THE APPLICATION OF STATISTICAL LINEARIZATION TO NONLINEAR RAIL VEHICLE DYNAMICS

by

AHMET VECDET ARSLAN

B.S., Middle East Technical University, Turkey
(1974)

M.S., California Institute of Technology
(1976)

SUBMITTED IN PARTIAL FULFILLMENT
OF THE REQUIREMENTS FOR THE
DEGREE OF

DOCTOR OF PHILOSOPHY

at the

MASSACHUSETTS INSTITUTE OF TECHNOLOGY

May 20, 1980

Signature of Author...
Department of Mechanical Engineering
May 20, 1980

Certified by...
J. Karl Hedrick
Thesis Supervisor

Accepted by..
Warren M. Rohsenow
Chairman, Department Committee

To my wife, Can

THE APPLICATION OF STATISTICAL LINEARIZATION TO NONLINEAR RAIL VEHICLE DYNAMICS

by

AHMET VECDET ARSLAN

Submitted to the Department of Mechanical Engineering on May 13, 1980, in partial fulfillment of the requirements for the degree of Doctor of Philosophy.

ABSTRACT

The applicability of statistical linearization as a design tool in the lateral stability and forced response analysis of nonlinear rail vehicles is investigated. A digital lateral half carbody locomotive model is developed to validate the results obtained by the statistical linearization method. Gaussian and trapezoidal probability density functions (PDF's) for the inputs to the nonlinearities are used, and it is shown that the trapezoidal PDF reduces the difference in r.m.s. values less than 15% for both low and high speeds whereas the Gaussian assumption produces differences as great as 30% in the high speed case. It is shown that the statistical linearization method is a useful tool in predicting the frequency content of the variables as well as the total r.m.s. values.

The extension of the half carbody model to a full carbody model indicates that the half carbody model is adequate to predict the lateral stability of the locomotive model. The developed and validated method is then used to determine the influence of wheel profile, track roughness, axle clearance and centerplate Coulomb friction level on the lateral stability of the locomotive.

Thesis Supervisor: J.K. Hedrick
Title: Associate Professor

ACKNOWLEDGEMENTS

I would like to thank many people for their guidance and help during the development and preparation of this work. I am grateful to my supervisor, Professor J. Karl Hedrick for his excellent guidance and patience. I would like to thank my committee members, Professor D.N. Wormley, Professor H.M. Paynter and Professor S.H. Crandall for their help and guidance in the committee meetings.

I would like to thank Mrs. Leslie Regan and Ms. Sandra Williams for their assistance and friendship during my academic years at M.I.T.

I would like to thank the Turkish Government and Association of American Railroads for their support of this work.

Finally, I would like to thank my wife, Can, for her unlimited patience and understanding.

Note: I still don't understand how the residents of Room 3-351 stand my noise. Thank you Kerim, Ismael, Dan, Charlie, George, Arnon, Jim, Garry, Misko, Ryan, Barry, and Amir.

NOMENCLATURE

Symbol		
a	1/2 track gauge	[in]
A	track roughness parameter	[in^2 -rd/ft]
a_1	wheelset roll coefficient in linearized expression	
C_{py}	lateral primary damping	[lb-sec/in]
$C_{p\psi}$	yaw primary damping	[lb-sec/in]
C_{sy}	lateral secondary damping	[lb-sec/in]
$C_{s\psi}$	yaw secondary damping	[lb-sec/in]
C_{pz}	vertical primary damping	[lb-sec/in]
$C_{p\phi}$	primary roll damping	[lb-sec/in]
$C_{s\phi}$	secondary roll damping	[lb-sec/in]
d_p	distance from truck c.g. to primary suspension	[in]
d_s	distance from truck c.g. to secondary suspension	[in]
f_{11}	lateral creep coefficient	[lb]
f_{12}	lateral/spin creep coefficient	[in-lb]
f_{22}	spin creep coefficient	[in^2-lb]
f_{33}	longitudinal creep coefficient	[lb]
h_{tp}	height to truck c.g. above axle center	[in]
h_{cs}	height of carbody c.g. above bolster spring center	[in]
h_{ts}	height of bolster spring center above truck c.g.	[in]
I_{wz}	wheelset yaw moment of inertia	[lb-in-sec^2]
I_{wy}	wheelset spin moment of inertia	[lb-in-sec^2]
I_{tz}	truck yaw moment of inertia	[lb-in-sec^2]
I_{tx}	truck roll moment of inertia	[lb-in-sec^2]
I_{cx}	carbody roll moment of inertia	[lb-in-sec^2]
I_B	bolster yaw moment of inertia	[lb-in-sec^2]

k_{py}	primary lateral stiffness	[lb/in]
$k_{p\psi}$	primary yaw stiffness (linear)	[lb/in]
$k_{p\phi}$	primary roll stiffness	[lb/in]
k_{pz}	primary vertical stiffness	[lb/in]
k_{sy}	secondary lateral stiffness	[lb/in]
$k_{s\psi}$	secondary yaw stiffness	[lb/in]
$k_{s\phi}$	secondary roll stiffness	[lb/in]
$k_{p\psi_1}$	primary yaw stiffness in the linear range	[lb/in]
$k_{p\psi_2}$	primary yaw stiffness after the linear range	[lb/in]
k_{ϕ}	equivalent linear gain for roll angle	
k_g	equivalent gravitational stiffness	
L_A	axle load	[lb]
ℓ_1	distance between truck center and leading axle	[in]
ℓ_2	distance between truck center and middle axle	[in]
ℓ_3	distance between truck center and trailing axle	[in]
ℓ	half distance between truck centers	[in]
M_W	wheelset mass	[lb-sec^2/in]
M_T	truck mass	[lb-sec^2/in]
M_c	carbody mass	[lb-sec^2/in]
N	sample size	
$N_{L,R}$	left, right normal forces	[lb]
r_L	left rolling radius	[in]
r_R	right rolling radius	[in]
r_o	rolling radius for centered wheelset	[in]
S	power spectral density	
$\bar{S}$	estimate of power spectral density	
$t_{n;\alpha}$	student t distribution	

T_{cp}	centerplate Coulomb breakaway torque	[lb-in]
V	vehicle forward speed	[mph]
δ_L	left contact angle	[rad]
δ_R	right contact angle	[rad]
δ_o	contact angle for centered wheelset	[rad]
δ_y	deadband amplitude of primary spring	[in]
δ_ψ	linear range for primary yaw spring	[in]
ϕ	wheelset roll angle	[rad]
ϕ_d	cant deficiency	[degrees]
ξ_x	longitudinal creepage	
ξ_y	lateral creepage	
ξ_{sp}	spin creepage	
$\Omega_A, \Omega_c, \Omega_s$	cut-off frequencies for track irregularity PSD's	[rad/ft]
λ	effective conicity	
Ω_o	V/r_o, nominal axle angular velocity	[rad/sec]
Ω	spatial frequency	[rad/sec]
σ_x	r.m.s. value of x	
$\bar{\sigma}_x$	sample r.m.s. value of x	
$\chi^2_{n;\alpha}$	Chi-Square distribution	
η	white noise	
Δ_L	equation (2.3)	
Δ_1	equation (2.4)	
Δ_2	equation (2.5)	

TABLE OF CONTENTS

Page

LIST OF FIGURES

FIGURE NUMBER	TITLE	PAGE

FIGURE NUMBER	TITLE	PAGE

LIST OF TABLES

CHAPTER 1

INTRODUCTION

The use of the analytical techniques to study rail vehicle dynamics has seen increasing application around the world during the past few decades. Most of these analytic studies have employed linear analysis techniques such as eigenvalue/vector and frequency response computations to study the stability and the forced response of the rail vehicles. The analysis of new rail vehicle truck designs has proceeded along these lines and a great deal has been learned about the complex lateral dynamic behavior by linear analytical techniques. The fundamental papers of Wickens [1], Matsudaira [2], and Cooperrider [3] made use of the linear matrix theory for rail vehicles with many degrees of freedom. Cooperrider and Law's survey paper, [4], outline the results of the linear theory.

Although the linearized theory often yields correct qualitative results, it cannot include the effects of worn wheel profiles, wheel flanges, suspension clearances, spring hardening, dry friction and creep force saturation. Cooperrider [5] found that flange contact can lead to sustained hunting at speeds well below the linear critical speed. Hobbs [6], King [7] and Law [8] showed that nonlinear creep may have a significant influence on the truck hunting.

One way of including these nonlinear effects is through digital simulations and this technique has been used successfully by many investigators [8,9]. Although an extremely useful method to make final checks of the design, this technique is not suitable as a design tool due to its complexity, cost and the difficulty in interpreting the results.

In order to develop nonlinear analytical tools for rail vehicle design, a number of approximation techniques have been investigated. DePater [10], Law [8], Law and Brand [11] applied the averaging method of Krylov and Bogoliubov to determine the hunting behavior of a wheelset. This method is difficult to extend to large order systems and is limited to the analysis of speeds above the onset of hunting. Cooperride and Hedrick, [12,13,14], applied the sinusoidal describing function method to predict the hunting behavior of wheelsets and higher degree of freedom vehicles. This technique, although very useful, is limited to speeds above the onset of hunting, like the K&B method. Stassen [15], Rus [16], Hedrick [17], Hedrick and Arslan [18], Hedrick and Castelazo [19] have applied the approximate method of statistical linearization to analyze the stationary statistical response of nonlinear rail vehicle models. The statistical linearization method replaces the nonlinear system with an equivalent linear system. This technique has the advantage of being applicable for speeds below and up to the onset of hunting. Thus it can be used to predict the forced response of the vehicle to statistical track irregularities as well as the influence of suspension parameters on the lateral stability. It also has the advantage of allowing the vehicle designer to interpret the nonlinear system response in familiar terms, i.e., natural frequencies, damping ratios, and modes of vibration. The disadvantage of the technique is that the probability density function of the inputs to the nonlinearities should be known. Booton [20] has shown that if the exact probability density functions are used the propagation of the mean and covaranice of the approximate system is identical to that of the nonlinear system.

Scope and Goals:

The major objective of this research is to investigate the applicability of the statistical linearization as a design tool in the lateral stability and forced response analysis of rail vehicles, and to validate the results against a time domain digital simulation model. The proposed research is:

- To develop a nonlinear locomotive model
- To develop a time domain digital simulation model
- To investigate (evaluate) the statistical linearization method as a design tool for rail vehicles
- To validate the results by time domain simulations
- To apply the developed and validated method to analyze the effects of the nonlinearities on the lateral dynamics of a six-axle locomotive.

In order to accurately describe the wheel/rail interaction forces the complete nonlinear wheelset equations are derived and presented in Appendix A. The nonlinear wheelset equations together with suspension nonlinear characteristics, which are obtained from

Martin-Marietta test data [21] are incorporated into a linear AAR locomotive model [22] in Chapter 2.

Chapter 3 describes the time domain digital simulation model. The digital program was developed to investigate the importance of wheel/rail nonlinearities and to validate the statistical linearization method. Chapter 3 also describes the digital simulations and the processing of time traces to compute probability density functions, power spectral densities and r.m.s. values.

In Chapter 4, the historic development of statistical linarization method and the approach used in this thesis are presented. Also, the flow chart of the developed computer program and the improvements made to increase the efficiency of the program are discussed.

Chapter 5 describes two types of probability density functions that are used in the evaluation of the statistical linearization method. These are Gaussian and trapezoidal density functions. It is shown that the trapezoidal density function assumption for the inputs to the nonlinearities is suitable as a design tool.

Chapter 6 presents the parametric studies performed using the developed and validated design tool. In the first part of the chapter the extension of the half-carbody model to full carbody model and the comparison of the two models are presented. It is shown that although the half carbody model is sufficient to investigate the lateral stability characteristics of rail vehicles, a full carbody model is recommended for the ride quality analysis. The second part of the chapter contains the parametric studies to investigate the effects of important nonlinearities on the lateral stability of the half carbody locomotive model. The results of parametric studies are summarized in Chapter 7.

The equations of motions of the digital and statistically linearized half carbody models and the extension to full carbody equations are presented in Appendix B. Finally, Appendix C contains the computer listing of the 12 D.O.F. statistically linearized half carbody model.

CHAPTER 2

MODEL DEVELOPMENT

In the first part of the research a nonlinear locomotive model has been developed for lateral stability and forced response analysis. It consists of the derivation of nonlinear wheelset equations and incorporation of these equations together with the suspension non-linearities obtained from Martin-Marietta test data into a lateral linear A.A.R. locomotive model [22].

The essential dynamic element of a rail vehicle is the wheelset. It is important to accurately describe the wheel/rail interaction forces and to include all of the terms that have a significant influence on the dynamic performance of the vehicle. Therefore, a rigorous derivation of the nonlinear wheelset equations has been completed. This nonlinear wheelset model has been incorporated into a twelve degrees of freedom half-carbody digital locomotive model to eliminate those nonlinearities which have a negligible influence on the lateral forced response and the stability of the locomotive. The detailed derivation of the nonlinear wheelset equations and simplifications of these equations to well-known approximations are presented in Appendix A, and the twelve d.o.f. locomotive equations with nonlinear wheelset equations are presented in Appendix B.1.

The resulting locomotive model is used in Chapter 5 to validate the statistical linearization method. Since the model is used for parametric studies it is important that while containing all important nonlinearities it must be a low order model to reduce the computation costs. It was felt that a half-carbody model achieved these goals [4]. In Chapter 6 a comparison of the half-carbody and full-carbody models are presented.

Also in this chapter, the time domain and frequency domain representation of random track irregularities are presented.

2.1 Locomotive Lateral Half-Carbody Model

2.1.1 Degrees of Freedom and Assumptions

The half-carbody model which is adapted from [22], Figure 2.1, consists of a half-carbody mounted on a single truck with three wheelsets. The twelve degrees of freedom of the model are:

$y_{1,3,5}$ = lateral displacement of wheelsets 1,2,3

$y_{2,4,6}$ = yaw displacement of wheelsets 1,2,3

y_7 = truck lateral displacement

y_8 = truck yaw displacement

y_9 = truck roll displacement

y_{10} = carbody lateral displacement

y_{11} = carbody roll displacement

y_{12} = bolster yaw displacement

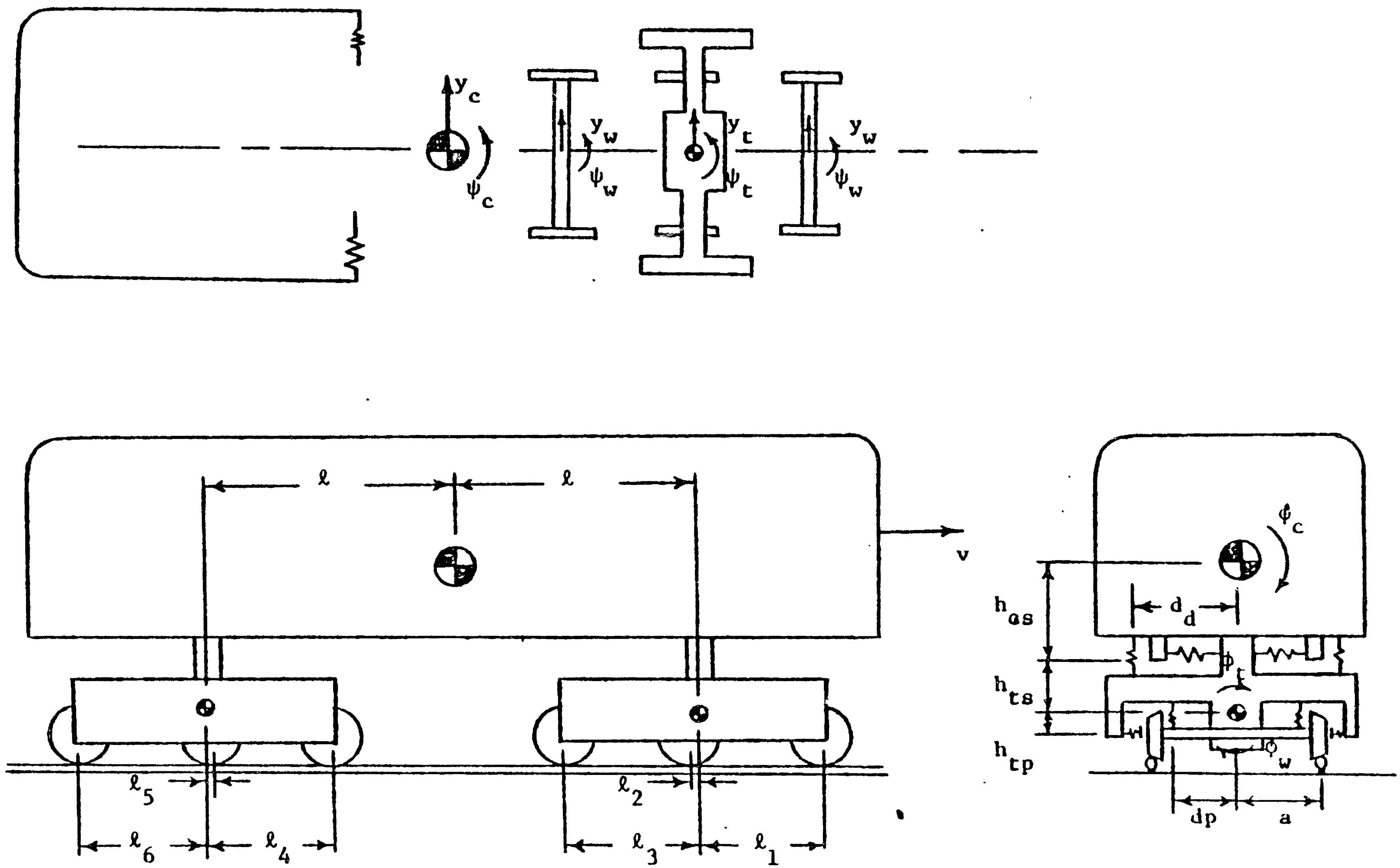

FIGURE 2.1: SIX-AXLE LOCOMOTIVE MODEL [22]

In this model the following assumptions are made:

- The vehicle is running at constant forward speed on tangent track
- All elements are rigid and their stiffnesses are lumped at the suspension connections
- There is no wheel lift
- The vehicle is symmetric about a vertical, longitudinal plane. Therefore, lateral and vertical motions are decoupled.

2.1.2 Wheel/Rail Profile Nonlinearities

In the nonlinear wheelset equations derived in Appendix A the following wheel/rail profile nonlinearities appear.

- $$\frac{r_L - r_R}{2} \qquad (2.1)$$
- $$\phi \qquad (2.2)$$
- $$\Delta_L(\Delta y) = \frac{\tan(\delta_L + \phi) - \tan(\delta_R - \phi)}{2 - \frac{1}{a}[r_L \tan(\delta_L + \phi) + r_R \tan(\delta_R - \phi)]} \qquad (2.3)$$
- $$\Delta_1(\Delta y) = \frac{\sin\delta_L \cos(\delta_L + \phi) - \sin\delta_R \cos(\delta_R - \phi)}{2} \qquad (2.4)$$
- $$\Delta_2(\Delta y) = \frac{\sin\delta_L \cos(\delta_L + \phi) - \sin\delta_R \cos(\delta_R - \phi)}{2 - \frac{1}{a}[r_L \tan(\delta_L + \phi) + r_R \tan(\delta_R - \phi)]} \qquad (2.5)$$

where r_L, r_R = left and right rolling radii [Figure 2.2]

δ_L, δ_R = left and right contact angles

ϕ = wheelset roll angle

a = half of the wheelbase

Equation (2.1) is the rolling radii difference, i.e., the difference between the left and right radius measured at the respective contact points as shown in Figure 2.2. Equation (2.2) is the wheelset roll angle. Equation (2.3) represents the lateral gravitational force normalized by the constant axle load, L_A. Equations (2.4) and (2.5) reduce to the contact angle difference for small contact angles. For a real wheel these geometric parameters are nonlinear functions of the wheelset excursion. Figures 2.3 and 2.4 are typical examples of these geometric nonlinearities [23].

2.1.3 Suspension Nonlinearities

There are three kinds of nonlinear suspension elements in the locomotive model [21]. These are:

- -Primary lateral suspension
- -Primary yaw suspension
- -Coulomb friction between bolster and the carbody yaw motions.

Primary Lateral Suspension:

The primary lateral suspension is modeled as a deadband spring in parallel with a viscous damper [21]. The characteristics

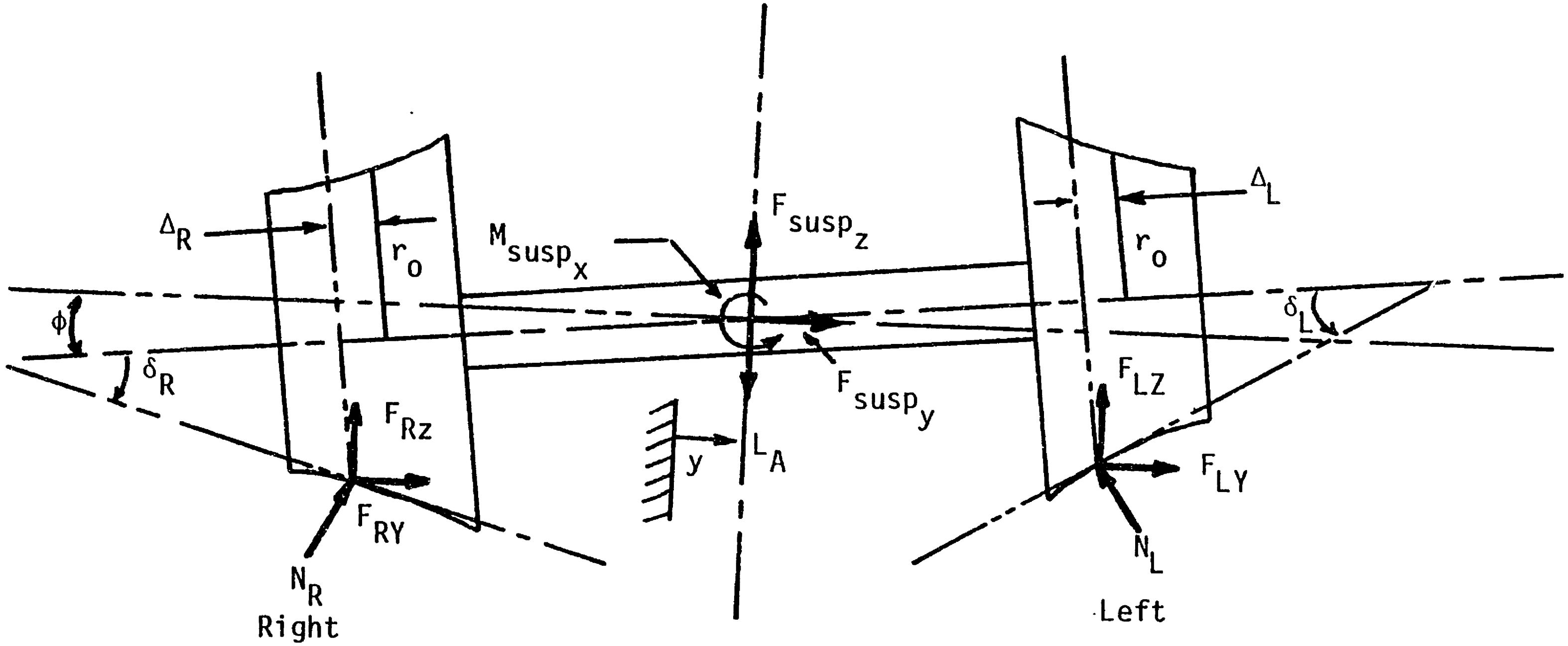

FIGURE 2.2: FREEBODY DIAGRAM OF A WHEELSET

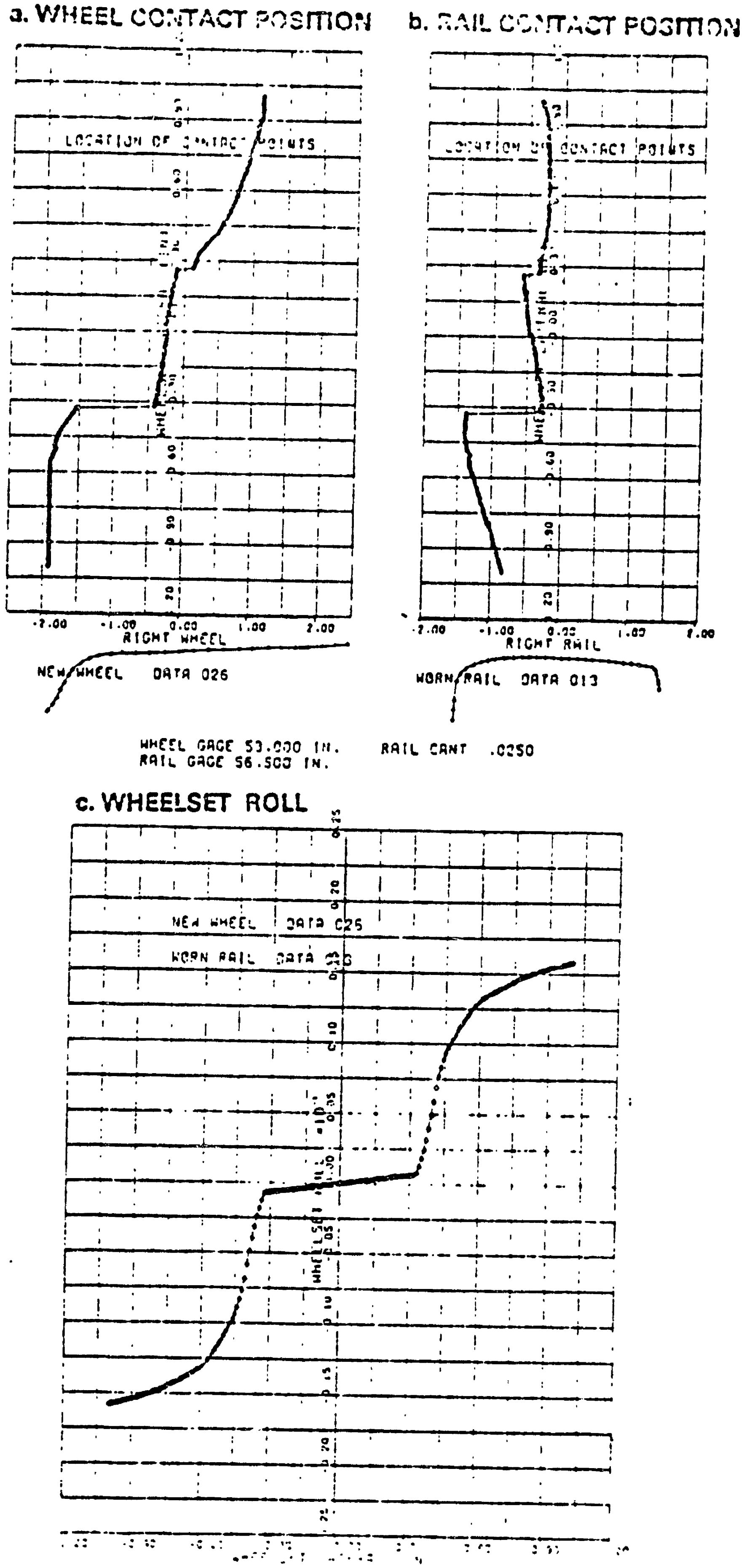

FIGURE 2.3: NEW WHEEL, WORN RAIL GEOMETRIC CONSTRAINTS [23]

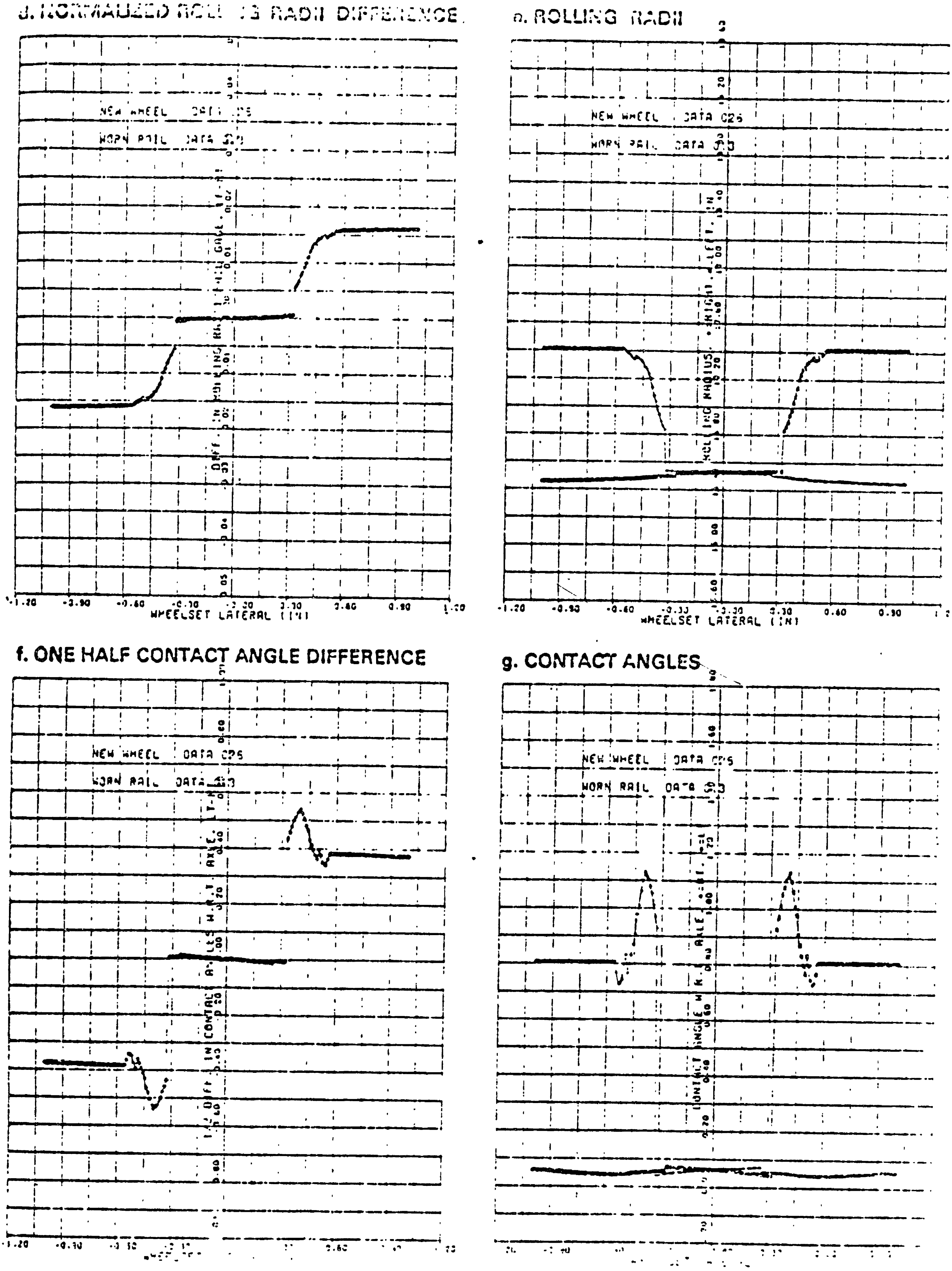

FIGURE 2.4: NEW WHEEL ON WORN RAIL GEOMETRIC CONSTRAINTS [23]

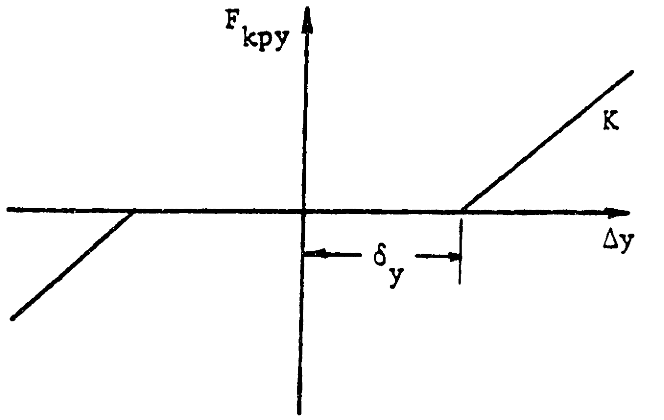

FIGURE 2.5.a: PRIMARY LATERAL DEADBAND SPRING

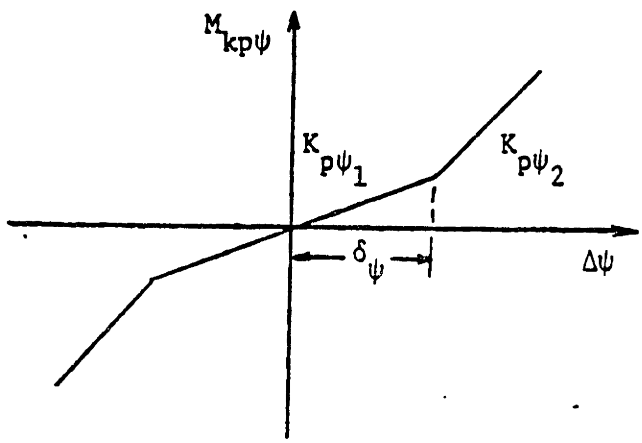

FIGURE 2.5.b: PRIMARY YAW SPRING

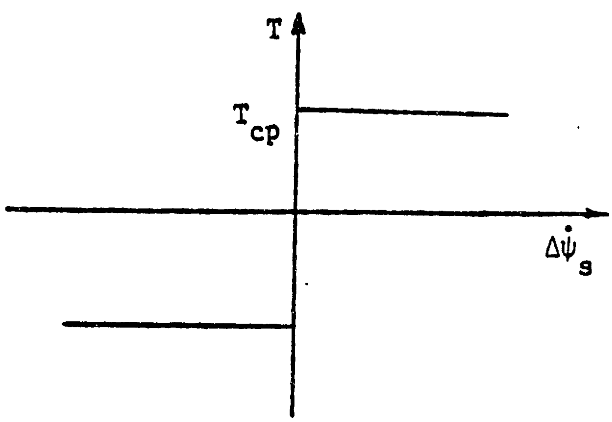

FIGURE 2.5.c: SECONDARY YAW COULOMB DAMPER

of the nonlinear spring are shown in Figure 2.5.a. The force-displacement relation of the spring is given by:

$$F_{kpy_i} = \begin{cases} k\,\xi_i & ; \quad (|\Delta y_i| > \delta_{yi}) \\ 0 & ; \quad (|\Delta y_i| \leq \delta_{yi}) \end{cases} \tag{2.6}$$

where $\xi_i = (|\Delta y_i| - \delta_{yi})\text{sign}(\Delta y_i)$

$\Delta y_i = y_i - y_7 \pm \ell_j y_8 - h_{tp} y_9 \qquad i = 1,3,5 \quad j = 1,2,3$

δ_{yi} = Deadband amplitude.

Primary Yaw Suspension:

The primary yaw suspension is modeled as a hardening spring in parallel with a viscous damper [21]. The hardening yaw spring has the piecewise linear shape as shown in Figure 2.5.b. The force-displacement relation of the spring is given by:

$$M_{kp\psi} = \begin{cases} k_{p\psi_1}\,\Delta\psi & ; \quad |\Delta\psi| \leq \delta_\psi \\ k_{p\psi_1}\,\delta_\psi\,\text{sign}(\Delta\psi) + k_{p\psi_2}[(\Delta\psi - \delta_\psi \cdot \text{sign}(\Delta\psi))] & ; \quad |\Delta\psi| > \delta_\psi \end{cases} \tag{2.7}$$

where $\Delta\psi = y_i - y_8$, $i = 2,4,6$

δ_ψ = Linear range of primary yaw spring

Secondary Yaw Suspension:

The secondary yaw suspension is modeled as an ideal Coulomb damper between the carbody and the bolster in series with a linear spring between the bolster and truck as shown in Figure 2.6. The characteristics of the Coulomb damper are shown in Figure 2.5.c. The force-displacement relation is given by:

$$M_{s\psi} = \begin{cases} k_{s\psi}\,\Delta\psi_s & ; \quad \Delta\psi_s < \dfrac{T_{cp}}{K_{s\psi}} \\ T_{cp} & ; \quad \Delta\psi_s \geq \dfrac{T_{cp}}{K_{s\psi}} \end{cases} \tag{2.8}$$

where $\Delta\psi_s = y_8 - y_{12}$

T_{cp} = centerplate breakout level

2.2 Track Input Description

Two types of rail irregularities are important in the analysis of lateral dynamics of rail vehicles: alignment and crosslevel. Alignment is defined as the average lateral position of the two rails. Crosslevel is defined as the difference in ele-

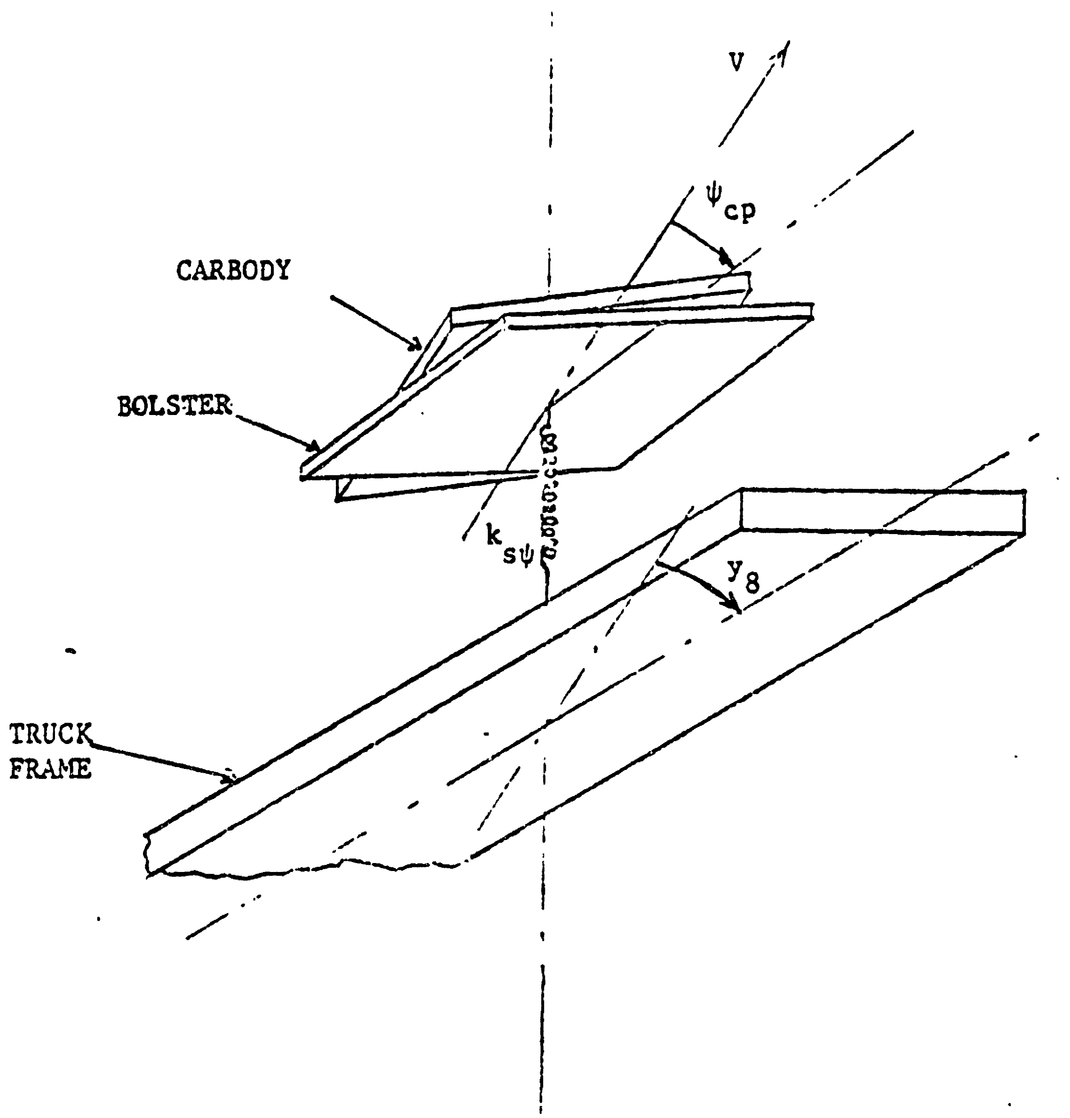

FIGURE 2.6: SECONDARY YAW SUSPENSION [25]

vation of the rails. Both displacements are illustrated in Figure 2.7. [24]

2.2.1 Frequency Domain Representation

The power spectral density of alignment and crosslevel have been measured for different kinds of tracks [24]. Figures 2.8 and 2.9 show the one sided spectral densities of alignment and crosslevel, respectively, for class 6 track [24].

These spectra have been approximated by a function which gives an analytic representation of the measured spectra. In practice, the track inputs are modeled as a stationary stochastic process whose spectral density fits that of the measured data in the frequency range of interest.

The spectral density functions obtained for the cases shown in Figures 2.8 and 2.9 are the following [24]:

Alignment:

$$S_A(\Omega) = \frac{2\pi A_a \Omega_c^2}{(\Omega^2 + \Omega_A^2)(\Omega^2 + \Omega_c^2)} \left[\frac{in^2\text{-}ft}{cycle}\right] \tag{2.9}$$

Crosslevel:

$$S_c(\Omega) = \frac{8\pi A_c \Omega_c^2}{(\Omega^2 + \Omega_s^2)(\Omega^2 + \Omega_c^2)} \left[\frac{in^2\text{-}ft}{cycle}\right] \tag{2.10}$$

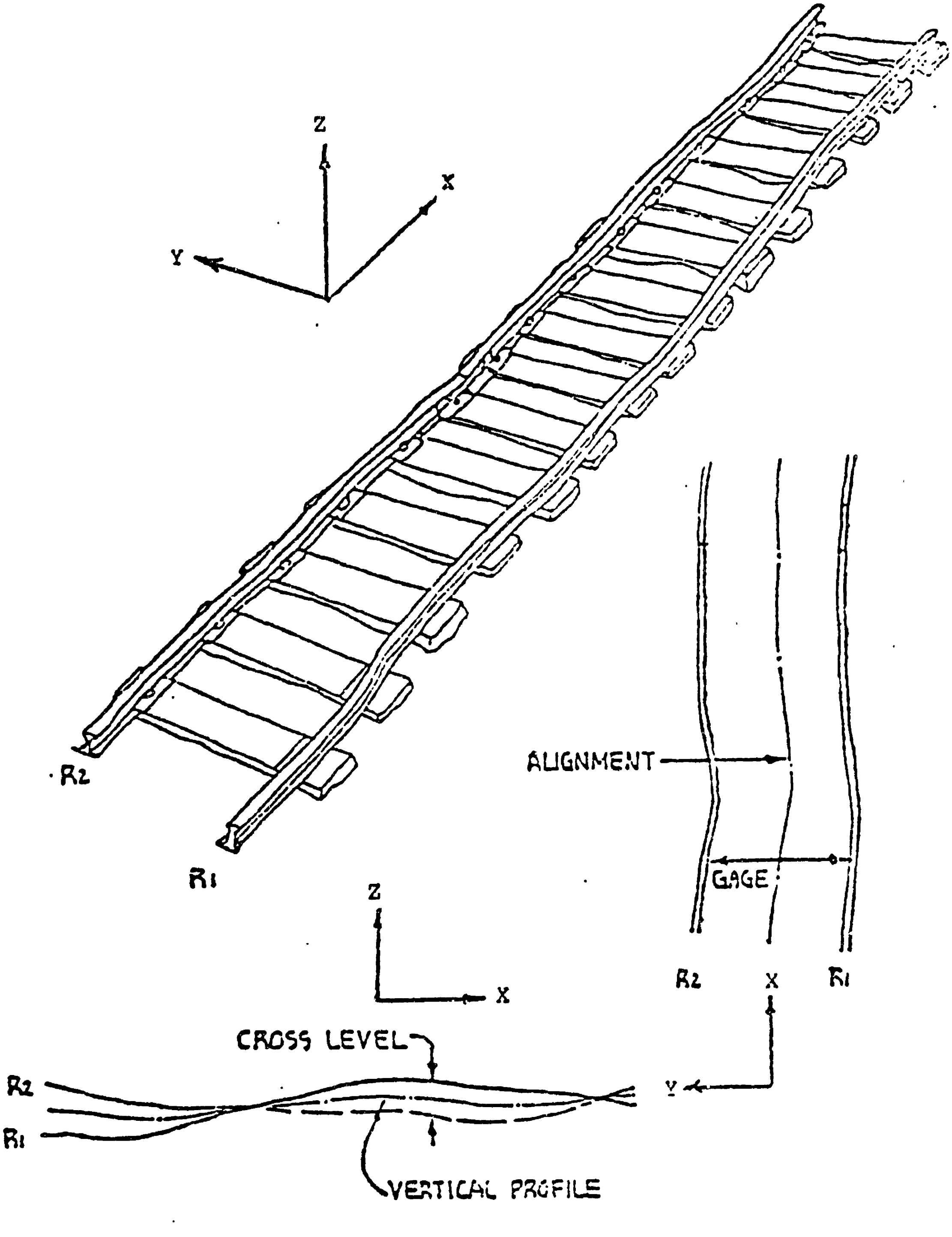

FIGURE 2.7: TRACK IRREGULARITIES DEFINITIONS
(Adapted from [24])

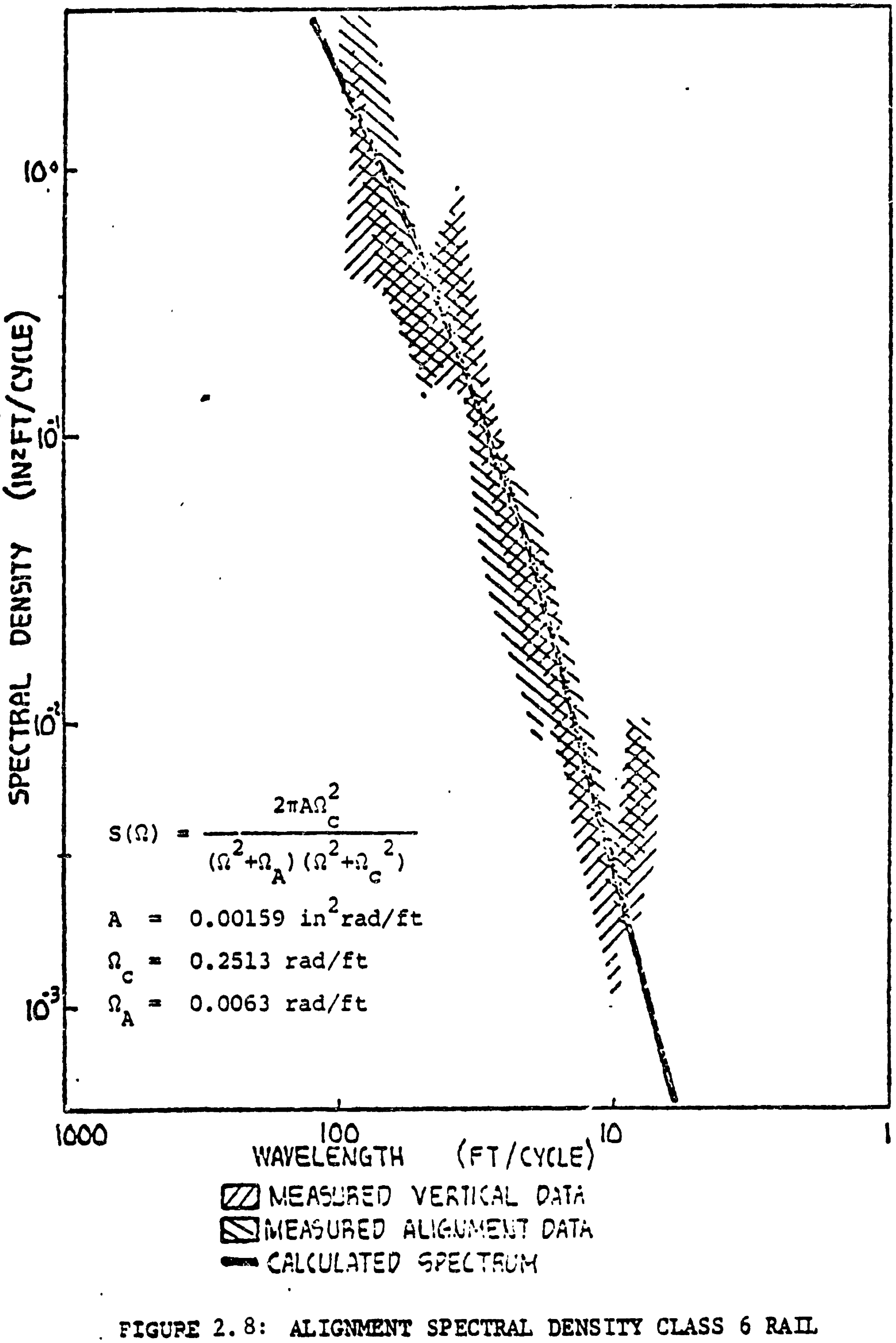

FIGURE 2.8: ALIGNMENT SPECTRAL DENSITY CLASS 6 RAIL (Adapted from [24])

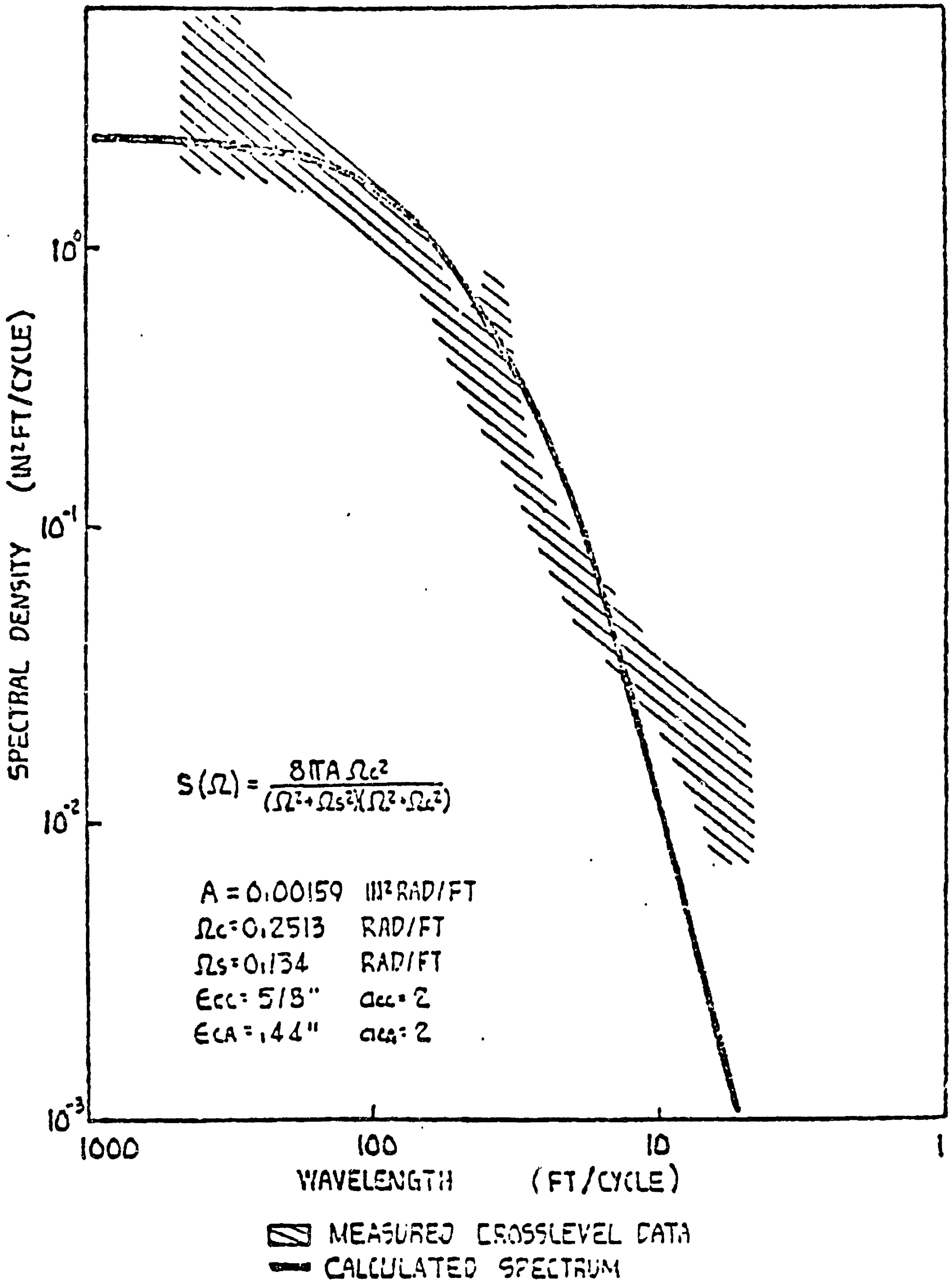

FIGURE 2.9: CROSSLEVEL SPECTRAL DENSITY CLASS 6 RAIL (Adapted from [24])

where Ω = spatial frequency [rad/ft]

A = track roughness parameter $[\frac{in^2/rad}{ft}]$

$\Omega_A, \Omega_c, \Omega_s$ = cut-off frequencies [rad/ft]

Table 2.1 shows the track roughness parameters and Ω_s as a function of Track Class Number. [25]

TABLE 2.1: TRACK INPUT PARAMETERS AS A FUNCTION OF TRACK CLASS NUMBER

T C N	1	2	3	4	5	6
A_c	0.05722	0.04808	0.03218	0.02543	0.00993	0.00159
A_a	0.1589	0.0572	0.0195	0.0143	0.0036	0.00159
Ω_s	0.1843	0.2837	0.2597	0.3448	0.2502	0.1335

2.2.2 Time Domain Representation

To obtain a time domain representation of the rail inputs suitable for digital simulation Gaussian white noise was passed through a linear shaping filter such that its output spectral density is equal to the spectra given by (2.9) and (2.10). A Gaussian random number generator which has a power spectral density shown in Figure 2.10 was used as the white noise. In this research only random alignment irregularities was used as track inputs.

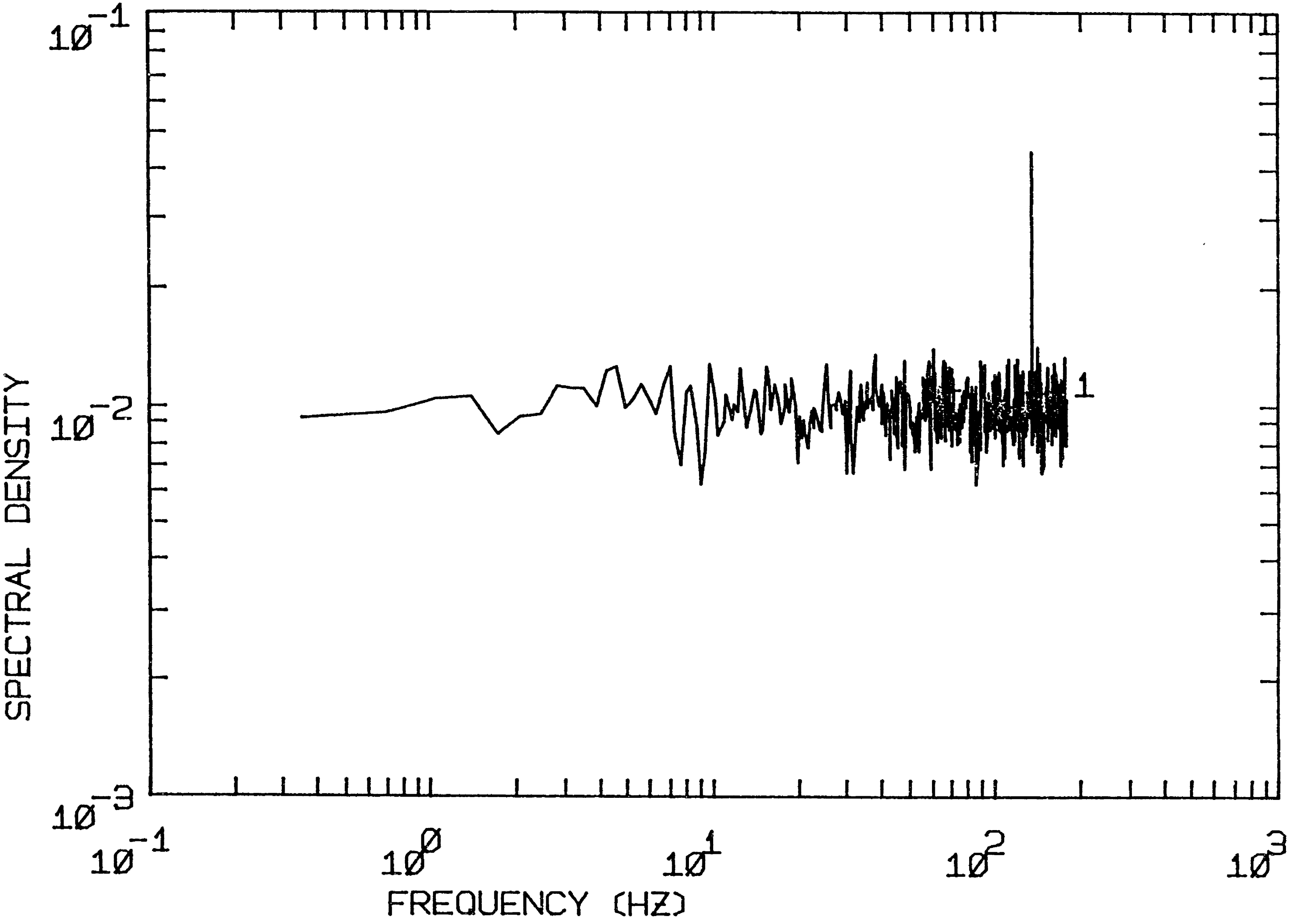

FIGURE 2.10: PSD OF THE GAUSSIAN RANDOM NUMBER GENERATOR

Derivation of Linear Shaping Filter:

The relationship between the input and output spectra for a linear time invariant system is given by:

$$S_o(\Omega) = H(\Omega)\ S_i(\Omega)\ H(-\Omega) \tag{2.11}$$

where $\Omega = \frac{\omega}{V}$ [rd/ft]

= spatial frequency

$S_i(\Omega)$ = PSD of input signal

$S_o(\Omega)$ = PSD of output signal

$H(\Omega)$ = Transfer function of the linear system

The transfer function $H(\Omega)$ can be obtained factorizing the output PSD and collecting all the factors with poles and zeros in the left hand plane. If such factorization is carried out $H(\Omega)$ is the transfer function of a stable, minimum phase system. This system is defined as the shaping filter.

Following this algorithm the factorization of (2.9) is given by:

$$S_A(\Omega) = \frac{2\pi A_a \Omega_c^2}{(S + \Omega_A)(S + \Omega_c)(S - \Omega_A)(S - \Omega_c)} \tag{2.12}$$

where $s = j\Omega$; $j = \sqrt{-1}$

The spectral density of white noise is given by:

$$S_i(\Omega) = \frac{q}{\pi} = \text{constant}$$

where q = intensity of the white noise.

Then the transfer function of the linear shaping filter can be expressed as:

$$H(\Omega) = \frac{1}{(S + \Omega_A)(S + \Omega_c)} \tag{2.13}$$

$$q = 2\pi^2 A_a \Omega_c^2 \tag{2.14}$$

Finally, we can express the system defined by the transfer function (2.13) by its time-domain differential equation with white noise input.

$$\ddot{y}_a + (\Omega_A + \Omega_c)\dot{y}_a + \Omega_A \Omega_c y_a = \eta_a(t) \tag{2.15}$$

$$E[\eta_a(t)\ \eta_a(t + \tau)] = q\delta(\tau)$$

<u>Verification of the Shaping Filter</u>:

The random sequence for alignment input produced by the shaping filter was verified by computing its power spectral density using a Fast Fourier Transform (FFT) algorithm. Figure 2.11

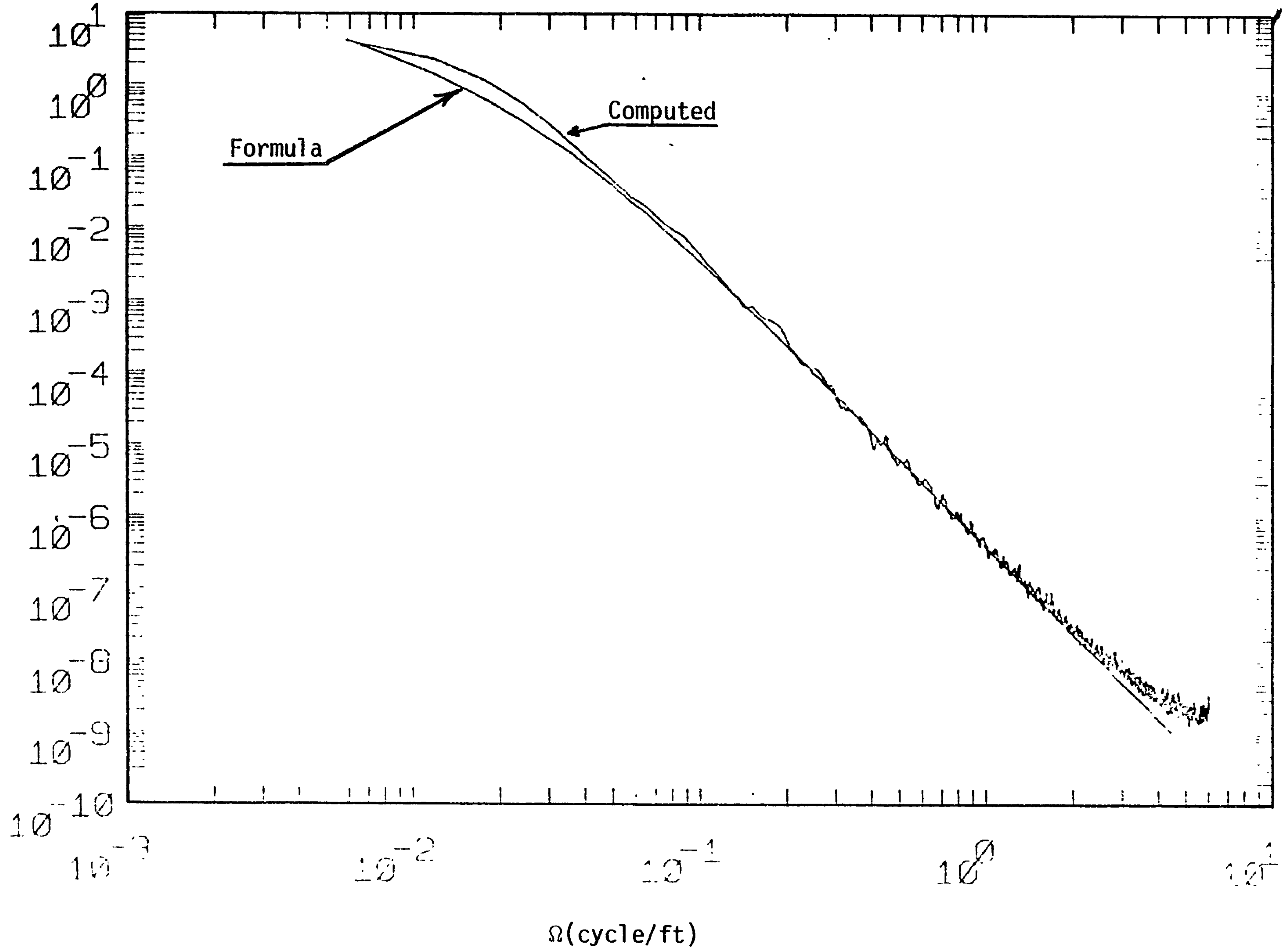

FIGURE 2.11: COMPARISON OF THE PSD OF CONSTRUCTED ALIGNMENT INPUT TO PSD GIVEN BY EQUATION (2.9)

shows the PSD of the constructed rail alignment irregularity compared with the formula given by (2.9). Figure 2.12 shows the computed probability density function of the constructed alignment irregularity from the digital simulation of equation (2.15).

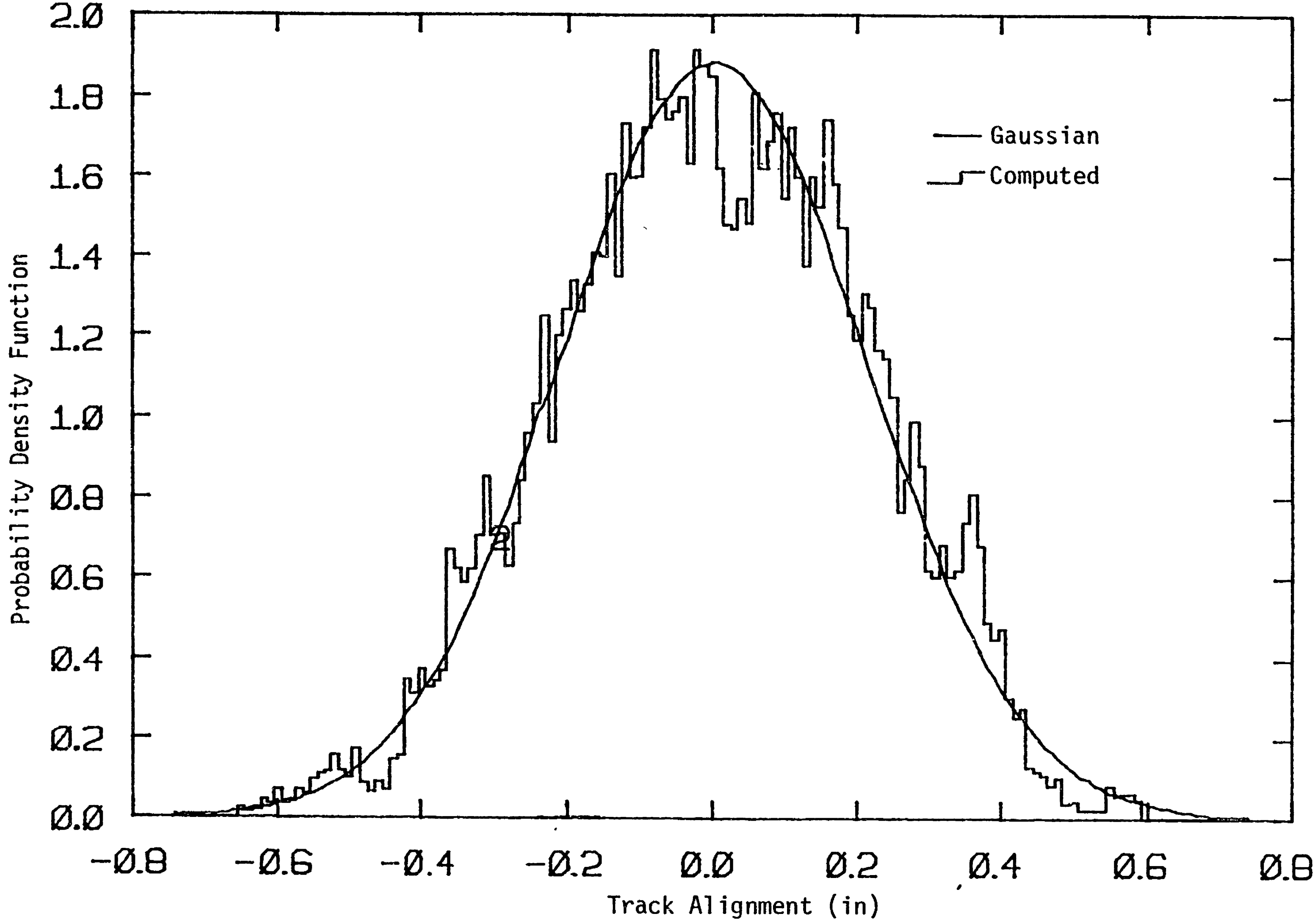

FIGURE 2.12: PROBABILITY DENSITY FUNCTION OF THE ALIGNMENT INPUT

CHAPTER 3

DIGITAL SIMULATION OF LOCOMOTIVE DYNAMICS

3.1 Introduction

The twelve degrees of freedom three-axle nonlinear half-carbody locomotive model presented in Chapter 2 has been simulated on a DEC/VAX 11/780 digital computer. In Chapter 5, the results of digital simulations are used to validate the statistical linearization method. The random track alignment input was generated and stored on disk as a stationary stochastic process. Twelve second order nonlinear ordinary differential equations which are presented in Appendix B.1 were represented by 24 first order nonlinear differential equations. These equations were integrated on the digital computer by a fourth order Runge-Kutta algorithm. The response of the locomotive model to random alignment irregularity was stored on disk files for further processing of the time traces.

Nonlinear characteristics of the model, specifically nonlinear wheel/rail profile geometry, is important during flange contact. Therefore a variable time step was used in the integration scheme in order to reduce the time step in the flange region and still allow larger time steps in the tread region. As a result of this variable time step a 30-60 percent reduction in computation time was achieved. The necessary time steps for the digital simulation were estimated by the eigenvalues of the linear frequency domain program.

The wheel/rail geometric functions as a function of wheelset excursion were stored on disk in tabular form at intervals of 0.01 inches in the excursion range of [-1.0, 1.0] inches. The array of 8x201 elements contains the following variables:

y	-	wheelset excursion	[in]
r_L	-	rolling radius, left wheel	[in]
r_R	-	rolling daius, right wheel	[in]
δ_L	-	contact angle, left wheel	[rd]
δ_R	-	contact angle, right wheel	[rd]
ϕ	-	wheelset roll angle	[rd]
ϕ'	-	$\partial\phi/\partial y$	[rd/in]
z	-	wheelset vertical displacement	[in]
z'	-	$\partial z/\partial y$	[in/in]

The locomotive equations presented in Appendix B.1 have many trigonometric functions of these wheel/rail geometric constraints. To reduce the computation time a second table was prepared and stored on disk. This table has the following variables:

$y, \sin\delta_L, \sin\delta_R, \cos(\delta_L + \phi), \cos(\delta_R - \phi),$

$\tan(\delta_L + \phi), \tan(\delta_R - \phi), \Delta_L(y).$

At each integration step these geometric constraints were computed from the tables by linear interpolation.

The computer program has the capability of including creep force saturation using an approximate creep force model. This nonlinear creep force model is presented in Appendix A.

The digital half-carbody locomotive model with nonlinear wheel/rail geometry, fully nonlinear suspensions and a linear creep force/creepage relationship was simulated on the digital computer to obtain the time response of the model to random track alignment irregularities. These time traces were processed to obtain the r.m.s. values, proability density functions and power spectral densities. The results were used in Chapter 5 to evaluate the statistical linearization method. In these digital simulations a high conicity (Heumann) wheel on new AAR rail at standard 56.5" gauge was used. The purpose of using a high conicity wheel was to evaluate the method of statistical linearization at both on-flange and off-flange conditions.

The computer ogram was coded in such a way that the user has many options. The program can be used:

- To obtain the initial condition response or response to track alignment irregularities
- To determine the effect of linear and nonlinear wheel/rail profile geometry on the performance of the vehicle
- To determine the effect of nonlinear suspensions on the performance separately or in any combinations

-To determine the effect of linear creep or creep force saturation. Also, the above options can be used in any combinations.

3.2 Digital Analysis of the Data

This section presents the methods used in the processing of the time traces generated by the digital half-carbody program. A complete and detailed treatment of these methods is given in reference [26].

3.2.1 Stationarity of the Data

The correct procedures for analyzing the random data are strongly influenced by the stationarity of the data. Because, the analysis procedures required for nonstationary data are generally more complicated than those which are appropriate for stationary data.

In this research, two methods were used to check the stationarity of the data.

Method 1: This method consisted of plotting the running mean and running variance of the data versus time. Figure 3.1 and 3.2 show the mean and variance vs time for the leading wheelset excursion at 60 mph. These figures indicated the stationarity of the data after 10 seconds.

Method 2 [26]: In this method, the stationarity of the data is tested by investigating the sample record as follows:

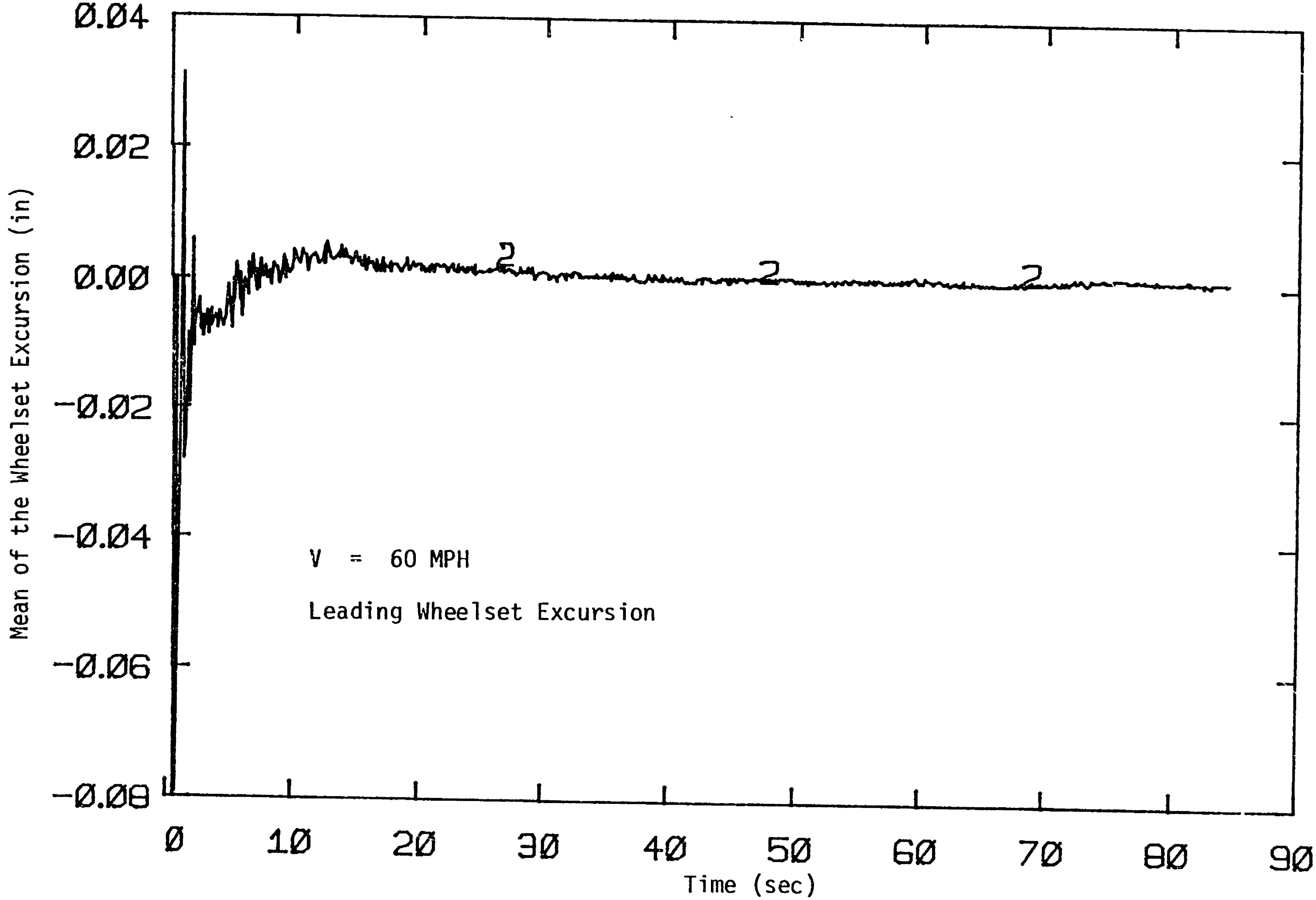

FIGURE 3.1: THE VARIATION OF MEAN w.r.t. TIME FOR STATIONARITY ANALYSIS

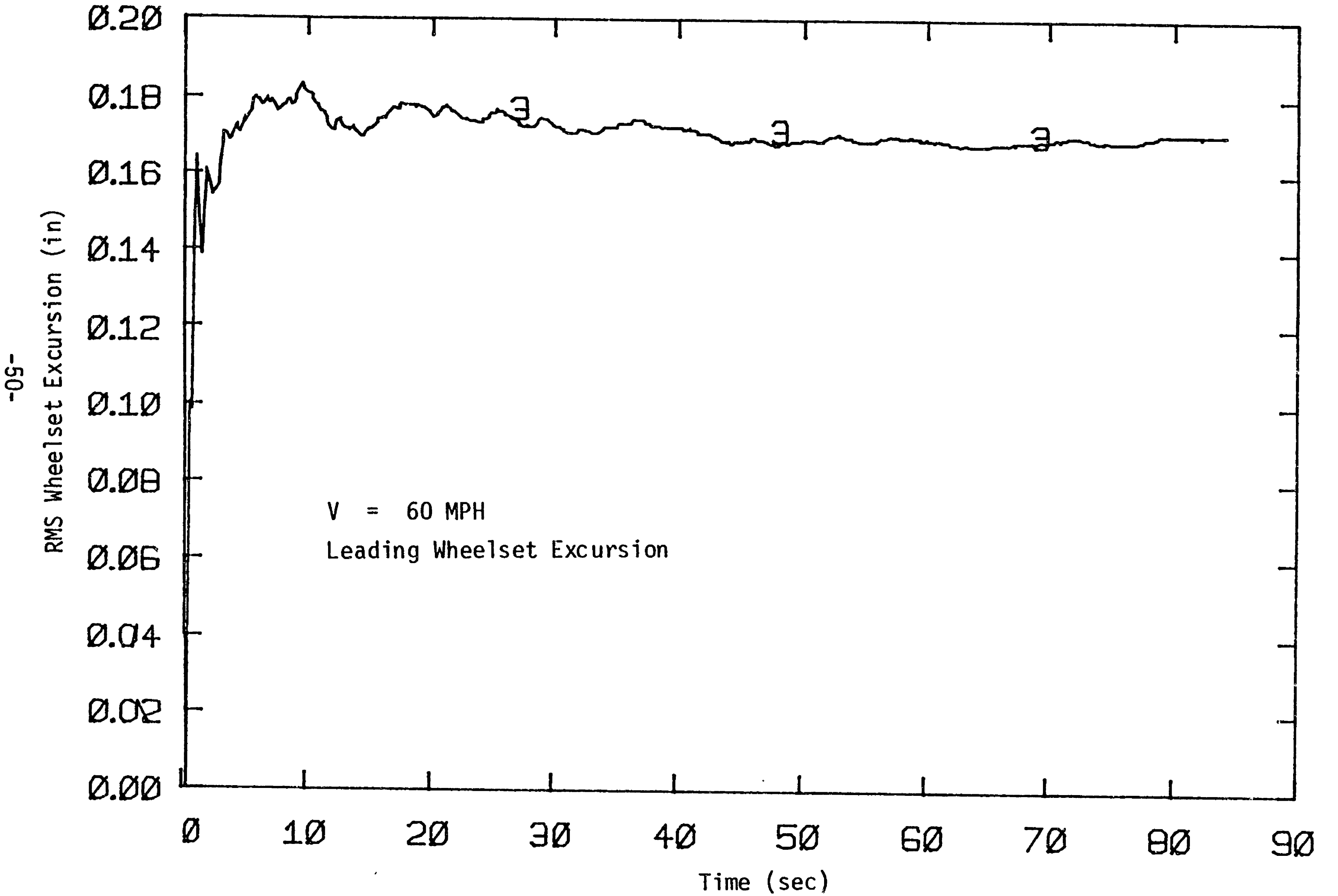

FIGURE 3.2: RMS VALUE OF WHEELSET EXCURSION vs TIME FOR STATIONARITY ANALYSIS

1. Divide the sample record into N equal time intervals where the data in each interval may be considered independent.

2. Compute a mean square value (or mean value and variance separately) for each interval and align these sample values in a time sequence, as follows.

$$\overline{x_1^2}\ , \overline{x_2^2}, \ldots, \overline{x_N^2}$$

3. Test the sequence of mean square values for the presence of underlying trends or variations other than those due to expected sampling variations.

The final test of the sample values for nonstationary trends may be accomplished in many ways. If the sampling distribution of the sample values is known, various statistical tests could be applied. However, the sampling distribution of mean square values requires a detailed knowledge of the frequency composition of the data. Such knowledge is generally not available at the time one wishes to establish whether or not the data is stationary. Hence a nonparametric approach which does not require a knowledge of the sampling distributions of data parameters is more desirable. One such nonparametric test is the <u>run test</u> which may be applied as follows.

Let it be hypothesized that the sequence of sample mean square values $(\overline{x_1^2}, \overline{x_2^2}, \ldots, \overline{x_N^2})$ are each independent sample values of a stationary random variable with a mean value of $\bar{x}$. If this hypothesis is true, the variations in the sequence of sample values are random and display no trends. Hence the number of runs in the sequence relative to, say, the median value, is as expected for a sequence of independent random observations of the random variable, as presented in Table A.6 of reference [26]. If the number of runs is significantly different from the expected number given in Table A.6 of reference [26], the hypothesis of stationarity is rejected. Otherwise, the hypothesis is accepted.

In this research both methods were used. The run test was a check of the stationarity. The first method was used to eliminate the transient part of the time traces in the processing of the data.

3.2.2 Sample Mean and Sample Variance Calculations

Estimators for Mean and Variance:

The sample mean and sample variances were computed using the following estimators.

$$\bar{x} = \frac{1}{N} \sum_{i=1}^{N} x_i \tag{3.1}$$

$$\bar{\sigma}_x^2 = \frac{1}{N-1} \sum_{i=1}^{N} (x_i - \bar{x})^2 \tag{3.2}$$

where $\bar{x}$ = sample mean

$\bar{\sigma}_x^2$ = sample variance

N = sample size

Estimators given by (3.1) and (3.2) are unbiased estimators for mean and variance x and σ_x [26].

Confidence Intervals for the Mean and Variance

Equations (3.1) and (3.2) give a point estimate for the mean and variance. It provides no indication how closely a sample value estimates the parameter. Therefore, a more satisfactory way is the estimation of an interval, rather than a single point, with a known degree of confidence.

A confidence interval for the mean value μ_x based upon the sample value $\bar{x}$ with unknown variance is given by [26]:

$$[\bar{x} - \frac{\bar{\sigma}_x \; t_{n;\alpha/2}}{\sqrt{N}} \leq \mu_x < \bar{x} + \frac{\bar{\sigma}_x \; t_{n;\alpha/2}}{\sqrt{N}}] \qquad (3.3)$$

where $n = N-1$

t = student t distribution

Equation (3.3) gives a $(1-\alpha)$ confidence interval for the mean value μ_x, and can be stated as: "The true mean value μ_x falls within the noted interval with a confidence of $100(1-\alpha)$percent".

Similarly, a $(1-\alpha)$ confidence interval for the variance σ_x^2 based upon a sample variance $\bar{\sigma}_x^2$ from a sample of size N is [26]

$$\frac{\bar{\sigma}_x^2}{(\chi^2_{n;\alpha/2})/n} \leq \sigma_x^2 < \frac{\bar{\sigma}_x^2}{(\chi^2_{n;1-\frac{\alpha}{2}})/n}] \qquad (3.4)$$

where σ_x^2 = actual variance

$\bar{\sigma}_x^2$ = sample variance

N = sample size

n = $N - 1$

$\chi^2_{n;\alpha}$ = Chi-Square distribution with n-degrees of freedom

3.2.3 Power Spectral Density (PSD) Calculations

The estimates of power spectral densities (PSD) were obtained by means of a Fast Fourier Transform (FFT) algorithm. A smooth cosine taper filter, which is shown in Figure 3.3, was used for FFT estimates to reduce the leakage [26]. In practice, the random error of an estimate produced by an FFT is reduced by smoothing the estimate in one of two ways. These are frequency and segment averging They can be used separately or together. Segment averaging is done by computing individual estimates from q independent segments and then averaging the q estimates at each frequency of a spectral component. Frequency averaging is done by averaging the spectra at adjacent frequencies. It can be shown that [26] the random errors for both cases are:

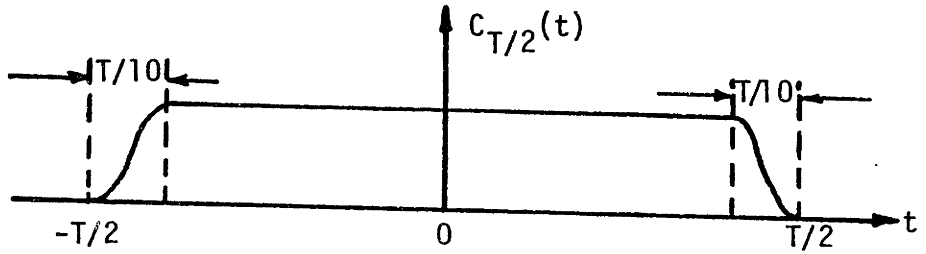

FIGURE 3.3: COSINE TAPER DATA WINDOW [26].

$$\varepsilon_s = \frac{1}{\sqrt{q}} \quad \text{(segment average)} \tag{3.5}$$

$$\varepsilon_f = \frac{1}{\sqrt{\ell}} \quad \text{(frequency average)} \tag{3.6}$$

where q = number of segments averaged

ℓ = number of adjacent frequencies averaged

Remarks on averaging: If we take a finite length time trace and consider that as a single segment, the normalized random error is 100% [26]. To reduce this error segment averaging can be done. But there is a lower limit on the smallest possible length of each segment based on the independency assumption of segments. If we further want to reduce the normalized random error frequency averaging can be done at the expense of losing the lowest resolution frequency. Then the total normalized random error is given by:

$$\varepsilon = \frac{1}{\sqrt{q\ell}} \tag{3.7}$$

where q = number of segments averaged

ℓ = number of adjacent frequencies averaged

Confidence Interval for a Power Spectral Density Estimate

After estimation of a power spectral density by a FFT algorithm, a smoothing operation is required to obtain a consistent estimate. The sampling distribution of a smoothed estimate is approximately chi-square [26] with $n = 2B_eT$ degrees of freedom. Hence a $(1-\alpha)$ confidence interval for a power spectral density function $S(f)$ based upon an estimate $\bar{S}(f)$ measured with a resolution bandwidth B_e and a record length T is given by [26]:

$$\left[\frac{\bar{S}(f)}{(\chi^2_{n;\alpha/2})/n} \leq S(f) < \frac{\bar{S}(f)}{(\chi^2_{n;(1-\frac{\alpha}{2})})/n}\right] \qquad (3.8)$$

where $n = 2B_eT$

3.3 Digital Simulation Results

The digital model with nonlinear wheel/rail profile geometry, fully nonlinear suspension and a linear creep force/creepage relationship was simulated to obtain the time response of the locomotive to random track alignment inputs at two speeds.

3.3.1 Low Speed Simulation

The locomotive with high conicity wheels (Heumann) on new rail at standard gauge was simulated at 40 mph. The flange clearance was 0.35 inches. The duration of the simulation was 100 seconds which was equal to 1.11 miles of track. Variable integration time steps of 0.003 and 0.001 seconds were used. The peak values of the wheelset excursions were:

- o 0.3684 inches for the leading wheelset
- o 0.3048 inches for the middle wheelset
- o 0.2125 inches for the trailing wheelset

These show that only the leading wheelset was flanging.

Figure 3.4 shows the leading wheelset excursion response to a random alignment input. The estimate of the mean and the rms values of the wheelset excursions, suspension strokes were computed by (3.1) and (3.2). The results are shown below.

TABLE 3.1: MEAN AND RMS VALUES AT 40 MPH

	WHEELSET EXCURSIONS			LATERAL PRIMARY STROKE LENGTH		
	#1	#2	#3	#1	#2	#3
Mean (in)	0.97E-3	0.72E-3	0.86E-4	0.34E-2	0.31E-2	0.26E-2
R.M.S.(in)	0.12474	0.096578	0.066809	0.18375	0.18563	0.21616

The 90% confidence intervals for the mean and variance are given by:

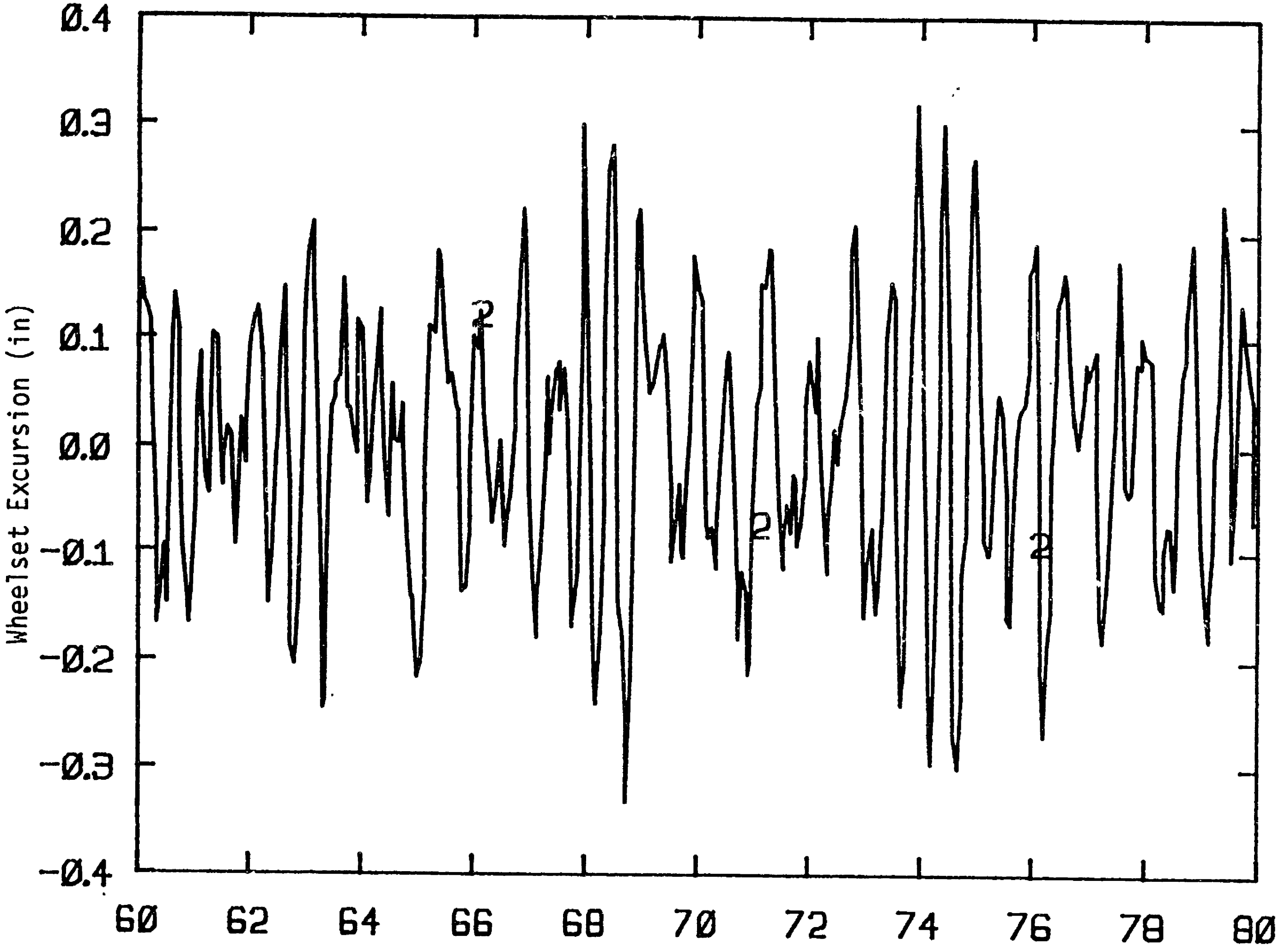

FIGURE 3.4: LEADING WHEELSET EXCURSION RESPONSE TO RANDOM ALIGNMENT INPUTS AT 40 MPH

Mean:

$$(\bar{x} - 5.2\text{E-}3 \;\; \bar{\sigma}_x) \leq \mu_x < (\bar{x} + 5.3\text{E-}3\bar{\sigma}_x)$$

Variance:

$$(0.9927 \; \bar{\sigma}_x^2) \leq \sigma_x^2 < (1.0074 \; \bar{\sigma}_x^2)$$

where $\bar{x}$ = sample mean

$\bar{\sigma}_x^2$ = sample variance

Figure 3.5 to 3.14 show the probability density functions of the inputs to the nonlinearities. The solid lines are the Gaussian density functions with the computed mean and variances and the computed probability density functions are shown in histogram forms. These PDF's are used in Chapter 5 to check the assumptions on the probability density functions.

Figures 3.15 to 3.17 show the PSD's of the wheelset excursions. The PSD's were obtained by an FFT algorithm with 48 segments averaging. Each segment had a length of 2.048 seconds corresponding to a resolution frequency of 0.488 Hz. The normalized error for 48 segments was 14.4%.

The 90% confidence interval for spectral points is given by:

$$0.807 \; \bar{S}(f) \leq S(f) < 1.3 \; \bar{S}(f)$$

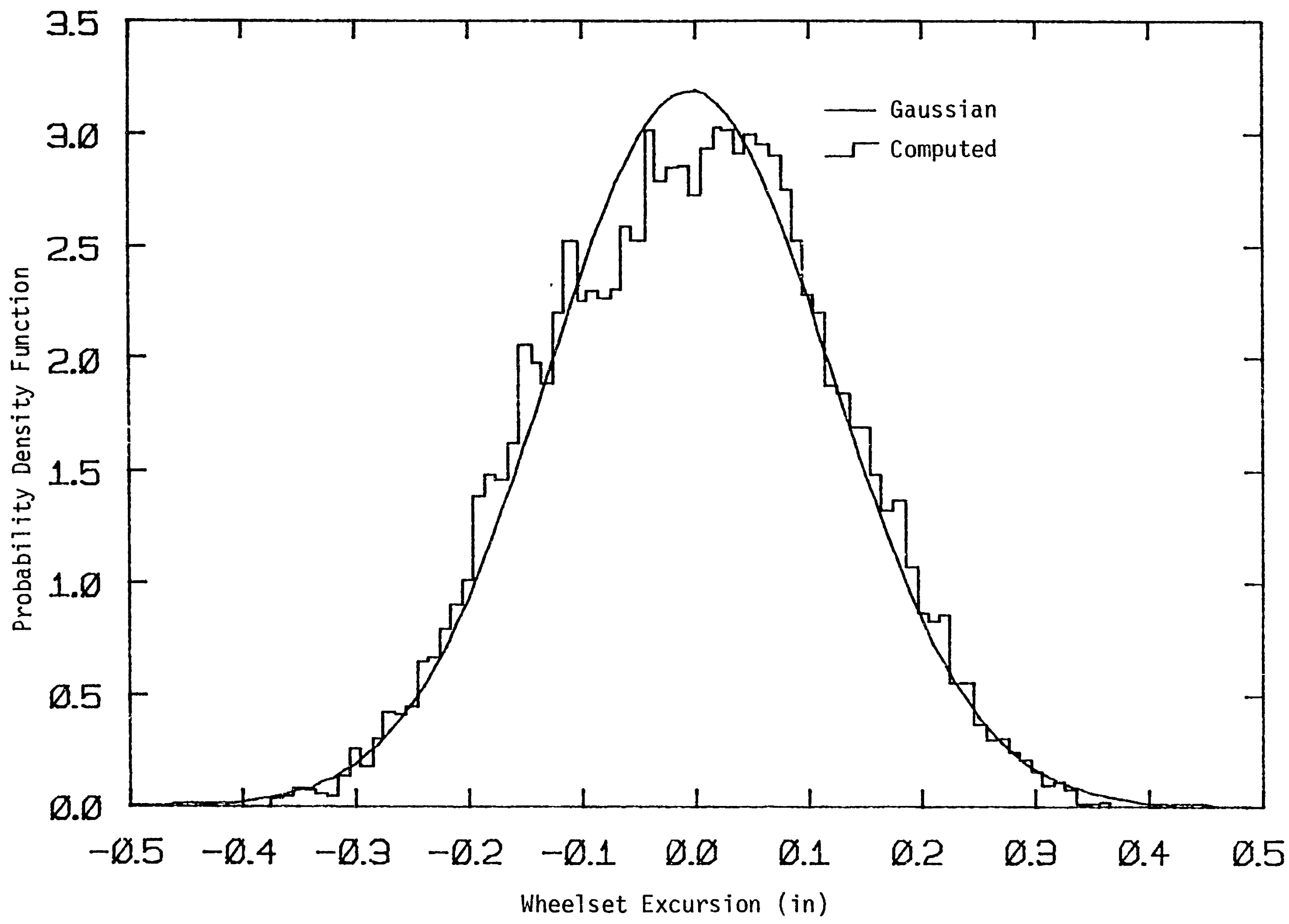

FIGURE 3.5: LEADING WHEELSET EXCURSION PDF AT 40 MPH

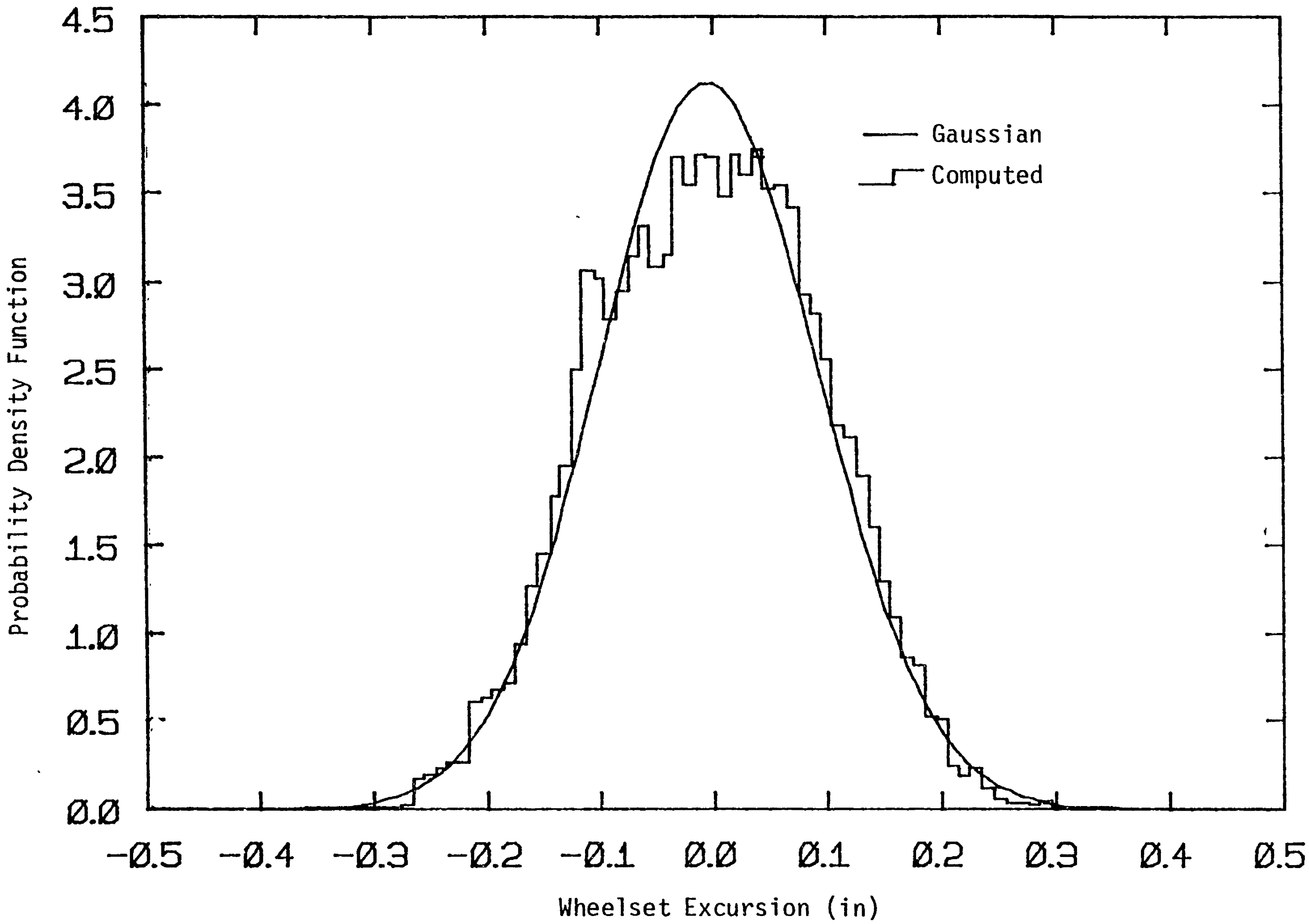

FIGURE 3.6: MIDDLE WHEELSET EXCURSION PDF AT 40 MPH

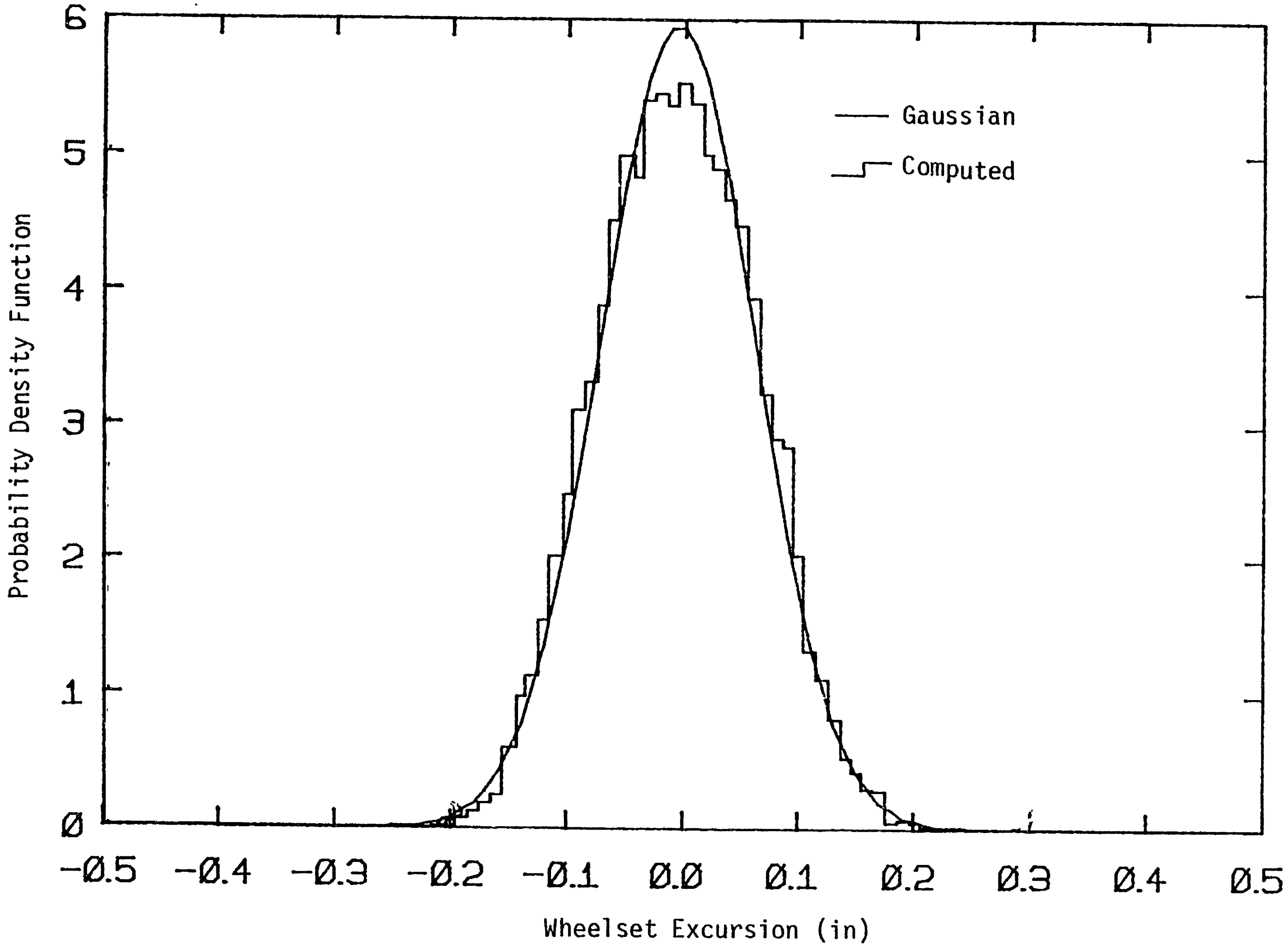

FIGURE 3.7: TRAILING WHEELSET EXCURSION PDF AT 40 MPH

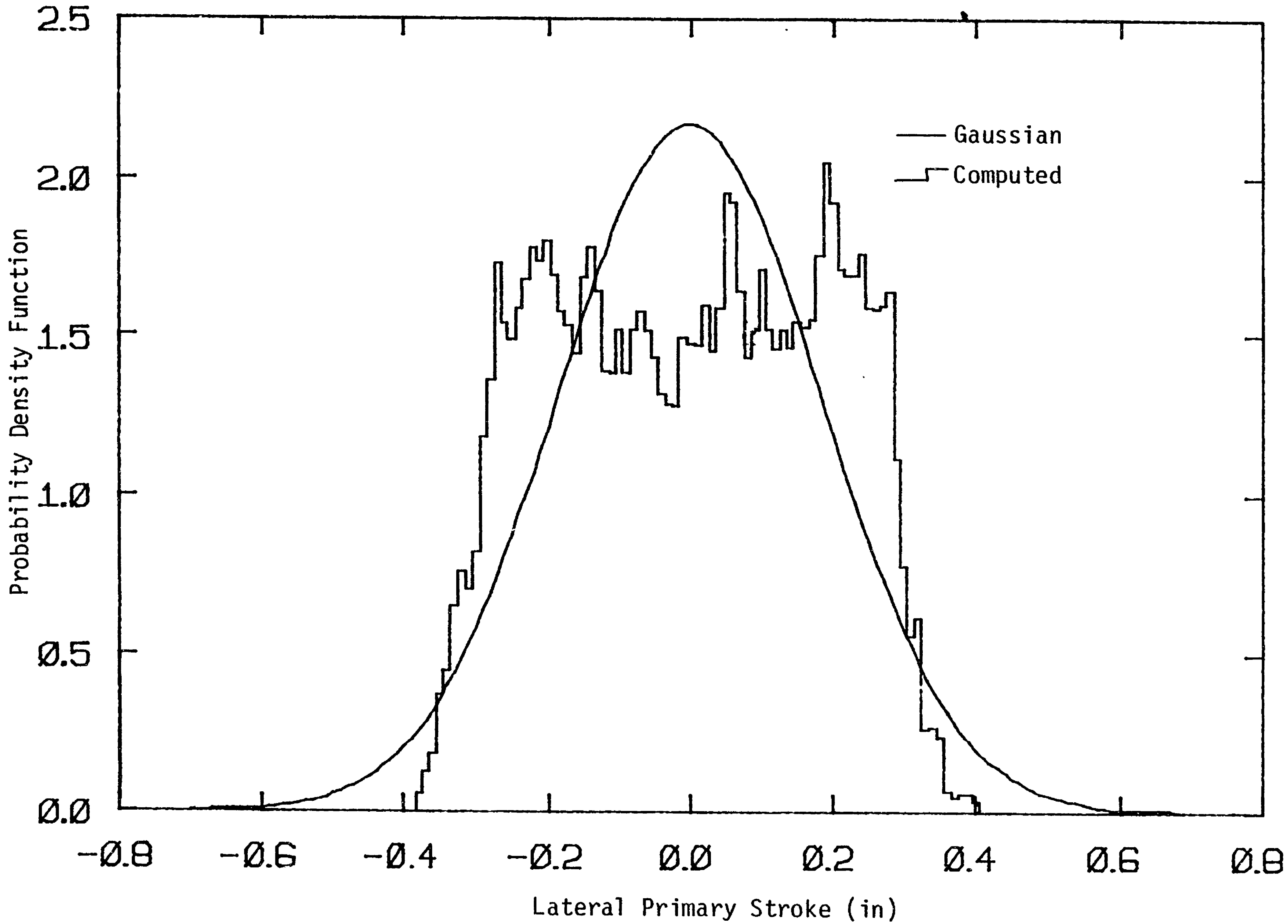

FIGURE 3.8: LEADING LATERAL PRIMARY STROKE PDF's AT 40 MPH

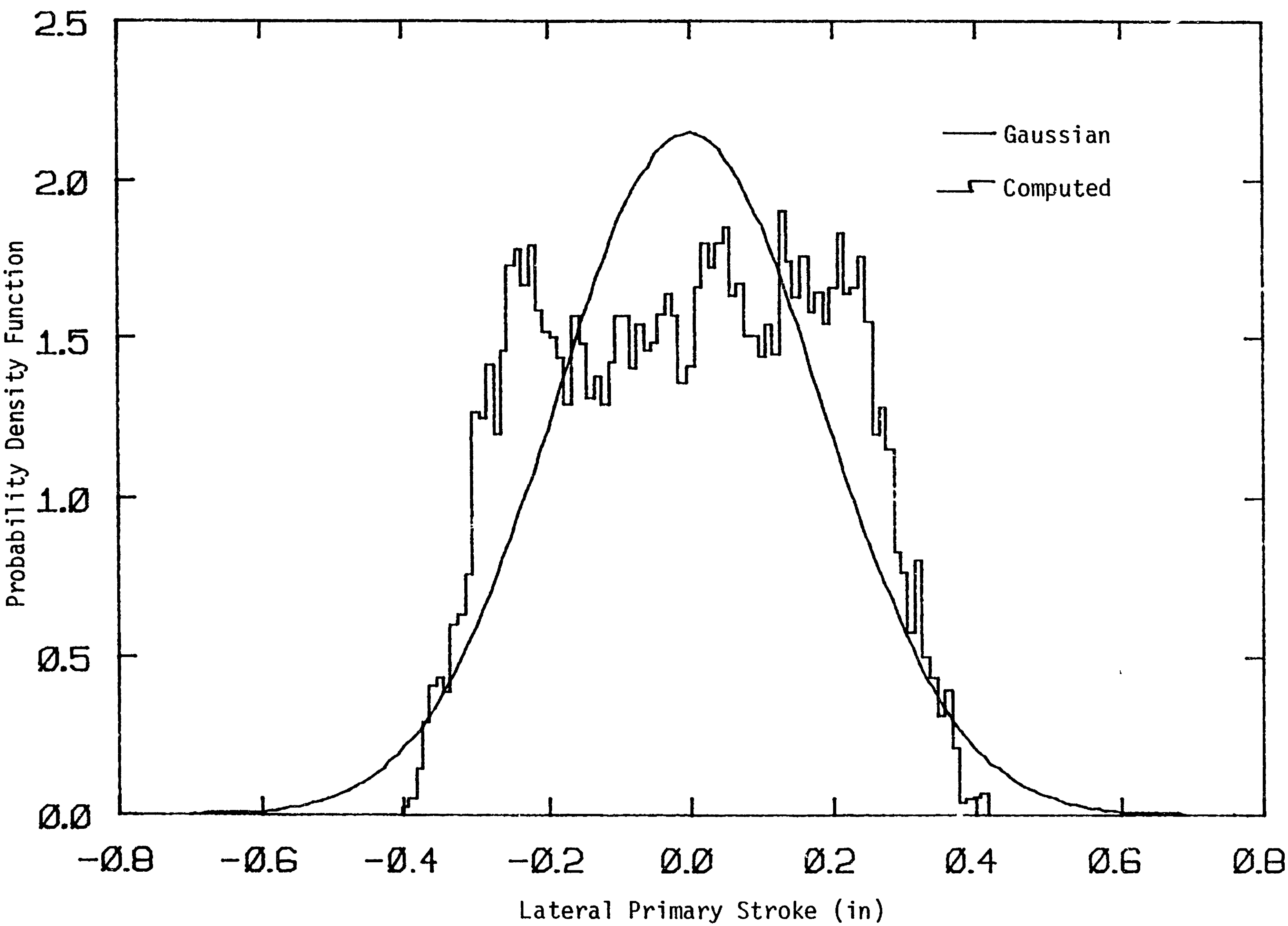

FIGURE 3.9: MIDDLE LATERAL PRIMARY STROKE PDF's AT 40 MPH

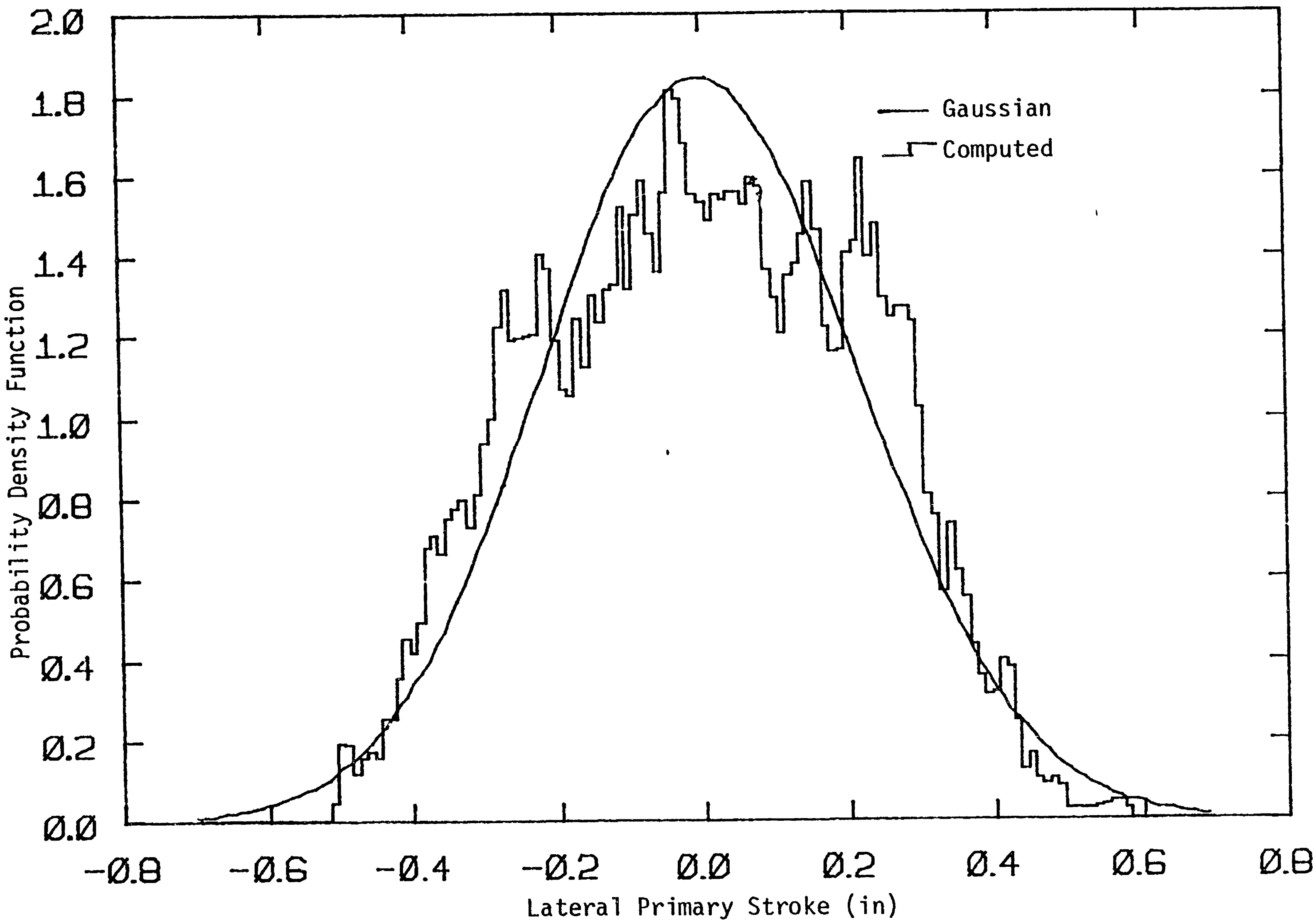

FIGURE 3.10: TRAILING LATERAL PRIMARY STROKE PDF's AT 40 MPH

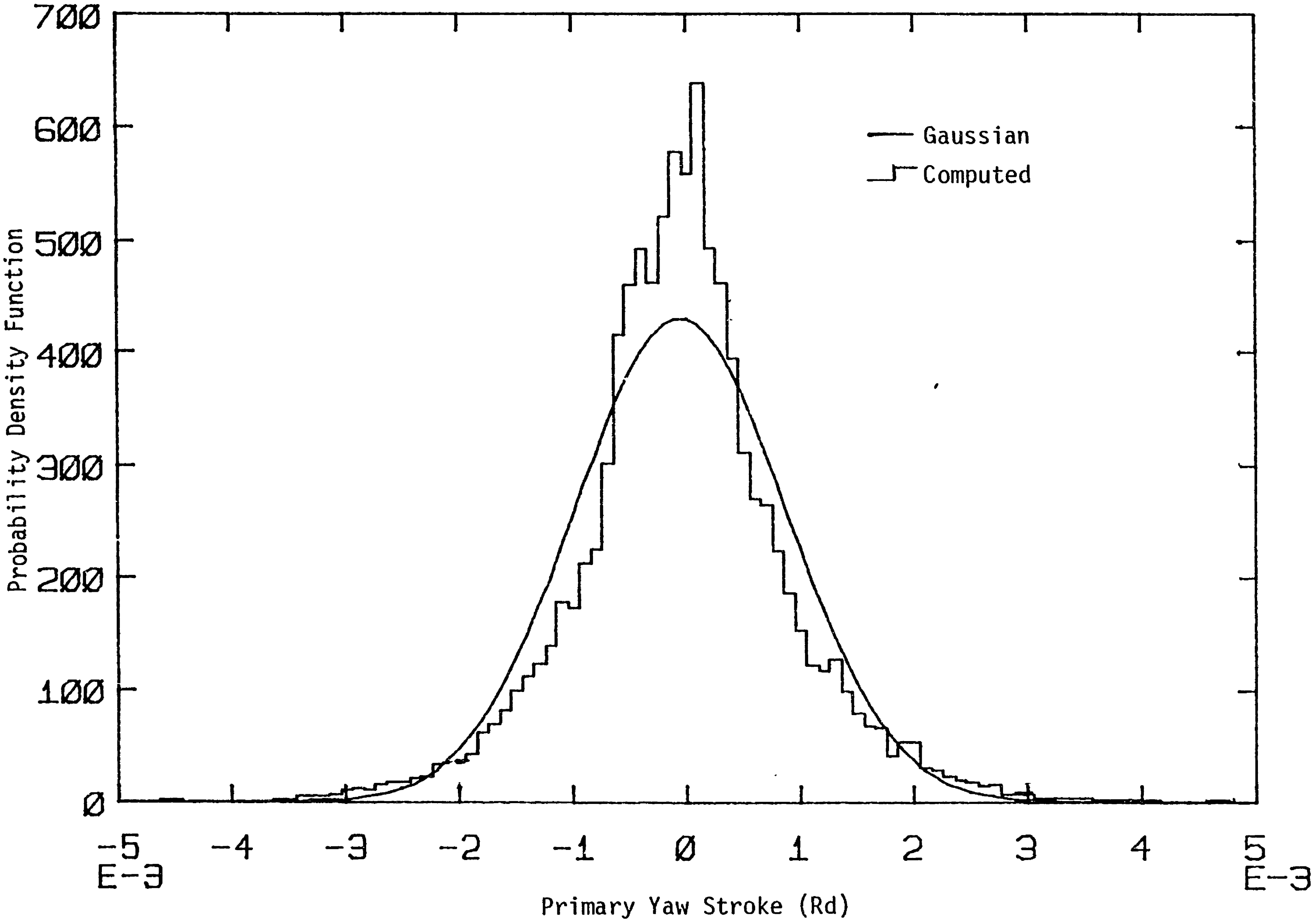

FIGURE 3.11: LEADING PRIMARY YAW STROKE PDF's AT 40 MPH

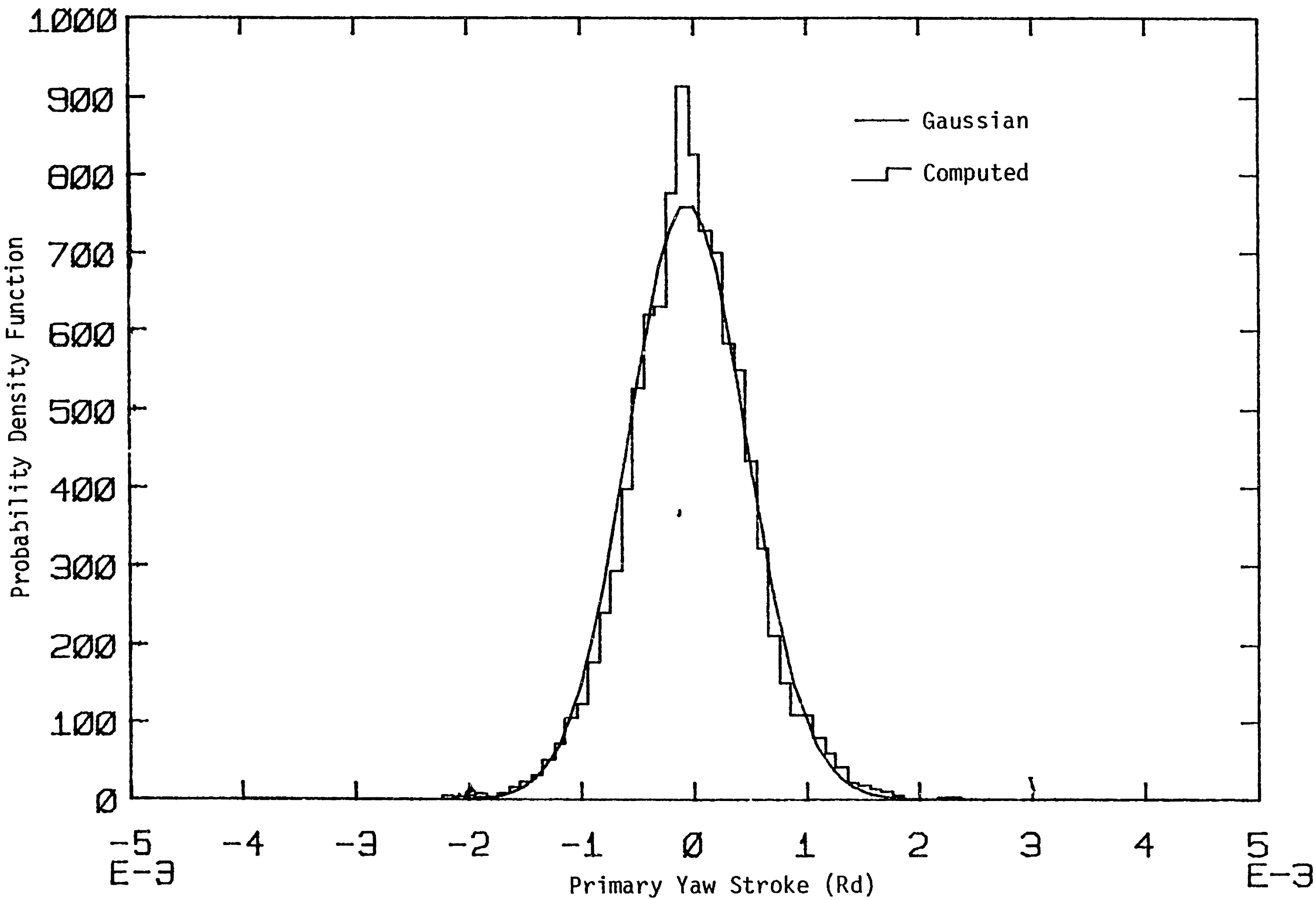

FIGURE 3.12: MIDDLE PRIMARY YAW STROKE PDF's AT 40 MPH

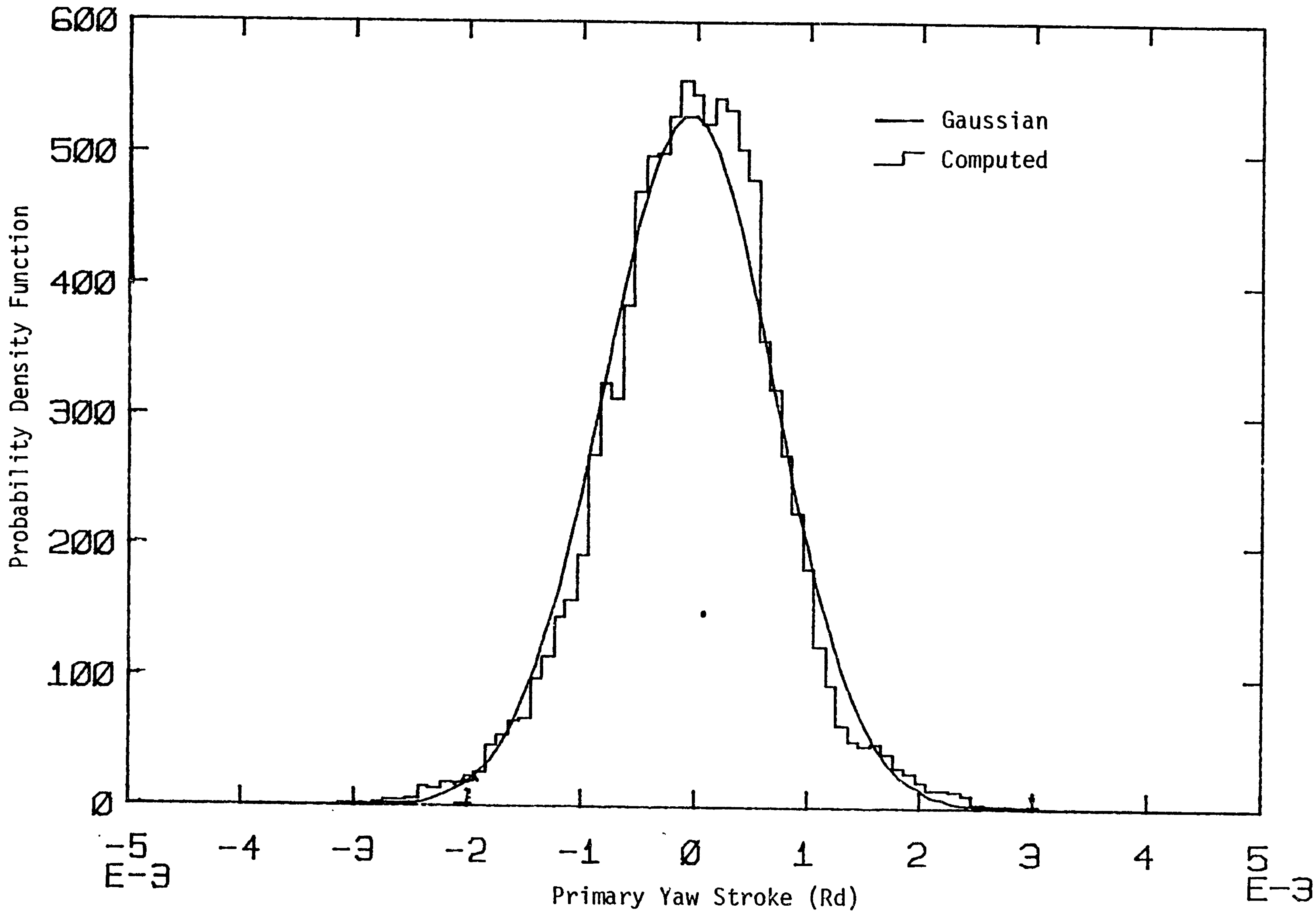

FIGURE 3.13: TRAILING PRIMARY YAW STROKE PDF's AT 40 MPH

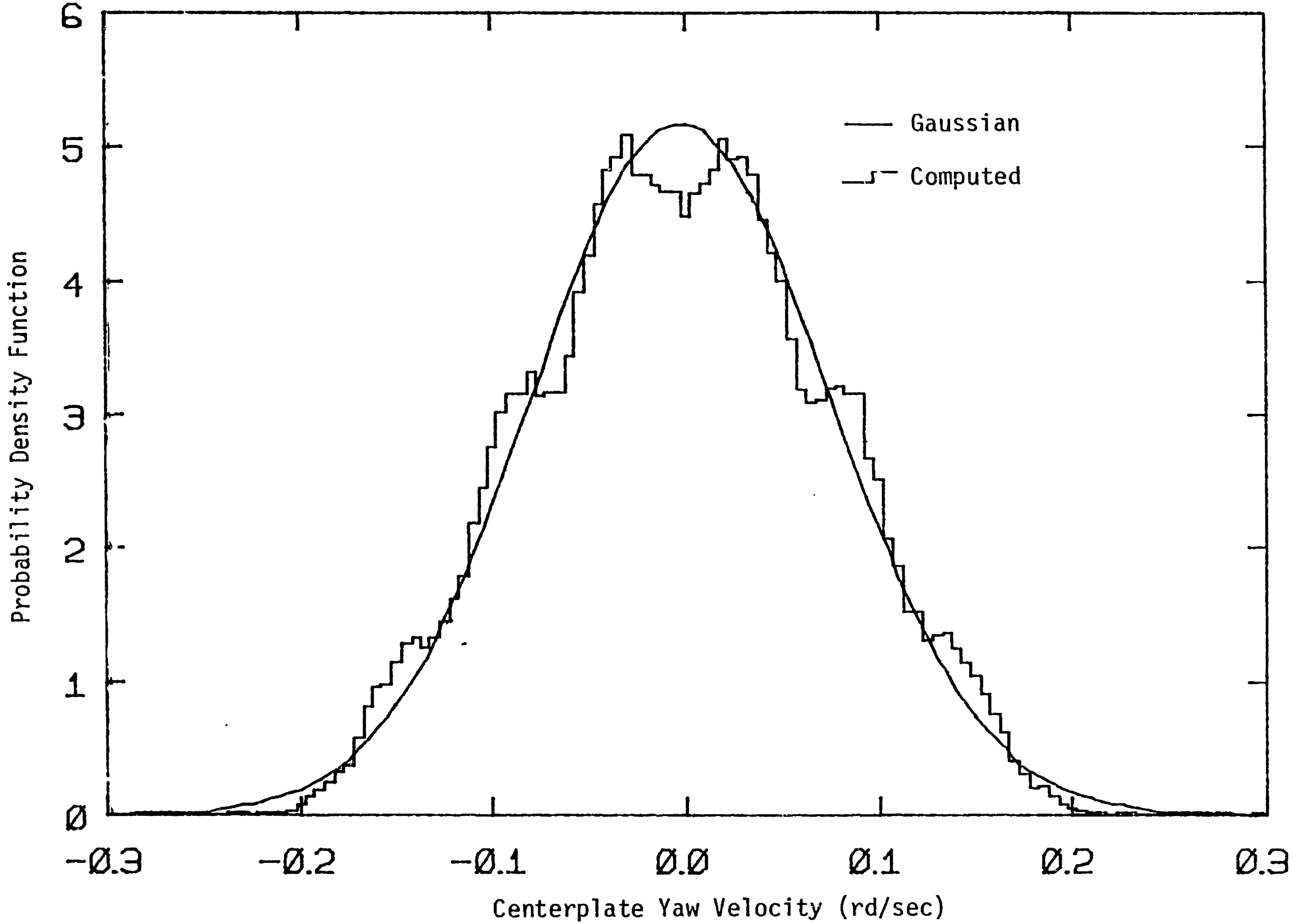

FIGURE 3.14: CENTERPLATE YAW VELOCITY PDF's AT 40 MPH

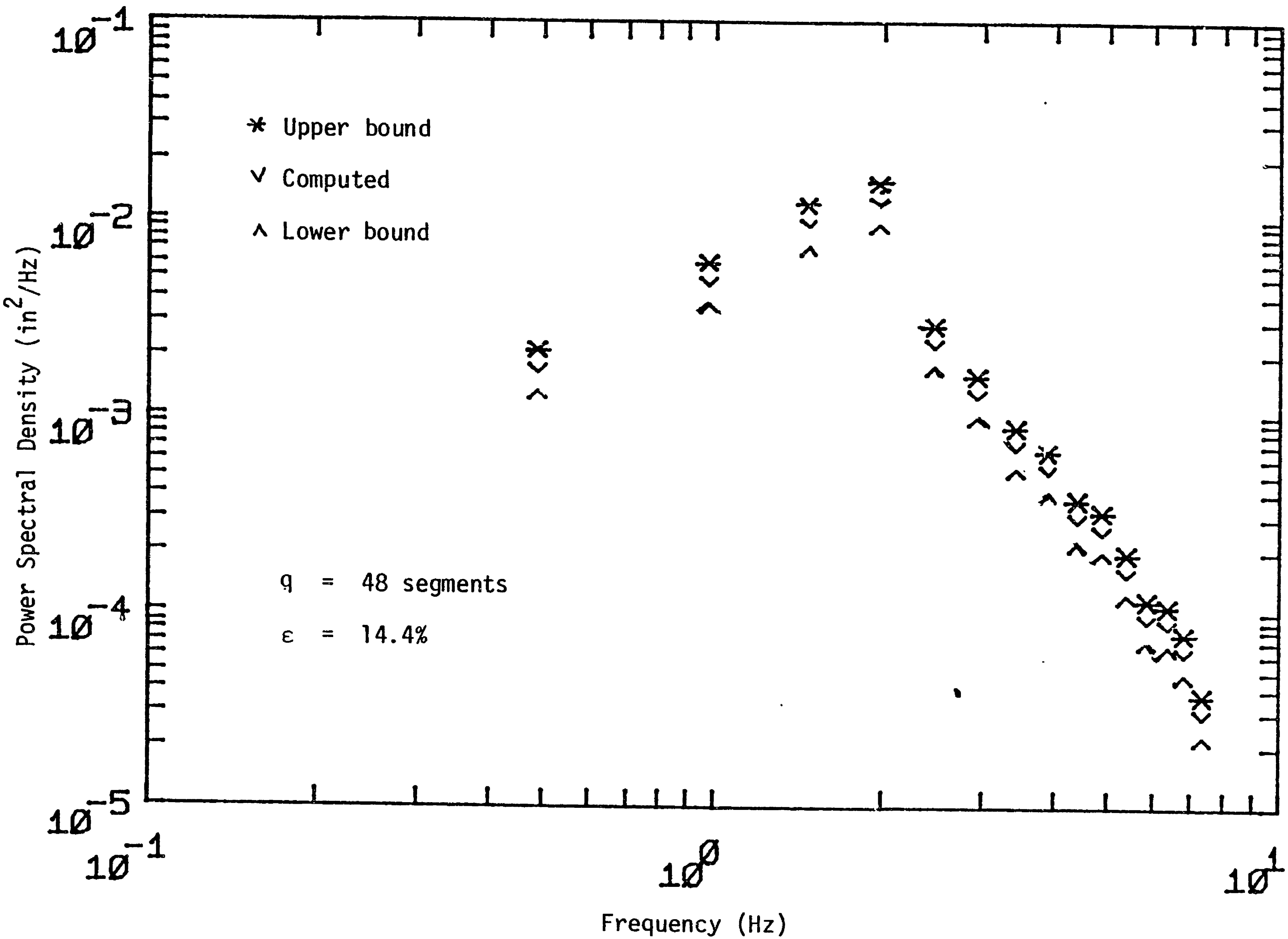

FIGURE 3.15: LEADING WHEELSET EXCURSION PSD

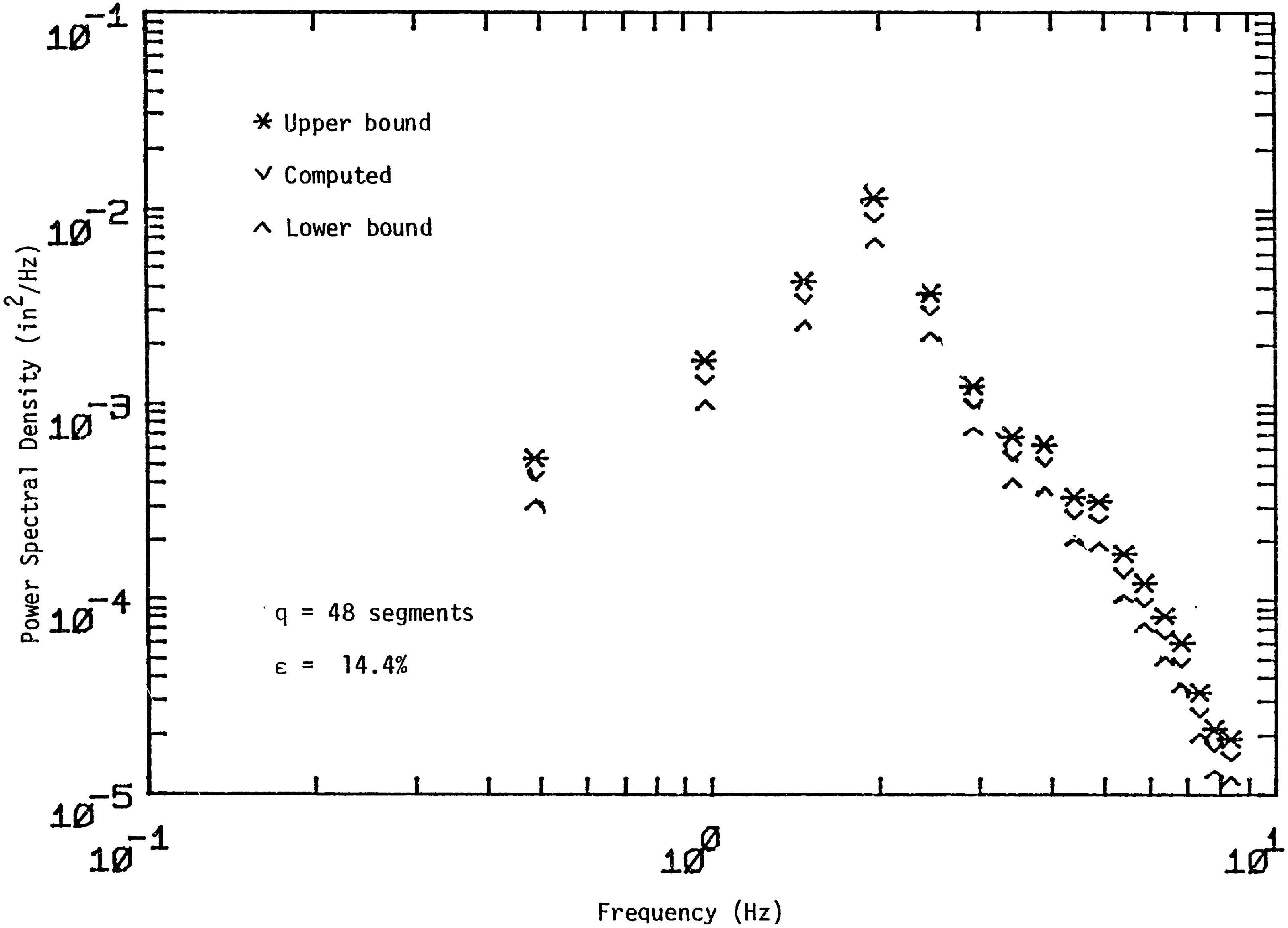

FIGURE 3.16: MIDDLE WHEELSET EXCURSION PSD

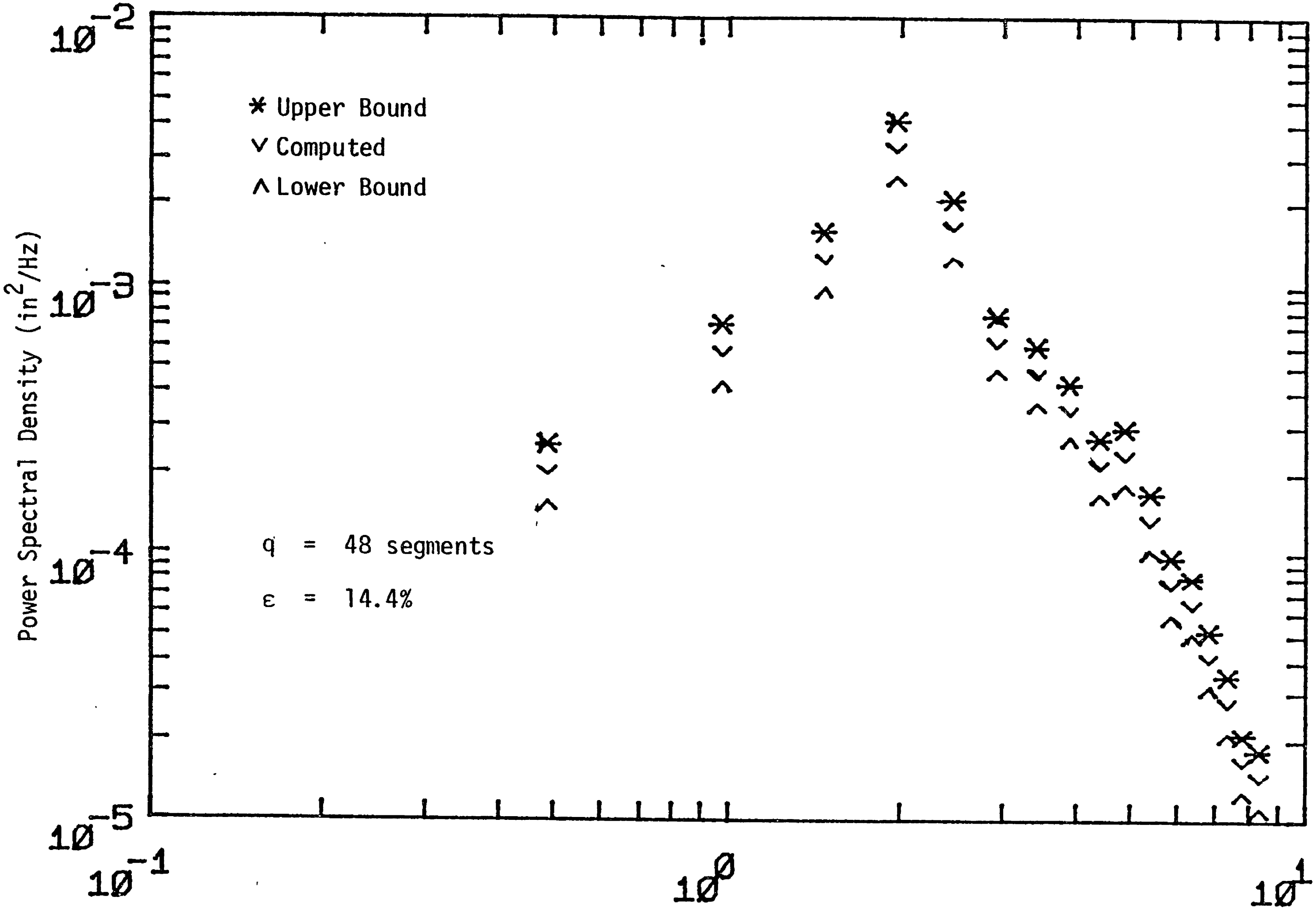

FIGURE 3.17: TRAILING WHEELSET EXCURSION PSD

The upper and lower bounds on spectral points are shown in Figures 3.15 to 3.17 together with the computed spectral point value.

3.3.2 High Speed Simulation (60 mph)

The duration of the high speed simulation was 84 seconds which corresponded to a 1.4 mile track. Variable integration time steps of 0.005 in thread region and 0.001 seconds in flange region were used. The peak values of the wheelset excursions were:

- o 0.3874 inches for the leading wheelset
- o 0.3794 inches for the middle wheelset
- o 0.3464 inches for the trailing wheelset

These show that the leading and middle wheelsets were flanging.

The estimate of the mean and the r.m.s. values at 60 mph are shown below.

TABLE 3.2: MEAN AND RMS VALUES AT 60 MPH

	WHEELSET EXCURSION			LATERAL PRIMARY STROKE LENGTH		
	#1	#2	#3	#1	#2	#3
Mean (in)	0.62E-3	0.13E-2	0.36E-3	0.31E-2	0.39E-2	0.25E-2
R.M.S. (in)	0.17014	0.15958	0.13771	0.28565	0.24280	0.35139

The 90% confidence intervals for the means and variances are given by:

Mean:

$$(\bar{x} - 5.67E\text{-}3\bar{\sigma}_x) \leq \mu_x < (\bar{x} + 5.67E\text{-}3\bar{\sigma}_x)$$

Variance:

$$0.992\ \bar{\sigma}_x^2 \leq \sigma_x^2 < 1.008\ \bar{\sigma}_x^2$$

Figures 3.18 to 3.27 show the PDF's of the inputs to the nonlinearities. Similarly, the computed PDF's are shown in histogram form and the Gaussian PDS's with the computed means and variances are shown as solid lines.

Figures 3.28 to 3.30 show the PSD's of the wheelset excursions. These were computed using 41 segments with a normalized random error of 15.6%. The 90% confidence interval for spectral points is given by:

$$0.788\ \bar{S}(f) \leq S(f) < 1.32\ \bar{S}(f).$$

These upper and lower limits are shown in Figures 3.28 to 3.30 together with the computed point value.

3.4 Conclusions

The purpose of the digital simulations has been to provide a basis for evaluations of the method of statistical linearization as a design tool for rail vehicles.

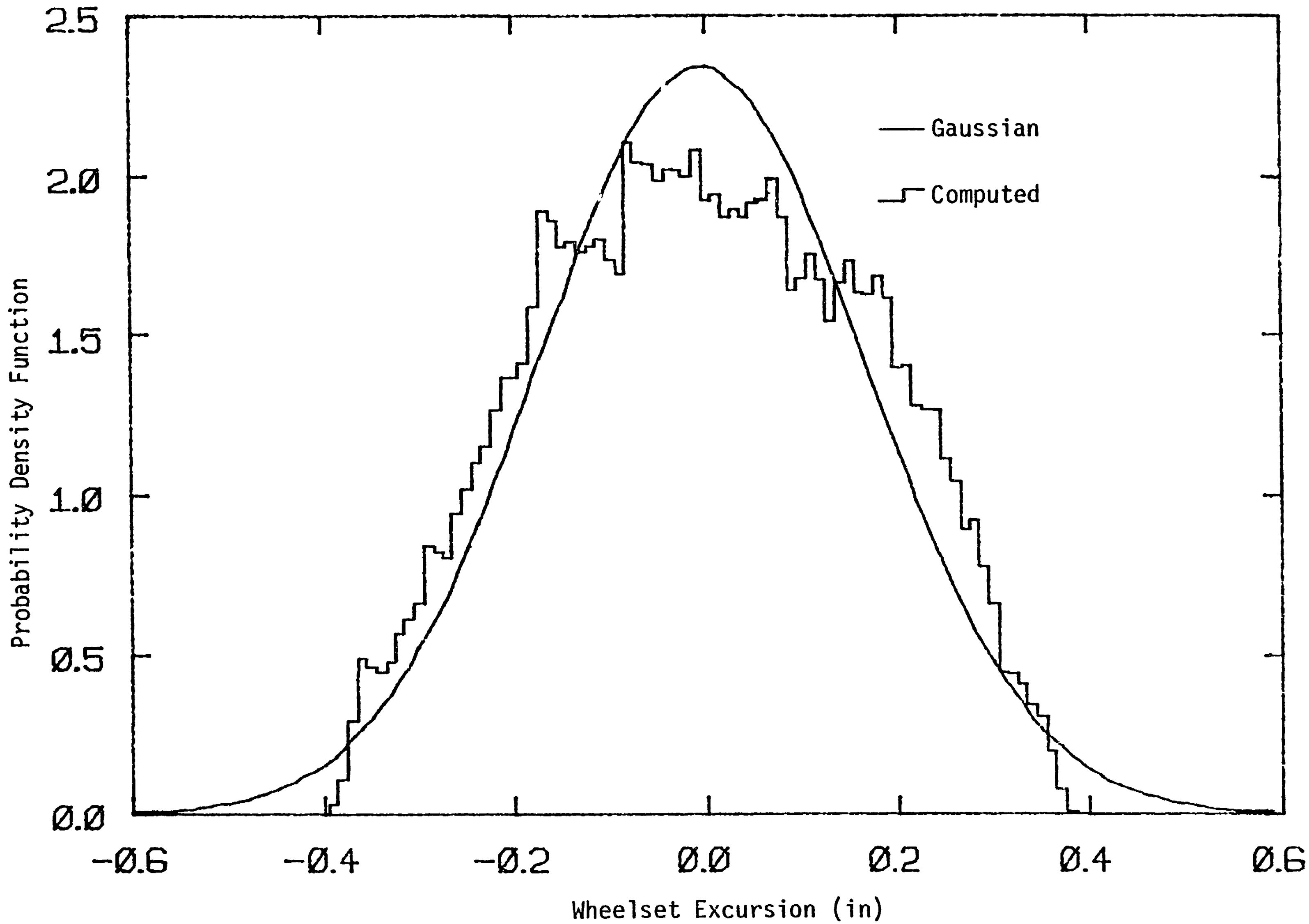

FIGURE 3.18: LEADING WHEELSET EXCURSION PDF AT 60 MPH

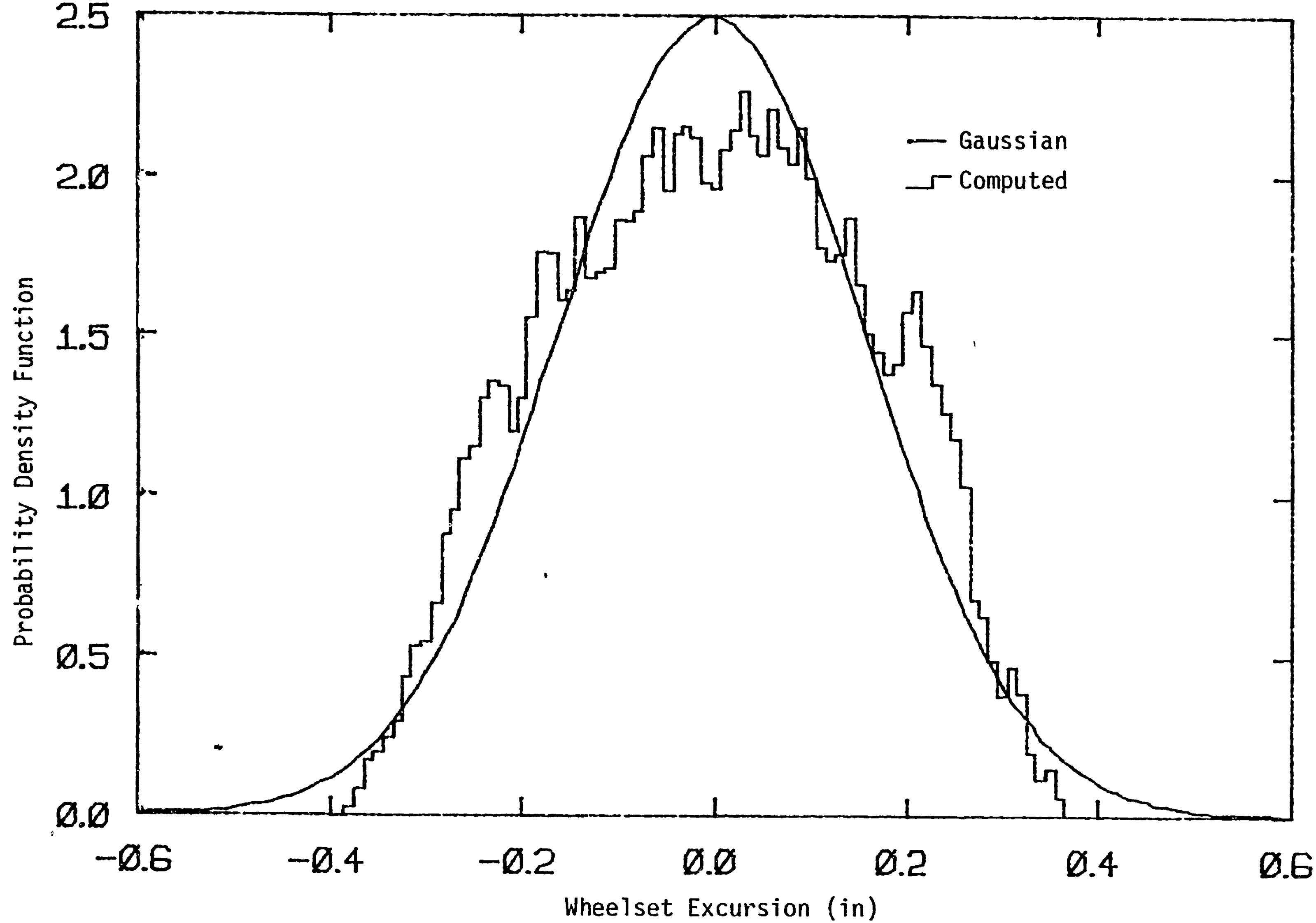

FIGURE 3.19: MIDDLE WHEELSET EXCURSION PDF AT 60 MPH

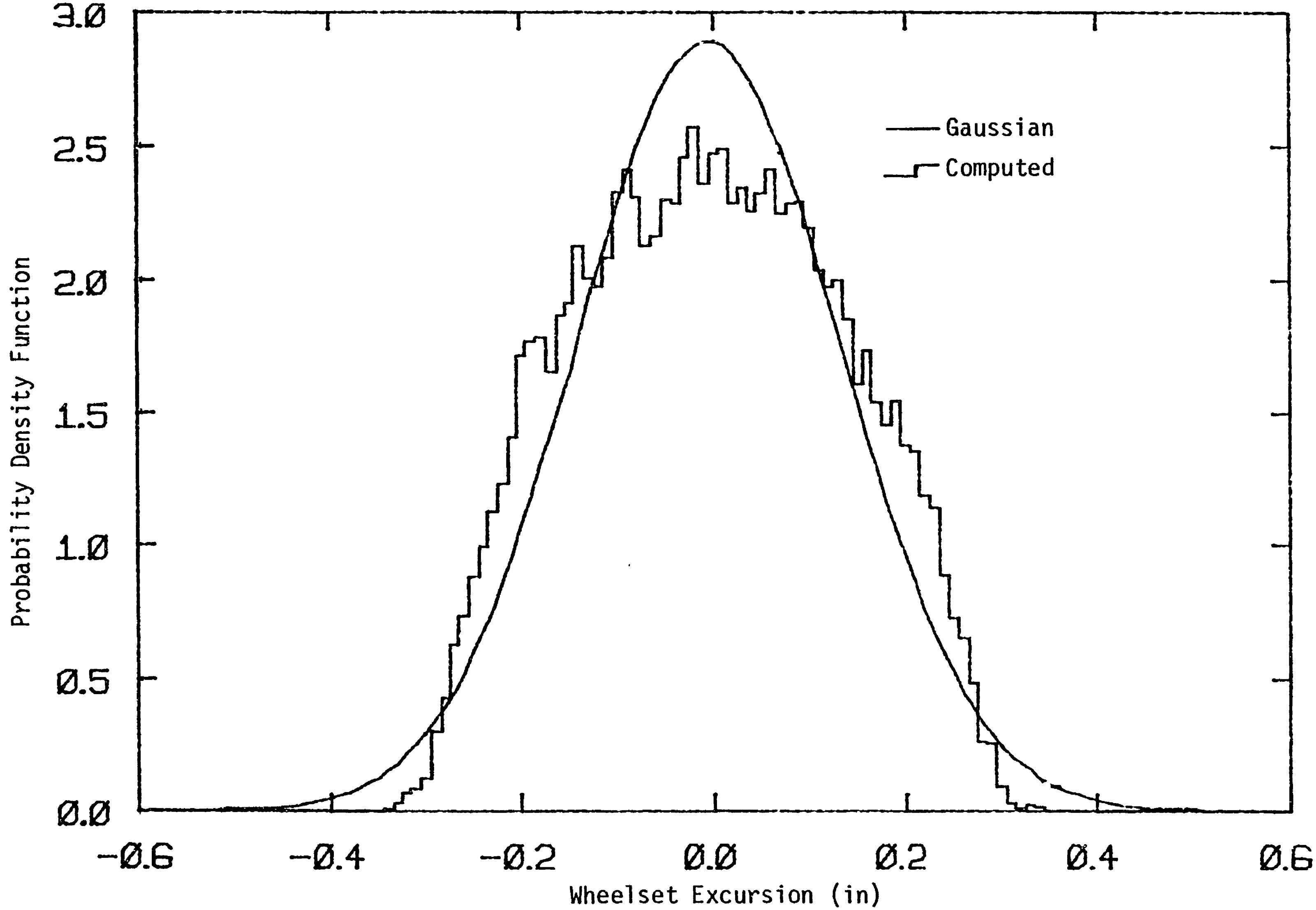

FIGURE 3.20: TRAILING WHEELSET EXCURSION PDF AT 60 MPH

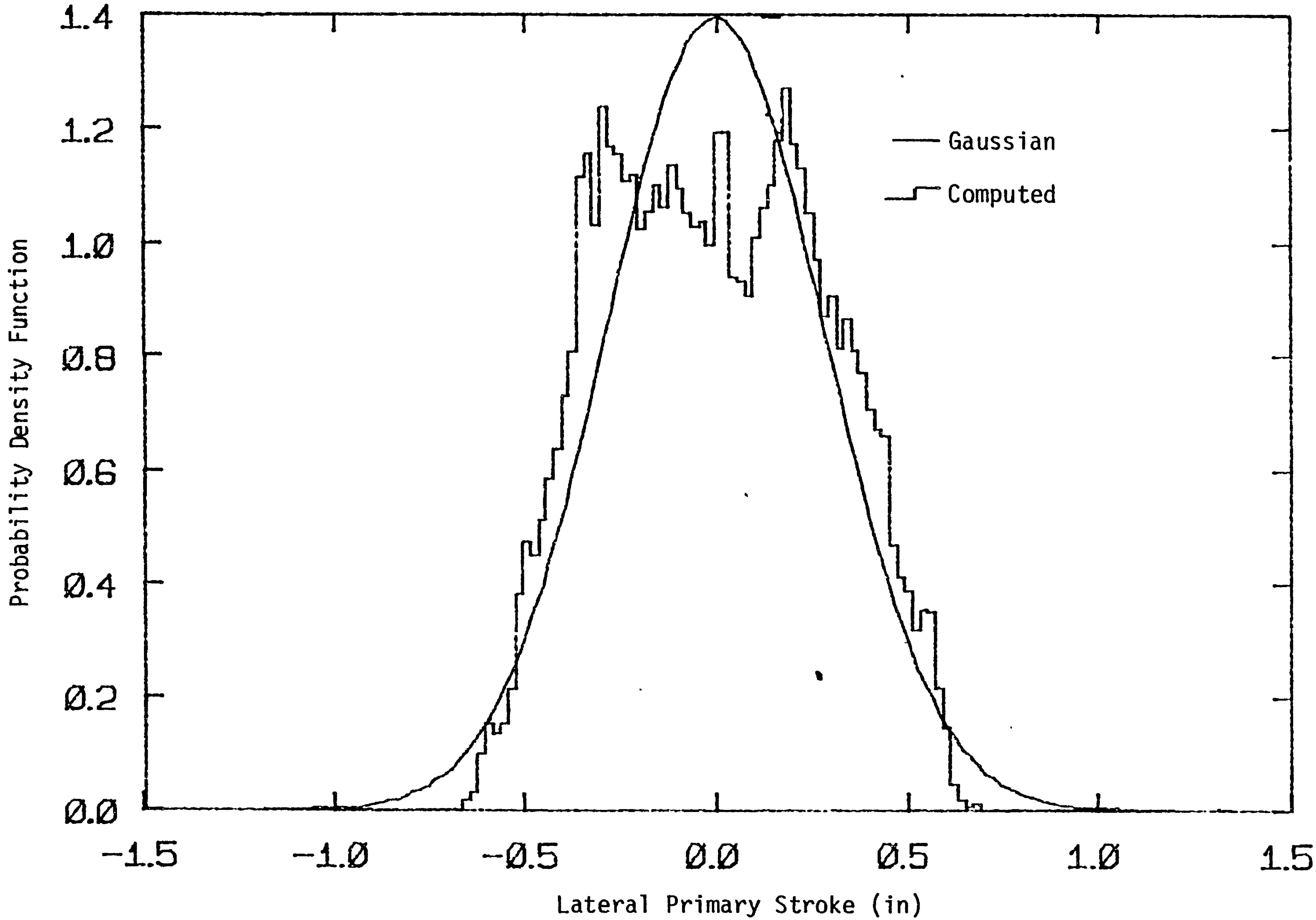

FIGURE 3.21: LEADING LATERAL PRIMARY STROKE PDF AT 60 MPH

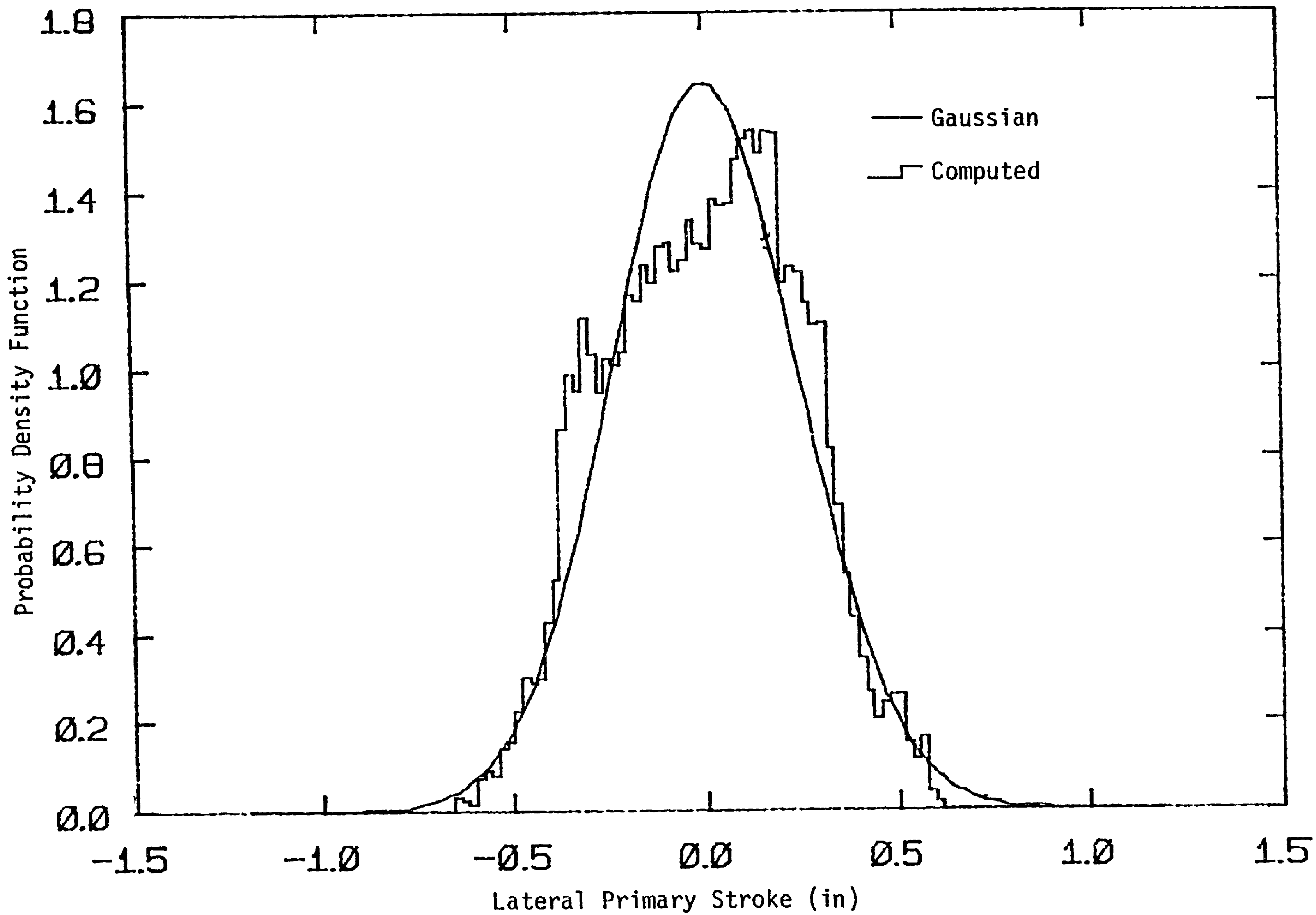

FIGURE 3.22: MIDDLE LATERAL PRIMARY STROKE PDF AT 60 MPH

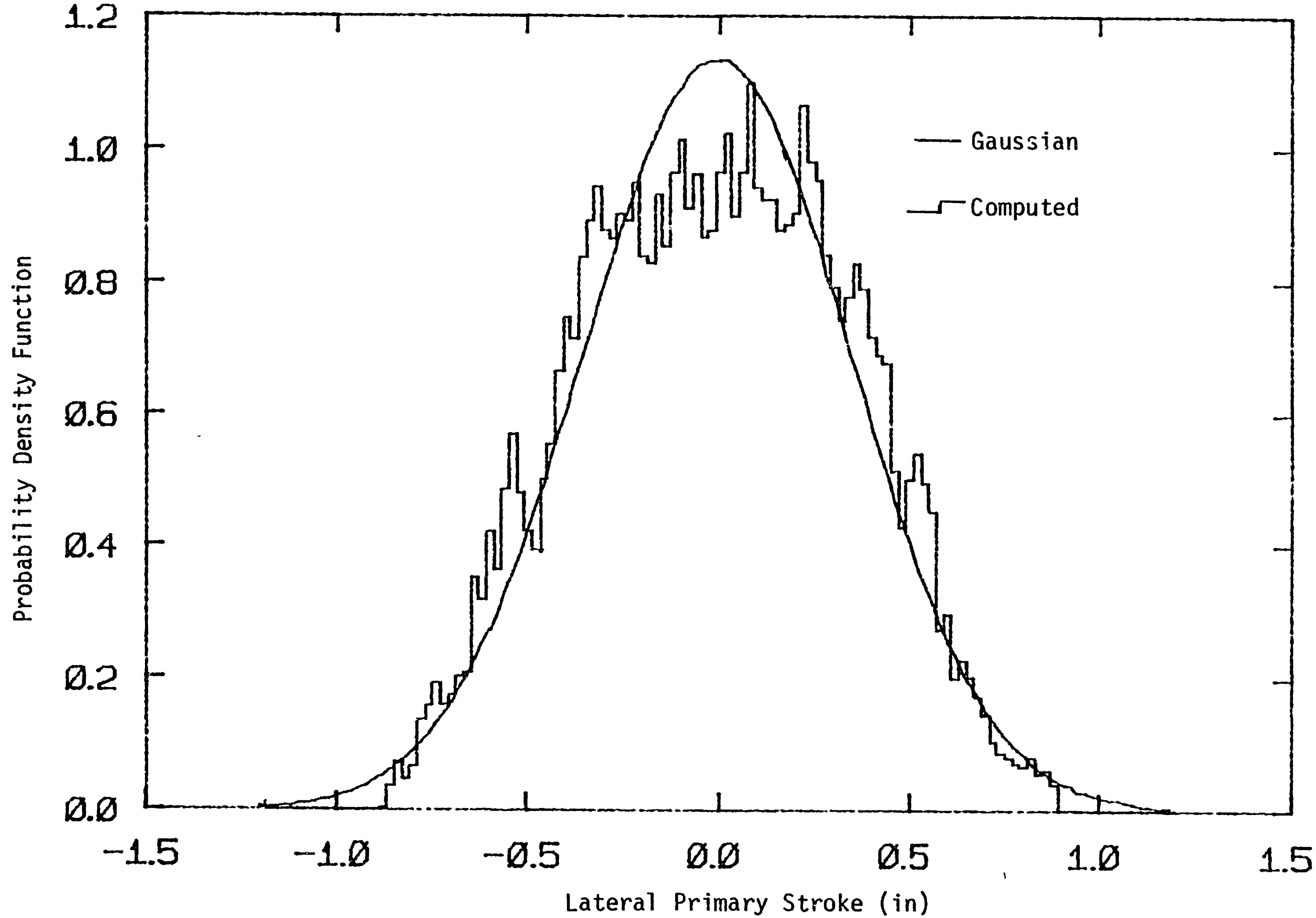

FIGURE 3.23: TRAILING LATERAL PRIMARY STROKE PDF AT 60 MPH

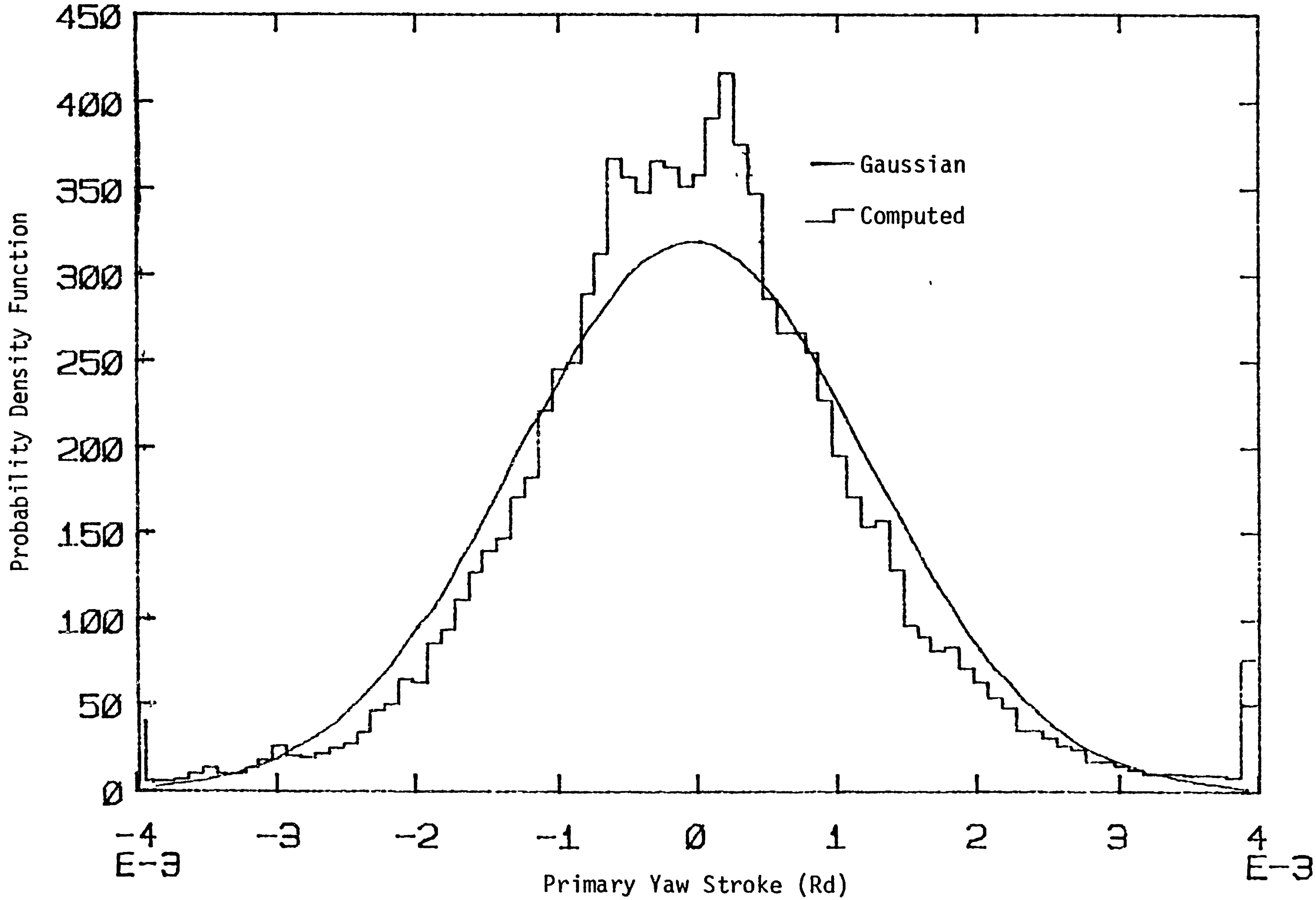

FIGURE 3.24: LEADING PRIMARY YAW STROKE PDF AT 60 MPH

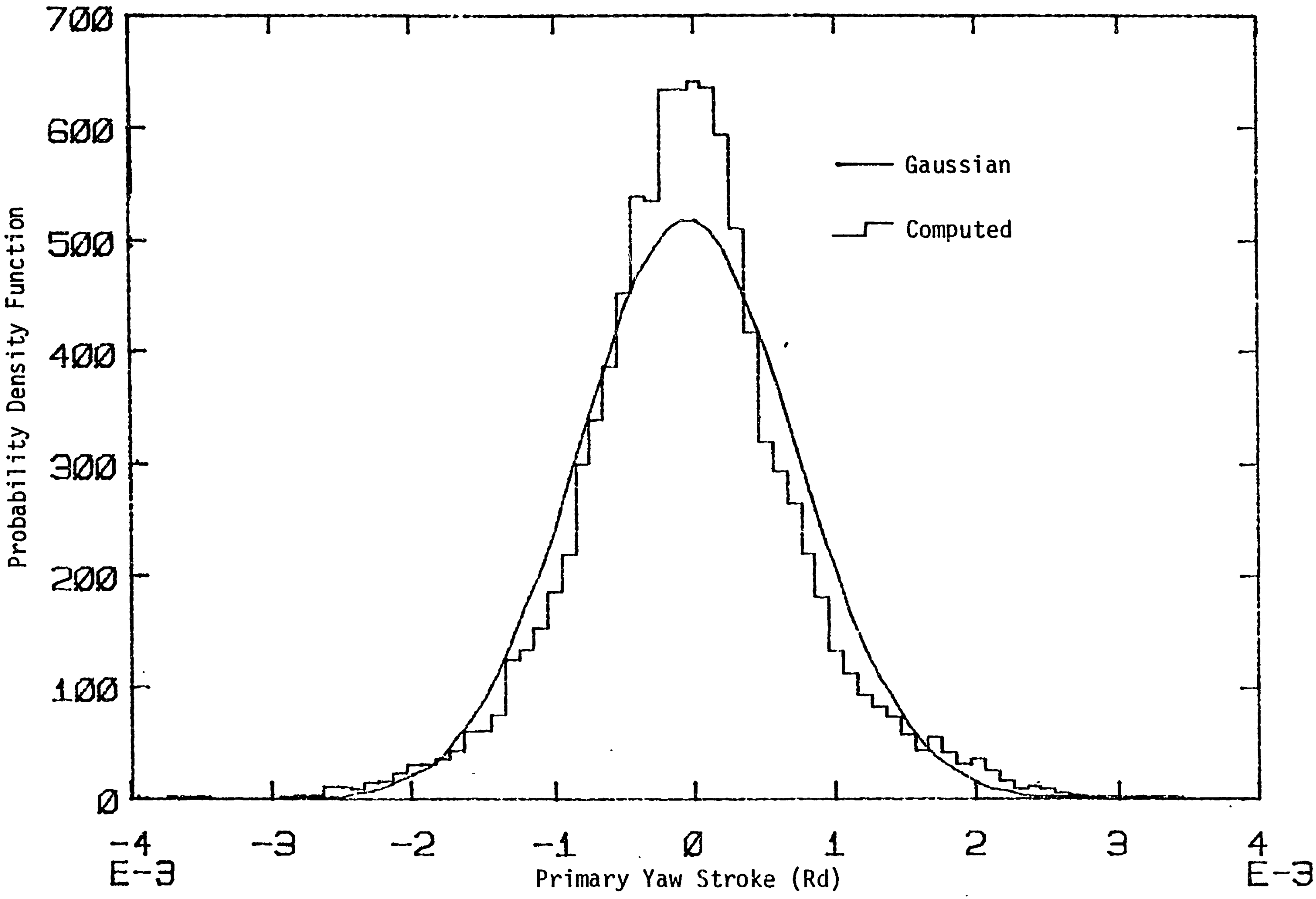

FIGURE 3.25: MIDDLE PRIMARY YAW STROKE PDF AT 60 MPH

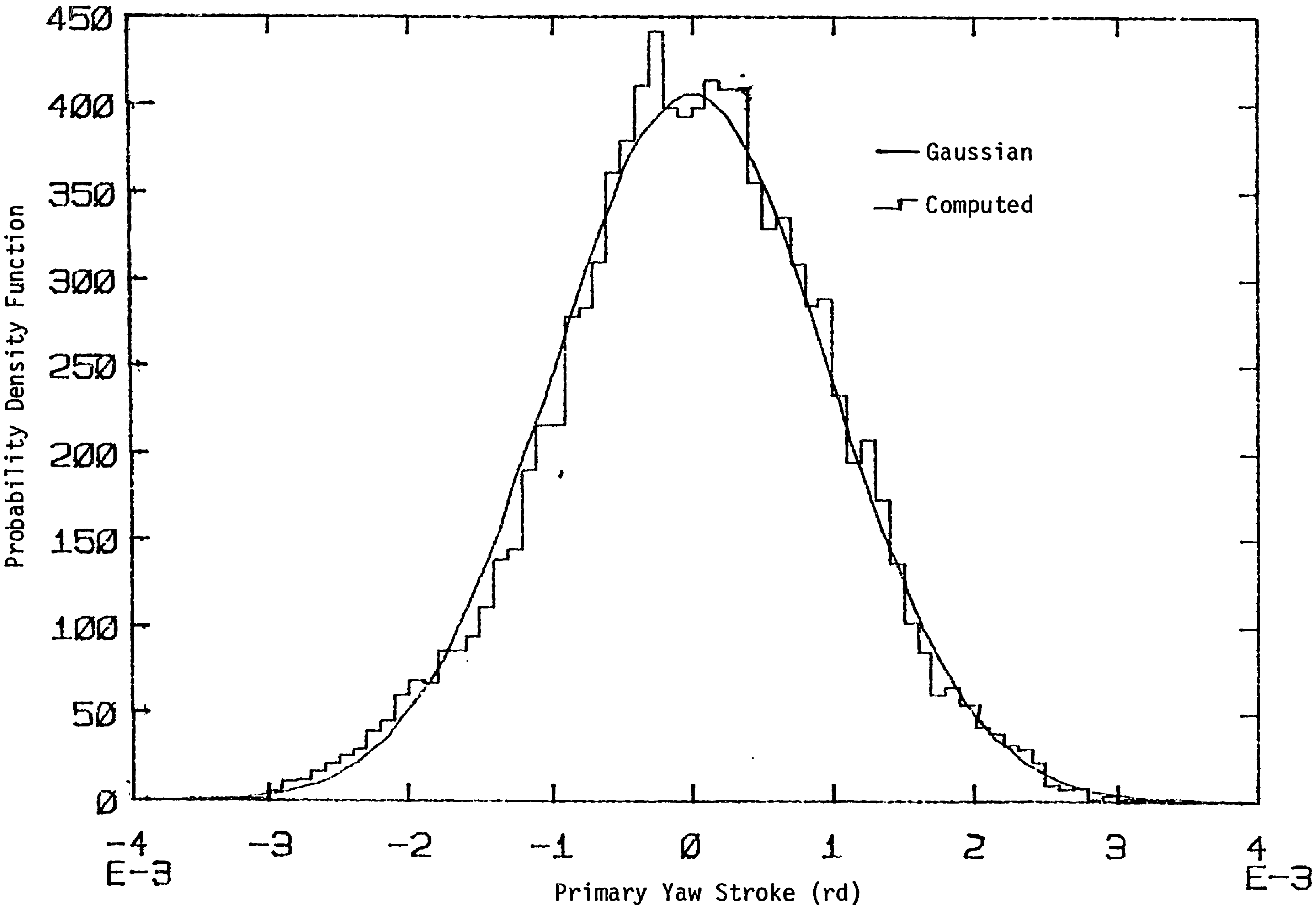

FIGURE 3.26: TRAILING PRIMARY YAW STROKE PDF AT 60 MPH

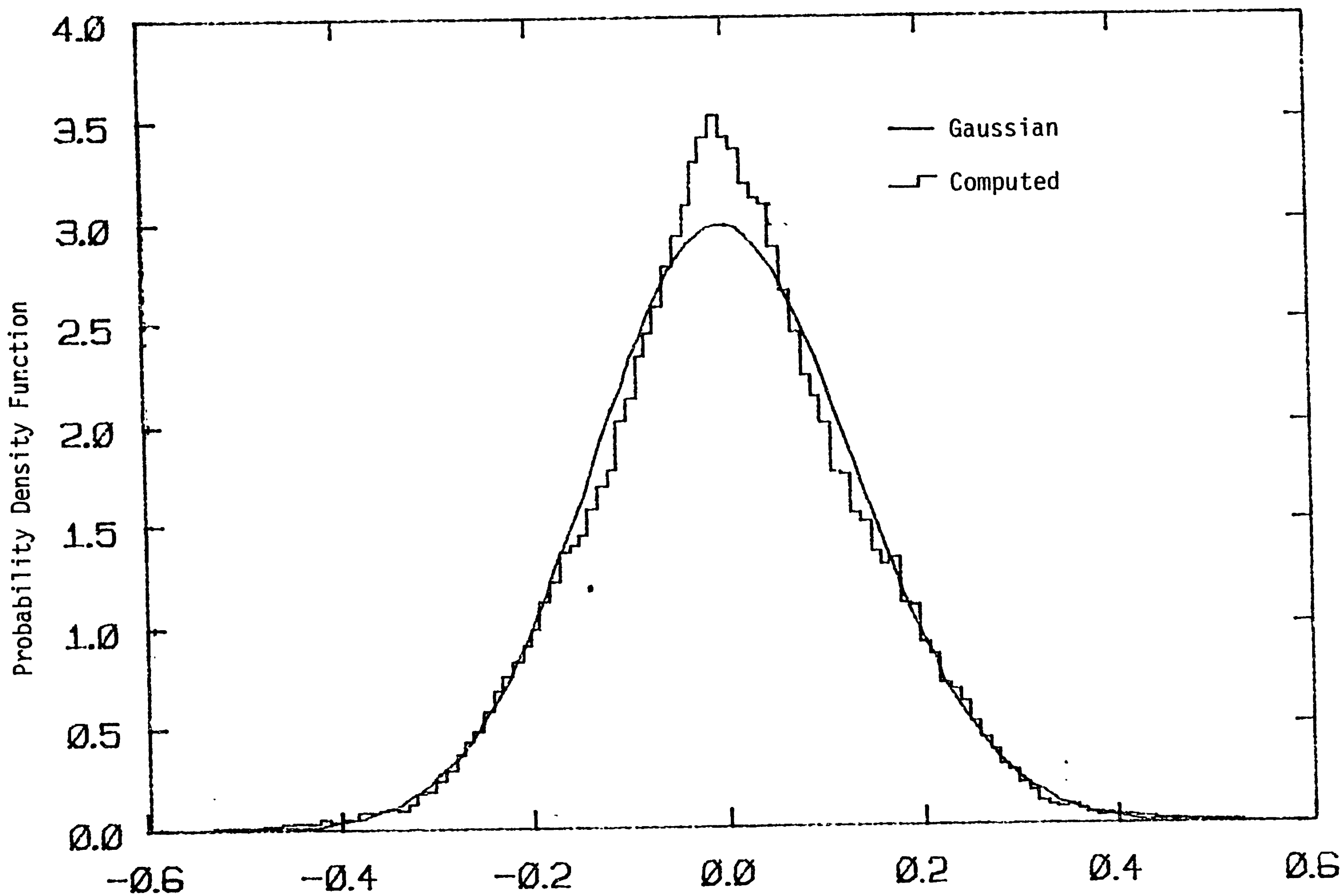

FIGURE 3.27: CENTERPLATE YAW VELOCITY PDF AT 60 MPH

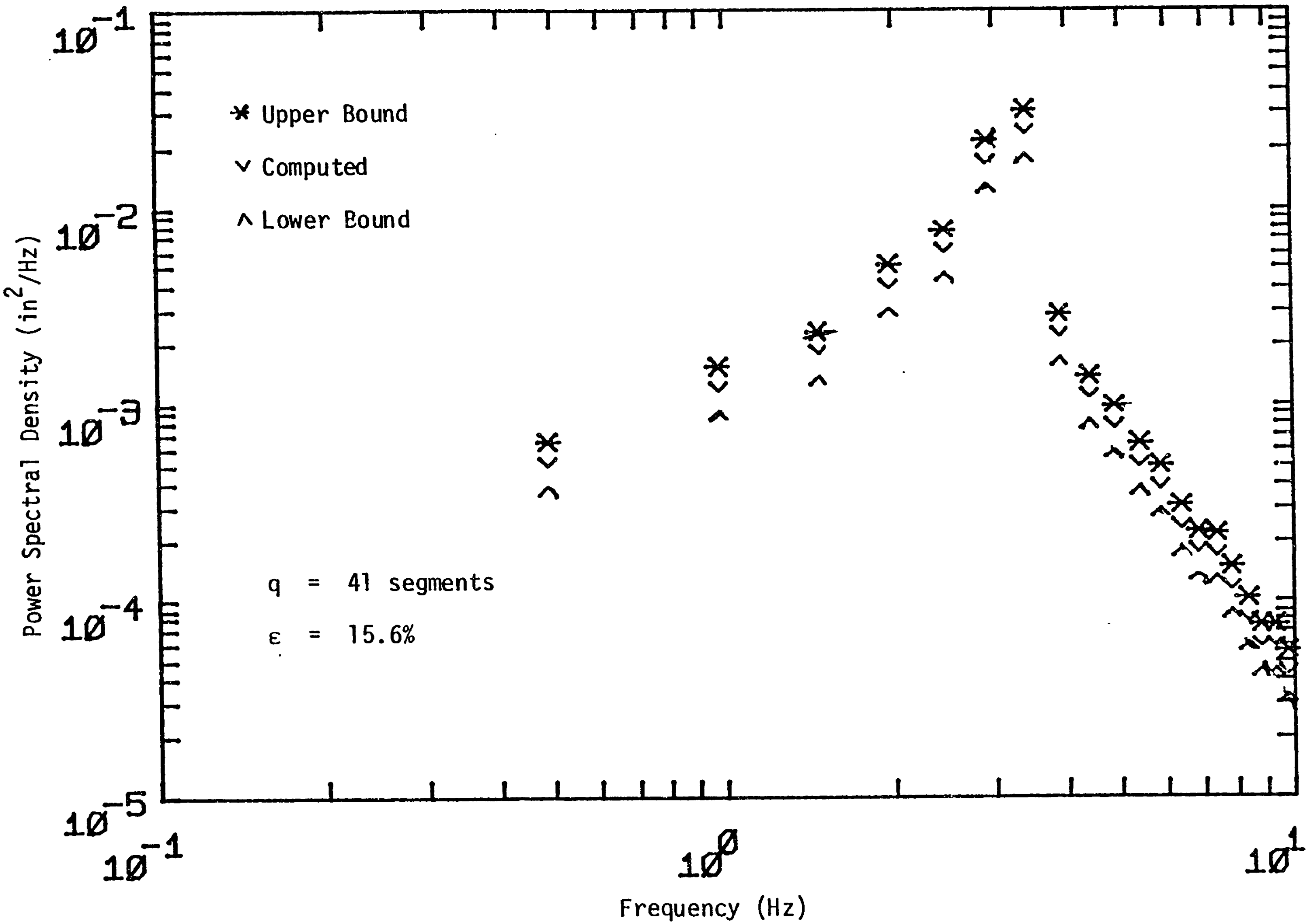

FIGURE 3.28: LEADING WHEELSET EXCURSION PSD

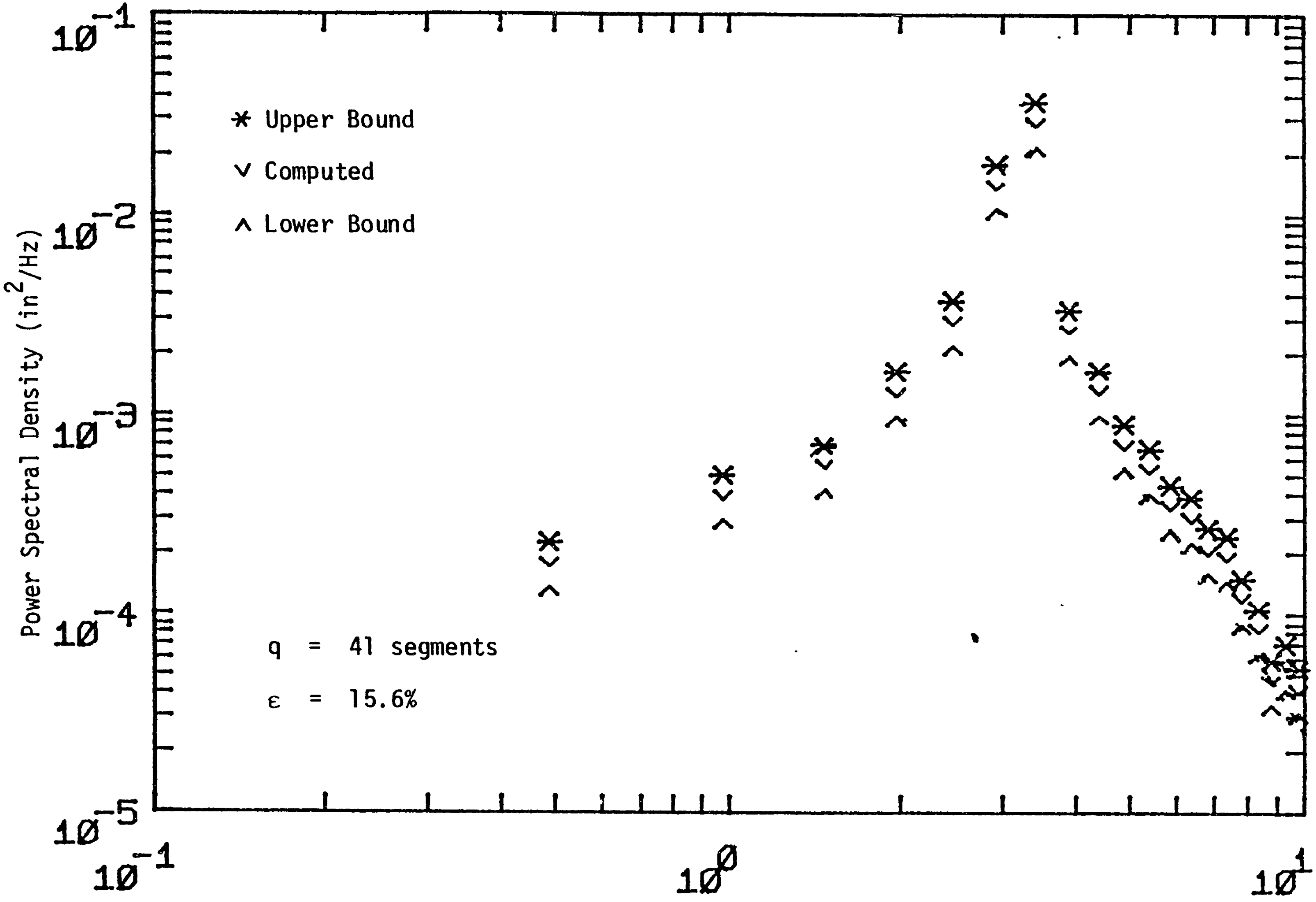

FIGURE 3.29: MIDDLE WHEELSET EXCURSION PSD

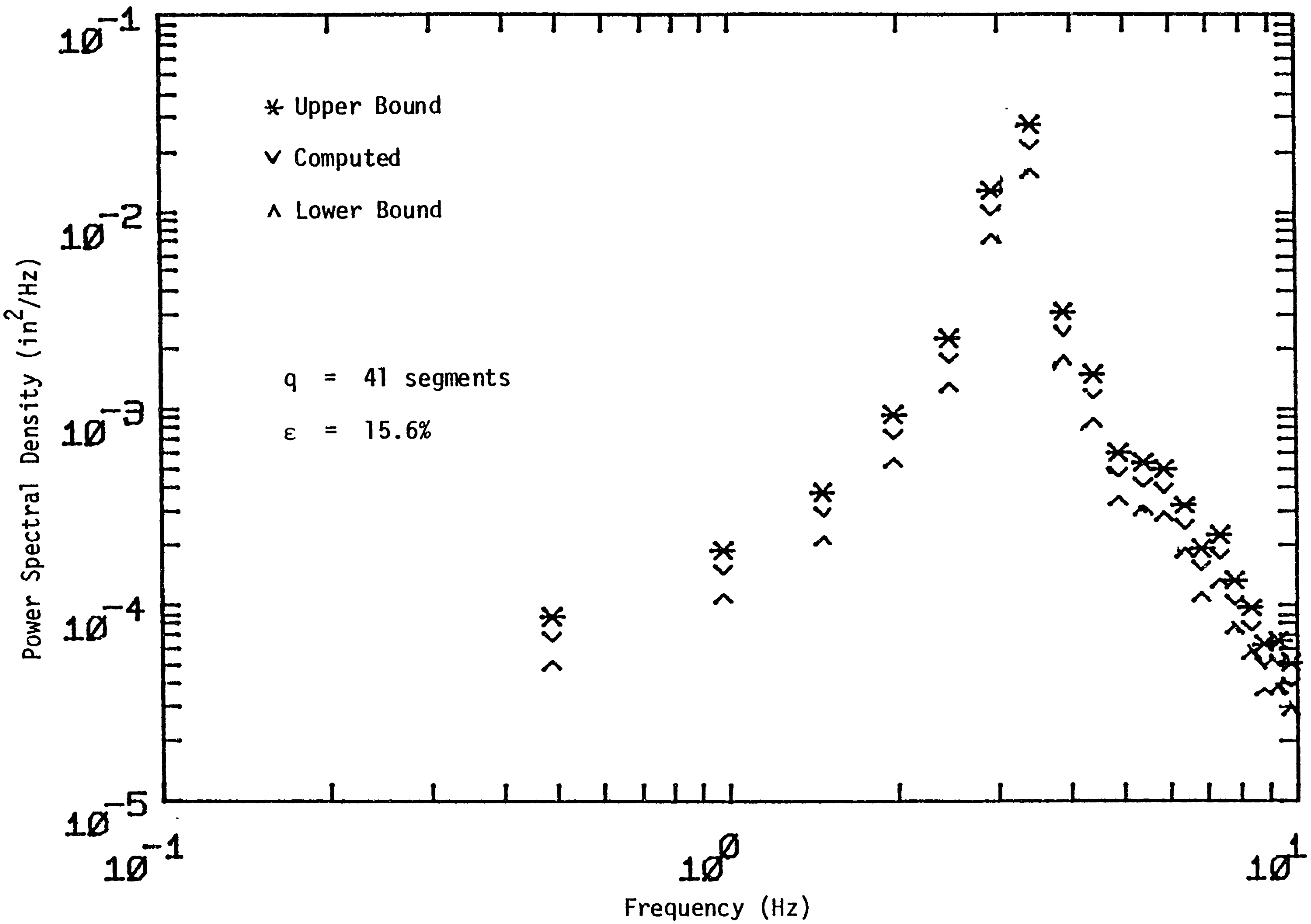

FIGURE 3.30: TRAILING WHEELSET EXCURSION PSD

The essential assumption of the statistical linearization is the knowledge of the probability density function of the inputs to the nonlinearities as explained in Chapter 4. If the exact probability density functions are known the statistical linearization gives a perfect estimate of the mean and rms values, Booton [20].

The shape of the PDF's at low speed can be summarized as:

- Wheelset Excursions (Figures 3.5 to 3.7), primary yaw strokes (Figures 3.11 to 3.13), the input to the Coulomb damper (Figure 3.14) and the lateral primary stroke of the trailing wheelset (Figure 3.10) are close to the Gaussian density functions.

- The PDF's of first and second lateral primary strokes (Figures 3.8 and 3.9) are far from the Gaussian shape.

These probability density functions can be interpreted physically as follows:

- Figures 2.3 to 2.5 show the type of nonlinearities that are effective in the system. The nonlinear effects of the wheel/rail geometry, and the primary yaw spring are small at low speed because of the small amplitude of the inputs to these nonlinearities. The deadband spring in the lateral primary can be considered as a piecewise linear (hardening) spring. At low speed, the wheelset behaves as if that spring is not there. Then, the wheelset equations given by (A.8.13) and (A.8.14) can be roughly approximated by a dominantly linear system:

$$\begin{bmatrix} \dot{y} \\ \\ \dot{\psi} \end{bmatrix} = \underline{\bar{A}} \begin{bmatrix} y \\ \\ \psi \end{bmatrix} + \Gamma\eta + \varepsilon$$ (Negligible nonlinear effects and truck coupling)

where $\underline{\eta}$ = Input which has a Gaussian density function.

From linear system theory, y and ψ should have PDF's which are close to the Gaussian shape. Since any linear operations on Gaussian random variables produce Gaussian random variables, the PDF's of the wheelset excursions and yaw strokes are close to Gaussian density functions.

- In the case of the lateral primary stroke, because of the deadband, the stroke has, roughly, the same probability of being at any point with $\mp\delta$ deadband value. Therefore, we can expect a flat (uniform) density functions corresponding to this range of values.

The shape of the PDF's at high speed can be summarized as:

- Excursions (Figures 3.15 to 3.16) and lateral primary strokes (Figures 3.17 to 3.19) are no longer Gaussian. Because the nonlinear part of the system, especially the flange contact of the wheelset, becomes more effective.

- The others are still close to the Gaussian probability density function.

CHAPTER 4

STATISTICAL LINEARIZATION

4.1 Historic Development [27,28]

The general problem of random excitation of physical systems was first investigated theoretically by Einstein (1905) and was generalized and extended by von Smoluchowski (1916) in the context of the theory of Brownian Motion. In 1931, Kolmogorov derived a precise mathematical formulation of the equations governing the probability densities satisfied by such processes.

The early studies were confined to the effects of additive noise on linear systems. The earliest work on the problem of random excitations of nonlinear systems was due to Andronov et al. (1933) who used the Kolmogrov-Fokker-Planck equations to study the motion of a general dynamic systems subject to random disturbances. Many others, Caughey [42], Crandall [43], Atkinson [39], Kramers [40], Sawaragi [41], etc., applied this technique to solve nonlinear dynamics and control problems.

In almost all of these investigations only first order statistical properties were obtained. There are some applications where additional statistical information is required. For example, the spectral density of a random process requires the second order statistics of the process. Then, a number of approximate techniques like Perturbational method by Crandall (1961), Eigenfunction expansions by Wang (1964) and Atkinson (1970) have been developed to obtain second order statistics for the response of nonlinear systems to random excitations. In many respects [28] the simplest and most useful development was statistical linearization. This method is simply a statistical extension of the well known equivalent linearization technique of Krylov and Bogoliubov (1937) for deterministic excitation. It was developed independently by Booton (1952), Kazakov (1954) and Caughey (1959). There are several types of statistical linearization techniques in the literature. The well known methods are due to Booton [20], Axelby [29], Pupkov [30], Somerville and Atherton [31].

Booton [20] has shown that if the exact probability density functions are used the propagation of the mean and covariance of the approximate system is identical to that of the nonlinear system. A description of the technique can be found in Gelb [32], Sunahara [33], Phaneuf [34] and Beaman [35].

The basic problem in linearization is to find an equivalent linear system which approximates the nonlinear system given by

$$\underline{\dot{x}}(t) = \underline{f}(\underline{x}(t), t) \quad . \tag{4.1}$$

One way is by approximating the nonlinearity as

$$\underline{f}(\underline{x}(t),t) \simeq \underline{a}(t) + N(t)(\underline{x}(t)-\underline{m}(t)) \tag{4.2}$$

where $\underline{m}$ is the expected value of $\underline{x}$. By defining the error vector $\underline{e}$ as

$$\underline{e} = \underline{f}(\underline{x}(t),t) - \underline{a}(t) - N(t)(\underline{x}(t)-\underline{m}(t)) \tag{4.3}$$

and, following Booton, choose $\underline{a}$ and N such that $E[\underline{e}^T\underline{e}]$ is minimized. The solution is [35]

$$\underline{a} = E[\underline{f}] \qquad (4.4)$$

$$N = E[\underline{f}(\underline{x}-\underline{m})^T]P^{-1} \qquad (4.5)$$

where P is the covariance matrix given by

$$P = E[(\underline{x}-\underline{m})(\underline{x}-\underline{m})^T] \qquad (4.6)$$

Equation [4.1] is then approximated as

$$\dot{\underline{x}} = N(\underline{x}-\underline{m}) + \underline{a} \qquad (4.7)$$

By defining r to be the zero mean process, $(\underline{x} - \underline{m})$, equation (4.7) can be written as

$$\dot{\underline{m}} + \dot{\underline{r}} = N\underline{r} + \underline{a} \quad . \qquad (4.8)$$

The choice of $\underline{a}$ and N to minimize the mean square error, $E[\underline{e}^T\underline{e}]$, yields an equivalent linear system (4.7) which has identical mean and covariance propagation equations with the nonlinear system (4.1). The expected values of equations (4.1) and (4.7) are identical, i.e.,

$$\dot{\underline{m}} = E[f] \qquad (4.9)$$

The covariance propagation of (4.7) is

$$\dot{P} = NP + PN^T \qquad (4.10)$$

and the covariance propagation of (4.1) is [36]

$$\dot{P} = E[\underline{f}\,\underline{r}^T] + E[\underline{r}\,\underline{f}^T] \tag{4.11}$$

Equation (4.11) can then be rewritten as

$$\mathring{P} = E[\underline{f}\,\underline{r}^T]P^{-1}P + PP^{-1}E[\underline{r}\,\underline{f}^T] = NP+PN^T \tag{4.12}$$

which is identical to(4.10). Therefore, the propagation of the mean and covariance of the approximate system (4.7) is identical to that of nonlinear system (4.1), provided both systems are assumed to have the same probability density function by which to evaluate the expectations.

Iwan [37] has given a formal solution for the equivalent linear system corresponding to an n-degree of freedom system with arbitrary stiffness and damping nonlinearities. He reported the existence and uniqueness of approximate solutions generated by the generalized method of equivalent linearization. Recently, Spanos and Iwan [38] have shown that a unique equivalent linear system exists whenever the elements of the solution vector:

$$\hat{\underline{x}} = \begin{bmatrix} \underline{x} \\ \dot{\underline{x}} \end{bmatrix}$$

are linearly independent. Also in the paper, the existence and uniqueness of a generalized equivalent linear system were examined in detail. It was shown that even though, in some cases, the equivalent linear system may not be unique, but a simple element-by-element substitute system always exists. Furthermore, the equivalent system defined by element-by-element substitution is at least as good as any other similarly defined substitute system. Finally, they concluded that the equivalent linear elements (gains) not only satisfy the minimization criterion for the system as a whole but also satisfy the condition the system error is minimized for each element of the system separately. All these conclusions were drawn for the following type of systems.

$$\underline{M}\ddot{x} + \underline{f}(x,\dot{x}) = \underline{g}(t) \qquad \text{(Nonlinear Dynamical System)}$$

$$\underline{M\ddot{x}} + \underline{\overline{C}\dot{x}} + \underline{\overline{K}\dot{x}} = \underline{g}(t) \qquad \text{(Equivalent Linear System)}$$

$$\underline{\varepsilon} = \underline{f}(\underline{x},\underline{\dot{x}}) - \underline{\overline{C}\dot{x}} - \underline{\overline{K}x} \qquad \text{(Error equation)}$$

where g(t) represents a stationary Gaussian random vector.

Up to now, a precise definition of the error bound on the equivalent linearization has not been developed. Kolovskii [44], Iwan and Yang [45] were able to evaluate the error in stationary mean square response for a restricted class of systems. Iwan and Patula [46] defined analytic bounds on the error for certain simple systems. They concluded that the solution error, in general, was considerably smaller than the one predicted. Beaman [35] has shown that for Hamiltonian systems the variance found by replacing the nonlinearity with Gaussian statistical linearized gains is a lower bound of the actual variance.

Phaneuf [34], Beaman and Hedrick [47] have given an interpretation to the eigenvalues of the equivalent linear system. Beaman and Hedrick [47] showed that the eigenvalues for the propagation of the perturbed mean were the stationary values of the Gaussian statistically linearized system. It was emphasized that if the Gaussian density approximation is valid then the stability and the speed of the perturbed mean response is characterized by the eigenvalues of the equivalent linear system.

4.2 Application to Rail Vehicle Dynamics

Statistical linearization was applied by Stassen [15] to a two-degrees-of-freedom rail vehicle model. His dissertation includes the verification of the method by analog/hybrid simulation and full scale bogie test by O.R.E. Rus [16], Hedrick [17], Hedrick and Arslan [18], Hedrick and Castelazo [19] have also applied the method to analyze the stationary statistical response of a nonlinear rail vehicle model.

In general, nonlinear rail vehicle equations can be expressed as:

$$\underline{\bar{M}}\,\ddot{\underline{y}} + \underline{g}(\underline{y},\dot{\underline{y}}) = \underline{\bar{B}}\,\underline{u}(t) \tag{4.13}$$

where $\underline{y}$ is an n-vector of generalized position coordinates, $\underline{\bar{M}}$ is the inertia matrix, $\underline{g}(\underline{y},\dot{\underline{y}})$ is a vector of linear and nonlinear elements including the wheel/rail profile, creep, and suspension nonlinearities, and $\underline{u}(t)$ is an m-vector of random inputs. In this research all the nonlinearities in the rail vehicle were isolated.

Therefore, an equivalent linear system may be constructed by a simple element-by-element substitution technique [37]. The resulting statistical linearization method for an isolated nonlinearity is shown in Figure 4.1 [48]. Here, the input to the nonlinearity was assumed to have a general form. It was considered to be the sum of any number of signals, $x_i(t)$, each of an identifiable type. In most cases, these input components $x_i(t)$ could be considered as constant signals, sinusoids and zero mean random variables, i.e.

$$x(t) = \bar{x} + r(t) + A \sin(\omega t + \phi) \quad . \tag{4.14}$$

Through physical considerations and digital simulations it was seen that, in this research, the inputs to the nonlinearities had zero means. Since we are concerned not only in predicting the hunting behavior of the rail vehicle but also in predicting the dynamic response of the vehicle to random disturbances, the sinusoidal input assumption is not valid. With these assumptions the general form of the statistical linearization shown in Figure 4.1 reduces to the original form by Booton [20] as shown in Figure 4.2.

In this method, the nonlinearity is replaced by a linear gain K_{eq} chosen so as to minimize the mean square of the difference between the outputs of the two devices, i.e., the error in the approximation is:

$$\varepsilon(t) = y(t) - y_a(t) \tag{4.15}$$

and its mean squared value

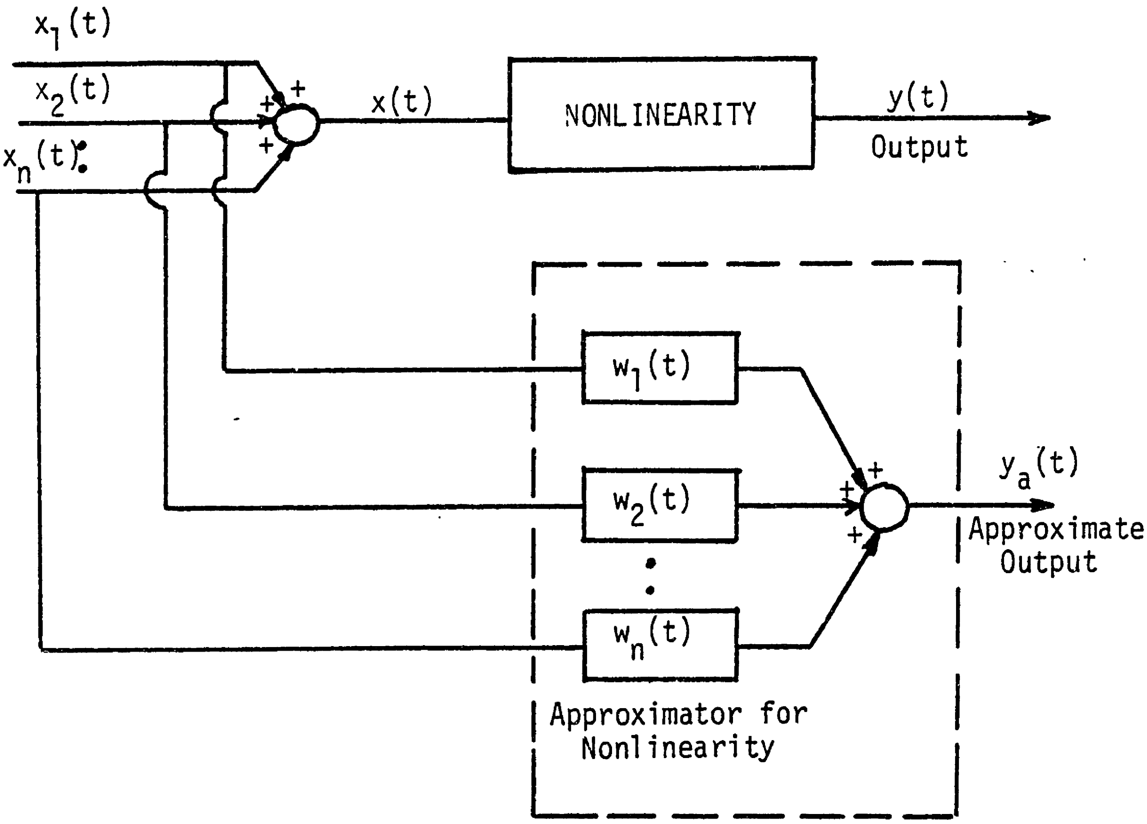

FIGURE 4.1: GENERAL LINEAR APPROXIMATOR FOR AN ISOLATED NONLINEARITY [48]

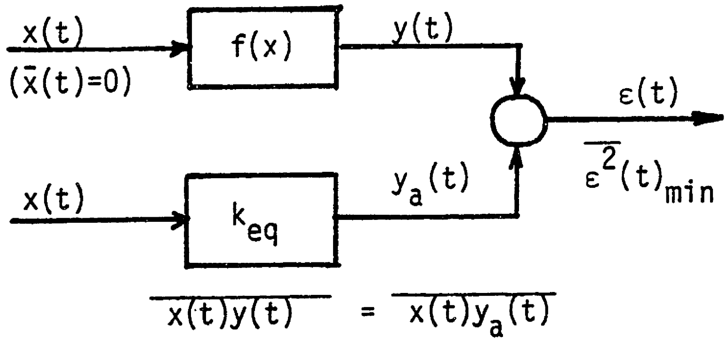

FIGURE 4.2: EQUIVALENT LINEAR MODEL OF BOOTON [56]

$$E[\varepsilon(t)^2] = E[y(t)^2] - 2E[y(t)y_a(t)] + E[y_a^2(t)] \tag{4.16}$$

K_{eq} is then chosen to minimize $\overline{\varepsilon(t)^2}$, the resulting expression for K_{eq} becomes [48]:

$$K_{eq} = \frac{E[x\ f(x)]}{E[x^2]} \triangleq \frac{\int_{-\infty}^{\infty} x\ f(x)\ p(x)dx}{\int_{-\infty}^{\infty} x^2 p(x)dx} \tag{4.17}$$

where

$E[(.)]$ = "expected" value of (.)

$p(x)$ = probability density function of $x(t)$.

The equivalent linear gain defined by (4.17) is thus a function of the parameters of the probability density function $p(x)$. The most common form that has been assumed for $p(x)$ is the Gaussian density function. If $p(x)$ is assumed to have a Gaussian form:

$$p(x) = \frac{1}{\sqrt{2\pi}\ \sigma_x} \exp\left(-\frac{x^2}{2\sigma_x^2}\right) \tag{4.18}$$

equation (4.17) becomes,

$$K_{eq} = \frac{1}{\sqrt{2\pi}\ \sigma_x^3} \int_{-\infty}^{\infty} x\ f(x)\ \exp\left(-\frac{x^2}{2\sigma_x^2}\right) dx \tag{4.19}$$

Crandall [49] has shown that improved results are obtained if the exact density function can be used. Simulation and experiments have shown that as the critical speed is approached the density functions deviate from a pure Gaussian and take the form of a Gaussian plus sinusoid as shown in Figure 4.3.

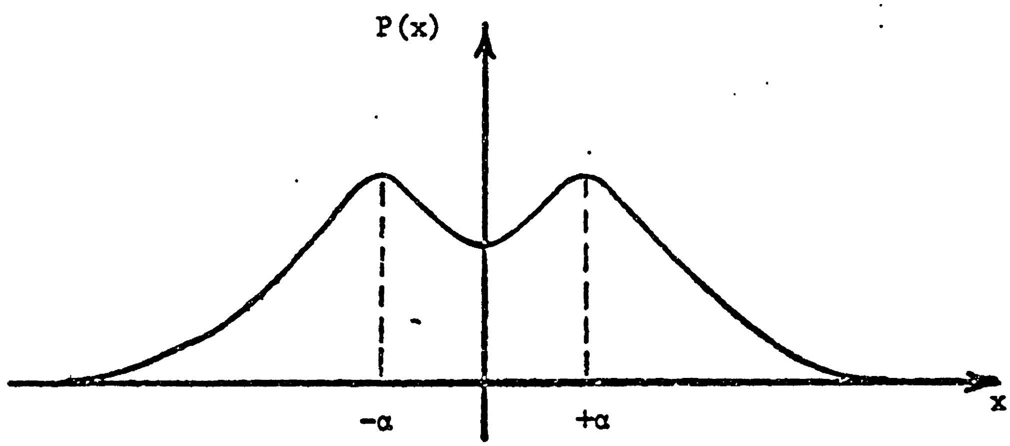

Figure 4.3 Gaussian Plus Sinusoidal Density Function

The non-Gaussian density function shown in Figure 4.3 can be characterized by two parameters, σ , the r.m.s. value, and α . The difficulty in using this density function is in determining the second parameter, α . In previous work Stassen [15] determined the second parameter, α , for his system by analog/hybrid simulation while Rus [16] assumed that α was equal to the wheelset flange clearance. Although both approaches yield slightly more accurate results than the purely Gaussian assumption, the first is not consistent with an analytical design method and the second is only valid when the hunting amplitude is known and equal to the flange clearance.

One of the purposes of this research is to find the probability density functions which are specified by only one parameter and are valid over a wide range of speeds. Chapter 5 also presents the probability density function chosen for the specific problem.

4.3 Solution Method

The statistical linearization method attempts to replace the nonlinear system defined by equation (4.13) with an equivalent linear one, i.e., we seek equivalent damping and stiffness matrices $\underline{\bar{D}}$ and $\underline{\bar{K}}$ such that:

$$\underline{g}(y,\underline{\dot{y}}) \simeq \underline{\bar{D}}\,\underline{\dot{y}} + \underline{\bar{K}}\,\underline{y} \tag{4.20}$$

If equation (4.20) is substituted into equation (4.13) the equivalent linear form becomes

$$\underline{\bar{M}}\,\underline{\ddot{y}} + \underline{\bar{D}}\,\underline{\dot{y}} + \underline{\bar{K}}\,\underline{y} = \underline{\bar{B}}\,\underline{u}(t) \tag{4.21}$$

where the equivalent linear damping and stiffness matrices are now functions of the equivalent gains defined by (4.17) or, in other terms, they are functions of the variances of the inputs to the nonlinearities.

The transfer function matrix between $\underline{y}$ and $\underline{u}$ of (4.21) is defined by:

$$\underline{y}(j\omega) = [\underline{\bar{K}} - \omega^2\underline{\bar{M}} + j\omega\underline{\bar{D}}]^{-1}\,\underline{\bar{B}}\,\underline{u}(j\omega) \tag{4.22}$$

Since we are considering the vector system to be made up of a number of scalar nonlinearities the equivalent gains are functions of the variances of the inputs to these nonlinearities. Therefore we need to compute these variances. Let $\underline{z}$ be an r-vector that represents the inputs to all of the nonlinear elements, then;

$$\begin{aligned} \underline{z}(j\omega) &= \underline{C}^T \underline{y}(j\omega) \\ &= \underline{C}^T[\overline{\underline{K}} - \omega^2 \overline{\underline{M}} + j\omega\overline{\underline{D}}]^{-1} \overline{\underline{B}} u(j\omega) \\ &= \overline{\underline{H}}(j\omega) \underline{u}(j\omega) \end{aligned} \quad (4.23)$$

where $\overline{\underline{H}}$ is an rxm matrix of transfer functions. The power spectral densities of the vector can be found from:

$$S_z(j\omega) = \overline{\underline{H}}(j\omega) S_u(j\omega) \overline{\underline{H}}^T(-j\omega) \quad (4.24)$$

where S_z is an rxr matrix containing the spectral densities of the $\underline{z}$ vector along the diagonal and the cross-spectral densities on the off-diagonal elements and S_u is an mxm matrix of input spectral and cross-spectral densities.

The equivalent linear gains defined by (4.17) depend on the mean square value, $\sigma_{z_i}^2$, of the input to the nonlinearity. Thus in order to evaluate the equivalent gains in the $\overline{\underline{K}}$ and $\overline{\underline{D}}$ matrices we need to compute the mean square value of the r variables in the $\underline{z}$ vector. This can be done by integrating the diagonal terms of S_z, i.e.,

$$\sigma_{z_i}^2 = \int_{-\infty}^{\infty} S_{z_i}(j\omega)\, d\omega \qquad ; \quad i=1,\ldots r \quad (4.25)$$

The <u>iterative</u> nature of the required solution procedure is apparent from (4.25). The spectral density functions, S_{z_i} , are dependent on the equivalent gains of the $\bar{\underline{K}}$ and $\bar{\underline{D}}$ matrices which are in turn dependent on the σ_{z_i}'s .

4.4 Numerical Algorithm

The following statistical linearization algorithm was used:

1. Place the system in equivalent linear form (Eq.(4.21)). This requires replacing all nonlinearities by their equivalent linear gains. In many cases, if the nonlinearities are common, the gains have been precomputed and are available in modern texts [32], otherwise the gains need to be computed and stored as a function of σ by integrating Eq. (4.17).

2. Select an initial set of rms (σ) values for the $\underline{z}$ vector , i.e., $\sigma_{z_1},\ldots,\sigma_{z_r}$ and using these σ's evaluate the equivalent linear gains.

3. Using Eqs. (4.23), (4.24), and (4.25) evaluate the <u>computed</u> values of σ_{z_i} . These values are then compared with the guessed values and the difference used to begin an iteration process until convergence occurs.

Figure 4.4 is a flowchart of the developed computer program. To increase the efficiency of the program the following improvements were made and they were incorporated into the program.

<u>Convergence Algorithm:</u> There are numerous convergence algorithms that can be used to seek convergence. It was found that a simple first-order gradient algorithm, which is given by equation (4.26), provided fast convergence.

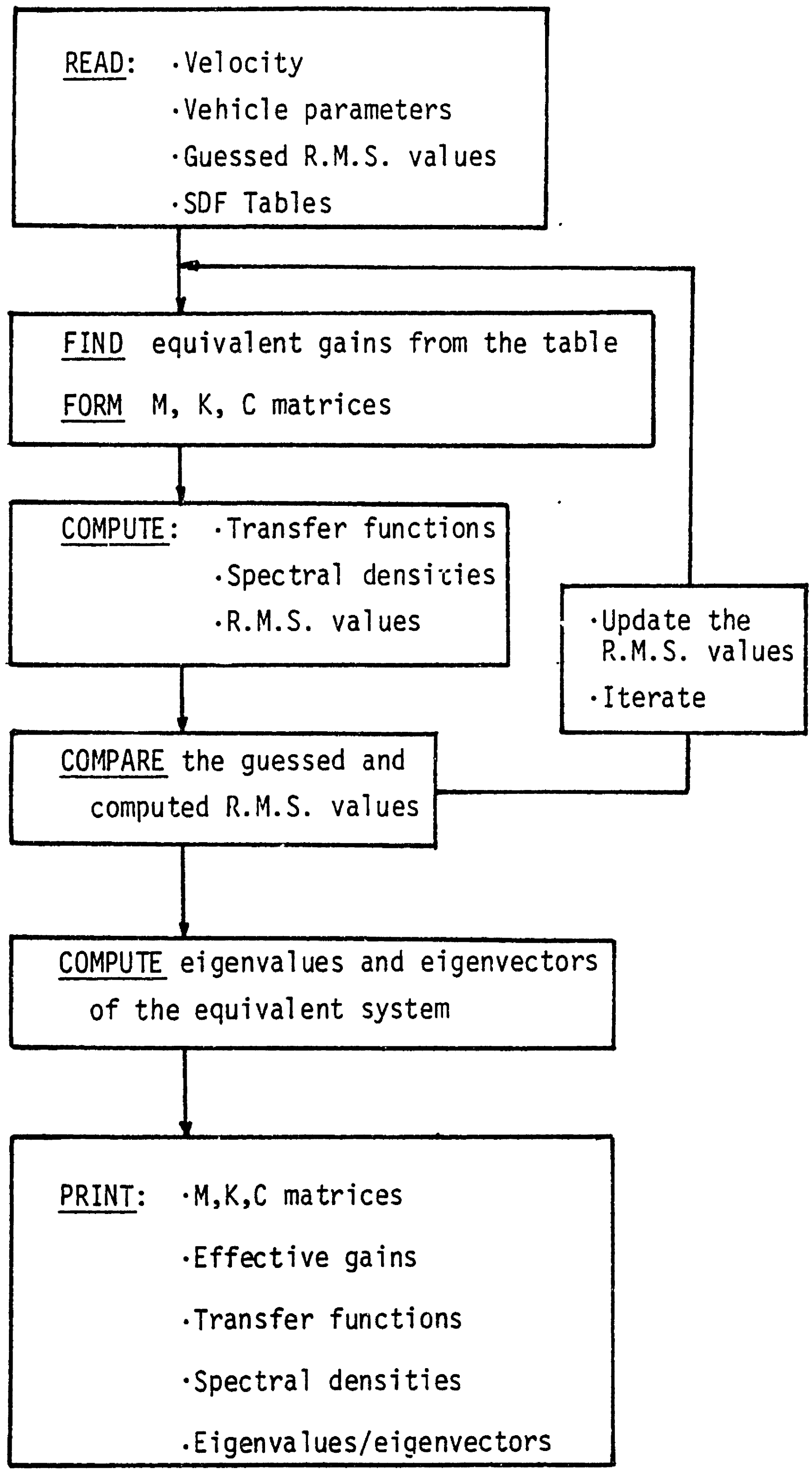

FIGURE 4.4: FLOWCHART OF THE PROGRAM

$$\sigma_{z_i}(n+1) = \sigma_{z_i}(n) + \varepsilon_i(n)[\sigma_{zc_i}(n) - \sigma_{z_i}(n)] \qquad (4.26)$$

where

n = the iteration number

$\sigma_{zc}(n)$ = computed variance using (4.25) at iteration n

$\sigma_z(n)$ = guessed variance at iteration n

and

$$\varepsilon_i(n) = \frac{1}{1 - \dfrac{d(\sigma_{zc_i}(n))}{d(\sigma_{z_i}(n))}} \qquad (4.27)$$

The derivative term in (4.15) is computed numerically by

$$\frac{d(\sigma_{zc_i}(n))}{d(\sigma_{z_i}(n))} \simeq \frac{\sigma_{zc_i}(n) - \sigma_{zc_i}(n-1)}{\sigma_{z_i}(n) - \sigma_{z_i}(n-1)}$$

After calculating $\varepsilon_L(n)$ from (4.27) it was bounded to be in an interval $[\varepsilon_1, \varepsilon_u]$. These bounds were found to be very useful in the convergence algorithm. In general, the number of nonlinearities in a system are greater than one. Then, equation (4.21) has n-coupled equations. Non-convergence of one variance affects the other variances. Usually, some variances are less sensitive to the changes of the others. Then, they converge to some values, not necessarily to the correct values, rapidly. As a result the ε's for those go to zero if there is no lower bound on the ε's. After this occurs, it is very difficult to update the estimated variances. In this research a non-zero value for ε_L (e.g., 0.1) was found to solve this problem. The upper bound was chosen to be one assuming that the guessed value at iteration (n+1) is not far from the two previous guesses.

In the program, there are two flags to terminate the iteration The first one is the limit on the allowable number of iteration and the second is the maximum allowable difference between the computed and guessed r.m.s. values.

Frequency Range of Interest: To calculate σ_{z_i} , equation (4.25) should be integrated numerically. To decrease the computation time a pre-analysis of the frequency range of interest was done. The approach was to find the frequency range which contained 95% of the r.m.s. values. It was found that for the lateral locomotive 0.4 - 10 Hz range was the frequency range of interest.

Inversion of the Complex Matrix in Equation (4.10) [24]: To determine the transfer function matrix we have to invert an (n×n) complex matrix. It is known that the inversion of two (n×n) real matrices takes less computer time than the inversion of an (n×n) complex matrix [ ]. Therefore, let

$$[\underline{\bar{K}} - \omega^2 \underline{\bar{M}} + j\omega\underline{\bar{D}}]^{-1} = \underline{\bar{D}}_R + j\,\underline{\bar{D}}_I \qquad (4.29)$$

where $\underline{D}_R$ and $\underline{D}_I$ are (n×n) real matrices. Premultiply equation (4.29) by $[\underline{\bar{K}} - \omega^2 \underline{\bar{M}} + j\omega\underline{\bar{D}}]$ to get:

$$\bar{\underline{I}} = [(\bar{\underline{K}} - \omega^2 \bar{\underline{M}}) + j\omega\bar{\underline{D}}][\bar{\underline{D}}_R + j\omega\bar{\underline{D}}_I] \tag{4.30}$$

where $\bar{\underline{I}}$ = Identity matrix.

Equation (4.30) is a complex identity, therefore:

$$(\bar{\underline{K}} - \omega^2 \bar{\underline{M}}) \bar{\underline{D}}_R - \omega \bar{\underline{D}} \bar{\underline{D}}_I = \bar{\underline{I}} \tag{4.31}$$

and

$$(\bar{\underline{K}} - \omega^2\bar{\underline{M}}) \bar{\underline{D}}_I + \omega \bar{\underline{D}} \bar{\underline{D}}_R = \bar{\underline{0}} \tag{4.32}$$

We can solve for $\bar{\underline{D}}_R$ and $\bar{\underline{D}}_I$ from equations (4.31) and (4.32) to get:

$$\bar{\underline{D}}_R = [(\bar{\underline{K}} - \omega^2 \bar{\underline{M}}) + \omega^2 \bar{\underline{D}}(\bar{\underline{K}} - \omega^2 \bar{\underline{M}})^{-1} \bar{\underline{D}}]^{-1} \tag{4.33}$$

and

$$\bar{\underline{D}}_I = -\omega(\bar{\underline{K}} - \omega^2 \bar{\underline{M}})^{-1} \bar{\underline{D}} \bar{\underline{D}}_R \tag{4.34}$$

Coulomb-Damper Lock-up: The secondary yaw suspension is modeled as an ideal Coulomb damper between the car body and the bolster in series with a linear spring between the bolster and the truck as shown in Figure 2.6. At high speeds truck yaw displacement exceeds $T_{cp}/K_{s\psi}$ so that the moment generated by the spring is sufficient to start the motion of the bolster. At low speeds, however, it is not enough and the bolster does not move, i.e. will lock up to the car body.

In digital programs this lock-up condition can be solved by a simple logical algorithm . In frequency domain programs the lock-up condition can be dealt with by either eliminating one degree of freedom from the system or increasing the equivalent gain to a very high value as shown below.

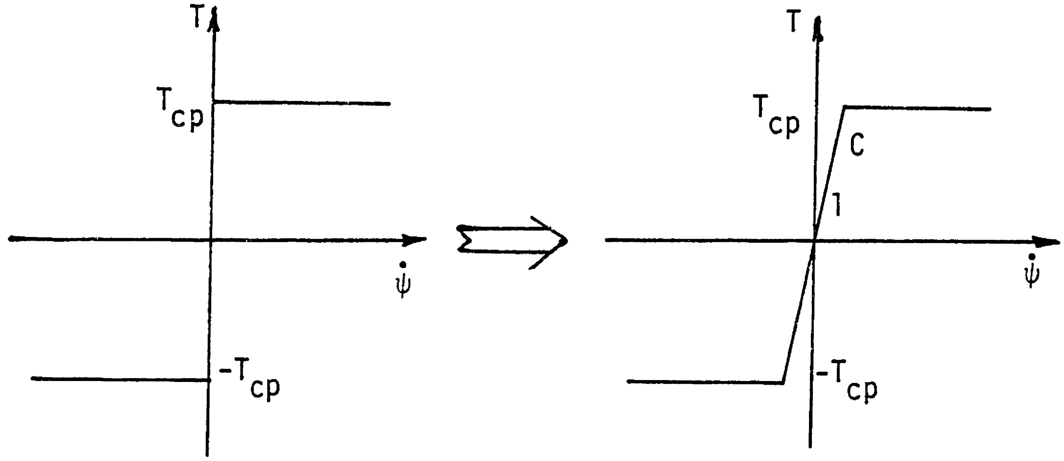

In this thesis, the second method was chosen and implemented in the program. If the equivalent gain is increased to infinity, i.e. $C \to \infty$, it causes numerical problems in the inversion of the matrix given by (4.29). To eliminate the problem the equivalent gain was saturated at a certain value, C^* , corresponding to a saturation in r.m.s. bolster velocity as shown below. C^* was chosen such that an

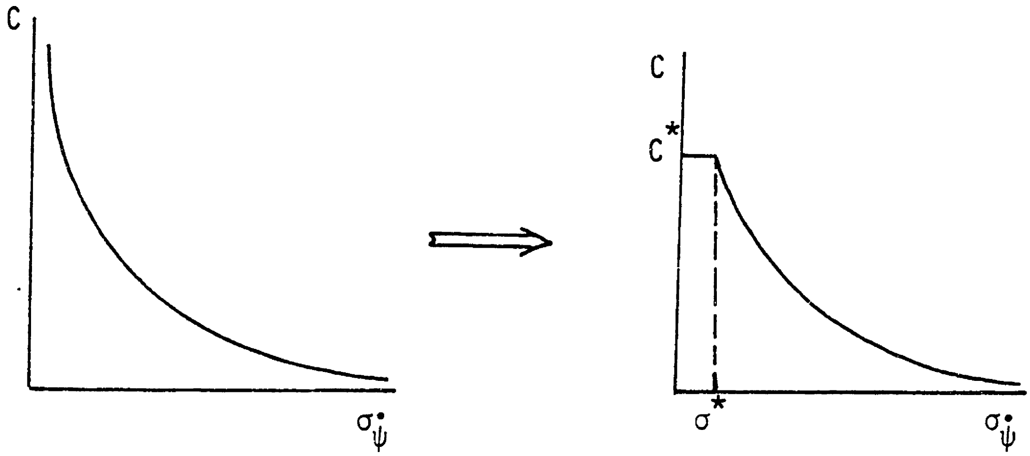

order of magnitude change in C^* did not affect the results. Also, the value of C^* was at least an order of magnitude greater than all the other viscous dampers in the system.

4.5 Application to 12 D.O.F. Locomotive Model

The statistical linearization method outlined in the previous sections is applied to the lateral, twelve degrees of freedom half car body locomotive model. The assumptions made in the Statistical Linearization Model (SLM) are those of the digital model. In this research a linear creep force/creepage relationship is assumed. The linear creep force assumption with nonlinear creepages reduces the general nonlinear wheelset equations to the equations (A.8.13) and (A.8.14) which are presented in Appendix A, i.e.,

Lateral Equation:

$$M_W\ddot{y} + \frac{2f_{11}}{V}(\dot{y} + r_o\dot{\phi} - V\psi) + \frac{2f_{12}}{V}\dot{\psi} - \frac{2f_{12}}{r_o}\Delta_2(\Delta y) + L_A\Delta_L(\Delta y) = F_{suspy} \tag{4.35}$$

Yaw Equation:

$$I_{wx}\ddot{\psi} + I_{wy}\frac{V}{r_o}\dot{\phi} + \frac{2a^2f_{33}}{V}\dot{\psi} + \frac{2af_{33}}{r_o}\left(\frac{r_L - r_R}{2}\right) + \frac{2f_{22}}{V}\dot{\psi} - \frac{2f_{12}}{V}(\dot{y} + r_o\dot{\psi} - V\psi) - \frac{2f_{22}}{r_o}\Delta_1(\Delta y) - aL_A\delta_o\psi = M_{suspz} \tag{4.36}$$

where

$$\Delta_L(\Delta y) = \frac{\tan(\delta_L + \phi) - \tan(\delta_R - \phi)}{2 - \frac{1}{a}[r_L \tan(\delta_L + \phi) + r_R \tan(\delta_R - \phi)]}$$

$$\Delta_1(\Delta y) = \frac{\sin\delta_L \cos(\delta_L + \phi) - \sin\delta_R \cos(\delta_R - \phi)}{2}$$

$$\Delta_2(\Delta y) = \frac{\sin\delta_L \cos(\delta_L + \phi) - \sin\delta_R \cos(\delta_R - \phi)}{2 - \frac{1}{a}[r_L \tan(\delta_L + \phi) + r_R \tan(\delta_R - \phi)]}$$

Δy = wheelset lateral displacement with respect to rail

4.5.1 Nonlinearities

The nonlinearities included in the dynamic model can be divided into wheel/rail geometry and suspension nonlinearities.

4.5.1.1 Wheel/Rail Geometry Nonlinearities - In the nonlinear wheelset equations the following wheel/rail geometry terms appear:

- $$\frac{r_L - r_R}{2} \tag{4.37}$$

- $$\phi \tag{4.38}$$

- $$L_A\Delta_L(\Delta y) = \frac{L_A[\tan(\delta_L + \phi) - \tan(\delta_R - \phi)]}{2 - \frac{1}{a}[r_L \tan(\delta_L + \phi) + r_R \tan(\delta_R - \phi)]} \tag{4.39}$$

$$\bullet \quad \Delta_1(\Delta y) = \frac{\sin\delta_L \cos(\delta_L + \phi) - \sin\delta_R \cos(\delta_R - \phi)}{2} \tag{4.40}$$

$$\bullet \quad \Delta_2(\Delta y) = \frac{\sin\delta_L \cos(\delta_L + \phi) - \sin\delta_R \cos(\delta_R - \phi)}{2 - \frac{1}{a}[r_L \tan(\delta_L + \phi) + r_R \tan(\delta_R - \phi)]} \tag{4.41}$$

Equation (4.37) is the rolling radii difference, i.e., the difference between the left and right radius measured at the respective contact points. Equation (4.39) represents the lateral gravitational stiffness force where L_A is a constant axle load. Equations (4.40) and (4.41) reduce to the contact angle difference for small contact angles. For a real wheel these geometric parameters are nonlinear functions of the wheelset excursion, i.e., the wheelset lateral displacement with respect to the rail. Numerous examples of wheel/rail geometry are given in reference [23].

The equivalent linear forms for the nonlinear terms in equations (4.37) to (4.41) are:

$$\frac{r_L - r_R}{2} \simeq \lambda(\sigma_{\Delta y}) \cdot \Delta y \tag{4.42}$$

$$\phi \simeq \frac{k_\phi(\sigma_{\Delta y})}{a} \cdot \Delta y \tag{4.43}$$

$$\Delta_L(\Delta y) \simeq \frac{k_g(\sigma_{\Delta y})}{L_A\, a} \Delta y \tag{4.44}$$

$$\Delta_1(\Delta y) \approx \frac{k_{\Delta_1}(\sigma_{\Delta y})}{a} \Delta y \qquad (4.45)$$

$$\Delta_2(\Delta y) \approx \frac{k_{\Delta_2}(\sigma_{\Delta y})}{a} \Delta y \qquad (4.46)$$

Thus there are five equivalent linear gains that are used to describe the nonlinear wheel/rail geometry, λ , k_ϕ, k_g , k_{Δ_1} , k_{Δ_2} . From the linear analysis we can give the gains λ , k_g the interpretation of:

λ = "effective conicity"

k_g = "effective lateral gravitational stiffness"

These five equivalent gains can be found using equation (4.17) for specified input probability density functions. If the input PDF is assumed to have the Gaussian form, then these five gains are given by:

$$\lambda = \frac{1}{\sqrt{2\pi}\,\sigma_{\Delta y}^3} \int_{-\infty}^{\infty} \frac{[r_L(\Delta y) - r_R(\Delta y)]}{2} \cdot \Delta y \cdot \exp\left(-\frac{\Delta y^2}{2\sigma_{\Delta y}^2}\right) \cdot d(\Delta y) \qquad (4.47)$$

$$k_\phi = \frac{a}{\sqrt{2\pi}\,\sigma_{\Delta y}^3} \int_{-\infty}^{\infty} \phi(\Delta y) \cdot \Delta y \quad \exp\left(-\frac{\Delta y^2}{2\sigma_{\Delta y}^2}\right) \cdot d(\Delta y) \qquad (4.48)$$

$$k_g = \frac{a}{\sqrt{2\pi}\,\sigma_{\Delta y}^3} \int_{-\infty}^{\infty} \Delta_L(\Delta y) \cdot \Delta y \cdot \exp\left(-\frac{\Delta y^2}{2\sigma_{\Delta y}^2}\right) \cdot d(\Delta y) \qquad (4.49)$$

$$k_{\Delta_1} = \frac{a}{\sqrt{2\pi}\,\sigma_{\Delta y}^3} \int_{-\infty}^{\infty} \Delta_1(\Delta y) \cdot \Delta y \cdot \exp(-\frac{\Delta y^2}{2\sigma_{\Delta y}^2}) \cdot d(\Delta y) \qquad (4.50)$$

$$k_{\Delta_2} = \frac{a}{\sqrt{2\pi}\,\sigma_{\Delta y}^3} \int_{-\infty}^{\infty} \Delta_2(\Delta y) \cdot \Delta y \cdot \exp(-\frac{\Delta y^2}{2\sigma_{\Delta y}^2}) \cdot d(\Delta y) \qquad (4.51)$$

<u>4.5.1.2 Suspension Nonlinearities</u> - The suspension nonlinearities in the locomotive model are:

-- Primary lateral deadband spring (Figure 2.5a)

-- Primary yaw hardening spring (Figure 2.5b)

-- Coulomb damper between centerplate and carbody (Figure 2.6)

<u>Deadband Spring:</u>

The force displacement relation for the deadband spring is given by equation (2.6). The equivalent linear form for the deadband spring can be expressed as:

$$F_{kpy} \simeq k_p(\sigma_{\Delta p}) \cdot \Delta p \qquad (4.52)$$

where (Gaussian assumption)

$$k_p = \frac{1}{\sqrt{2\pi}\,\sigma_{\Delta p}^3} \int_{-\infty}^{\infty} F_{kpy} \cdot \Delta y \cdot \exp(-\frac{\Delta p^2}{2\sigma_{\Delta p}^2})\, d(\Delta p)$$

$$= k[1 - \mathrm{erf}(\frac{\delta_y}{\sqrt{2}\,\sigma_{\Delta p}})] \qquad (4.53)$$

$-\Delta p$ = lateral primary stroke

$\mathrm{erf}(\cdot)$ = Gaussian error function tabulated in Reference [50].

Hardening Spring:

The force displacement relation for the piecewise linear hardening spring is given by equation (2.7). The equivalent linear form for the hardening spring can be expressed as:

$$M_{kp\psi} \simeq k_{\psi}(\sigma_{\Delta\psi}) \cdot \Delta\psi \qquad (4.54)$$

where (for Gaussian assumption)

$$k_{\psi}(\sigma_{\Delta\psi}) = \frac{1}{\sqrt{2\pi}\,\sigma_{\Delta\psi}^{3}} \int_{\infty}^{\infty} M_{kp\psi} \cdot \Delta\psi \cdot \exp\left(- \frac{\Delta\psi^{2}}{2\sigma_{\Delta\psi}^{2}}\right) d(\Delta\psi)$$

$$(4.55)$$

$$= k_{p\psi_1} + (k_{p\psi_2} - k_{p\psi_1})\left[1 - \mathrm{erf}\left(\frac{\delta\psi}{\sqrt{2}\,\sigma_{\Delta\psi}}\right)\right]$$

$\Delta\psi$ = primary yaw stroke

$\mathrm{erf}(\cdot)$ = Gaussian error function

Coulomb Friction:

The governing equation for the Coulomb friction between the centerplate and carbody is given by:

$$T = T_0 \,\mathrm{Sgn}(\dot{\psi}_b - \dot{\psi}_c) \quad , \qquad \dot{\psi}_c \equiv 0 \qquad (4.56)$$

where

T = torque

$\dot{\psi}_b$ = angular velocity of the bolster

T_o = breakout level of the torque

Sgn = Signum function

Then the equivalent linear form for Coulomb friction can be expressed as:

$$T \simeq C_{cp}(\sigma_{\dot{\psi}_b})\dot{\psi}_b \tag{4.57}$$

where (for Gaussian Assumption)

$$C_{cp} = \frac{1}{\sqrt{2\pi}\,\sigma^3_{\dot{\psi}_b}} \int_{-\infty}^{\infty} T \cdot \dot{\psi}_b \cdot \exp\left(-\frac{\dot{\psi}_b}{2\sigma^2_{\dot{\psi}_b}}\right) d(\dot{\psi}_b)$$

$$= \frac{\sqrt{2/\pi}\,T_o}{\sigma_{\dot{\psi}_b}} \tag{4.58}$$

4.5.2 Alignment Input

There are three wheelsets, thus there are three inputs to the wheelset lateral equations and three inputs to the wheelset yaw equations. Also the alignment input enters the truck roll equation through the wheelset roll. The input to each trailing wheelset is just the input to the leading wheelset delayed by the time it takes for each wheelset to reach the same point in the rail; i.e.,

$$u_L(t) = \begin{bmatrix} u_{1L}(t) \\ u_{1L}(t - \tau_1) \\ u_{1L}(t - \tau_2) \end{bmatrix} \tag{4.59}$$

where

$$\tau_1 = \frac{\ell_1 - \ell_2}{V}$$

$$\tau_2 = \frac{\ell_1 + \ell_3}{V}$$

ℓ_i = distance of the wheelset c.g. from truck c.g. (Figure 2.1)

In the frequency domain:

$$\underline{u}_L(j\omega) = \begin{bmatrix} 1 \\ e^{-j\omega\tau_1} \\ e^{-j\omega\tau_2} \end{bmatrix} \cdot u_1(j\omega) \tag{4.60}$$

or in general,

$$\underline{u}(j\omega) = \underline{B}_3 \; u_1(j\omega) \quad . \tag{4.61}$$

In matrix notation the equivalent linear equations of motion of the locomotive become:

$$\underline{\bar{M}}\,\ddot{\underline{y}} + \underline{\bar{D}}\,\dot{\underline{y}} + \underline{\bar{K}}\,\underline{y} = \underline{\bar{B}}_1\,\dot{\underline{u}}(t) + \underline{\bar{B}}_2\,\underline{u}(t) \tag{4.62}$$

where $\underline{u}(t)$ = random rail irregularity.

The transfer function matrix between $\underline{y}$ and $\underline{u}$ is then defined by

$$\underline{y}(j\omega) = \underline{H}(j\omega)\ u_1(j\omega) \tag{4.63}$$

where

$$\underset{(12\times 1)}{\underline{H}(j\omega)} = \underset{(12\times 12)}{[\,\underline{\bar{K}} - \omega^2\,\underline{M} + j\omega\underline{\bar{D}}\,]^{-1}}\ \underset{(12\times 6)}{[\,\underline{\bar{B}}_2 + j\omega\underline{\bar{B}}_1\,]}\underset{(6\times 1)}{\underline{B}_3} \tag{4.64}$$

In the locomotive model all the nonlinearities are single input nonlinearities, thus the equivalent linear gains are a function of the variances of the inputs to these nonlinearities. In the model there are ten nonlinearities, the inputs to these nonlinearities are:

$z_1 = y_1 - u_1(t)$	Wheelset Excursion (#1)
$z_2 = y_3 - u_1(t - \tau_1)$	Wheelset Excursion (#2)
$z_3 = y_5 - u_1(t - \tau_2)$	Wheelset Excursion (#3)
$z_4 = y_1 - y_7 - \ell_1\, y_8 - h_{tp}\, y_9$	Displacement Across Primary Lateral Spring (#1)

$$z_5 = y_3 - y_7 - \ell_2 y_8 - h_{tp}\, y_9$$ Displacement Across Primary Lateral Spring (#2)

$$z_6 = y_5 - y_7 + \ell_3 y_8 - h_{tp}\, y_9$$ Displacement Across Primary Lateral Spring (#3)

$$z_7 = y_2 - y_8$$ Displacement Across Primary Yaw Spring (#1)

$$z_8 = y_4 - y_8$$ Displacement Across Primary Yaw Spring (#2)

$$z_9 = y_6 - y_8$$ Displacement Across Primary Yaw Spring (#3)

$$z_{10} = \dot{y}_{12}$$ Velocity Across Coulomb Damper

The transfer function matrix between z_i and u_1 can be obtained from:

$$\begin{aligned} z_i(j\omega) &= \underline{C}_i^T\, \underline{y}(j\omega) \\ &= \underline{C}_i^T\, \underline{H}(j\omega)\, u_1(j\omega) \quad . \end{aligned} \tag{4.65}$$

The power spectral densities of the nonlinearities can be found from:

$$S_{z_i}(j\omega) = \underline{C}_i^T\, \underline{H}(j\omega)\, \underline{S}_u(j\omega)\, \underline{H}^T(-j\omega)\underline{C}_i \tag{4.66}$$

where S_u is the input spectral density.

These statistically linearized locomotive equations are presented in Appendix B.1.

CHAPTER 5

EVALUATION OF STATISTICAL LINEARIZATION AS A DESIGN TOOL

5.1 Introduction

In rail vehicle dynamic analysis, linear models have been developed and used extensively to investigate the complex dynamic behavior of rail vehicles. These models are coded and available to the rail industry to provide guidance in the design and evaluation of new and existing vehicles. Linear models, however, cannot include the critical nonlinear effects of worn wheel profiles, flanges, suspension clearances, hardening springs, dry friction and creep force saturation. The importance of these nonlinearities have been observed through simulations and experiments [4]. For example, it is known that the lateral primary stiffness strongly affects the stability of rail vehicles [4], locomotives have nonlinear axle clearances in their primary, as shown in Figure 2.5.a. This nonlinear suspension cannot be included in linear models, therefore an equivalent spring constant which has a value in the range of 0 to k should be chosen. This wide range gives a critical speed ranging from 5 mph to 145 mph. Therefore, if these linear models are to be used an "effective" spring constant needs to be selected, for example through field tests, which is not in general a practical alternative.

One way of including these nonlinear effects is through digital simulation as presented in Chapter 3. Digital simulation, however, is a limited technique as a design tool since it is too complex for a designer, very expensive in parametric studies and also it is extremely difficult to interpret the results.

Many approximation techniques for representing nonlinear effects which are reviewed in Chapter 1, have been investigated. In this research, the statistical linearization method, described in Chapter 4, has been evaluated as a design tool for rail vehicles. This approximation technique is a compromise between the efficiency of the linear methods and the accuracy of digital simulations. It was shown in Chapter 4 that if the correct probability density function of the input to the nonlinearity is known, then the statistical linearization method provides a perfect representation of the mean and covariance of the system. Unfortunately, these PDF's are not known apriori, and they must be assumed.

In the following sections, the statistical linearization method is evaluated and the results are compared with those of digital simulations presented in Chapter 3. The comparison includes not only the r.m.s. values but also the frequency content of the input to the nonlinearities since natural frequencies and transfer functions are as important to the vehicle designer as r.m.s. values.

5.2 Gaussian Probability Density Functions

If the density functions are unknown, they are usually assumed to have a Gaussian form. This assumption is based on the "filter hypothesis" which appeals to the central theorem for validity, however, Beaman [35] has shown that the filter hypothesis can give misleading results in nonlinear random systems.

If the probability density functions of the inputs to the nonlinearities are assumed to be Gaussian equation (4.17) reduces to:

$$K_{eq} = \frac{1}{\sqrt{2\pi}\,\sigma_x^3} \int_{-\infty}^{\infty} x f(x) \exp(-\frac{x^2}{2\sigma_x^2}) dx \qquad (5.1)$$

Using equation (5.1), the equivalent gains for the nonlinearities can be found as follows.

Wheel/Rail Profile Nonlinearities

The equivalent gains for the nonlinearities given by equations (4.37) to (4.41) are given by equations (4.47) to (4.51).

Wheel/rail profile data for a wide variety profile types and gauges are available in reference [23]. Figures 5.1 and 5.2 show the equivalent gains obtained by integrating equations (4.47) and (4.49) numerically.

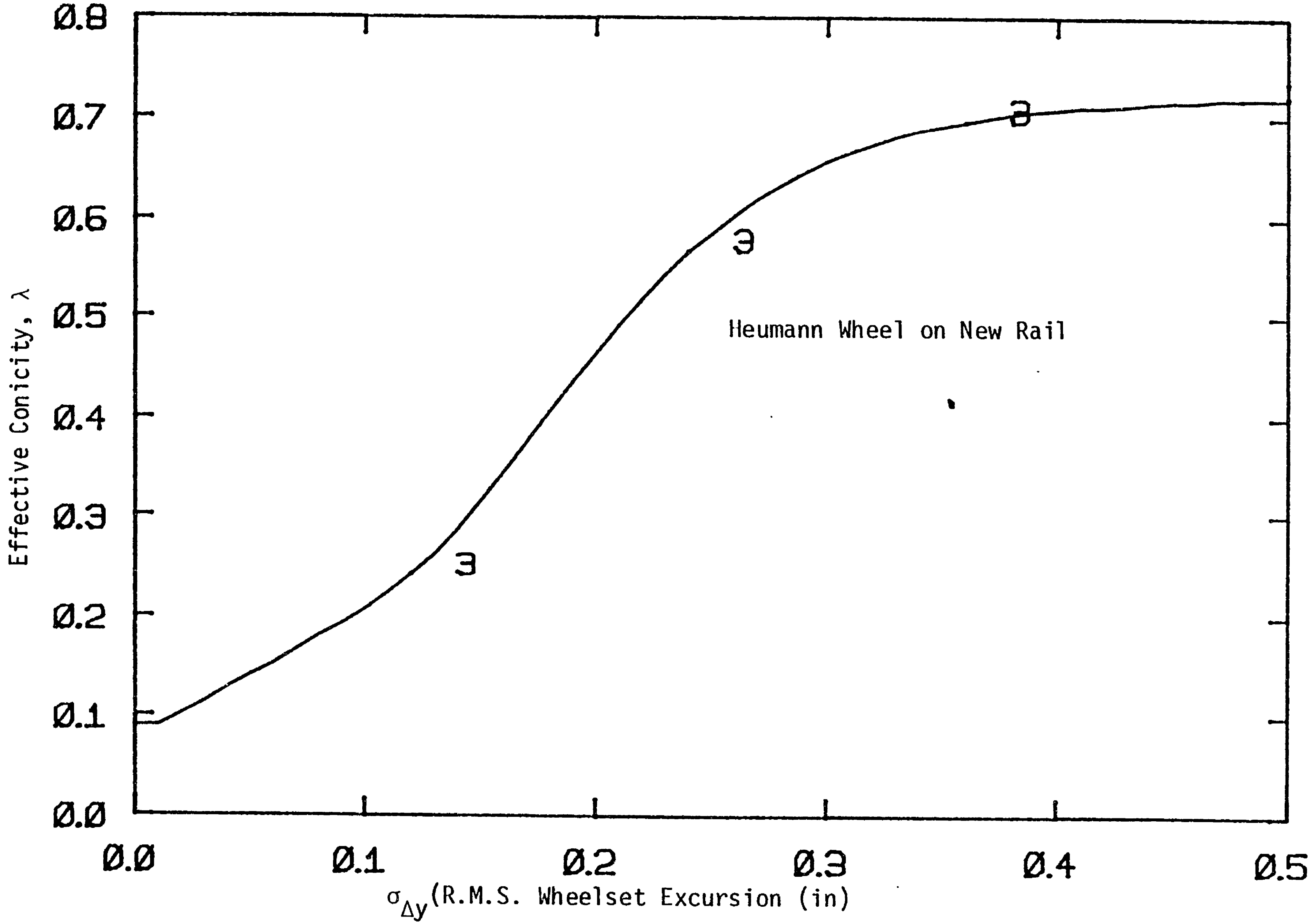

FIGURE 5.1: STATISTICALLY LINEARIZED EFFECTIVE CONICITY

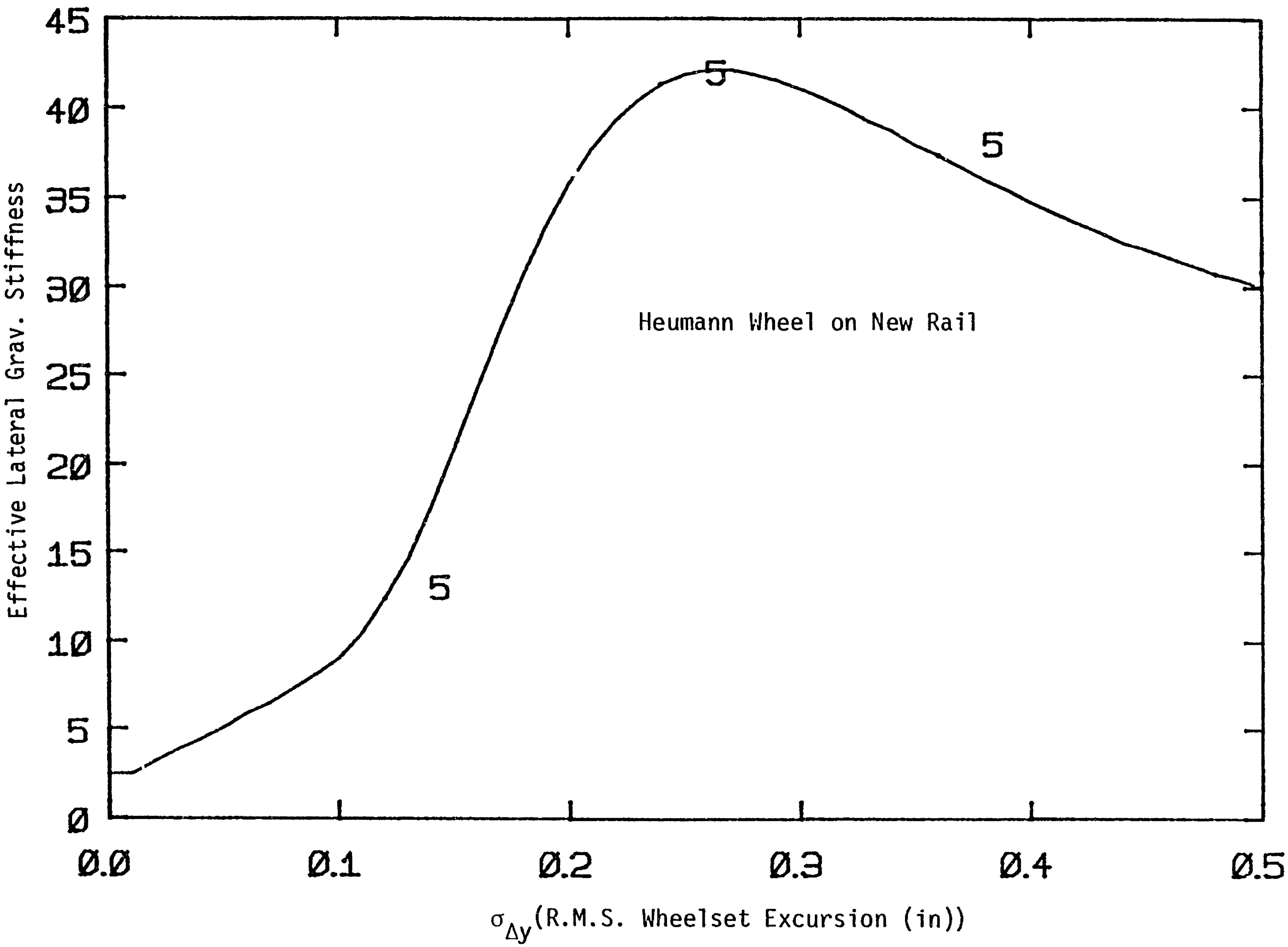

FIGURE 5.2: STATISTICALLY LINEARIZED LATERAL GRAVITATIONAL STIFFNESS

Suspension Nonlinearities:

The equivalent gains for a deadband spring, linear hardening spring and Coulomb damper are given by equations (4.53), (4.55) and (4.58). Figure 5.3 shows the "effective" spring constant for a deadband spring.

The twelve degrees of freedom statistically linearized equations with Gaussian equivalent gains were implemented on a digital computer to predict the response of the model to random alignment inputs. The output of the program was r.m.s. values of the inputs to the nonlinearities, transfer functions, power spectral densities, mass, stiffness, and damping matrices, and eigenvalue/eigenvectors of the equivalent linear system after convergence has been obtained.

5.2.1 Low Speed Run (40 mph)

The frequency range chosen was 0.4 to 10 Hz with 50 frequency points. The frequency points were equally spaced in $\log_{10}$ scale and convergence was achieved after 7 iterations. The results are compared to the digital simulation presented in Chapter 3.

Table 5.1 shows the comparison of the r.m.s. values, and Figures 5.4 to 5.6 show the wheelset excursion PSD's obtained from the digital simulation and statistical linearization.

The results presented in Table 5.1 and in Figures 5.4 to 5.6 can be summarized as follows:

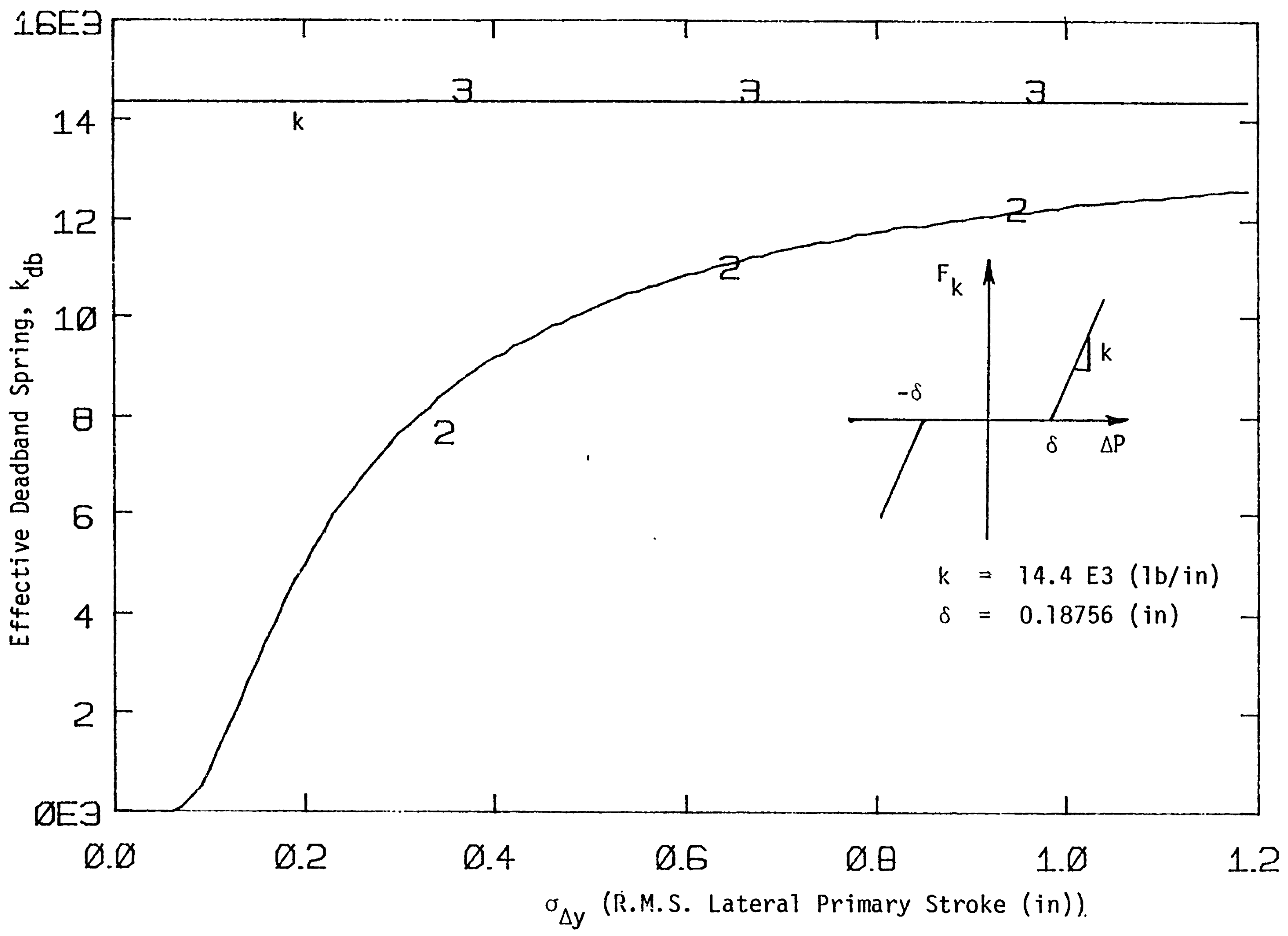

FIGURE 5.3: STATISTICALLY LINEARIZED DEADBAND SPRING STIFFNESS

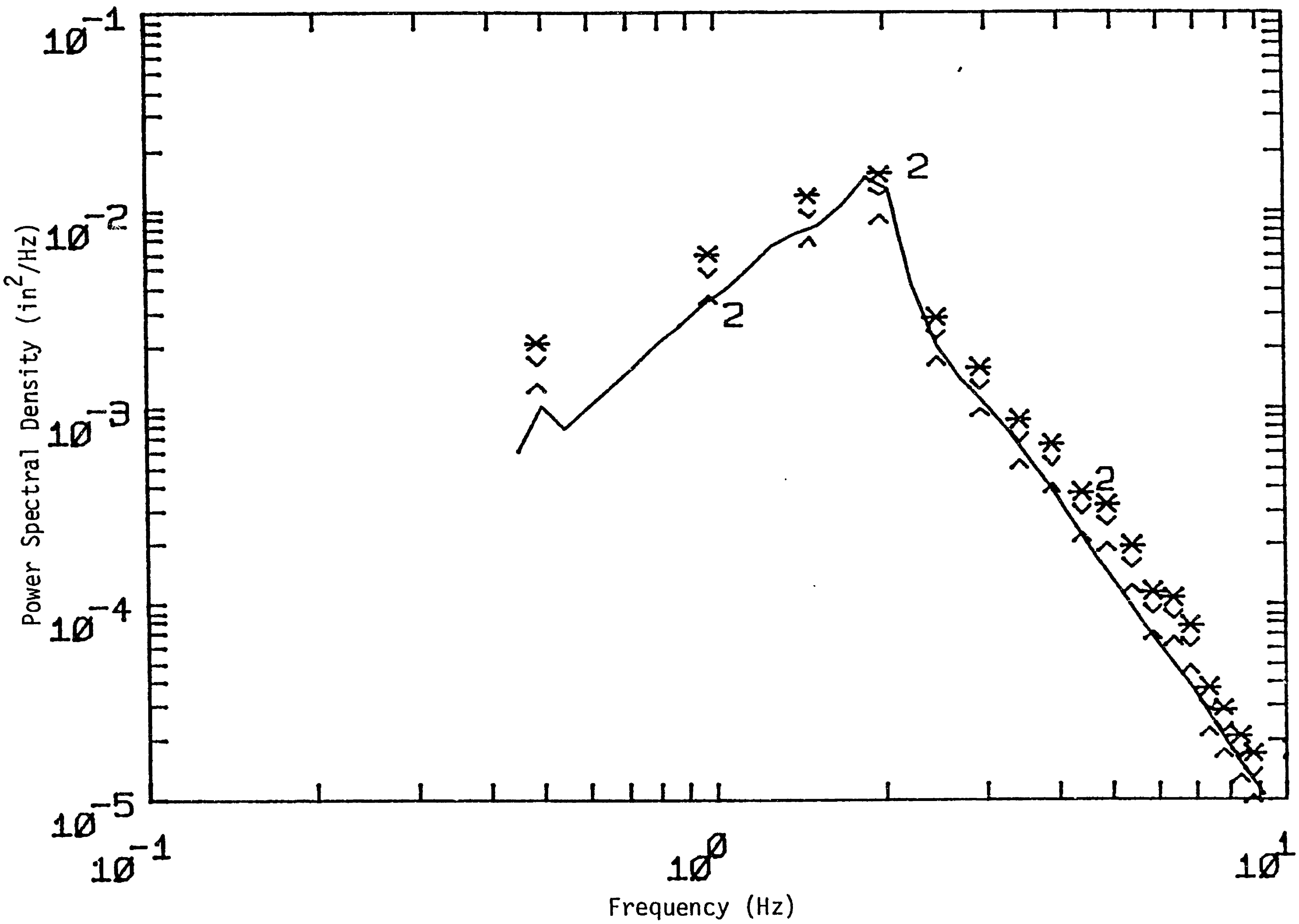

FIGURE 5.4: LEADING WHEELSET EXCURSION PSD AT 40 MPH

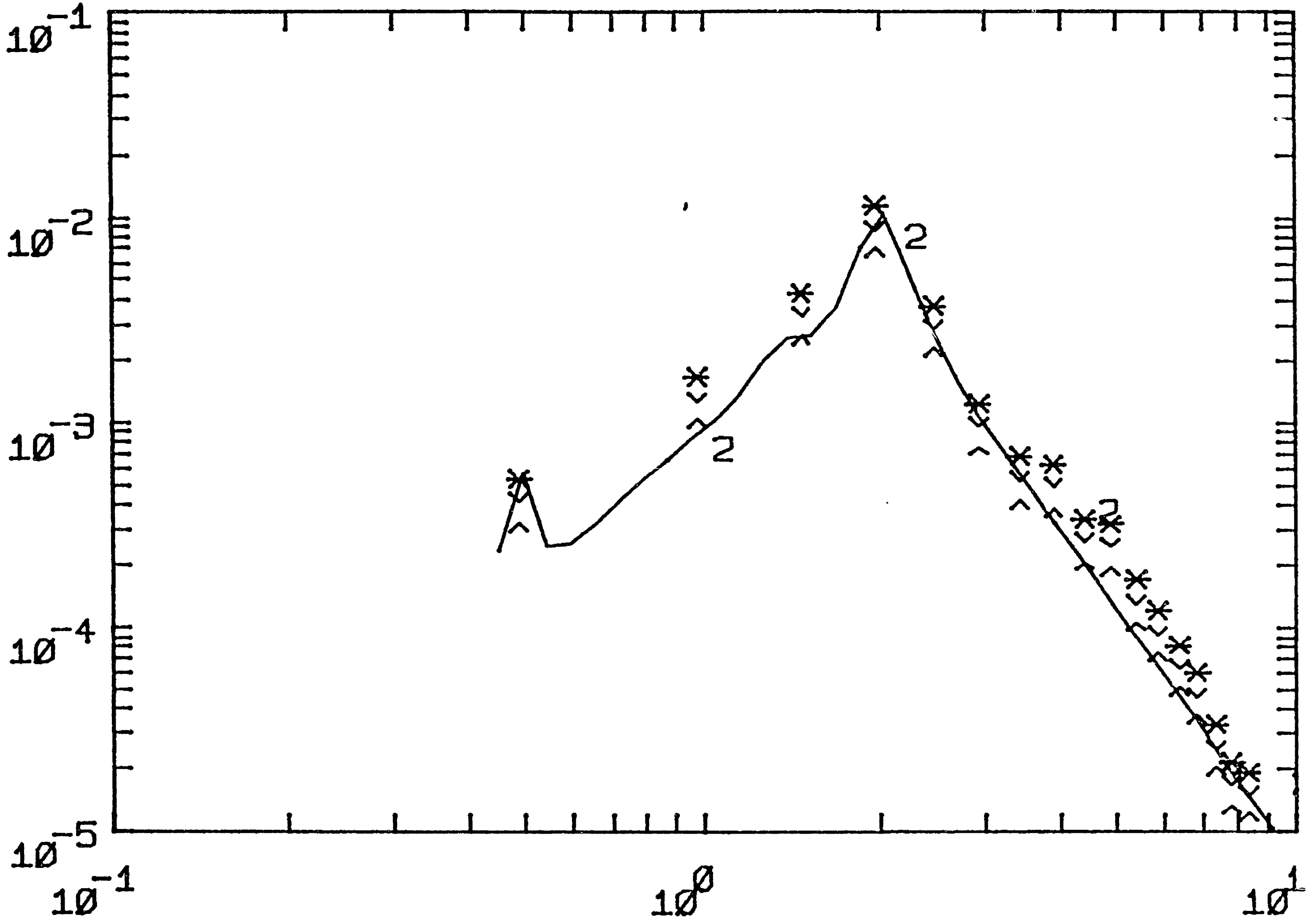

FIGURE 5.5: MIDDLE WHEELSET EXCURSION PSD AT 40 MPH

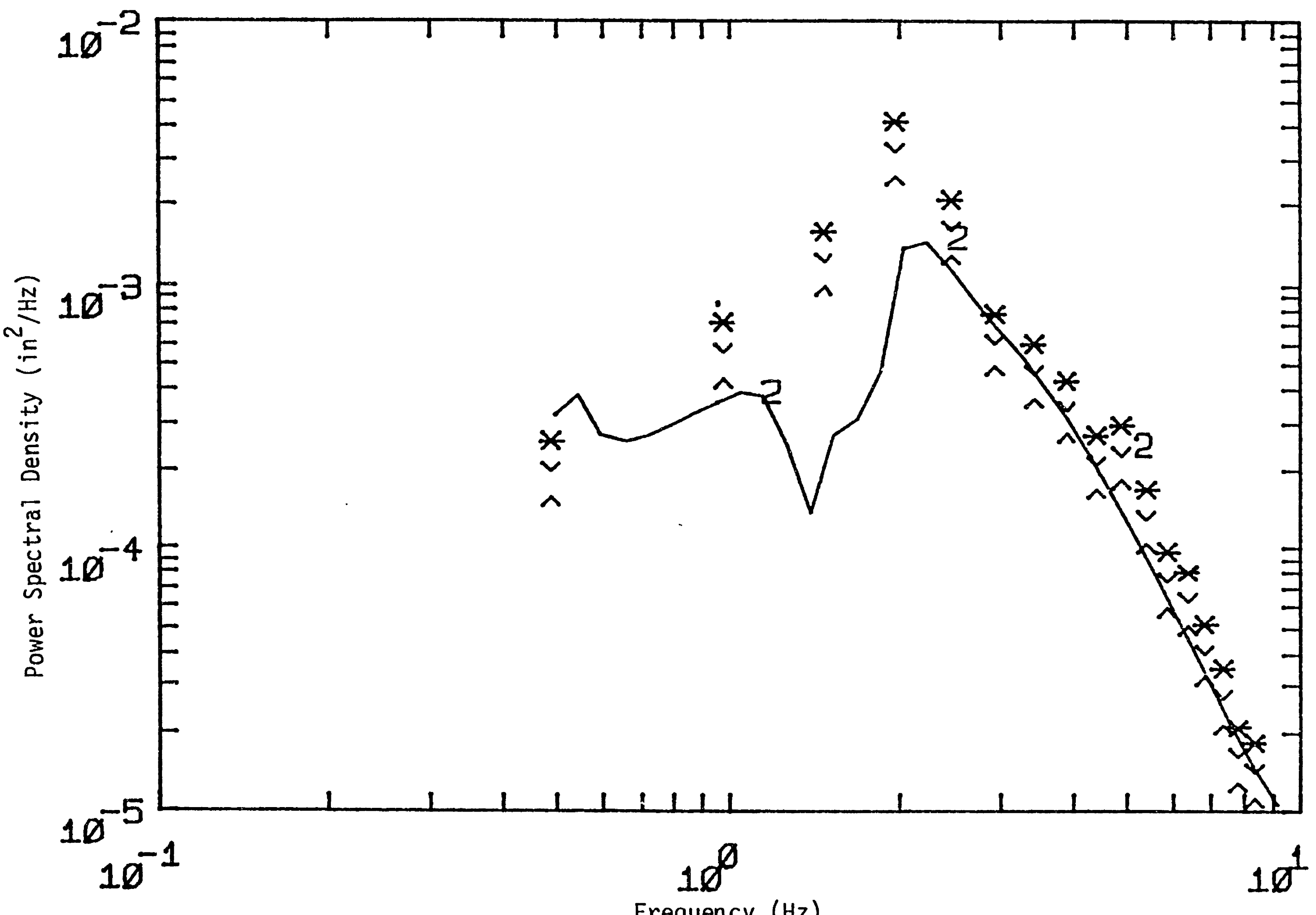

FIGURE 5.6: TRAILING WHEELSET EXCURSION PSD AT 40 MPH

TABLE 5.1: COMPARISON OF DIGITAL SIMULATION AND GAUSSIAN STATISTICAL LINEARIZATION RESULTS AT 40 MPH (RMS Values, inches)

40 MPH	Wheelset Excursions			Lateral Primary Stroke Length		
	#1	#2	#3	#1	#2	#3
Digital	0.12474	0.096578	0.066809	0.18375	0.18563	0.21616
Gaussian	0.12492	0.09809	0.05579	0.16602	0.18006	0.22215
% Difference	0.1	1.5	16	9.6	3	2.6

• The maximum difference in r.m.s. values is in the trailing wheelset. The peak value in the digital simulation ($3\sigma \approx 0.167$ inches) is less than the axle clearance of 0.18756 inches. This shows that the trailing wheelset can move almost "freely" within the deadband. As far as a vehicle design is concerned, this value is not important due to its small size. Therefore it can be concluded that the r.m.s. values are predicted quite well.

• Figures 5.4 to 5.6 show that the spectral density of the statistically linearized system is very close to that of digital simulation. For the first and second wheelset the PSD's of the system fall within the 90% confidence interval at most of the frequencies. These show that statistical linearization is predicting not only the r.m.s. values but also the shape of the power spectrum. Specifically, the location of the peaks and the decay rates are predicted quite accurately.

5.2.2 High Speed Run (60 Mph)

The frequency range and frequency points selected were the same as that for the 40 mph analysis and convergence was achieved after 8 iterations. Table 5.2 shows the comparison of the r.m.s. values.

TABLE 5.2: COMPARISON OF DIGITAL SIMULATION AND GAUSSIAN STATISTICAL LINEARIZATION RESULTS AT 60 MPH (RMS Values, inches)

	WHEELSET EXCURSIONS			LATERAL PRIMARY STROKE LENGTH		
60 MPH	#1	#2	#3	#1	#2	#3
Digital	0.17014	0.15958	0.13771	0.28565	0.24280	0.35139
Gaussian	0.14887	0.12900	0.094359	0.22224	0.21657	0.27831
% Difference	12	19	31	22	10.8	20.8

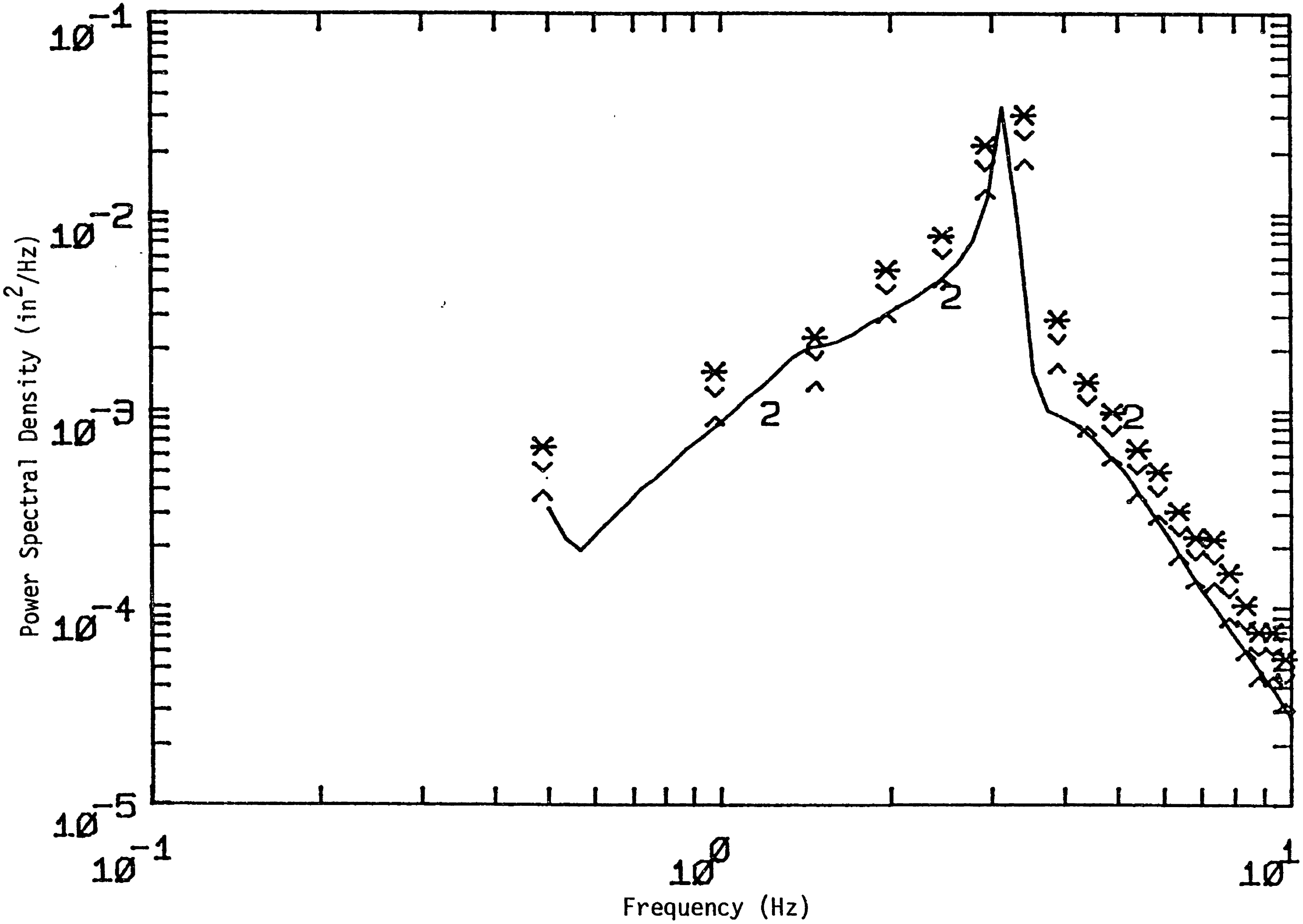

FIGURE 5.7: LEADING WHEELSET EXCURSION PSD AT 60 MPH

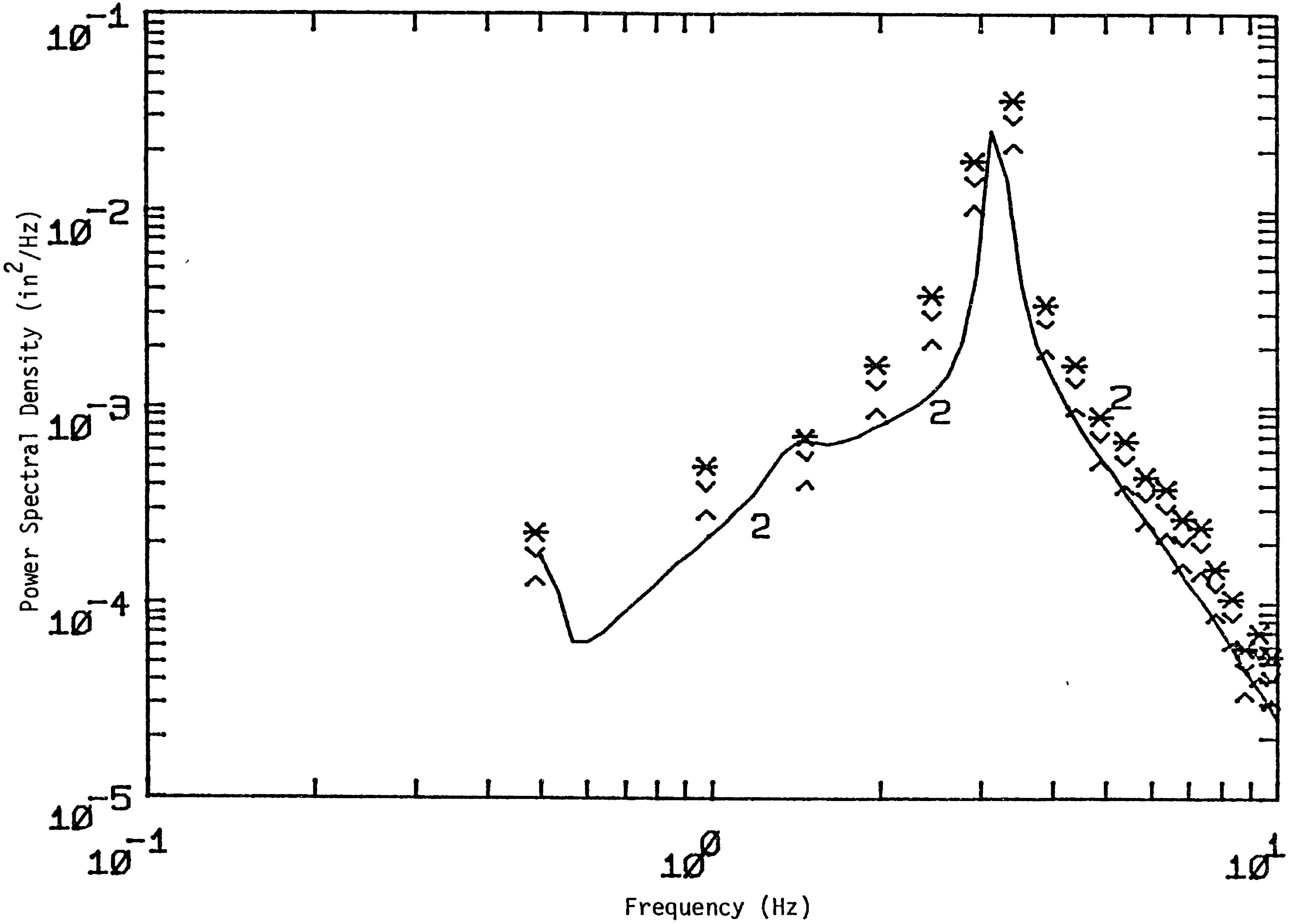

FIGURE 5.8: MIDDLE WHEELSET EXCURSION PSD AT 60 MPH

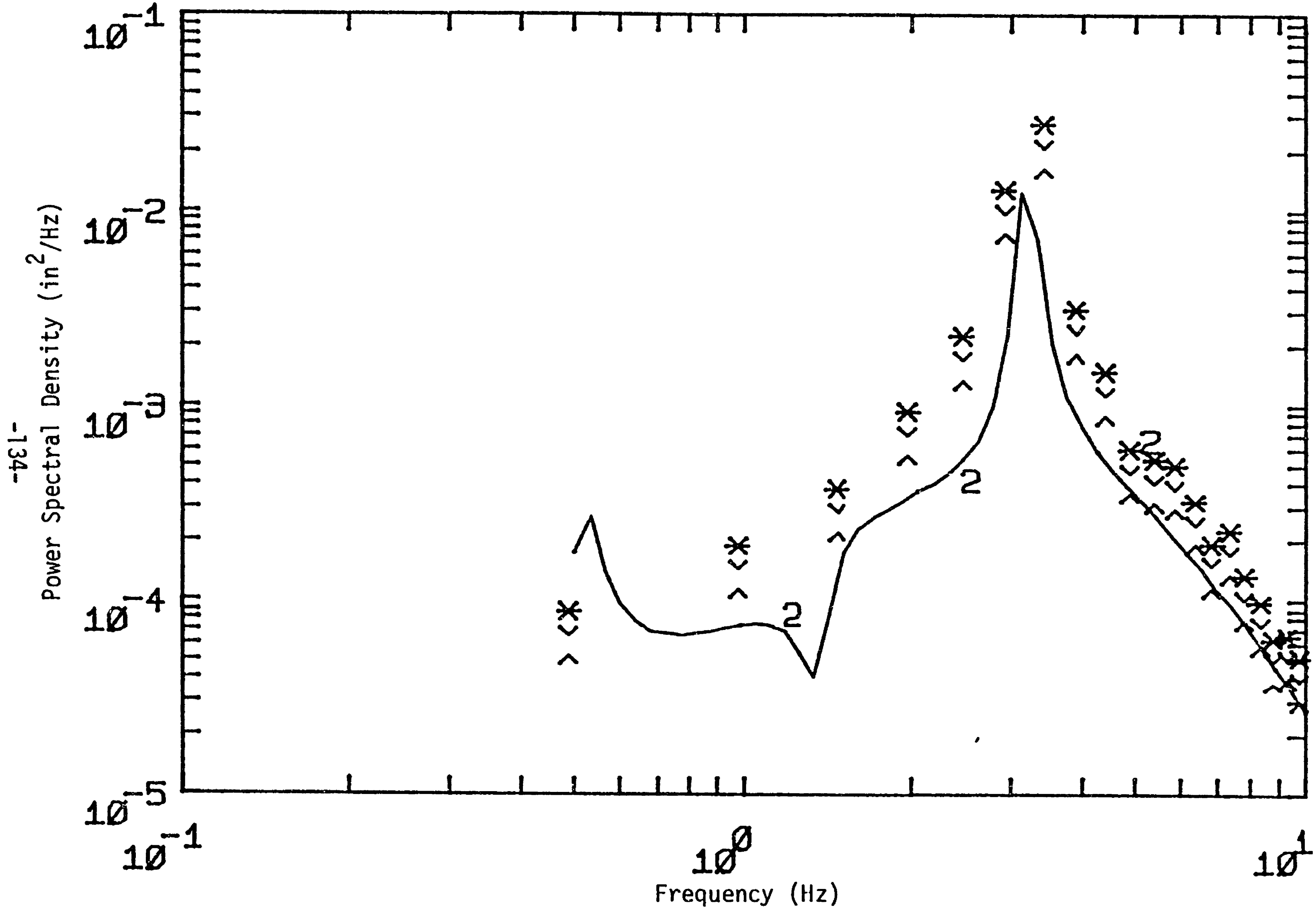

FIGURE 5.9: TRAILING WHEELSET EXCURSION PSD AT 60 MPH

Figures 5.7 to 5.9 show the wheelset excursion PSD's obtained from the digital simualtion and statistical linearization at 60 mph. These figures indicate that despite the big differences in excursion r.m.s. values the prediction of the shape of power spectrum and specifically the peaks are very good. But the differences in the r.m.s. values are as much as 31%. In addition, if we assume that the digital results are correct, the statistical linearization method underestimates the correct value which is not good from a design point of view.

5.3 Trapezoidal Probability Density Functions

The Gaussian density function assumption for the inputs to the nonlinearities is simple to use, however, the results are not acceptable in predicting the performance of the lateral half carbody locomotive model due to the 31% difference in results between the predicted r.m.s. values by Gaussian statistical linearization method and digital simulations.

In this section, the trapezoidal probability density function and its degenerate forms, i.e., triangular and rectangular, are proposed and applied to the twelve d.o.f. lateral half carbody locomotive model. The choice of trapezoidal PDFs and its degenerate forms is based on the type of nonlinearities which exist in the model.

The exact steady-state probability density function for any first order nonlinear system excited by white noise can be determined by the direct integration of the Fokker-Planck equaton [27]. For a stochastic differential equation of the type

$$\dot{x} = -f(x) + w(t)$$

where w(t) = white noise

the steady state probability density function is

$$P(x) = C^{-1} \exp[-\int_0^x f(\xi)D\, d\xi]$$

where D = positive constant

$$C = \int_{-\infty}^{\infty} \exp[-\int_0^x f(\xi)\, Dd\xi]dx$$

The probability density function of a first order system with a deadband nonlinearity is shown in Figure 5.10.a.

Figure 5.10.b shows a trapezoidal density function. The choice of the trapezoidal density function is based on the need for the continuity in the PDF's as the r.m.s. value increases.

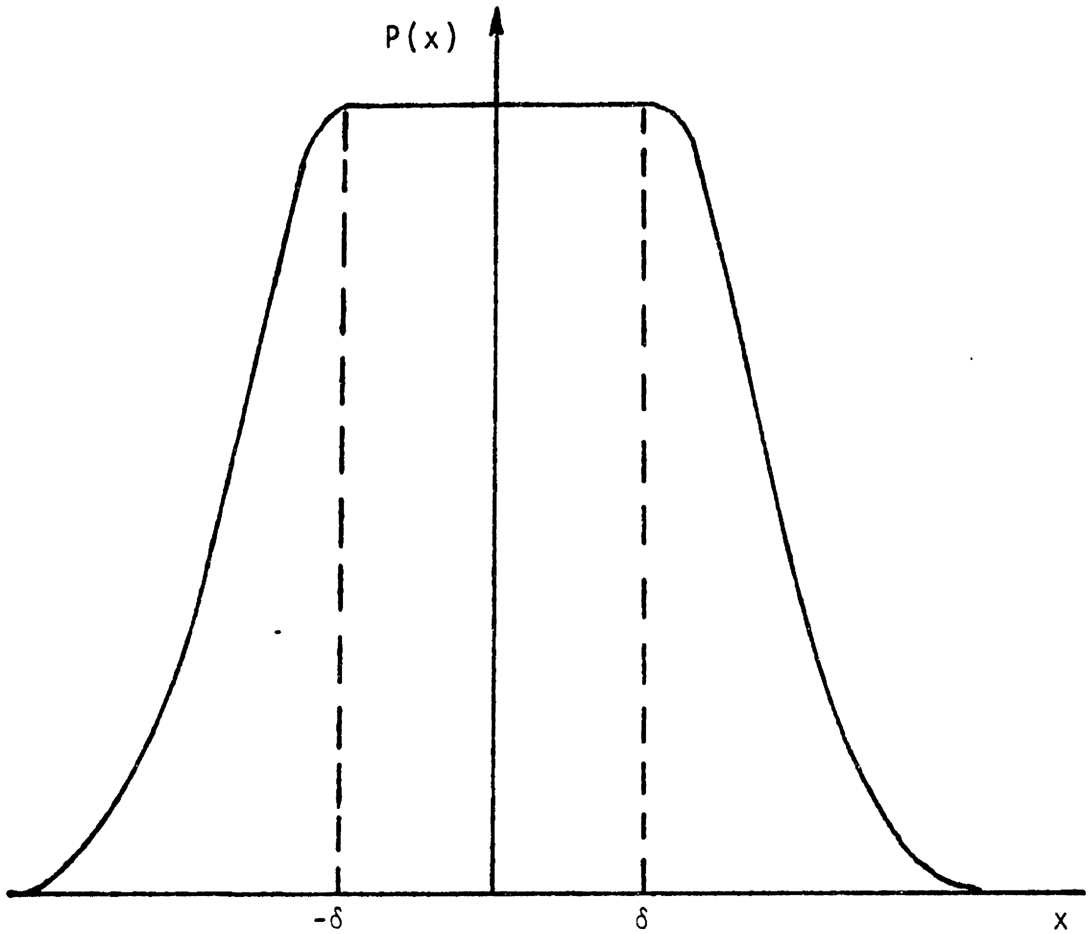

$$P(x) = \begin{cases} C^{-1} & |x| < \delta \\ C^{-1}\exp(-D/2(x-\delta)^2) & |x| > \delta \end{cases}$$

where C and D are constants.

FIGURE 5.10.a: PDF OF A FIRST ORDER SYSTEM WITH DEADBAND NONLINEARITY

The variance of the trapezoidal density function is given by:

$$\sigma^2 = \int_{-b}^{b} x^2 \, p(x)dx$$

$$= \frac{a^2 + b^2}{6} \qquad (5.2)$$

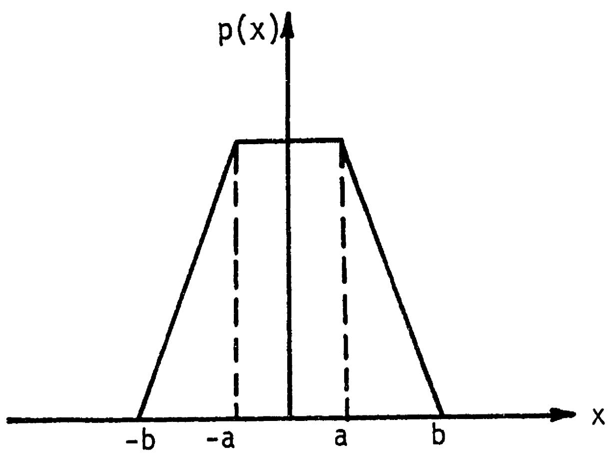

FIGURE 5.10.b: TRAPEZOIDAL DENSITY FUNCTION

In order to have a probability density function which is a function of one variable either a or b should be fixed. The important non-linearities in the locomotive equations are the ones which have wheelset excursions and lateral primary strokes as inputs. Therefore, the choice of the fixed parameter in the probability density function is based on the characteristics of these two inputs.

Because of the axle clearance in the lateral primary suspension, the lateral primary stroke has the same probability of being at any point within the axle clearance of δ. Thus the fixed parameter of the trapzeoidal density function, a, can be chosen to be equal to the axle clearance.

The choice of the fixed parameter in the trapezoidal density function for wheelset excursion is not as easy as that of the lateral primary stroke. The lateral motion of the wheelset can roughly be represented as shown in Figure 5.11.

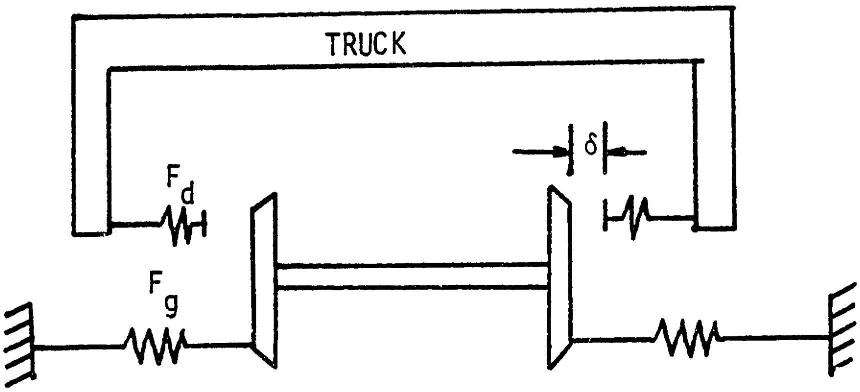

F_d = deadband spring
F_g = gavitational stiffness force

FIGURE 5.11: SIMPLE TRUCK-WHEELSET LATERAL MODEL

The characteristics of the deadband spring and the gravitational stiffness are shown below.

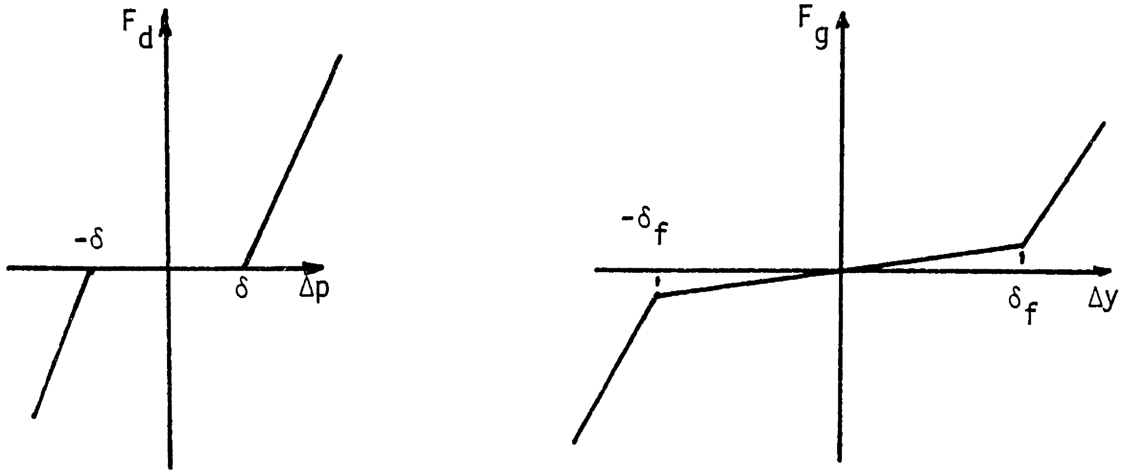

where δ = axle clearance

δ_f = flange clearance

The total lateral spring force acting on the wheelset is a combination of these forces. Then, the first stop that the wheelset experiences depends on the magnitude of the axle clearance, flange clearance and the speed of the vehicle, in other words, the r.m.s. wheelset excursions.

The model selected for the validation of the statistical linearization has the following axle and flange clearances.

Axle clearance, δ = 0.18756 inches

Flange clearance, δ_f = 0.36 inches

Therefore, the following discussion on the choice of the first stop for the wheelset excursion is based on the knowledge that the axle clearance is less than the flange clearance. Similar arguments can be made for other combination of clearances.

From a rail vehicle designer's point of view, the approximate method should predict the extreme cases like high r.m.s. wheelset excursions and r.m.s. lateral primary stroke lenghts to reduce the amount of flanging and spring bottoming. In rail vehicles, these extreme cases occur at high speeds where the natural frequency (kinematic) of the wheelset is 2-5 times that of the truck lateral motion. Therefore, the first stop that the wheelset experiences is, most of the time, due to the axle clearance when $\delta < \delta_f$. Also, as explained in Section 5.1, the critical speed of 5 mph for the vehicle with zero lateral primary stiffness indicates that even at low speeds, 20-40 mph, the vehicle uses up the available primary stroke clearance in order to generate an effective lateral primary stiffness for stability at all speeds.

In summary, the fixed value of the trapezoidal, density function, a, was chosen to be equal to the axle clearance. Then the value of b can be determined from:

$$b = \sqrt{6\sigma^2 - \delta^2} \tag{5.3}$$

Figure 5.12 shows the trapezoidal density functions and its degenerate forms as the r.m.s. value changes. Note that for the lateral primary stroke only Case 5 can exist whereas the wheelset excursion can have all the possibilities depending on the r.m.s. wheelset excursion. The occurrence of the degenerate forms of the trapezoidal PDFs for the wheelset excursion is based on the need for the continuity in the PDFs as the r.m.s. value increases so that a continuous equivalent gain tables can be prepared without any smoothing and/or curve fitting.

The change from one form to another can be described as follows. For a low r.m.s. value, Case 1, the PDFs for wheelset excursions are given by the Gaussian density function, as explained in Section 3.4, and it can be approximated by triangular PDFs. Figure 5.15 shows the PDFs of the trailing wheelset excursion at 40 mph. Note that in this case a is free and is determined by:

$$a = \sqrt{6}\ \sigma \tag{5.4}$$

As the velocity increases, the r.m.s. value increases and the peak value, a, reaches the value of the axle clearance, δ, which is shown as Case 2 in Figure 5.12. A further increase in speed, Case 3, does not increase the peak value, δ, but the PDF becomes flat and the

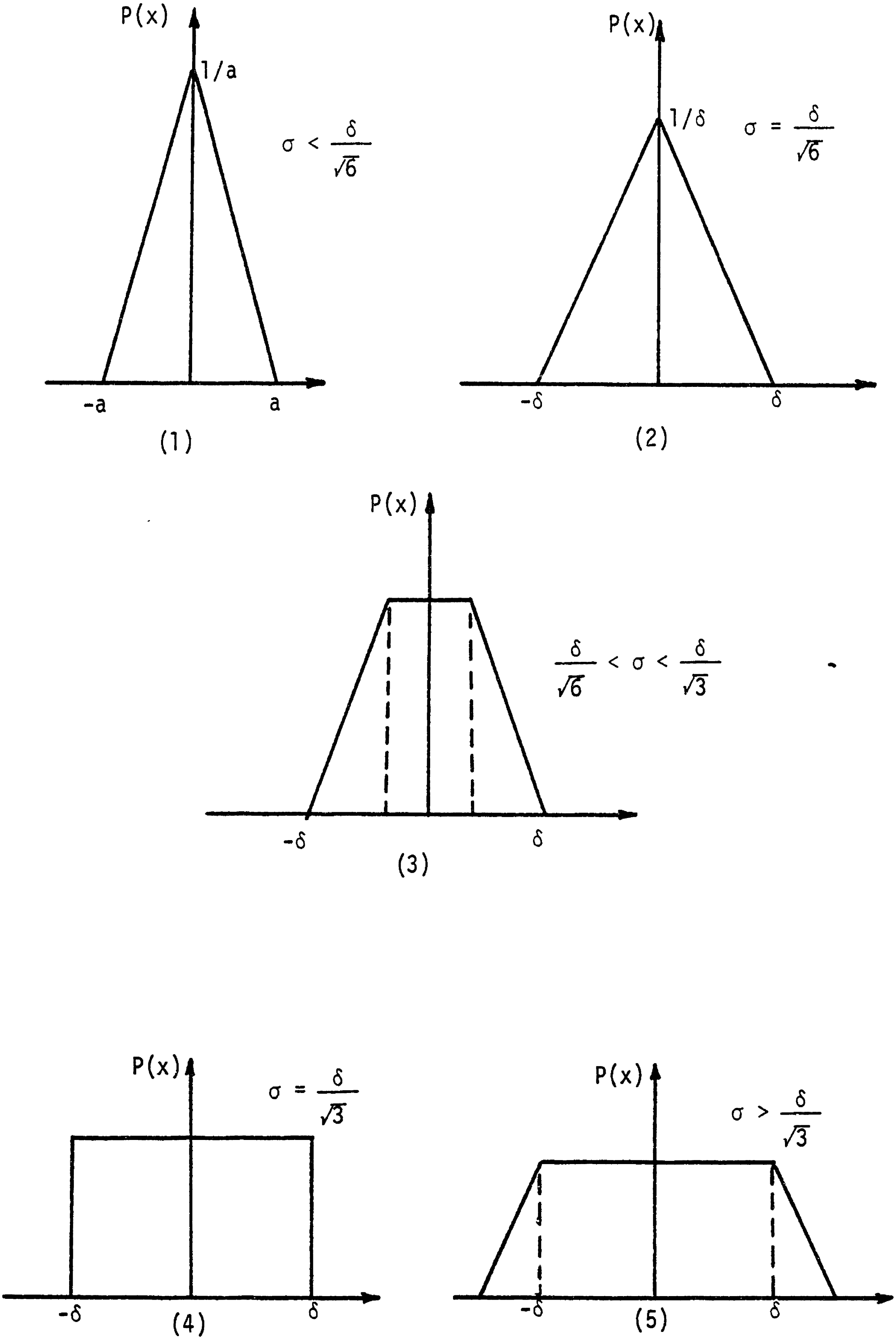

FIGURE 5.12: TRAPEZOIDAL DENSITY FUNCTION AND ITS DEGENERATE FORMS

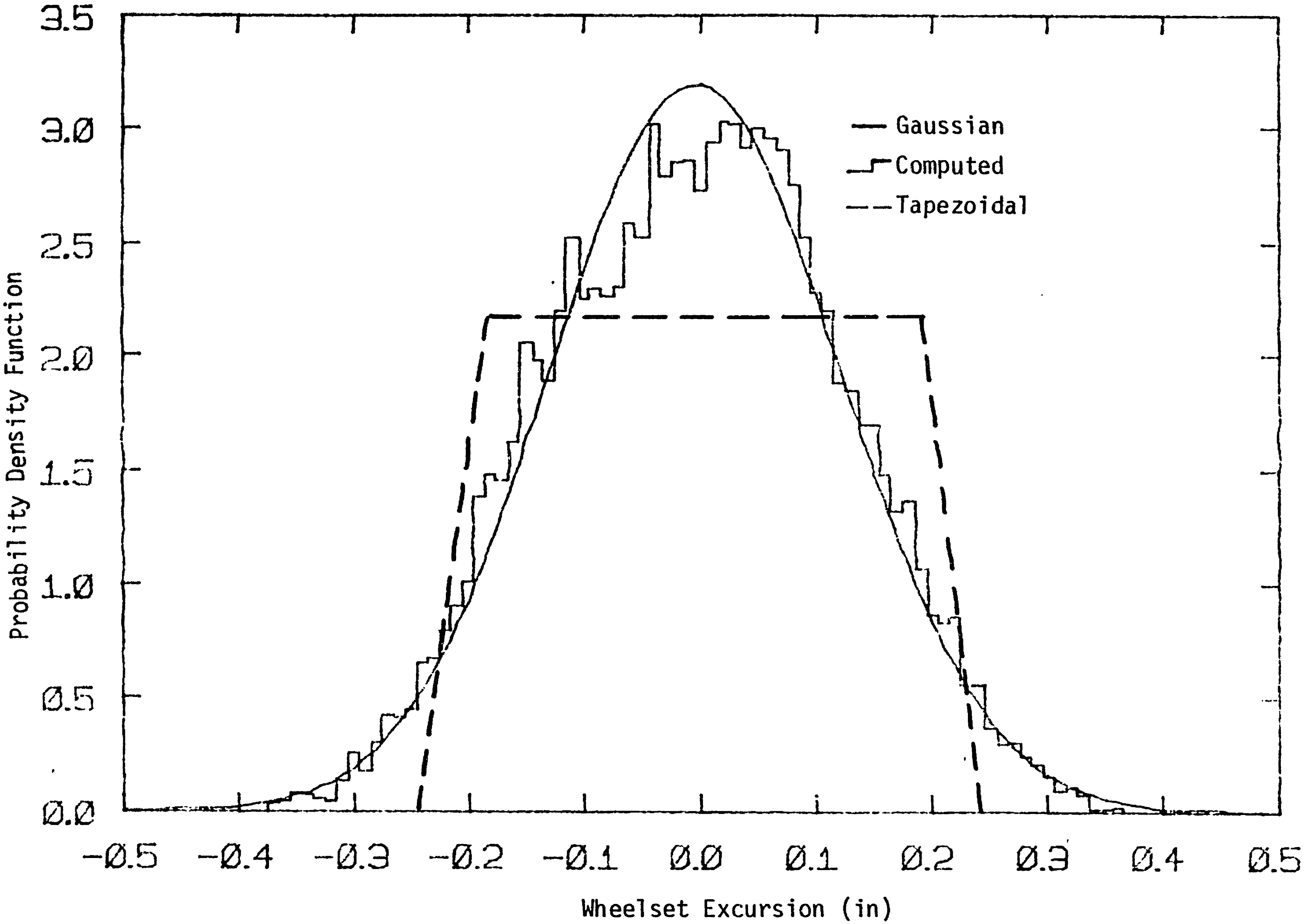

FIGURE 5.13: LEADING WHEELSET AT 40 MPH

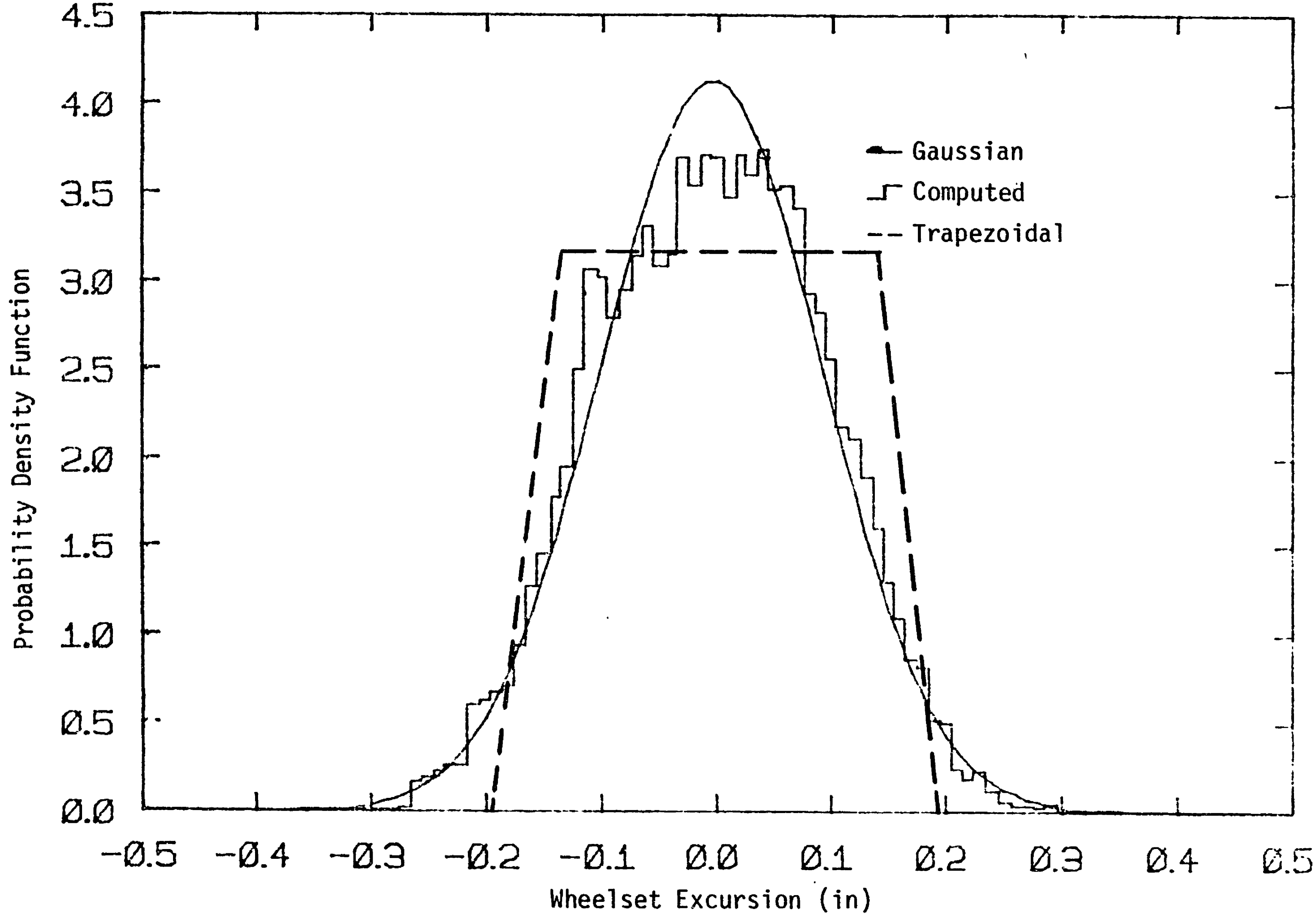

FIGURE 5.14: MIDDLE WHEELSET AT 40 MPH

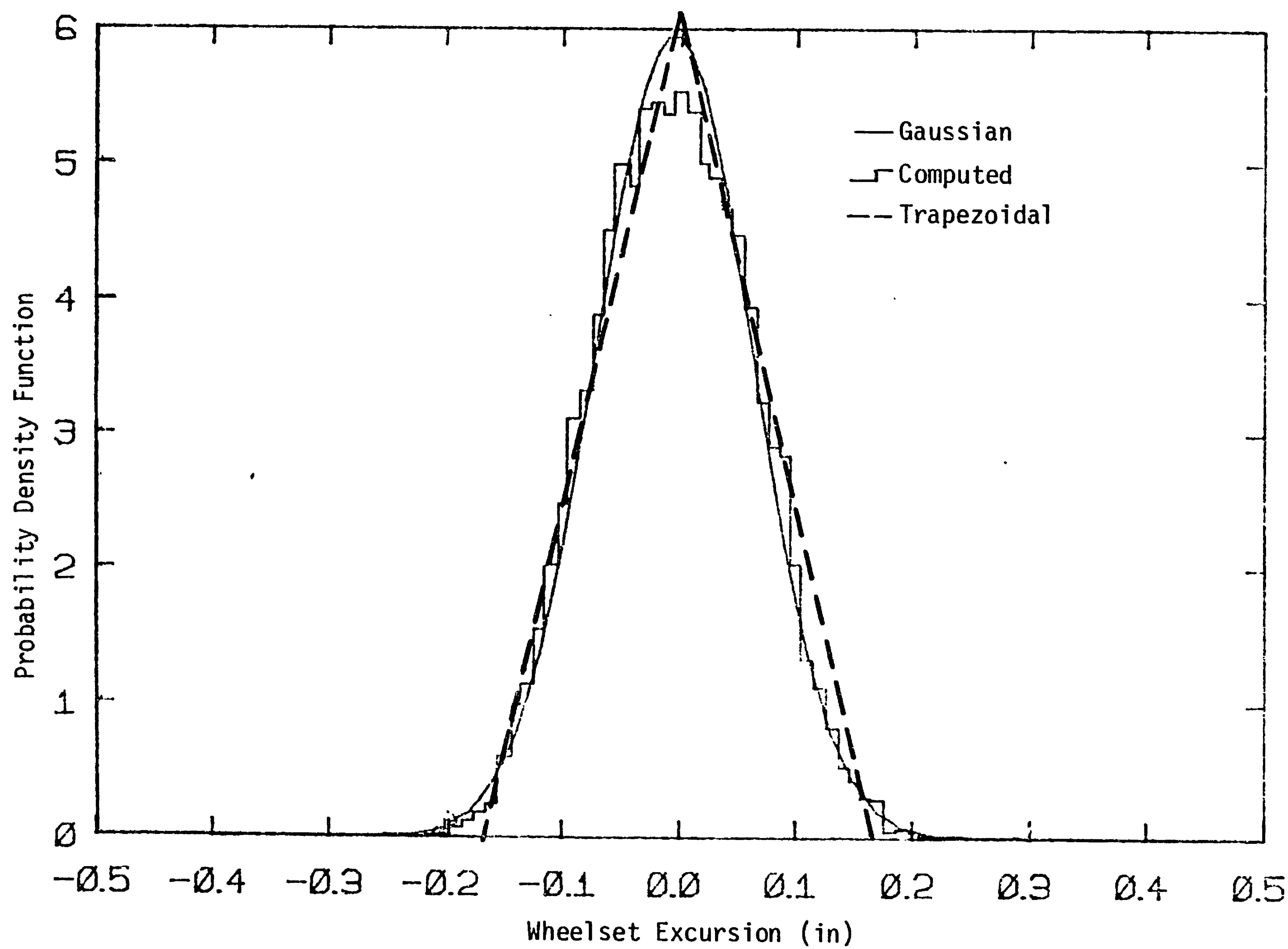

FIGURE 5.15: TRAILING WHEELSET AT 40 MPH

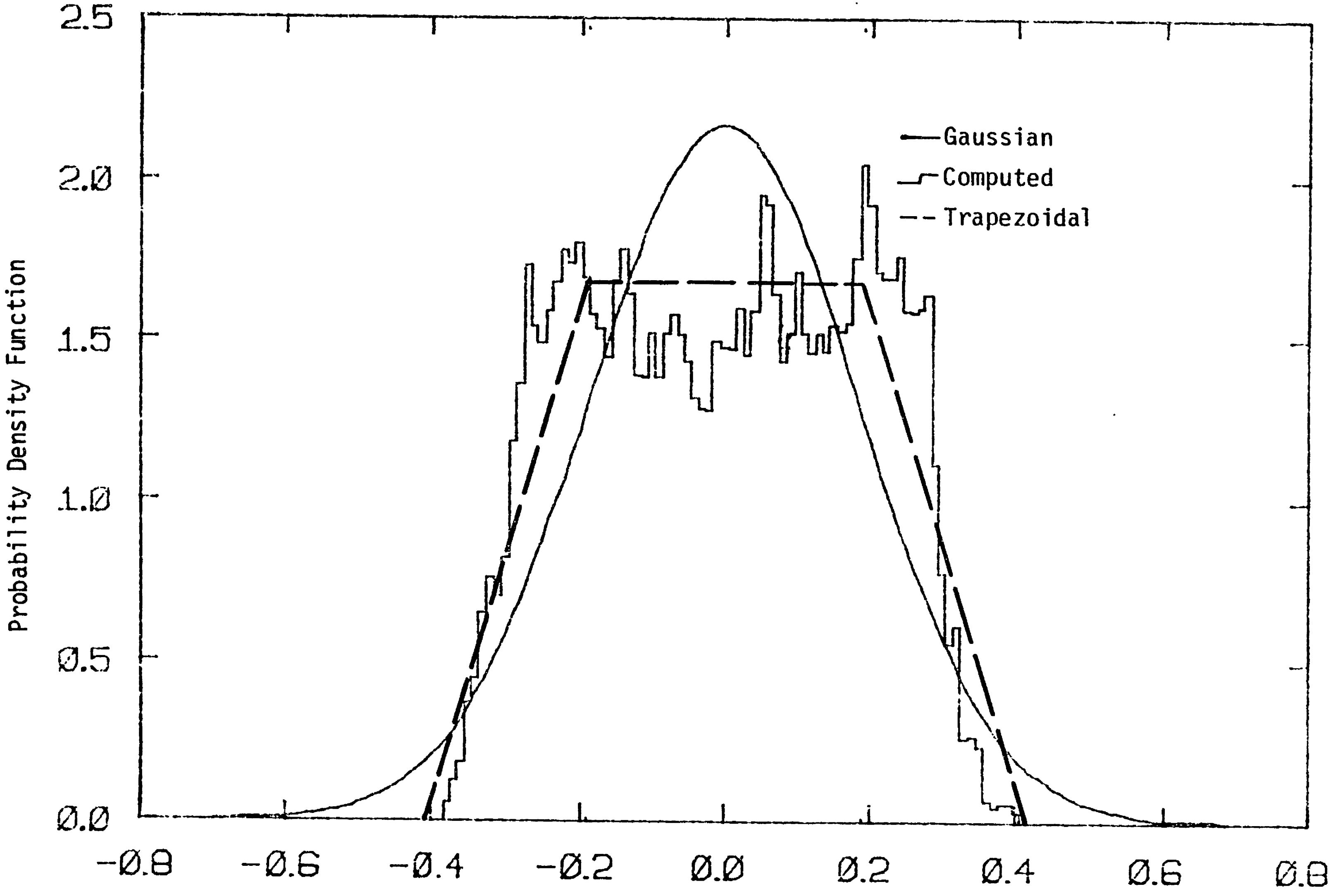

FIGURE 5.16: LEADING WHEELSET AT 40 MPH

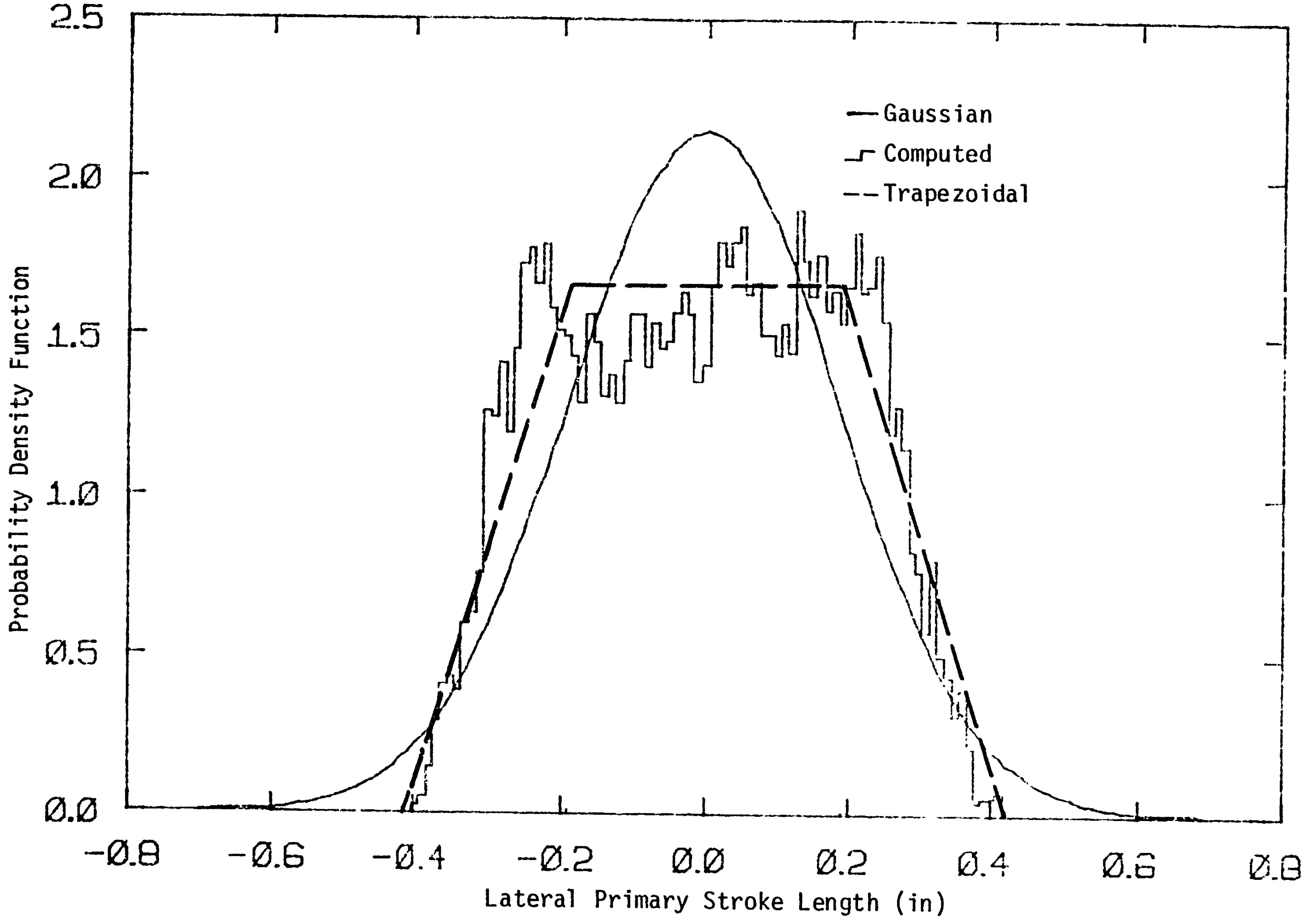

FIGURE 5.17: MIDDLE WHEELSET AT 40 MPH

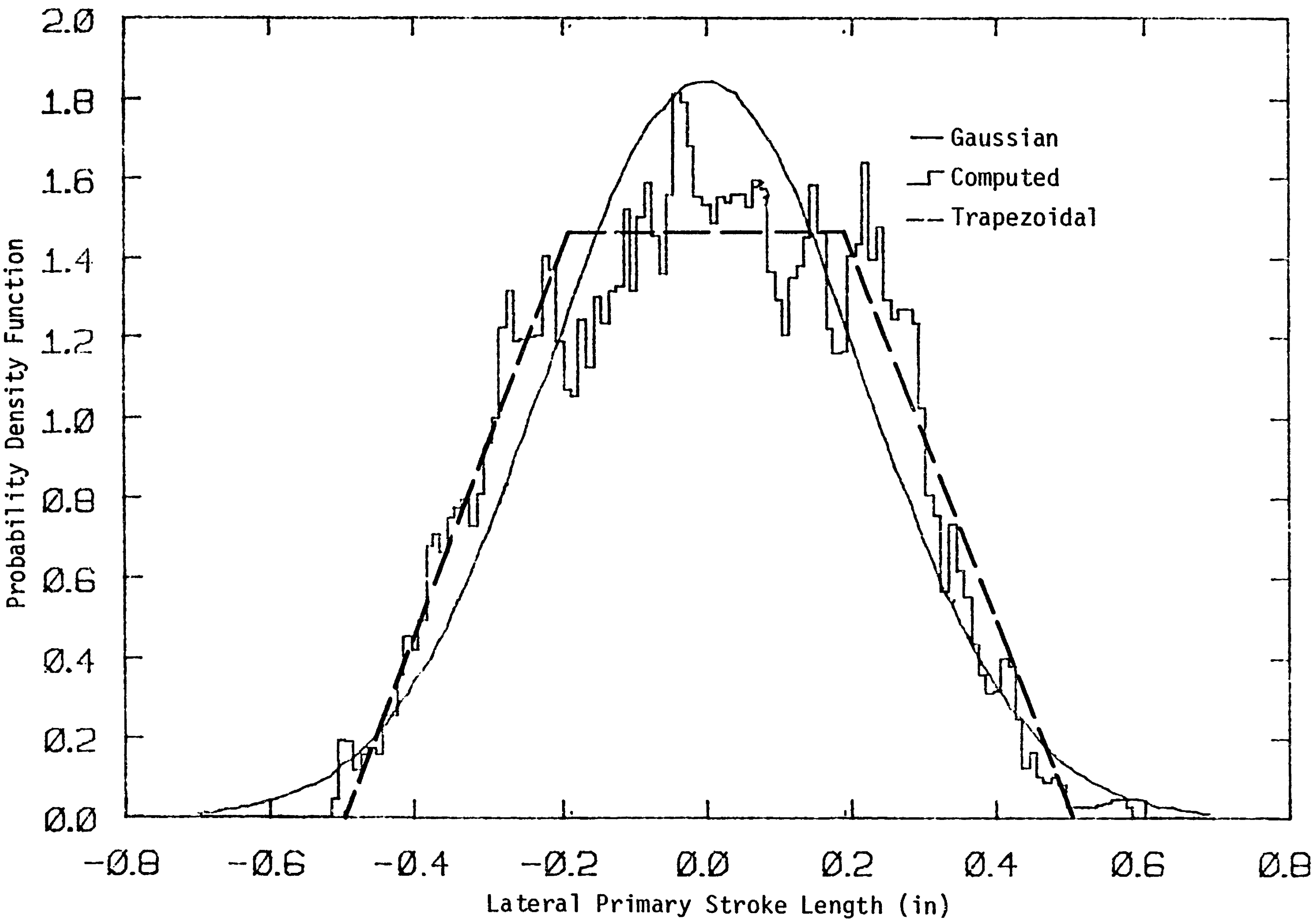

FIGURE 5.18: TRAILING WHEELSET AT 40 MPH

range of flatness is given by the parameter b which can be computed from equation (5.3). The extreme of Case 3 is shown as Case 4 which is the uniform density function where $\sigma = \frac{\delta}{\sqrt{3}}$. Finally, Case 5 corresponds to the r.m.s. value which is greater that $\frac{\delta}{\sqrt{3}}$.

In summary, the form of the density function should be chosen from Figure 5.12 depending on the magnitude of the r.m.s. value of the input to the nonlinearity.

Figures 5.13 to 5.18 show the comparison of the trapezoidal density functions with the digital and Gaussian density functions at 40 mph and Figures 5.19 to 5.24 show the comparison of PDFs at 60 mph. The best feature of the trapezoidal density function is in predicting the peak values closely for high r.m.s. values.

5.3.1 Application to the Half Carbody Locomotive Model

5.3.1.1 Wheel/Rail Nonlinearities

The effective gains given by equations (4.47) to (4.51) were computed using the trapezoidal PDFs and its degenerate forms. Figure 5.25 shows the effective conicity which is obtained by integrating equation (4.17) numerically.

5.3.1.2 Effective Stiffness for the Deadband Spring

The effective gain for the deadband spring is given by equation 4.17, i.e.,

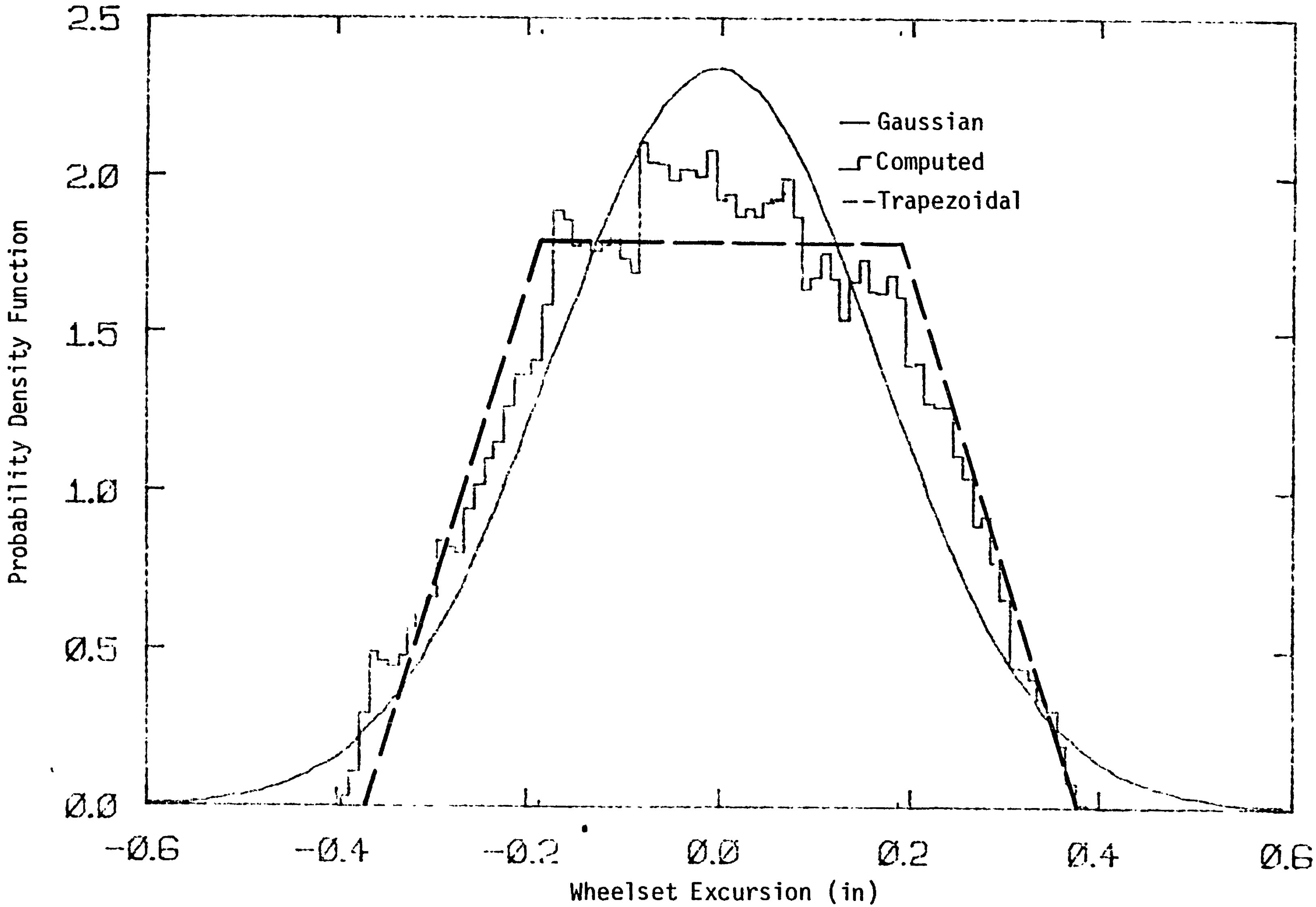

FIGURE 5.19: LEADING WHEELSET AT 60 MPH

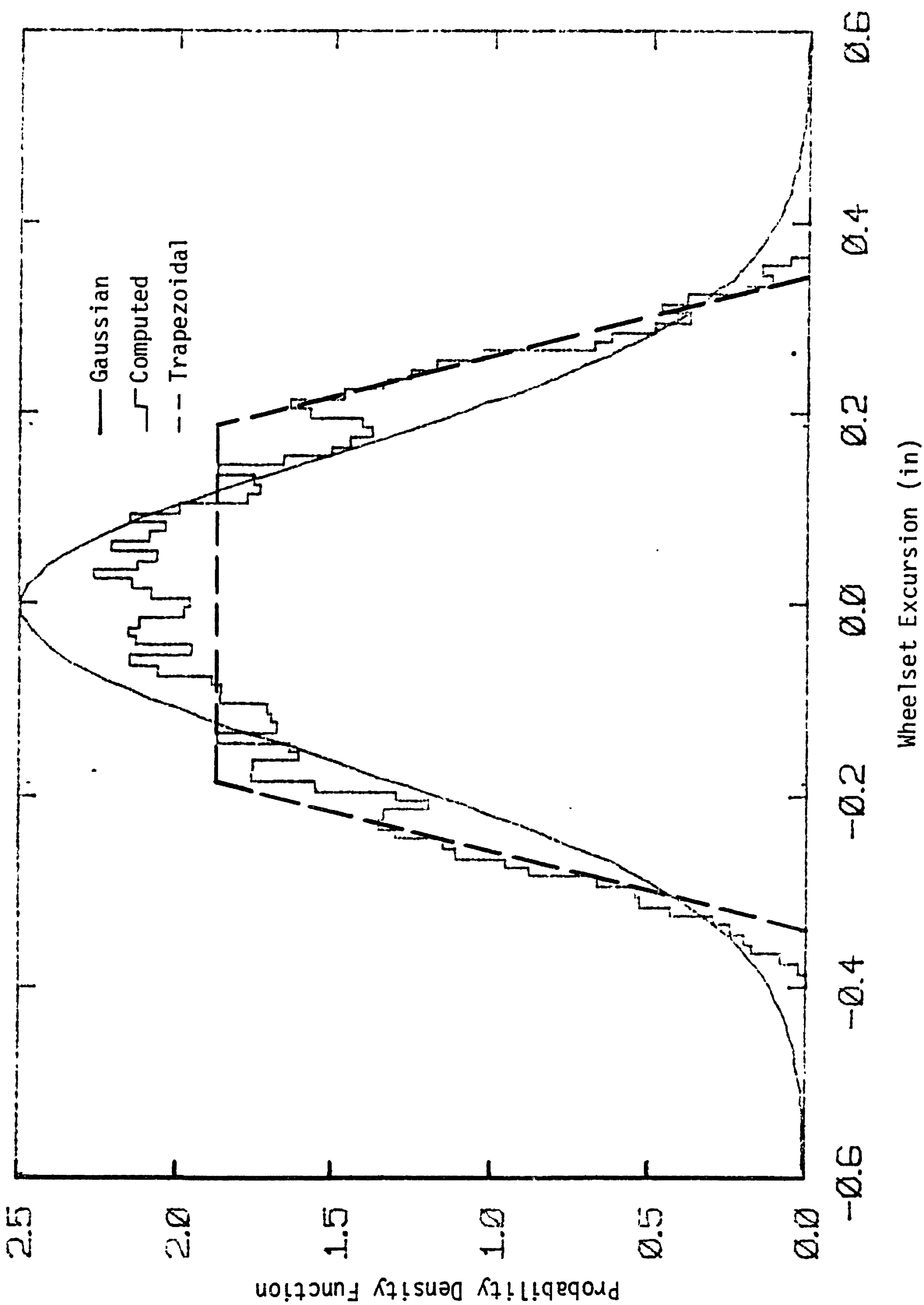

FIGURE 5.20: MIDDLE WHEELSET AT 60 MPH

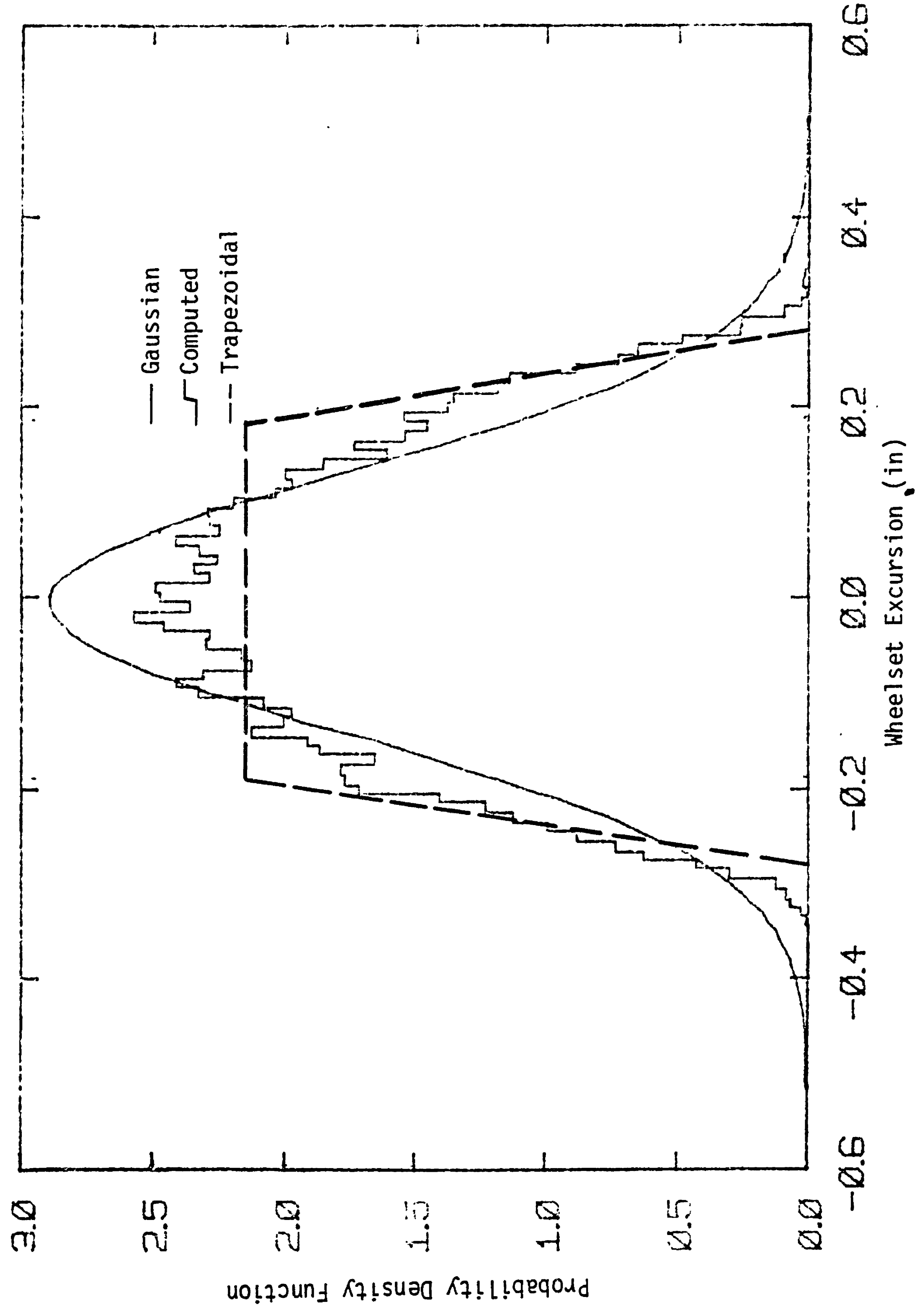

FIGURE 5.21: TRAILING WHEELSET AT 60 MPH

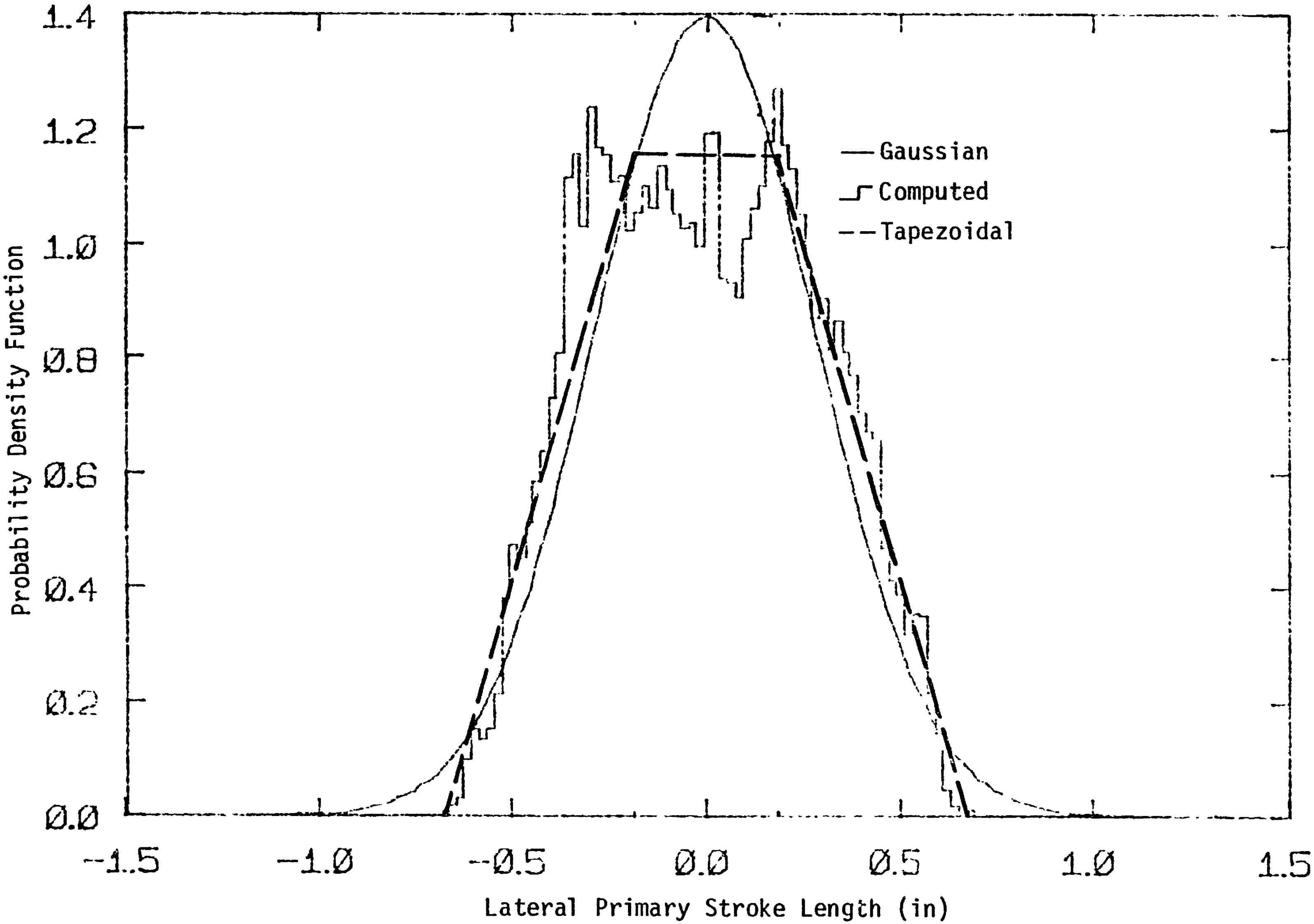

FIGURE 5.22: LEADING WHEELSET AT 60 MPH

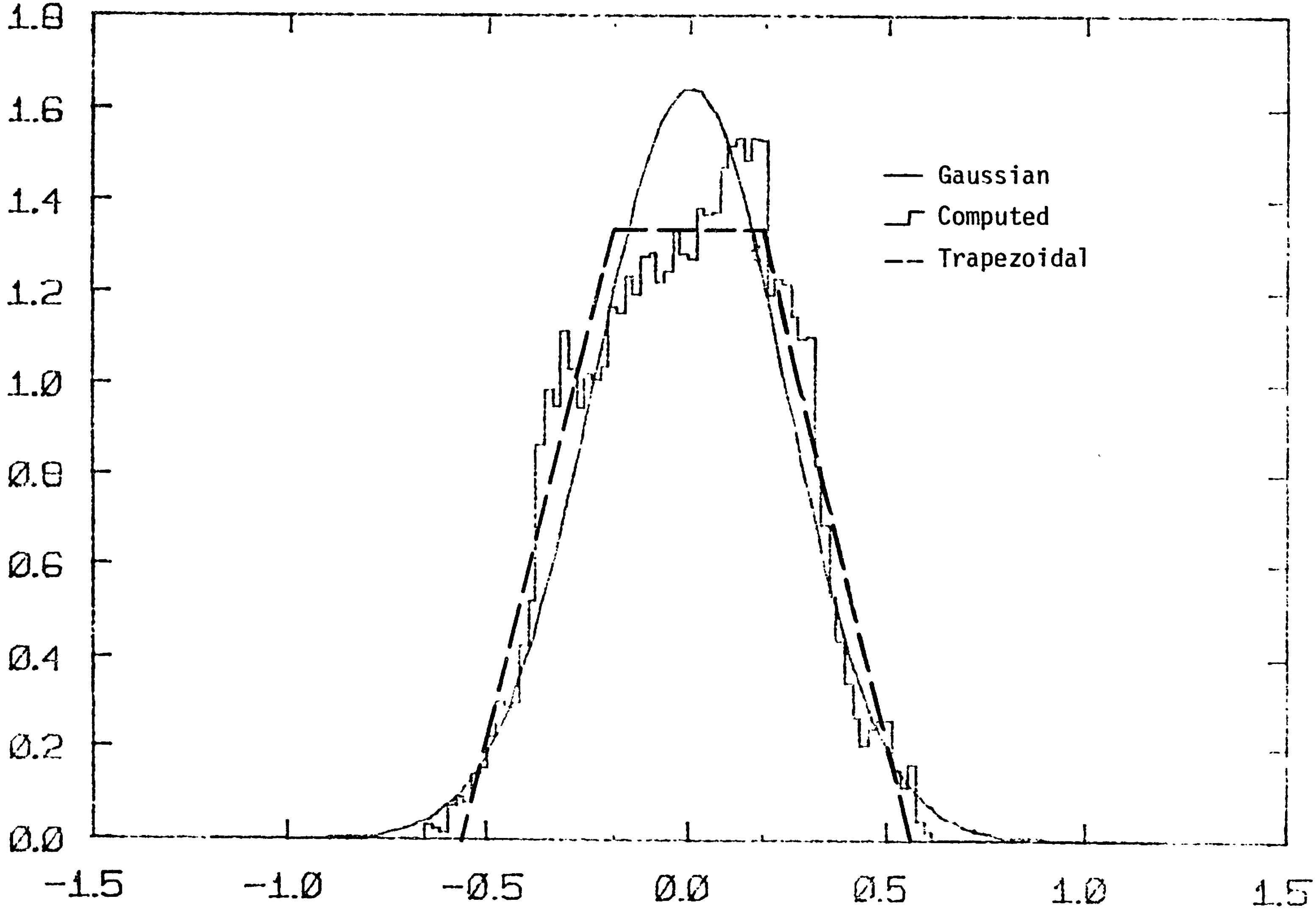

Lateral Primary Stroke Length (in)

FIGURE 5.23: MIDDLE WHEELSET AT 60 MPH

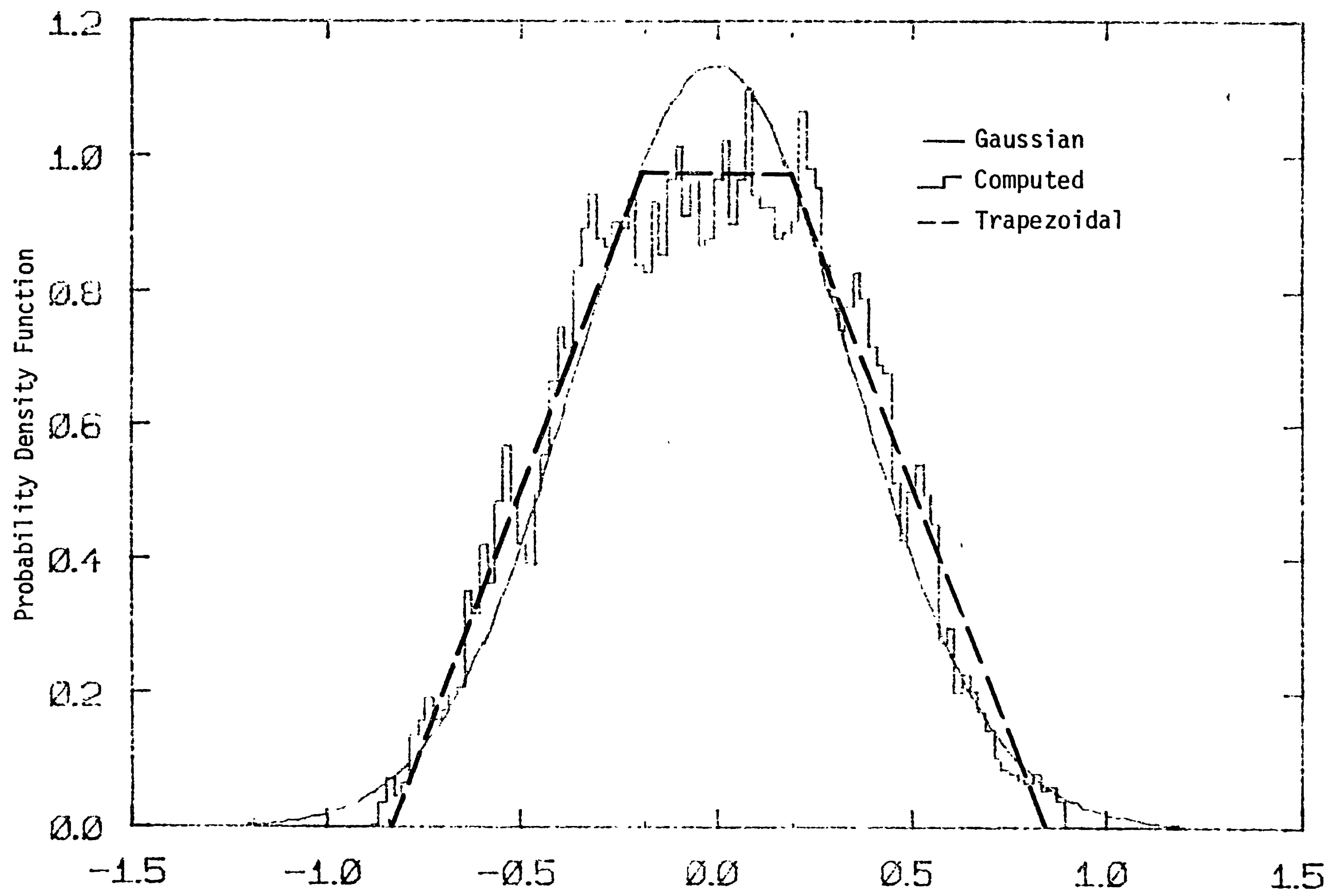

Figure 5.24: TRAILING WHEELSET AT 60 MPH

$$K_{eff} = \frac{\int_{-\infty}^{\infty} x\ f(x)p(x)dx}{\int_{-\infty}^{\infty} x^2\ p(x)dx} \tag{5.5}$$

where f(x) is given by equation (2.6). Equation (5.5) can be integrated analytically and the effective stiffness for the deadband spring is given by:

$$K_{eff} = \begin{cases} 0 & ; \quad \sigma \leq \frac{\delta}{\sqrt{3}} \\ k\,\frac{(b-\delta)^2}{(b^2-\delta^2)} & ; \quad \sigma > \frac{\delta}{\sqrt{3}} \end{cases} \tag{5.6}$$

Note that $\sigma = \frac{\delta}{\sqrt{3}}$ corresponds to $b = \delta$.

5.3.2 Trapezoidal PDF Results

Tables 5.3 and 5.4 show the comparison of the digital simulation and the results for trapezoidal PDFs at 40 mph and 60 mph. The frequency range chosen was 0.4-10 Hz with 50 frequency points. Convergence was achieved after 7 iterations at 40 mph and after 8 iterations at 60 mph. The results indicate that the difference in r.m.s. values are within 14.3% of the digital simulations as compared

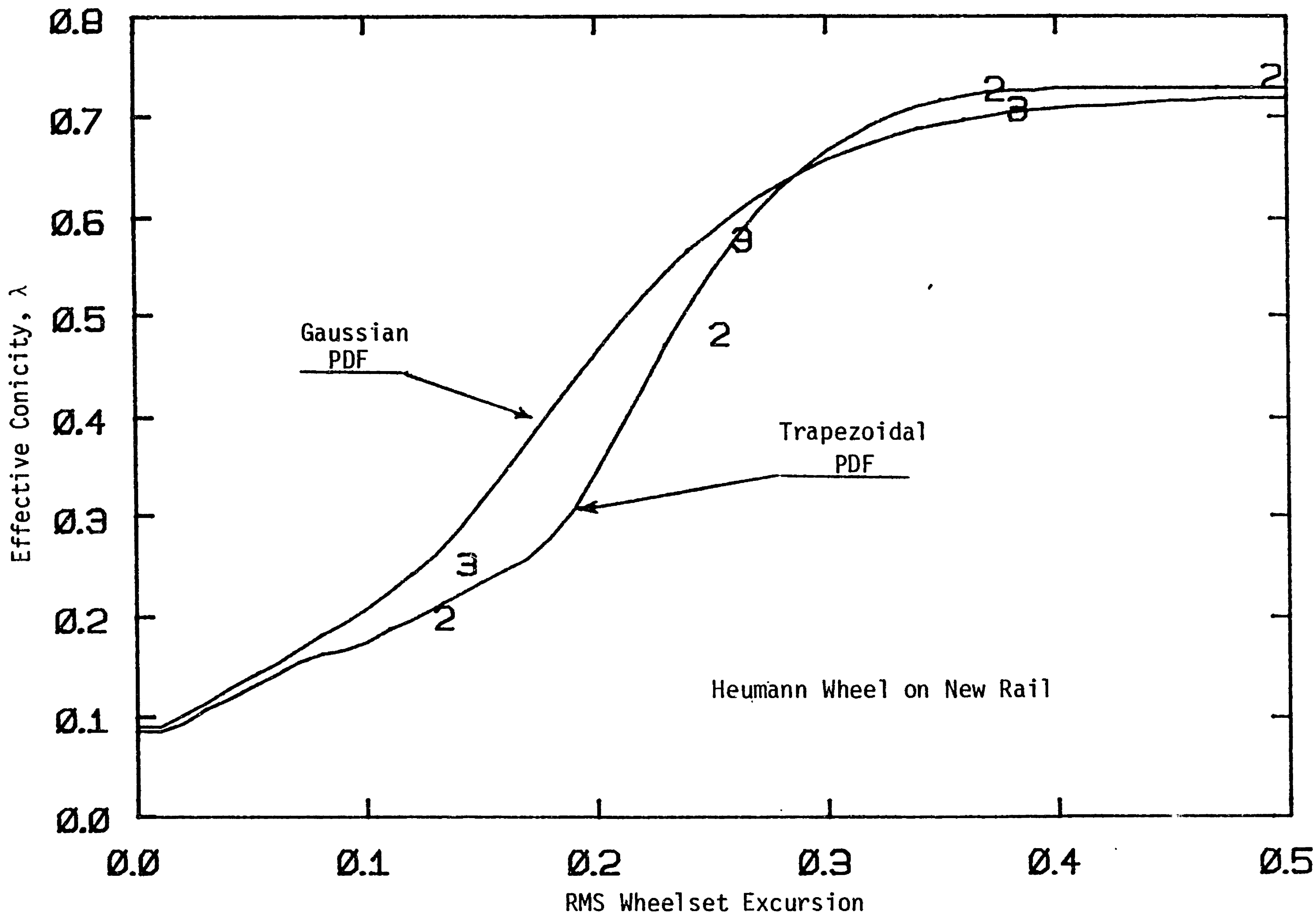

FIGURE 5.25: STATISTICALLY LINEARIZED EFFECTIVE CONICITY

to 31% difference with Gaussian density functions. Comparison of Tables 5.1 and 5.3 indicates that Gaussian density function predicts the r.m.s. wheelset excursions better than the trapezoidal density functions. This is due to the fact that at low speeds the wheelset excursions have PDF closer to the Gaussian density function as explained in Section 3.4 and as shown in Figures 5.13 to 5.15. An improved way to prepare the equivalent gain tables for wheel/rail geometric nonlinearities is to use Gaussian density function at low speed, trapezoidal density function at high speed with a smoothing of the describing function table at intermediate speeds to avoid discontinuities. Table 5.5 shows the comparison of the results obtained for this case at 40 mph.

5.4 Conclusions

In this chapter the method of statistical linearization has been evaluated as a design tool using Gaussian and trapezoidal density functions for the inputs to the nonlinearities. The Gaussian density function was the first choice because:

- it is the most common density function that was used in literature

- it does not require any knowledge about the type of nonlinearities in the system

- the effective gains for the nonlinearities are easy to obtain

TABLE 5.3: COMPARISON OF DIGITAL SIMULATION AND "TRAPEZOIDAL" STATISTICAL LINEARIZATION RESULTS AT 40 MPH

40 MPH	WHEELSET EXCURSIONS (in)			PRIMARY STROKE LENGTH (in)		
	1	2	3	1	2	3
DIGITAL	0.12474	0.096578	0.066809	0.18375	0.18563	0.21616
TRAPEZOIDAL PDF	0.14321	0.11198	0.067639	0.18109	0.19373	0.24622
% DIFFERENCE	12.8	13.7	1.2	1.4	4.2	12

TABLE 5.4: COMPARISON OF DIGITAL SIMULATION AND "TRAPEZOIDAL" STATISTICAL LINEARIZATION RESULTS AT 60 MPH

	WHEELSET EXCURSIONS (in)			PRIMARY STROKE LENGTH (in)		
60 MPH	1	2	3	1	2	3
DIGITAL	0.17014	0.15958	0.13771	0.28565	0.24280	0.35139
TRAPEZOIDAL PDF	0.17649	0.15021	0.12844	0.24623	0.20805	0.30686
% DIFFERENCE	3.6	5.8	6.7	13.8	14.3	12.6

TABLE 5.5: COMPARISON OF DIGITAL SIMULATION AND "TRAPEZOIDAL-GAUSSIAN" STATISTICAL LINEARIZATION RESULTS AT 40 MPH

	WHEELSET EXCURSIONS			PRIMARY STROKE LENGTH		
	1	2	3	1	2	3
Digital	0.12474	0.096578	0.066809	0.18563	0.18563	0.21616
Trapezoidal and Gaussian Density Function	0.12564	0.099269	0.0591	0.17795	0.18811	0.22660
% Difference	0.7	2.7	11.5	8.6	1.3	4.6

However, the Gaussian method produced a maximum difference of 31% as compared to the digital simulations. To reduce the difference in r.m.s. values as compared to the digital simulation trapezoidal density functions have been proposed and applied to the half carbody locomotive model. The trapezoidal density function is simple to use, the difference in r.m.s. values are reduced to 14.3%, and the trapezoidal density function predicts the peak values of the inputs to the nonlinearities accurately at extreme cases.

In Chapter 6, the trapezoidal density function and its degenerate forms are used as PDFs in the statistical linearization method for parametric studies.

CHAPTER 6

PARAMETRIC STUDIES

This chapter presents the extension of the half carbody model to a full carbody model and the comparison of the response of the two models. The second part contains a parametric study of locomotive dynamics utilizing the trapezoidal density-statistical linearization technique.

6.1 Extension to a Full Carbody Model

In the development and the validation of the statistical linearization method as a design tool, a 12 D.O.F. half carbody locomotive model was used. The reason for using the half carbody model was to reduce the computation costs in the validation process while still including the important nonlinearities. In addition, studies with linear models have indicated that [4] truck and carbody motions are usually weakly coupled in the truck hunting mode which determines the stability of conventional rail vehicles.

To compare the half carbody and full carbody models, the 12 D.O.F. model was extended to a 23 D.O.F. full carbody model. The degrees of freedom and equations of motion for the full carbody model are presented in Appendix B.3.

The half carbody and full carbody models with a low conicity wheel (New AAR wheel on New AAR rail [23]) have the same baseline parameters which are given in Appendix B.4. The critical speed of the half carbody model with a low conicity wheel is 105 mph (Section 6.2.1). The speed chosen to compare the results of the two models was 95 mph.

The results which are presented in Table 6.1 shows that the difference in the r.m.s. values of wheelset excursions are less than 2.4%. The maximum difference in the lateral primary stroke r.m.s. values is 17%. Figure 6.1 shows the power spectral densities of the leading lateral primary stroke length for the half carbody and full carbody models. The two PSDs have similar peaks, but the full carbody PSD has an extra peak at 1 hertz which corresponds to the carbody yaw degree of freedom.

The eigenvalues which correspond to the least damped mode at this speed are:

$$-1.04 \pm j\,23.33 \text{ with } \rho = 0.0445 \text{ (half carbody)}$$

$$-1.18 \pm j\,23.02 \text{ with } \rho = 0.0512 \text{ (full carbody)}$$

The least damped mode indicates that the full carbody model is slightly more stable than the half c- ody model. This is due to the fact that the r.m.s. lateral primary strokes in the full carbody are higher than that of the half carbody, and higher r.m.s. strokes mean higher effective stiffnesses in the lateral primary which yields a more stable system. However, the damping ratios for these two models are very close and the difference in predicted critical speed will be less than 10%.

TABLE 6.1 COMPARISON OF R.M.S. VALUES OF HALFCARBODY AND FULLCARBODY MODELS AT 95 MPH.

		Halfcarbody Model	Fullcarbody Model		% Difference	
			Front Truck	Rear Truck	Front Truck	Rear Truck
Wheelset Excursion(in.)	1 (4)	0.19816	0.19696	0.20029	0.6	1.0
	2 (5)	0.19259	0.19076	0.19424	0.9	0.8
	3 (6)	0.16514	0.16330	0.16930	1.1	2.4
Primary Stroke Length (in.)	1 (4)	0.23237	0.28006	0.24144	17.0	3.4
	2 (5)	0.25437	0.29773	0.26564	14.6	4.2
	3 (6)	0.28550	0.30361	0.30416	6.0	6.1
Accelerations (G)	Carbody	0.03145	0.019598		37	
	Truck(s)	0.12569	0.13939	0.16782	9.8	25.0

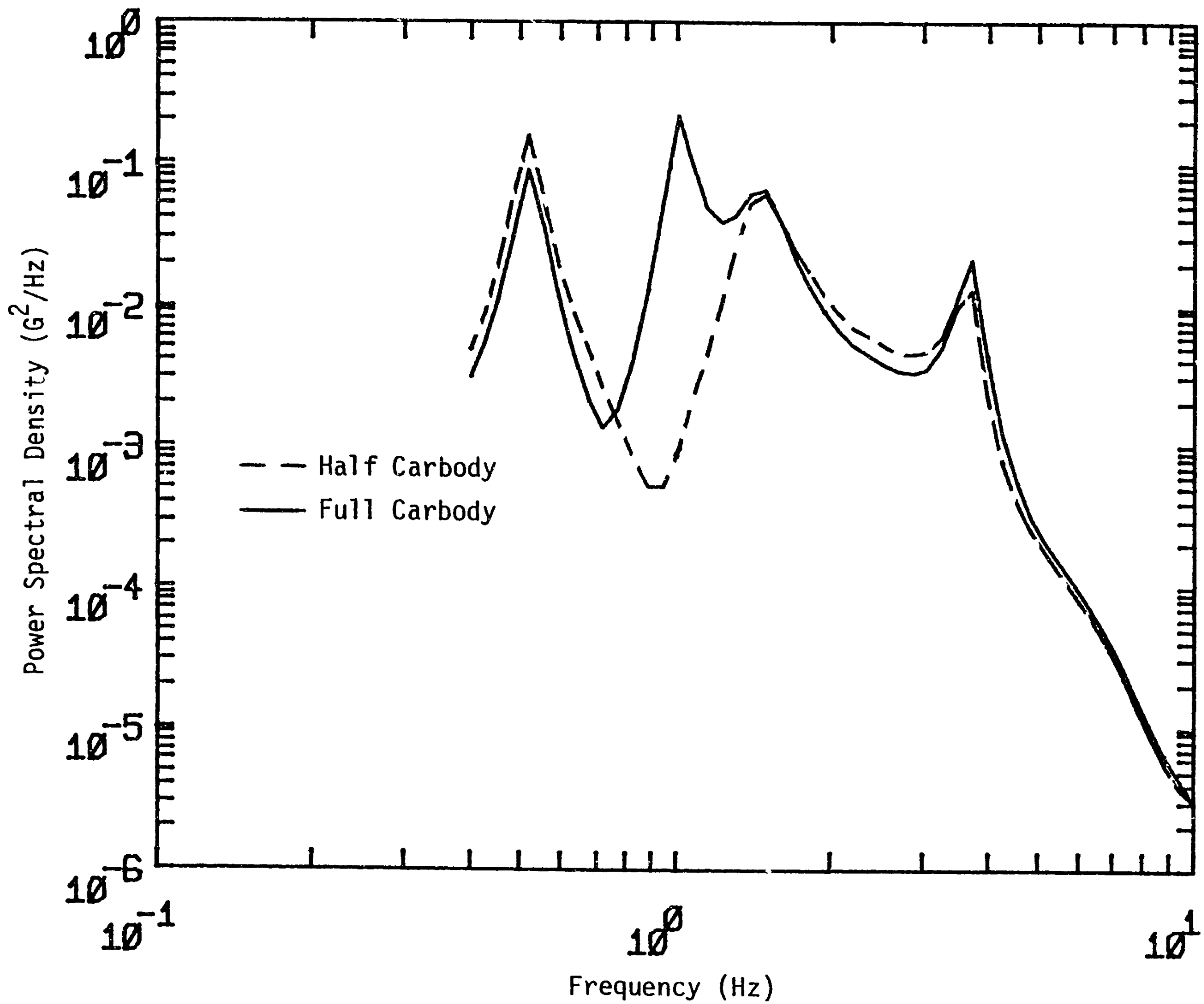

FIGURE 6.1: PSD OF THE LEADING LATERAL PRIMARY STROKE LENGTH FOR HALF CARBODY AND FULL CARBODY MODEL AT 95 MPH

The biggest difference in Table 6.1 is the lateral carbody acceleration levels. Table 6.1 shows that the half carbody model overestimates the acceleration by 37%. This change in the carbody acceleration levels can be explained by noting the half carbody model has only lateral and roll degrees of freedom for the carbody, thus the lateral acceleration of the carbody is the same at any point along the car length. In other words, the half carbody model can be thought of a full carbody model with two trucks moving in phase. The extension to the full carbody model allows a variable acceleration level to exist along the car length, due to the fact that the two trucks can now move in opposite directions which, in turn, reduces the acceleration at the geometric center of the car.

As a result, the half carbody model appears to be sufficient to investigate the lateral stability characteristics of rail vehicles. The results indicate that the half carbody model underestimates the lateral primary strokes and overestimates the lateral acceleration levels, therefore, a full carbody model is recommended for ride quality analyses.

6.2 Parametric Studies Using the Half Carbody Model

The statistical linearization method with trapezoidal PDFs was used to investigate the effects of important nonlinearities on the lateral stability of the 12 degrees of freedom half carbody locomotive model.

6.2.1 Wheel Profile Variations

Figure 6.2 shows the effective conicity of two types of profiles. They are a Heumann wheel [23] (high conicity) and a New AAR wheel (low conicity) on new AAR rail at standard gauge (56.5"). Figure 6.3 shows the least damped mode *vs* speed for both profiles. It is seen that the change of wheel/rail profile from low conicity to high conicity decreases the critical speed from 105 mph to 65 mph.

6.2.2 Track Roughness Variations

Figure 6.4 shows the lateral truck acceleration spectral densities at 60 mph for the equivalent linear system for three track class specifications. The r.m.s. lateral accelerations on track classes 6, 5, and 4 were $\sigma_{a_6} = 0.0466g$, $\sigma_{a_5} = 0.05875g$, $\sigma_{a_4} = 0.0976g$. It is interesting to note that for a purely linear model the ratio of the mean square accelerations would be equal to the ratio of the track roughness parameters, A, i.e.

$$\frac{\sigma_{a_5}^2}{\sigma_{a_6}^2} = \frac{A_5}{A_6} = 2.25$$

whereas the nonlinear equivalent linear results yield:

$$\frac{\sigma_{a_5}^2}{\sigma_{a_6}^2} = 1.59$$

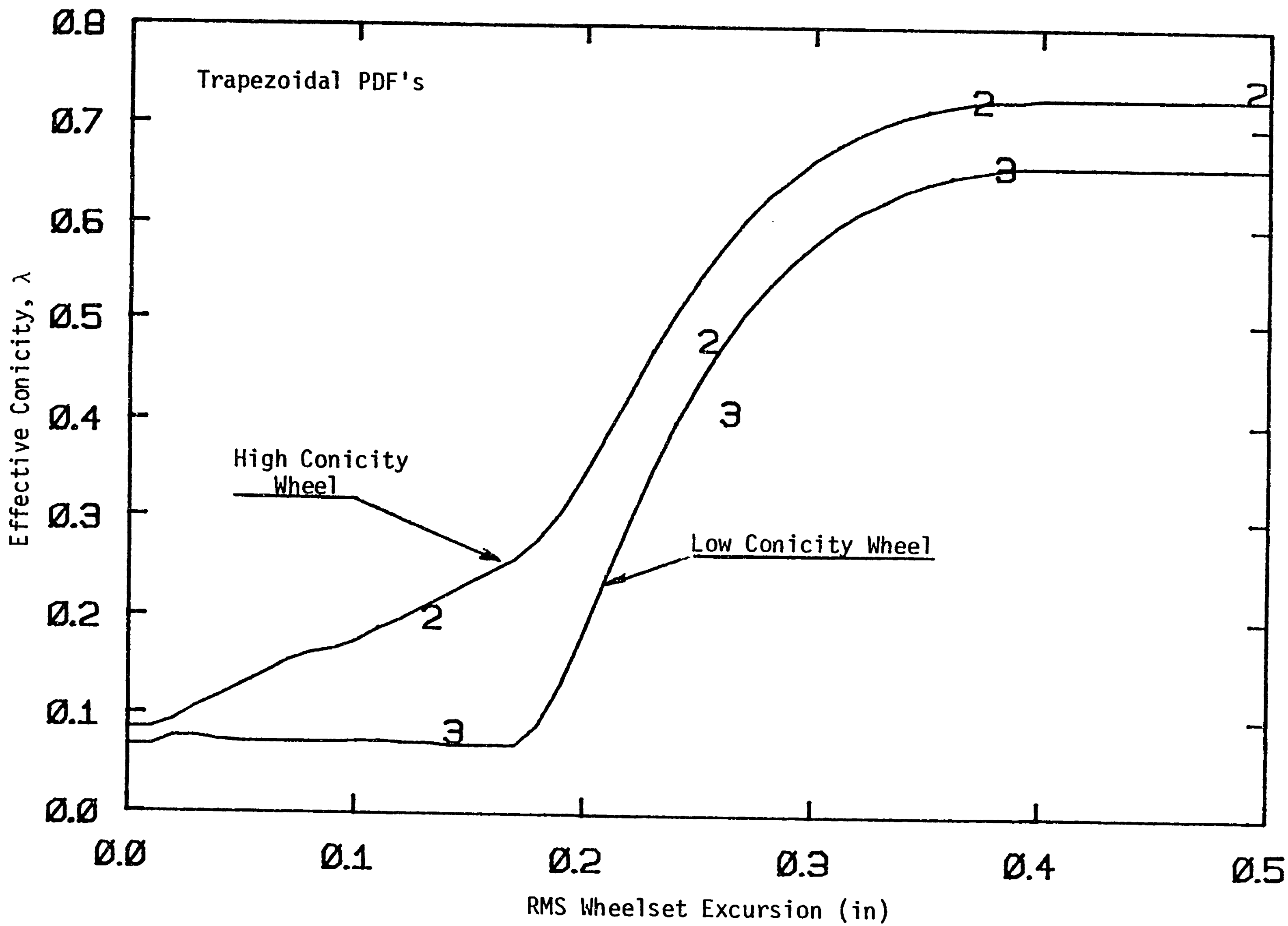

FIGURE 6.2: STATISTICALLY LINEARIZED EFFECTIVE CONICITY

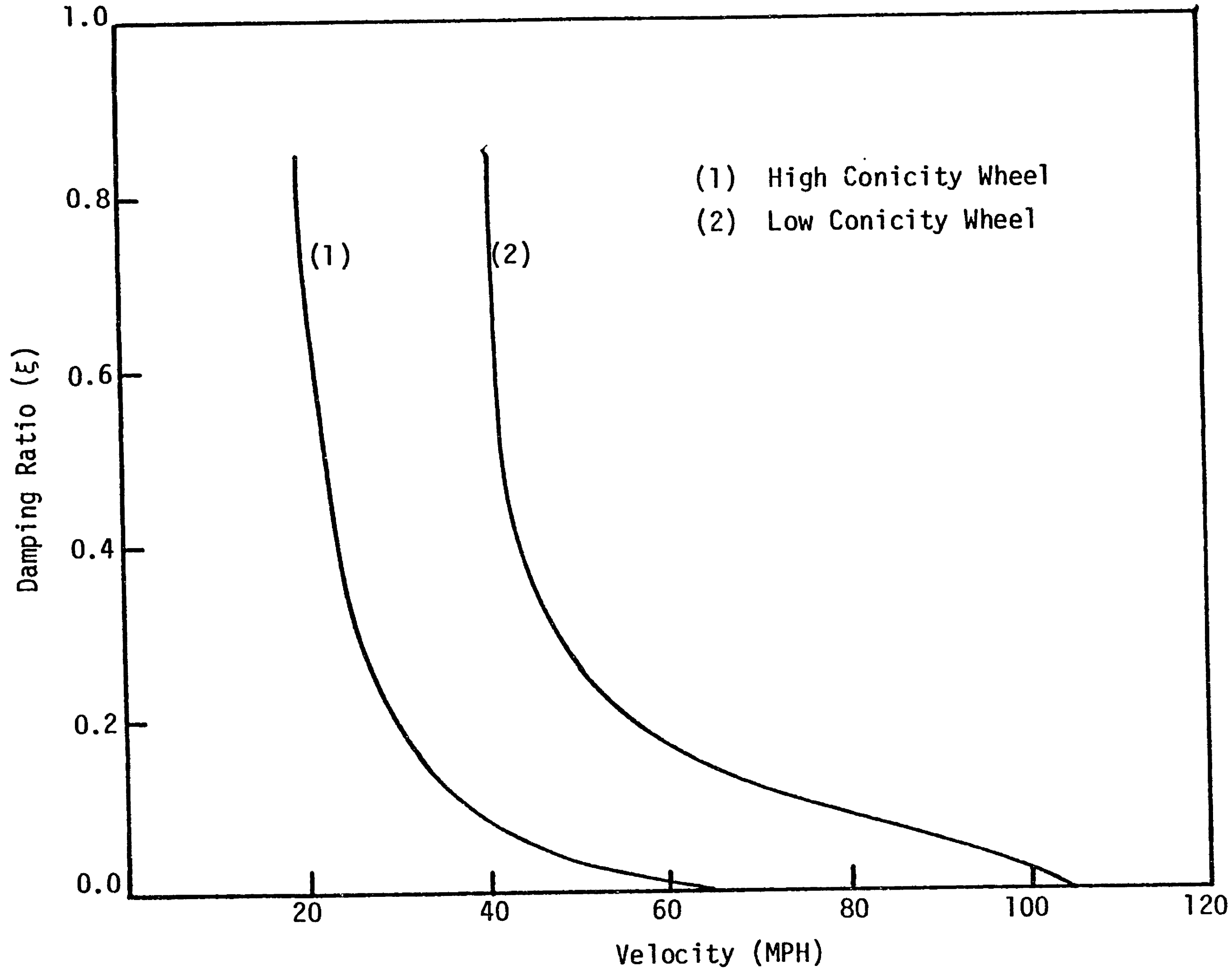

FIGURE 6.3: EFFECT OF WHEEL/RAIL PROFILE ON LATERAL STABILITY

Figure 6.4 shows that the lateral truck acceleration psds in the half carbody model have two major peaks corresponding to the carbody lateral and truck lateral motions. The location of the first peak is the same for all track classes, but the peak corresponding to the truck lateral motion occurs at higher frequencies on rougher tracks. The reason for this is that on rougher tracks the r.m.s. lateral primary strokes are higher than those occurring on smoother tracks at the same speed. As a result, the effective lateral primary stiffness and natural frequency corresponding to the truck lateral motion is higher.

Figure 6.4 shows that there is a sharp drop at the frequency of 4 Hz for class 6 track corresponding to the first drop in the spacing function as shown in Figure 6.5. The spacing function does not go to zero due to the unequal spacing of the wheelsets with respect to the geometric center of the truck. This drop does not exist for the rougher tracks because the kinematic frequency of the leading wheelset

$$\omega = V\sqrt{\frac{\lambda}{ar_o}}$$

$$= 4.02 \text{ Hz}$$

corresponds to the frequency at which the drop occurs.

To determine the influence of the track class on the stability of the half carbody locomotive model the least damped modes for the speeds up to 105 mph were compared and it was found that the half carbody locomotive model was stable up to 105 mph on track classes

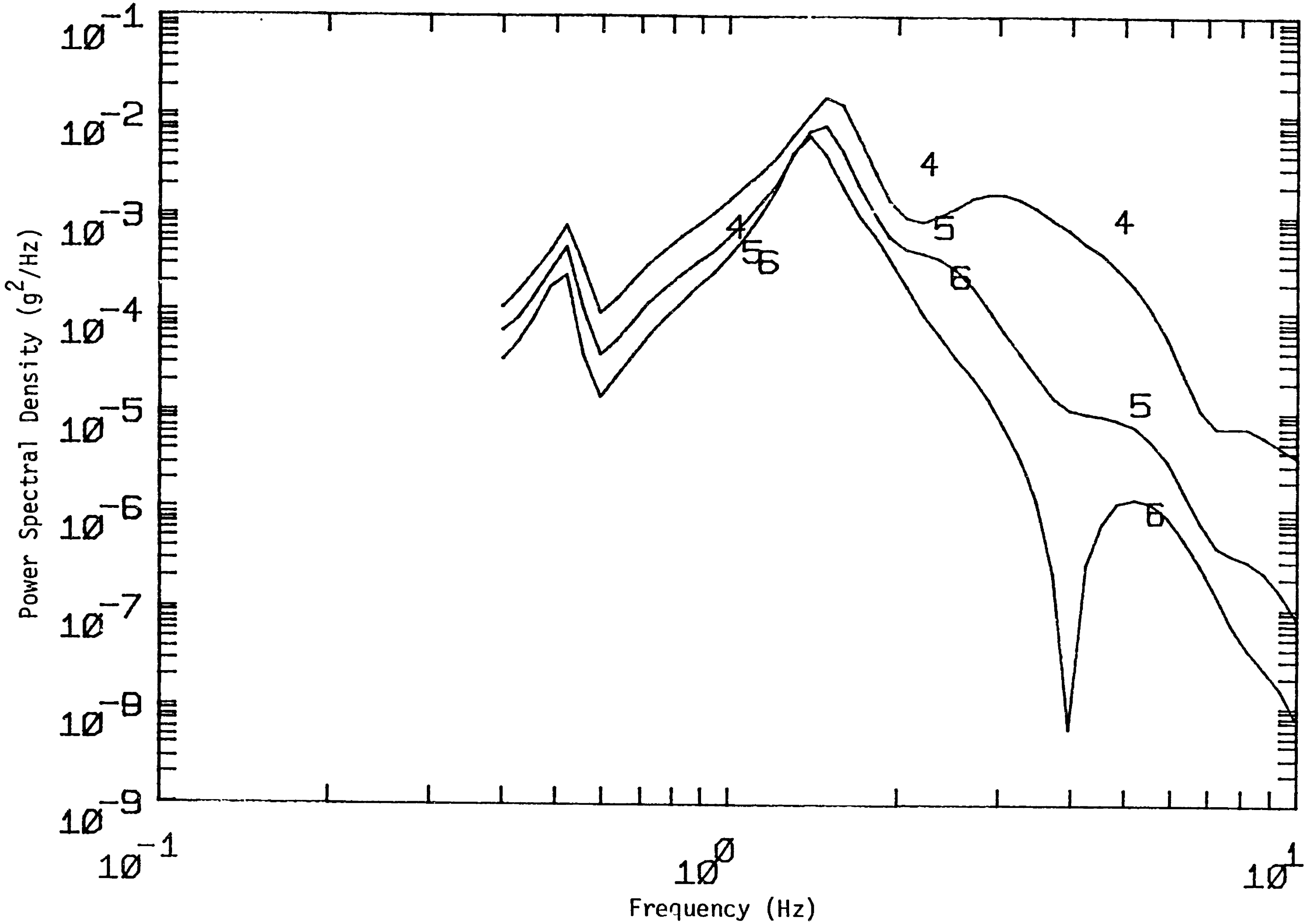

FIGURE 6.4: LATERAL TRUCK ACCELERATION PSDs AT 60 MPH

4, 5 and 6. This result can be explained as follows. Wickens [51] has formulated the effects of the longitudinal, lateral stiffnesses and the conicity on the stability of a simple wheelset suspended from a stationary truck as:

$$V_{cr} = \left[\frac{2[\alpha_1 k_x + \alpha_2(k_y + k_g)]}{\alpha_3 \lambda} \right]^{1/2}$$

where V_{cr} = critical speed

k_x = longitudinal stiffness

k_y = lateral stiffness

k_g = gravitational stiffness

$\alpha_1 = d_p^2 f_{11}$

$\alpha_2 = a^2 f_{33}$ and $\alpha_3 = \dfrac{a^2 f_{11} M_w + f_{33} I_w}{a r_0}$

For a model with a linear suspension and nonlinear wheel/rail geometry the critical speed is basically determined by the effective conicity. The r.m.s. wheelset excursion and, as a result, the effective conicity increases as the track class number reduces. Thus a low critical speed is expected for low (rough) track class numbers. However, the half carbody model has a hardening spring in the longitudinal and a deadband spring in the lateral primary suspension as shown in Figure 2.5. Therefore, the effective lateral and longitudinal stiffnesses are higher on the lower track classes at the same speed due to higher

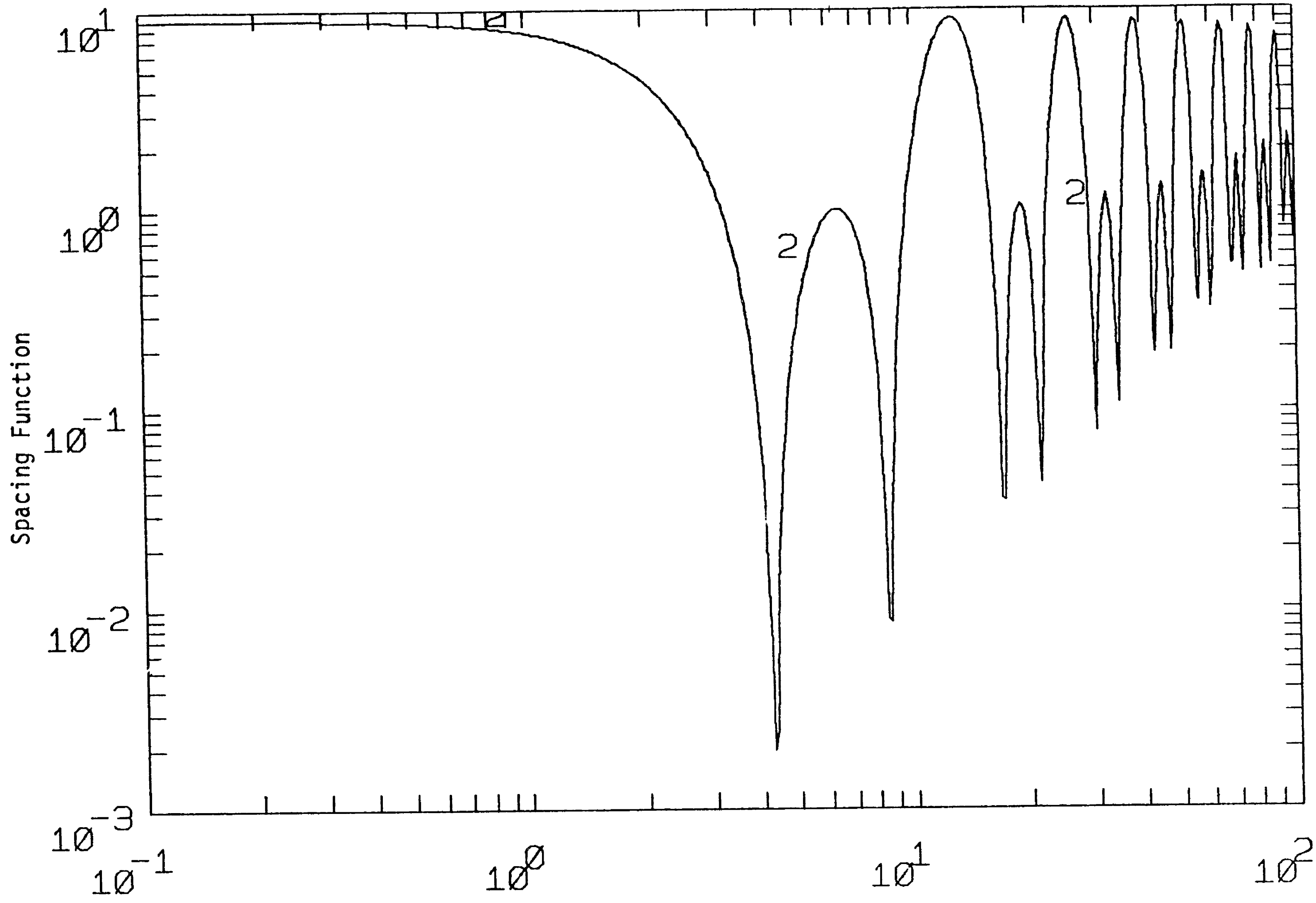

FIGURE 6.5: SPACING FUNCTION FOR THREE AXLE TRUCK

r.m.s. strokes, thus yielding a more stable system than expected. For example, at 80 mph on track class 4 the longitudinal stiffness is 1.5 times, the lateral stiffness is 1.6 times, the gravitational stiffness is 2.9 times and the effective conicity is 3.3 times greater than the values on track class 6.

To investigate the influence of the longitudinal hardening spring shown in Figure 2.5 on the lateral stability, the hardening spring was replaced by a linear spring with a stiffness of k_1. It was seen that the critical speed of the half carbody model is reduced from 105 mph on track class 6 to 75 mph on track class 4. Thus it is clear that the hardening spring has a strong influence on the lateral stability characteristics.

6.2.3 Effect of Axle Clearances

Axle clearances are important in the curving performance of the six-axle locomotive, but they degrade the lateral stability of the locomotive by decreasing the effective lateral stiffness. The magnitude of the axle clearances are chosen such that the locomotive can negotiate the tightest curves in a yard. In practice, axle clearances are generally chosen to be equal at each axle. Simple geometric analysis has shown that [57] the sum of the leading and middle axle clearances determine the curving ability of the locomotives in yard curves. It is clear from Figure 6.6 that the leading wheelset always has the highest r.m.s. excursion, or in other words, has the highest effective conicity. If the clearance

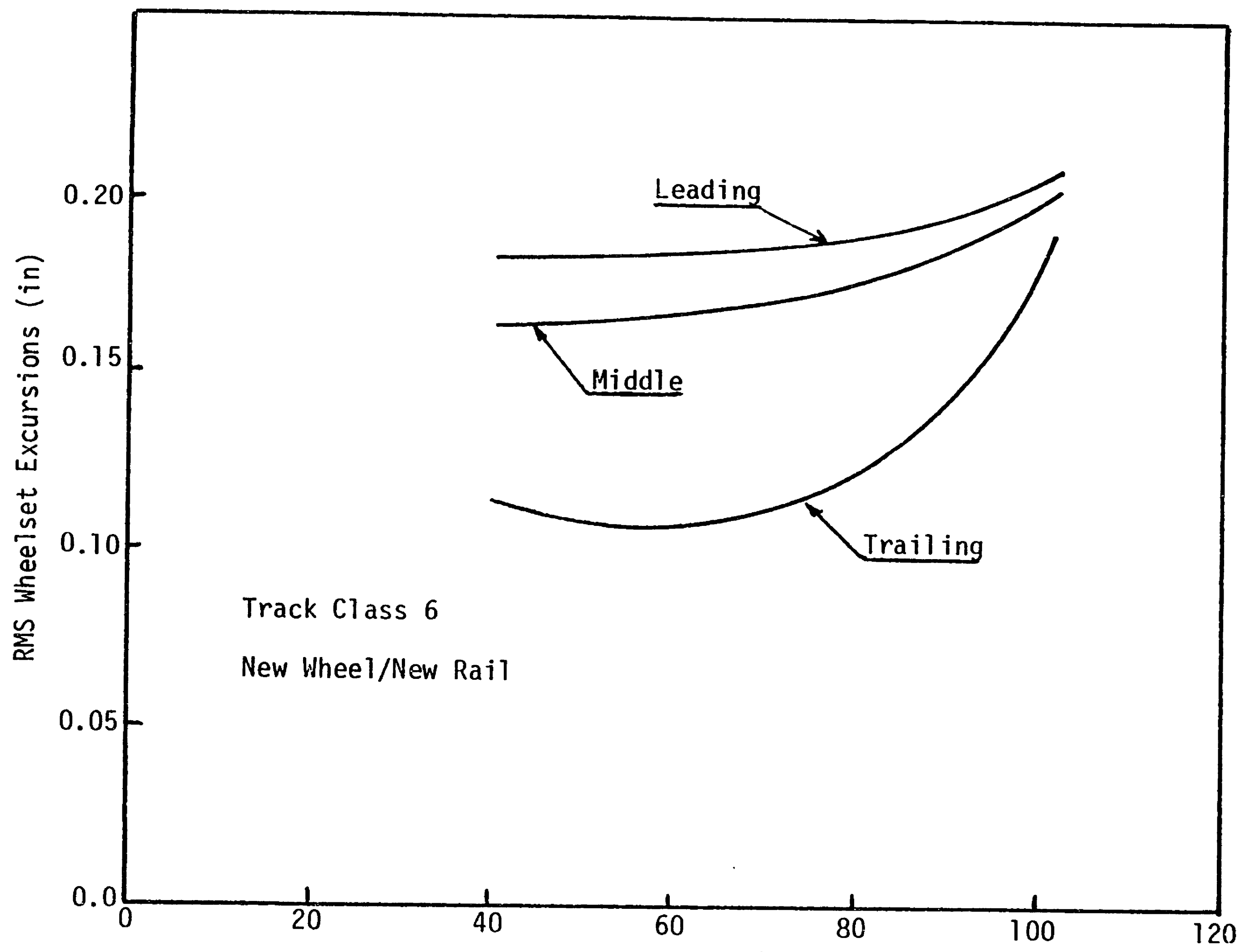

FIGURE 6.6: RMS WHEELSET EXCURSIONS VS SPEED

in the leading axle is reduced and the clearance in the middle axle is increased by the same amount such that the total axle clearance for the leading and middle axle stays the same, the same effective conicity can be obtained at higher speed. Therefore an increase in the critical speed is expected. Figure 6.7 shows the least damped mode vs speed for two types of axle clearances (Case 7 in Table 6.2). Curve 1 corresponds to the baseline case which has equal clearances of 0.18756 in. at all axles. In Curve 2, the leading and trailing axle clearances were reduced by 50% whereas the clearances in the middle axle was increased by 50%. As expected, the critical speed was increased from 105 mph to 113 mph.

To determine the effect of each axle clearance on the lateral stability of the locomotive the axle clearances were increased/decreased by 50% at the same speed, 80 mph, and the results are tabulated in Table 6.2 with the damping value of the mode which becomes unstable at the critical speed. Table 6.2 indicates that to increase the critical speed the first axle clearance should be reduced. The comparison of cases 4 and 7 shows the effect of the third axle clearance on the stability. The decrease in the third axle clearance increases the effective stiffness without changing the other terms in equation (6.1) significantly.

6.2.4 Effect of Bolster Dry Friction Level

In this section the effect of the bolster dry friction level on the lateral stability of a locomotive is investigated.

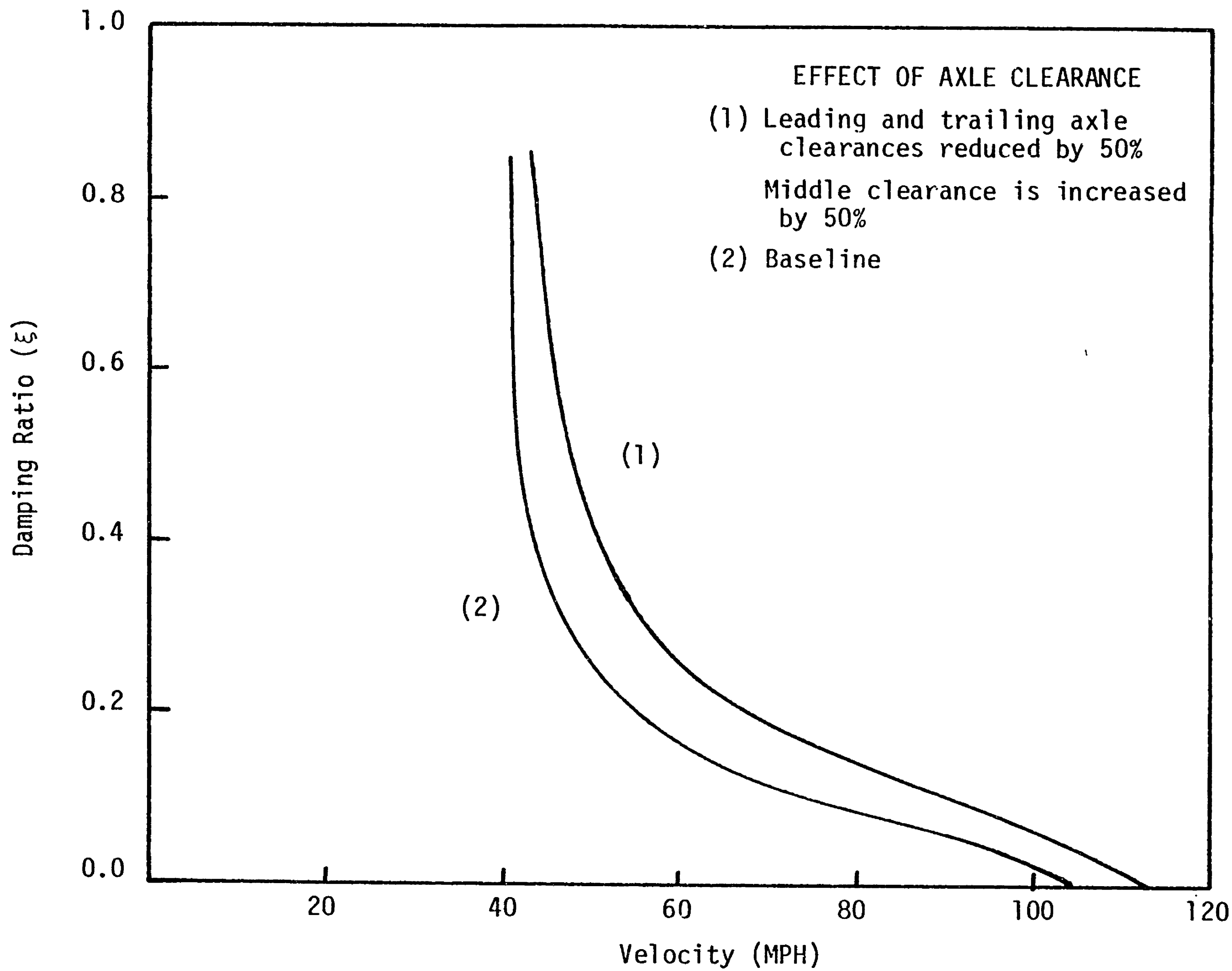

FIGURE 6.7: EFFECT OF AXLE CLEARANCE ON STABILITY

TABLE 6.2 : PARAMETRIC STUDY ON AXLE CLEARANCES AT 80 MPH.

(New Wheel On New Rail)

Cases	1	2	3	4	5	6	7
Axle 1	→	↑	↓	↓	↓	↓	↓
Axle 2	→	→	→	↑	↑	↓	↑
Axle 3	→	→	→	→	↑	↓	↓
Damping	0.09736	0.06900	0.12750	0.14097	0.12377	0.14307	0.15700

→ Nominal Value, 0.18756 in.

↑ Increased By 50%

↓ Decreased By 50%

It was observed that the critical speed of the halfcarbody model was reduced from 105 mph to 95 mph when the dry friction level was decreased by 10 times from 100,000 lb-in to 10,000 lb-in. The reason for this reduction in the critical speed is that the truck can move more in the yaw direction as the dry friction level decreases, and this increase in yaw motion of the truck increases the wheelset excursions and, in turn, increases the effective conicity to decrease the critical speed of the halfcarbody model.

6.3 Conclusions

The extension of the halfcarbody model to a fullcarbody model indicated that the halfcarbody model is sufficient for predicting the lateral stability of the locomotive model.

The developed nonlinear technique was used to determine the influences of the wheel/rail profile, the track roughness, axle clearances and the bolster dry friction level on the lateral stability of the locomotive model. The parametric studies were selected to show the advantages of the nonlinear technique over the linear techniques in determining the effects of the various nonlinearities on the performance of the rail vehicles.

CHAPTER 7

CONCLUSIONS AND RECOMMENDATIONS

7.1 Conclusions

In this thesis the applicability of the statistical linearization method as a design tool in nonlinear rail vehicle dynamics was investigated. The first part of the research involved the nonlinear wheelset equations and the development of a digital half carbody lateral locomotive model to validate the results obtained by the statistical linearization method.

The traditional statistical linearization method using a Gaussian density function was found to produce large errors at high speeds, thus a different form for the assumed density function was developed. The trapezoidal density function was found to compare more favorably with the digitally computed probability density functions while not increasing the computational complexity. It was shown that the r.m.s. values obtained by the Gaussian probability density function assumption deviate from the r.m.s. values obtained from the digital simulation by as much as 31%. To reduce the difference in r.m.s. values the trapezoidal density function and its degenerate forms were used as the input probability density functions to the nonlinearities. It was shown that the trapezoidal density function reduces the difference in r.m.s. values to within 14.3% of the r.m.s. values of the digital simulations, and that they are as simple to use for a design tool. It was also shown that the statistical linearization method is a useful tool both in predicting the r.m.s. values and the frequency contents of the inputs to the nonlinearities.

The most important aspect of the statistical linearization method is that the computation time required to obtain the r.m.s. values and the power spectral densities was reduced from 30-40 minutes for the digital simulation to 1.5 - 2 minutes for the statistical linearization method.

The developed and validated design tool, the statistical linearization with the trapezoidal density function, was used to check the assumption of using the half carbody model in the lateral stability analysis of locomotives. The 12 D.O.F. half carbody model was extended to a 23 D.O.F. full carbody model and it was shown that the half carbody model is sufficient for predicting the lateral stability of the locomotive model. However, the full carbody model is recommended for ride quality analyses.

Finally, the developed design tool was used to investigate the influence of the nonlinearities on the lateral stability of the 12 D.O.F. half carbody model. The parametric studies indicated that:

- The effect of changing the wheel profile from a high conicity (Heumann) wheel to a low conicity (new AAR wheel) was to increase the critical speed by 38 percent

- The effect of operating the vehicle over a rougher track was to increase the r.m.s. lateral acceleration of the truck by 26 percent for class 6 to class 5 and 109 percent for class 6 to class 4.

- By changing the axle clearances the critical speed can be increased by 10% without hurting the curve negotiation.

- The effect of decreasing the dry friction level by 10 times was to decrease the critical speed by 10 percent.

7.2 Recommendations for Future Work

The future directions to improve the developed method as a design tool for the nonlinear rail vehicles could be divided into three areas as follows.

7.2.1 The Improvement of the Method

In this study, the probability density functions for the inputs to the nonlinearities are restricted to be a function of only one variable to develop a simple design tool. To improve the accuracy in predicting the r.m.s. values the method could be extended by including the higher moments [35] or by taking into account for the possibility of the multiple inputs to the nonlinearities.

In this study only the second order moments were computed and compared. To have a better description of the probability density function of the inputs to the nonlinearities the calculation of the fourth moment will be useful. However, the addition of the fourth moment in the convergence algorithm will complicate the technique and it will be expensive as a design tool.

7.2.2 The Creep Force Saturation

In this study a linear creep force/creepage relationship due to Kalker [53] was used. Law [4] showed that the creep force saturation could have significant influence on truck hunting. Therefore, the creep force saturation, e.g. the approximate model presented in Section A.9, could be included in the model.

7.2.3 Verification of the Method and the Modles by Field Tests

In this study the statistical linearization was validated against a time domain digital simulation mathematical model. The rail vehicle models should be verified by field tests to make sure that the mathematical models represent the actual behavior of rail vehicles.

REFERENCES

1. Wickens, A.H., "General Aspects of the Lateral Dynamics of Railway Vehicles," Journal of Engineering for Industry, Trans. ASME, Series 8, Vol. 91, No. 3, August 1969, pp. 868-878.

2. Matsudaira, T., "Hunting Problems of High Speed Railway Vehicles with Special Reference to Bogie Design for the New Tokaido Line," Proceedings of the Institution of Mechanical Engineer, Interaction Between Vehicle and Track, Vol. 180, Part 3F, 1966, pp. 58-66.

3. Cooperrider, N.K., "High Speed Dynamics of Conventional Railway Trucks," Ph.D Thesis, Department of Mechanical Engineering, Stanford University, Stanford, CA,1968.

4. Law, E.H. and Cooperrider, N.K., "A Survey of Rail Vehicle Dynamics Research," Journal of Dynamic Systems, Measurement and Control, Trans. ASME, Series G, Vol. 96, No. 2. June 1974, pp. 132-146.

5. Cooperrider, N.K., "The Hunting Behavior of Conventional Railway Trucks," Journal of Engineering for Industry, Trans. ASME, Series B, Vol. 94, No. 2, May 1972, pp. 752-762.

6. Hobbs, A.E.W., "A Survey of Creep," DYN/52, April 1967, British Railways Research Dept., Derby, England.

7. King, B.L., "An Evaluation of the Contact Conditions Between a a Pair of Worn Wheels and Worn Rails in Straight Track," DYN/37, Sept. 1966, British Railways Research Dept., Derby, England.

8. Law, E.H., "Nonlinear Wheelset Dynamic Response to Random Lateral Rail Irregularities," Journal of Engineering for Industry, Trans. ASME, Vol. 96, Series B, Nov. 1974, pp. 1168-1176.

9. Chang, E.H., Garg, V.K. and Goodspeed, C.H., "Comparative Study on the Linear and Non-Linear Response of Locomotive," presented at the 1977 ASME Winter Annual Meeting, Atlanta, GA, December 1977.

10. DePater, A.D., "The Approximate Determination of the Hunting Movement of a Railway Vehicle by Aid of the Method of Krylov and Bogoliubov,". Paper delivered at the Xth International Congress of Applied Mechanics at Stressa, 1960.

11. Law, E.H. and Brand, R.S., "Analysis of the Nonlinear Dynamics of a Railway Wheelset," Journal of Dynamic Systems, Measurement and Control, Trans. ASME, Series G, Vol. 95, No. 1, March 1973. pp. 28-35.

12. Cooperrider, N.K., Hedrick, J.K., Law, E.H., and Malstrom, C., "The Application of Quasi-Linearization Techniques to the Prediction of Nonlinear Railway Vehicle Response," Vehicle System Dynamics, Vol. 6, No. 2-3, July 1975, pp. 141-148.

13. Hannebrink, D.N., Lee, H., Weinstock, H., Hedrick, J.K., "Influence of Axle Load, Track Gage, and Wheel Profile on Rail Vehicle Hunting," Journal of Engineering for Industry, Trans. ASME, Vol. 99, No. 1, February 1977, pp. 186-195.

14. Hull, R. and Cooperrider, N.K., "Influence of Nonlinear Wheel/Rail Contact Geometry on Stability of Rail Vehicles," Journal of Engineering for Industry, Trans. ASME, Vol. 99, No. 1, Feb. 1977.

15. Stassen, H.G., "Random Lateral Motions of Railway Vehicles," WTHD. No. 49, Laboratory for Measurement and Control, Delft University of Technology, the Netherlands, 1973.

16. Rus, L., "Running Stability, and Railway Vehicle Transfer Functions, Solved by the Method of Statistical Linearization," 5th VSD-2nd IUTAM Symposium, Vienna, Austria 1977.

17. Hedrick, J.K., "Application of Statistical Linearization to Nonlinear Rail Vehicle Dynamics," 6th International Congress on Nonlinear Oscillations (ICNO), Prague, Czech., Sept. 1978.

18. Hedrick, J.K., Arslan, A.V., "Nonlinear Analysis of Rail Vehicle Forced Lateral Response and Stability," ASME Trans. Journal of Dynamic Systems, Measurement and Control, Volume 101, Number 3, pp. 230-237, Sept. 1979.

19. Hedrick, J.K., Castelazo, I.A., "Statistical Linearization of the Nonlinear Wheelset," Presented at 6th IUTAM Symposium on Dynamics of Vehicles on Roads and Tracks, Berlin, September 1979.

20. Booton, R.C., "Nonlinear Control Systems with Random Inputs," IRE Trans. Circuit Theory, Vol. CT-1, March 1954, pp. 9-17.

21. Denovchek, J.H., and Cooperrider, N.K., "Locomotive Dynamic Curving Analysis Program User's Manual," Interim Report FRA-TSC, DOT, July 1978.

22. Chang, E.H., Garg, V.K., and Hartman, P.W., "Technical Documentation, Locomotive Response Model," AAR Report R-295, February 1978.

23. Cooperrider, N.K., Law, E.H., "Data Book, Wheel/Rail Geometry for Five Wheel Profiles and Three Rail Profiles," Report No. ERC-R-75015, Arizona State University, October, 1975.

24. Sayers, M.W., "Analytical Methods to Reduce the Combined Track, Vehicle Suspension Costs of Rail Systems," M.S. Thesis, Department of Mechanical Engineering, M.I.T., August 1976.

25. Hedrick, J.K., et.al., "Nonlinear Analysis and Design Tools for Rail Vehicles: Nonlinear Locomotive Dynamics," Final Report for AAR, December 31, 1979.

26. Bendat, J.S., and Piersol, A.G., "Random Data: Analysis and Measurement Procedures," Wiley-Interscience, John Wiley and Sons, Inc., N.Y., 1971.

27. Caughey, T.K., "Nonlinear Theory of Random Vibrations," Advances in Applied Mechanics, Volume 11, Academic Press, 1971.

28. Crandall, S.H., "Nonlinear Problems in Random Vibration," Presented at the 7th International Conference on Nonlinear Oscillations, Berlin 1975.

29. Axelby, G., "Random Noise with Bias Signals in Nonlinear Devices," Trans. IRE Professional Group on Automatic Control, AC-4, No. 2, 167, 1959.

30. Pupkov, K.A., "Method of Investigating the Accuracy of Essentially Nonlinear Automatic Control Systems by Means of Equivalent Transfer Functions," Aut. Ren. Con., 21, 2, 1960.

31. Somerville, M.J. and Atherton, D.P., "Multigain Representation for a Single-Valued Nonlinearity with Several Inputs, and the Evaluation of Their Equivalent Gains by a Cursor Method," Proc. IEE, Monograph No. 309M, 105C, 537, 1958.

32. Gelb, A., "Applied Optimal Estimation", M.I.T. Press, 1974.

33. Sunahara, Y., "An Approximation Method of State Estimation for Nonlinear Dynamical Systems," JACC, University of Colorado, 1969.

34. Phaneuf, R.J., "Approximate Nonlinear Estimation," Ph.D. Thesis, M.I.T., May 1968.

35. Beaman, J.J., "Statistical Linearization for the Analysis and Control of Nonlinear Stochastic Systems," Ph.D. Thesis, M.I.T., December 1978.

36. Jazwinski, A.H., "Stochastic Processes and Filtering Theory," Academic Press, 1970.

37. Iwan, W.D., "A Generalization of the Concept of Equivalent Linearization," Int. J. Non-Linear Mechanics, Vol. 8, 1973.

38. Spanos, P-T.D., Iwan, W.D., "On the Existence and Uniqueness of Solutions Generated by Eqivalent Linearization," Int. J., Non-linear Mechanics, Vol. 13, 1978.

39. Atkinson, J.D., "A Variational Method for Randomly Excited Systems," Tech. Note D-1, Dep. Mech. Eng., University of Sydney, Australia.

40. Kramers, H.A., "Brownion Motion in a Field of Force and the Diffusion Model of Chemical Reactors," Physica 7, 284-304.

41. Sawaragi, Y., et.al., Reports, Vol. VIII, No. 10; Vo. IX, Nos. 57, 60, 61, 68 and 79. Eng. Res. Inst., Kyoto University.

42. Caughey, T.K., and Dienes, J.K., "The Behavior of Linear Systems with Random Parametric Excitation," J. Math. Phys., 41, No. 4, 300-318.

43. Crandall, S.H., "Random Vibrations of a Nonlinear System with a Set-Up Spring," J. Appl. Mech, 29, 477-482, pp. 306-314.

44. Kolovskii, M.Z., "Estimating the Accuracy of Solutions Obtained by the Method of Statistical Linearization," Autom. Rem. Cont., Vol. 22, No. 10, 43-53, 1966.

45. Iwan, W.D., Yang, I.M., "Application of Statistical Linearization Techniques to Nonlinear Multidegree-of-Freedom Systems," Journal of App. Mechanics, June 1972.

46. Iwan, W.D., Patula, E.J., "The Merit of Different Error Minimization Criteria in Approximate Analysis," Journal of App. Mechanics March 1972.

47. Beaman, J.J., Hedrick, J.K., "Improved Statistical Linearization for Analysis and Control of Nonlinear Control Systems," Presented at the 1979 JACC, Denver Colorado, 1979.

48. Gelb, A. and VanderVelde, W.E., Multiple-Input Describing Functions and Nonlinear System Design, McGraw-Hill, New York, 1968.

49. Crandall, S.H., "On Statistical Linearization for Nonlinear Oscillators," Problems of the Asymptotic Theory of Nonlinear Oscillators, Academy of Sciences of the Ukranian S.S.R., Naukova Duma, Kiev, 1977, pp. 115-122.

50. Abranowitz, M., and Stegun, I.A., "Handbook of Mathematical Functions with Formulas, Graphs, and Mathematical Tables," National Bureau of Standards, Applied Mechanics, Series 55.

51. Wickens, A.H., "The Dynamic Stability of Rail Vehicle Wheelsets and Bogies Having Profiled Wheels," Int. J. Solid Structures, 1965, Vol. 1, pp. 319-341.

52. Vermuelen, P.J., Johnson, K.L., "Contact of Nonspherical Elastic Bodies Transmitting Tangential Forces," Journal of Applied Mechanics, ASME Trans., pp. 338-340, June 1964.

53. Kalker, J.J., "Simplified Theory of Rolling Contact," Delft Progr. Rep., Series C: Mechanical and Aeronautical Engineering and Shipbuilding, 1 (1973) pp. 1-10.

54. Goree, J.G., Law, E.H., "User's Manual for Kalker's Simplified Nonlinear Creep Theory," Interim Report, August, 1977.

55. White, R.C., Limbert, D.L., Hedrick, J.K., and Cooperrider, N.K., "Guideway-Suspension Tradeoffs in Rail Vehicle Systems," Final Report to D.O.T., January 31, 1978.

56. Smith, H.W., "Approximate Analysis of Randomly Excited Nonlinear Controls", M.I.T. Press, Research Monograph No. 34, 1966.

57. Smith, H.W., "Approximate Analysis of Randomly Excited Nonlinear Controls", M.I.T. Press, Research Monograph No. 34, 1966.

58. Bell, C., Vehicle Dynamics Laboratory Memorandum, April 1980.

APPENDIX A

NONLINEAR WHEELSET EQUATION FORMULATION

The wheelset is the essential dynamic element of a rail vehicle. It is important to accurately describe the wheel/rail interaction forces and to include all of the terms that have a significant influence on the dynamic performance of the rail vehicle. In this appendix a complete derivation of the equations of motion for a rail vehicle wheelset are presented. This nonlinear wheelset model will be incorporated into twelve degrees of freedom, lateral locomotive models (digital simulation and statistical linearization models) in Chapters 3 and 5. Section A.8 shows how further simplifications can be made in the equations to yield the well known approximations. Section A.9 presents the approximate nonlinear creep force model.

A.1 Definition of Axes

Three axes are used to represent the steady state motion of the wheelset on the tangent truck, Figure A.1. Axes systems (e_{1L}, e_{2L}, e_{3L}) are attached to the left and right rail instantaneous contact points as shown in Figure A.2. They are used to represent the direction of the wheel/rail contact forces.

The coordinate transformations between the axes are given by:

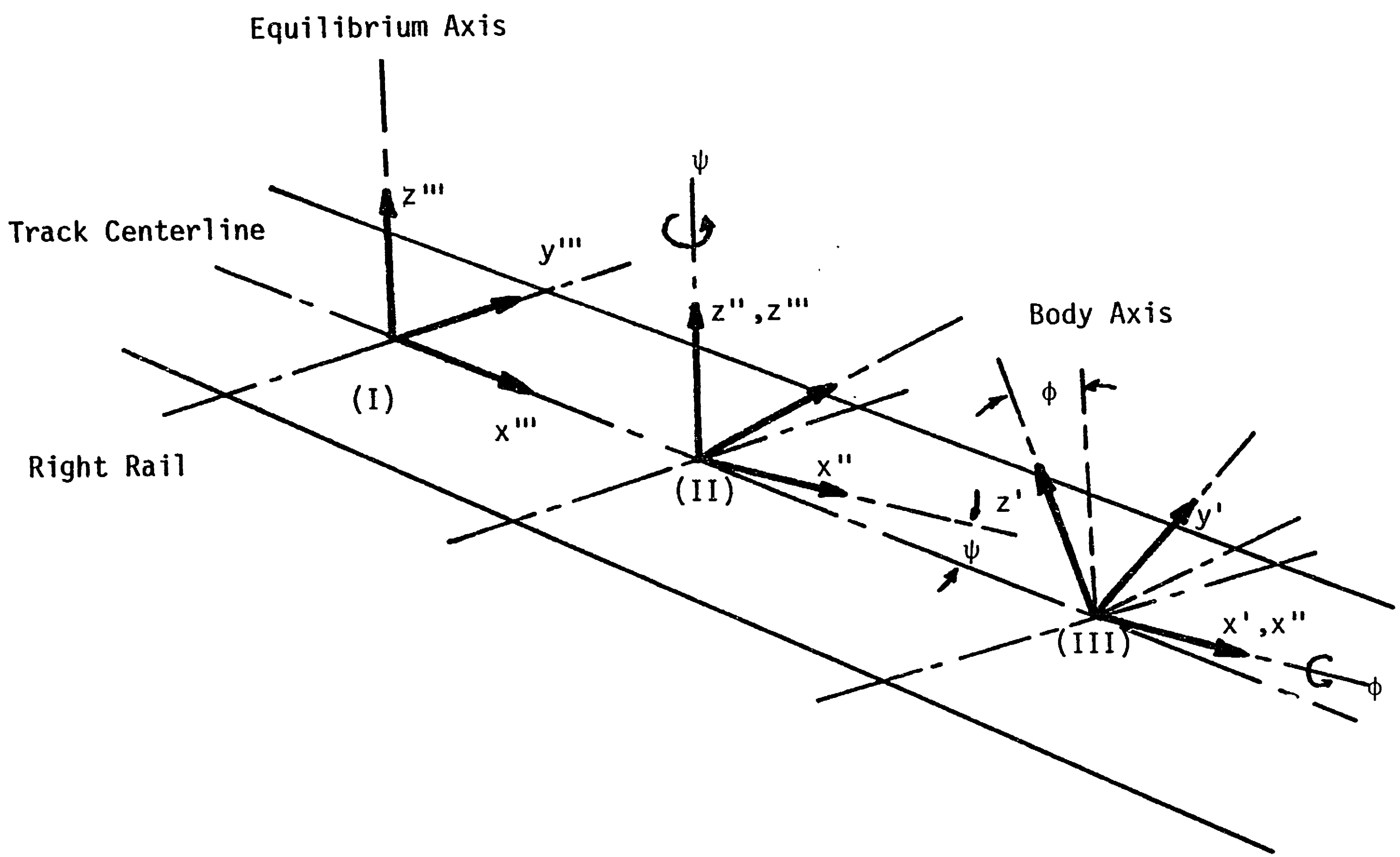

FIGURE A.1: AXES SYSTEMS

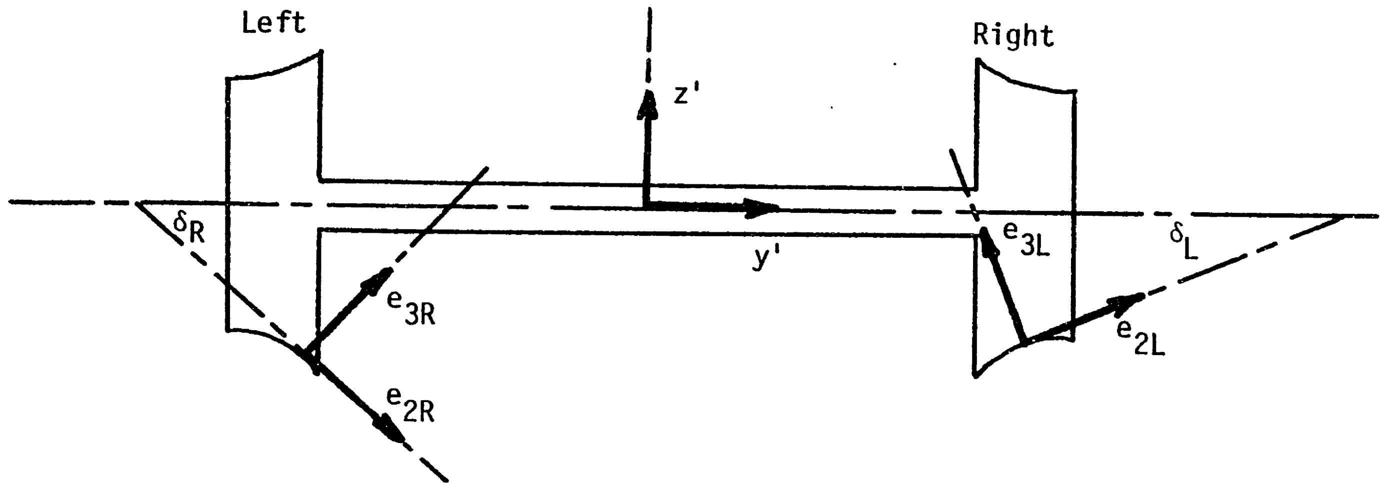

FIGURE A.2: CONTACT PLANE AXES

$$\begin{bmatrix} i' \\ j' \\ k' \end{bmatrix} = \begin{bmatrix} 1 & 0 & 0 \\ 0 & \cos\phi & \sin\phi \\ 0 & -\sin\phi & \cos\phi \end{bmatrix} \begin{bmatrix} i'' \\ j'' \\ k'' \end{bmatrix} \quad \text{(A.1.1)}$$

and

$$\begin{bmatrix} i'' \\ j'' \\ k'' \end{bmatrix} = \begin{bmatrix} \cos\psi & \sin\psi & 0 \\ -\sin\psi & \cos\psi & 0 \\ 0 & 0 & 1 \end{bmatrix} \begin{bmatrix} i''' \\ j''' \\ k''' \end{bmatrix} \quad \text{(A.1.2)}$$

then the relation between the body and the equilibrium axis is:

$$\begin{bmatrix} i' \\ j' \\ k' \end{bmatrix} = \begin{bmatrix} \cos\psi & \sin\psi & 0 \\ -\cos\phi\cdot\sin\psi & \cos\phi\cdot\cos\psi & \sin\phi \\ \sin\phi\cdot\sin\psi & -\sin\phi\cdot\cos\psi & \cos\phi \end{bmatrix} \begin{bmatrix} i''' \\ j''' \\ k''' \end{bmatrix} \quad \text{(A.1.3)}$$

The relations between contact-point axes and the body axis are given by:

$$\begin{bmatrix} e_{1R} \\ e_{2R} \\ e_{3R} \end{bmatrix} = \begin{bmatrix} 1 & 0 & 0 \\ 0 & \cos\delta_R & -\sin\delta_R \\ 0 & \sin\delta_R & \cos\delta_R \end{bmatrix} \begin{bmatrix} i' \\ j' \\ k' \end{bmatrix} \quad \text{(A.1.4)}$$

and

$$\begin{bmatrix} e_{1L} \\ e_{2L} \\ e_{3L} \end{bmatrix} = \begin{bmatrix} 1 & 0 & 0 \\ 0 & \cos\delta_L & \sin\delta_L \\ 0 & -\sin\delta_L & \cos\delta_L \end{bmatrix} \begin{bmatrix} i' \\ j' \\ k' \end{bmatrix} \quad \text{(A.1.5)}$$

A.2 Degrees of Freedom and Constraints

The coordinates that are used in the derivation are:

x: Longitudinal displacement of c.g.

y: Lateral displacement of c.g.

z: Vertical displacement of c.g.

ψ: Yaw displacement about z''' axis

ϕ: Roll displacement about x'' axis

β: Perturbation, angular displacement from nominal value of Ω about y' axis.

In the derivation it is assumed that the wheels are always in contact with the rails, i.e., there is no wheel lift. Using this assumption, two constraint equations for vertical and roll displacements are obtained in terms of lateral and yaw displacements of the wheelset.

Cooperrider [23] stated that yaw dependence of vertical and roll displacements is second order w.r.t. lateral displacement dependence.

Consequently, two constraint equations and their time derivatives are:

Vertical:

$$\begin{aligned} z &= z(y) \\ \dot{z} &= z'\dot{y} \\ \ddot{z} &= z''\dot{y}^2 + z'\ddot{y} \end{aligned} \tag{A.2.1}$$

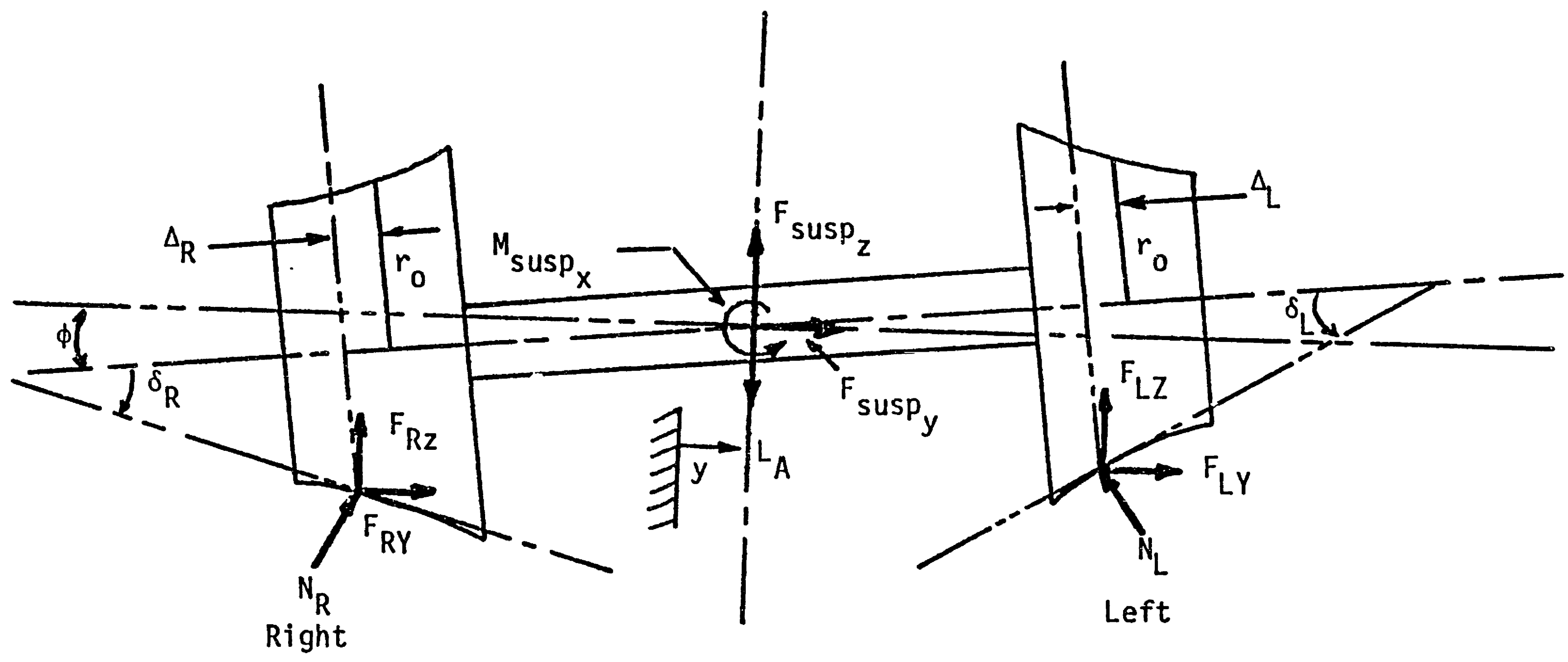

FIGURE A.3 : FREEBODY DIAGRAM OF A WHEELSET

Roll:

$$\phi = \phi(y)$$
$$\dot{\phi} = \phi'\dot{y} \qquad (A.2.2)$$
$$\ddot{\phi} = \phi''\dot{y}^2 + \phi'\ddot{y}$$

where $(\cdot) = (\frac{d}{dt})$; $(') = (\frac{\partial}{\partial y})$

A.3 Complete Wheelset Equations

The angular velocity of the wheelset is:

$$\omega = (\dot{\phi})i'' + (\Omega+\dot{\beta})j' + \dot{\psi}k''$$
$$= \omega_x i' + \omega_y j' + \omega_z k' \qquad (A.2.3)$$

where

$$\omega_x = \dot{\phi}$$
$$\omega_y = \Omega + \dot{\beta} + \dot{\psi}\sin\phi$$
$$\omega_z = \dot{\psi}\cos\phi$$

The angular momentum of the wheelset at the c.g. is:

$$H_{cg} = I_{wx}\omega_x i' + I_{wy}\omega_y j' + I_{wz}\omega_z k' \qquad (A.3.2)$$

where

$I_{wx} = I_{wz}$ for a wheelset.

Then

$$\frac{dH_{cg}}{dt} = I_{wx}\dot{\omega}_x i' + I_{wy}\dot{\omega}_y j' + I_{wx}\dot{\omega}_z k'$$

$$+ [\omega_{axis} \times H_{cg}] \qquad (A.3.3)$$

where

$$\omega_{axis} = \dot{\phi} i' + \dot{\psi} k'' \qquad (A.3.4)$$

$$= \dot{\phi} i' + \dot{\psi}\sin\phi j' + \dot{\psi}\cos\phi k'$$

Small roll and yaw angle assumption reduces Equation A.3.3 in equilibrium axis to:

$$\frac{dH_{cg}}{dt} = (I_{wx}\ddot{\phi} - I_{wy}\Omega\dot{\psi})i''' + I_{wy}\ddot{\beta}\, j'''$$

$$+ (I_{wy}\Omega\dot{\phi} + I_{wx}\ddot{\psi})\, k''' \qquad (A.3.5)$$

The moments due to creep, normal, and suspension forces shown in Figure A.3 are:

$$M = [R_R \times (F_R + N_R)] + [R_L \times (F_L + N_L)] + M_L + M_R + M_{susp} \qquad (A.3.6a)$$

where

$$R_R = -(a + \Delta_R)j' - r_R k' \qquad (A.3.6b)$$

$$R_L = (a - \Delta_L)j' - r_L k'$$

and Δ_L, Δ_R: Displacements of the contact points w.r.t. axle

F_L, F_R: Creep forces at left, right contact points

M_L, M_R: Creep moments at left, right contact points

N_L, N_R: Normal forces at left, right contact points

M_{susp}: Suspension moment

Applying Newton's Law for the equilibrium axis yields the following six equations.

Longitudinal equation

$$M\ddot{x} = F_{Lx} + F_{Rx} + F_{susp_x} \qquad (A.3.7)$$

Lateral equation

$$M\ddot{y} = F_{Ly} + F_{Ry} + N_{Ly} + F_{susp_y} \qquad (A.3.8)$$

Vertical equation

$$M\ddot{z} = F_{Lz} + F_{Rz} + N_{Rz} + N_{Lz} + F_{susp_z} - L_A \qquad (A.3.9)$$

Roll equation

$$I_{wx}\ddot{\phi} = I_{wy}\frac{V}{r_o}\dot{\psi} + R_{Ry}(F_{Rz} + N_{Rz}) - R_{Rz}(F_{Ry}+N_{Ry})$$

$$+ R_{Ly}(F_{Lz} + N_{Lz}) - R_{Lz}(F_{Ly} + N_{Ly}) \qquad (A.3.10)$$

$$+ M_{Lx} + M_{Rx} + M_{susp_x}$$

Spin equation

$$I_{wy}\ddot{\beta} = R_{Rz}F_{Rx} - R_{Rx}(F_{Rz} + N_{Rz}) + R_{Lz}F_{Lx}$$

$$- R_{Lx}(F_{Lz} + N_{Lz}) + M_{Ly} + M_{Ry} + M_{susp_y} \qquad (A.3.11)$$

Yaw equation

$$I_{wx}\ddot{\psi} = -I_{wy}\frac{V}{r_o}\dot{\phi} + R_{Rx}(F_{Ry} + N_{Ry}) - R_{Ry}F_{Rx}$$

$$+ R_{Lx}(F_{Ly} + N_{Ly}) - R_{Ly}F_{Lx} + M_{Lz} + M_{Rz} + M_{susp_z}$$

(A.3.12)

where

$$\begin{aligned}
L_A &= \text{axle load} \\
R_{LX} &= [-(a-\Delta_L)\cos\phi\,\sin\psi - r_L\sin\phi\sin\psi] \\
R_{Ly} &= [(a-\Delta_L)\cos\phi\,\cos\psi + r_L\sin\phi\,\cos\psi] \\
R_{Lz} &= [(a-\Delta_L)\sin\phi - r_L\cos\phi] \qquad (A.3.13) \\
R_{Rx} &= [(a+\Delta_R)\cos\phi\,\sin\psi - r_R\sin\phi\sin\psi] \\
R_{Ry} &= [-(a+\Delta_R)\cos\phi\cos\psi + r_R\sin\phi\cos\psi] \\
R_{Rz} &= [-(a+\Delta_R)\sin\phi - r_R\cos\psi]
\end{aligned}$$

A.4 Normal Forces

Normal forces at the left and right contact points are given by the relations:

Left wheel:

$$N_L = -N_L \sin(\delta_L+\phi)j''' + N_L\cos(\delta_L+\phi)k''' \qquad (A.4.1)$$

Right wheel:

$$N_R = N_R\sin(\delta_R - \phi)j''' + N_R\cos(\delta_R - \phi)k''' \qquad (A.4.2)$$

Normal forces N_L, N_R are obtained from the vertical and the roll equations. Solution of the equations (A.3.9) and (A.3.10) gives the magnitude of the normal forces as:

$$N_R\cos(\delta_R-\phi) = \frac{[R_{Ly} + R_{Lz}\tan(\delta_L+\phi)]F_z^* - M_\phi^*}{R_{Ly}-R_{Ry} + [R_{Lz}\tan(\delta_L+\phi)+R_{Rz}\tan(\delta_R-\phi)]} \qquad (A.4.3)$$

and

$$N_L\cos(\delta_L+\phi) = \frac{[-R_{Ry} + R_{Rz}\tan(\delta_R-\phi)]F_z^* + M_\phi^*}{R_{Ly}-R_{Ry} + [R_{Lz}\tan(\delta_L+\phi)+R_{Rz}\tan(\delta_R-\phi)]} \qquad (A.4.4)$$

where

$$F_z^* = M\ddot{z} + L_A - (F_{Rz} + F_{Lz} + F_{susp_z})$$

and

$$M_{\phi}^{*} = I_{wx}\ddot{\phi} - I_{wy}\Omega\ddot{\psi} + R_{Rz}F_{Ry} - R_{Ry}F_{Rz}$$

$$+ R_{Lz}F_{Ly} - R_{Ly}F_{Lz} - (M_{Lx} + M_{Rx} + M_{susp_x})$$

<u>Static Wheel Lift Condition</u>:

The vertical component of the creep forces given by equations (A.4.3) and (A.4.4) can be decomposed into two parts, namely, static part and dynamic part. Static parts of normal forces can also be obtained from the force moment balance of a wheelset. In Section A.6 this decomposition will be examined in gravitational stiffness derivation. It will be shown that the creep forces appear as a multiplicative factor in equations (A.6.18) and (A.6.19).

Static part of the equations (A.4.3) and (A.4.4) becomes:

$$\frac{N_R}{L_A}\cos(\delta_R-\phi) = \frac{a - r_L\tan(\delta_L+\phi)}{2a-[r_L\tan(\delta_L+\phi)+r_R\tan(\delta_R-\phi)]} \qquad (A.4.5)$$

$$\frac{N_L}{L_A}\cos(\delta_L+\phi) = \frac{a - r_R\tan(\delta_R-\phi)}{2a-[r_L\tan(\delta_L+\phi)+r_R\tan(\delta_R-\phi)]} \qquad (A.4.6)$$

In order not to have a wheel lift, the normal forces N_R and N_L should always be greater than zero. Assume that the wheel-set is moving to the left. The following cases are possible:

Case 1: $r_L \tan(\delta_L + \phi) < a$

It is clear that N_R and N_L are positive.

Case 2: $r_L \tan(\delta_L + \phi) = a$

This case corresponds to $N_R = 0$ and N_L takes its maximum value, i.e.,

$$N_L = \frac{L_A}{\cos(\delta_L + \phi)} \tag{A.4.7}$$

Case 3: $r_L \tan(\delta_L + \phi) > a$

When $r_L \tan(\delta_L + \phi)$ exceeds the value a, static wheel lift occurs, i.e., $N_R < 0$ and $N_L > 0$.

Therefore, the angles at which static wheel lift occurs are 56° for locomotive wheels and 60° for passenger wheels. In reality, wheel lift can occur at lower contact angles due to the high dynamic forces in the system.

A.5 Creep Forces

The creep forces, in general, are defined with respect to the contact plane. Since the derivation is done in the equilibrium axis, after the coordinate transformation, creep forces and creep moments in equilibrium axis are:

Left Wheel:

$$
\begin{aligned}
F_{Lx} &= F'_{Lx}\cos\psi - F'_{Ly}\cos(\delta_L + \phi)\sin\psi \\
F_{Ly} &= F'_{Lx}\sin\psi + F'_{Ly}\cos(\delta_L + \phi)\cos\psi \\
F_{Lz} &= F'_{Ly}\sin(\delta_L + \phi) \\
M_{Lx} &= M'_{Lz}\sin(\delta_L + \phi)\sin\psi \\
M_{Ly} &= -M'_{Lz}\sin(\delta_L + \phi)\cos\psi \\
M_{Lz} &= M'_{Lz}\cos(\delta_L + \phi)
\end{aligned}
\qquad (A.5.1a)
$$

Right Wheel:

$$
\begin{aligned}
F_{Rx} &= F'_{Rx}\cos\psi - F'_{Ry}\cos(\delta_R - \phi)\sin\psi \\
F_{Ry} &= -F'_{Rx}\sin\psi + F'_{Ry}\cos(\delta_R - \phi)\cos\psi \\
F_{Rz} &= -F'_{Ry}\sin(\delta_R - \phi) \\
M_{Rx} &= -F'_{Rz}\sin(\delta_R - \phi)\sin\psi \\
M_{Ry} &= M'_{Rz}\sin(\delta_R - \phi)\cos\psi \\
M_{Rz} &= M'_{Rz}\cos(\delta_R - \phi)
\end{aligned}
\qquad (A.5.1b)
$$

where

F'_{Ri}, F'_{Li}: $i^{\underline{th}}$ component of the creep forces at the contact plane

M'_{Ri}, M'_{Li}: $i^{\underline{th}}$ component of the creep moments at the contact plane.

A.6 Final Equations

Six rigid body equations were derived in Section A.3. Using the vertical and roll equations to find normal forces N_L, N_R equations A.4.3 and A.4.4 were obtained. The longitudinal and the spin equations decouple from the lateral and yaw equations for tangent track motions.

Substitution of the normal forces into the yaw and lateral equations gives:

Lateral equation:

$$M\ddot{y} = F_{Ly} + F_{Ry} + F_{susp_y} + N_R \sin(\delta_R - \phi) - N_L \sin(\delta_L + \phi) \tag{A.6.1}$$

Yaw equation:

$$\begin{aligned} I_{wx}\ddot{\psi} = & -I_{wy} \frac{V}{r_o} \dot{\phi} + (R_{Rx}F_{Ry} - R_{Ry}F_{Rx}) + (R_{Lx}F_{LY} - R_{Ly}F_{Lx}) \\ & + R_{Rx}N_R \sin(\delta_R - \phi) - R_{Lx}N_L \sin(\delta_L + \phi) \\ & + M_{Lz} + M_{Rz} + M_{susp_z} \end{aligned} \tag{A.6.2}$$

A.6.1 Lateral Gravitational Stiffness Derivation

Lateral "gravitational stiffness force", F_{grav}, is defined as the net lateral (in j''' direction) component of the normal forces:

$$F_{grav} = -N_R \sin(\delta_R - \phi) + N_L \sin(\delta_L + \phi) \qquad \text{(A.6.3)}$$

A small yaw and roll angle assumption together with equations (A.4.3) and (A.4.4) reduces the equation (A.6.3) to:

$$F_{grav} = F_z^* \Delta_L(\Delta y) + \frac{M_\phi^*}{a} \Delta_\psi(\Delta y) + \frac{F_z^*}{a} \Delta_c(\Delta y) \qquad \text{(A.6.4)}$$

where

$$F_z^* = L_A - [F'_{Ly} \sin(\delta_L + \phi) - F'_{Ry} \sin(\delta_R - \phi)] + M\ddot{z} - F_{susp_z} \qquad \text{(A.6.5)}$$

$$F_{susp_z} = 0 \text{ at equilibrium} \qquad \text{(A.6.6)}$$

$$M_\phi^* = I_{wx} \ddot{\phi} - I_{wy} \Omega_o \dot{\psi} - \psi\, [r_R F'_{Rx} + r_L F'_{Lx}]$$

$$-[r_R F'_{Ry} \cos(\delta_R - \phi) + r_L F_{Ly} \cos(\delta_L + \phi)]$$

$$+\psi [M'_{Lz} \sin(\delta_L + \phi) - M'_{Rz} \sin(\delta_R - \phi)] - M_{susp_x} \qquad \text{(A.6.7)}$$

$$M_{susp_x} \equiv 0 \text{ at equilibrium} \qquad \text{(A.6.8)}$$

$$\Delta_L(\Delta y) = \frac{\tan(\delta_L + \phi) - \tan(\delta_R - \phi)}{2 - \frac{1}{a}[r_L \tan(\delta_L + \phi) + r_R \tan(\delta_R - \phi)]} \quad (A.6.9)$$

$$\Delta_\psi(\Delta y) = \frac{\tan(\delta_L + \phi) + \tan(\delta_R - \phi)}{2 - \frac{1}{a}[r_L \tan(\delta_L + \phi) + r_R \tan(\delta_R - \phi)]} \quad (A.6.10)$$

$$\Delta_c(\Delta y) = \frac{(r_L - r_R) \cdot \tan(\delta_L + \phi) \cdot \tan(\delta_R - \phi)}{2 - \frac{1}{a}[r_L \tan(\delta_L + \phi) + r_R \tan(\delta_R - \phi)]} \quad (A.6.11)$$

Δy = Lateral displacement of the wheelset w.r.t. rail

In general, three wheelset positions are possible:

a) Both of the wheels are in the linear range, i.e. wheelset excursion is less than the flange clearance

b) Left wheel is on the flange

c) Right wheel is on the flange

Case a:

$$\Delta_L(\Delta y) \simeq \frac{\delta_L + \delta_R}{2}$$

$$\frac{\Delta_c(\Delta y)}{a} \simeq \frac{(r_L - r_R)}{a} (\delta_L + \phi)(\delta_R - \phi)$$

The result is $\frac{\Delta_c(\Delta y)}{a} << \Delta_L(\Delta y)$

Case b:

$$\Delta_L(\Delta y) \simeq \frac{\tan(\delta_L + \phi)}{2 - \frac{1}{a}[r_L \tan(\delta_L + \phi)]}$$

$$\frac{\Delta_c(\Delta y)}{a} = \frac{(r_L - r_R)}{a} \frac{\tan(\delta_L + \phi) \cdot (\delta_R - \phi)}{2 - \frac{1}{a}[r_L \tan(\delta_L + \phi)]}$$

The result is $\frac{\Delta_c(\Delta y)}{a} << \Delta_L(\Delta y)$

Case c:

$$\Delta_L(\Delta y) \simeq \frac{-\tan(\delta_R - \phi)}{2 - \frac{1}{a}[r_R \tan(\delta_R - \phi)]}$$

$$\frac{\Delta_c(\Delta y)}{a} \simeq \frac{(r_L - r_R)}{a} \frac{(\delta_L + \phi) \tan(\delta_R - \phi)}{2 - \frac{1}{a}[r_R \tan(\delta_R - \phi)]}$$

The result is $\frac{\Delta_c(\Delta y)}{a} << \Delta_L(\Delta y)$

Therefore, $F_z^* \frac{\Delta_c(\Delta y)}{a} << F_z^*\Delta_L(\Delta y)$, always, and equation (A.6.4) reduces to:

$$F_{grav} = F_z^*\Delta_L(\Delta y) + \frac{M_\phi^*}{a}\Delta_\psi(\Delta y) \qquad \text{(A.6.12)}$$

A small yaw and roll angle assumption together with equations (A.6.6) and (A.6.8), and by neglecting the vertical force and vertical component of the creep force reduces F^* and M_ϕ^* :

$$F_z^* \approx L_A \qquad \text{(A.6.13)}$$

and

$$M_\phi^* = -r_R F'_{Ry}\cos(\delta_R-\phi) - r_L F'_{Ly}\cos(\delta_L+\phi) \qquad \text{(A.6.14)}$$

A.6.2 Yaw Gravitational Stiffness Derivation

Yaw gravitational stiffness (monent), M_{grav} is defined as:

$$M_{grav} = -R_{Rx}N_R\sin(\delta_R-\phi) + R_{Lx}N_L\sin(\delta_L+\phi) \qquad \text{(A.6.15)}$$

where

$$R_{Lx} = [-(a-\Delta_L)\cos\phi\sin\psi - r_L\sin\phi\sin\psi]$$

$$R_{Rx} = [(a+\Delta_R)\cos\phi\sin\psi - r_R\sin\phi\sin\psi].$$

Assuming small yaw and roll angles, equation (A.6.15) reduces to:

$$M_{grav} = -a\psi[F_z^* \Delta_\psi(\Delta y) + \frac{M_\phi^*}{a} \Delta_L(\Delta y)]$$

$$+ a\psi \, F_z^* \, \Delta_{c\psi}(\Delta y) \qquad \text{(A.6.16)}$$

where

$$\Delta_{c\psi}(\Delta y) = \frac{(r_L + r_R)}{a} \cdot \frac{\tan(\delta_L + \phi)\tan(\delta_R - \phi)}{2 - \frac{1}{a}[r_L \tan(\delta_L + \phi) + r_R \tan(\delta_R - \phi)]}$$

Case a: Wheelset is within the flange clearance:

then

$$\Delta_{c\psi}(\Delta y) \simeq (\frac{r_L + r_R}{a}) \frac{(\delta_L + \phi)(\bar{\delta}_R - \phi)}{2}$$

$$\Delta_\psi(\Delta y) \simeq \frac{(\delta_L + \delta_R)}{2}$$

Since $\frac{r_L + r_R}{a}$ is of order one, the result is;

$$\Delta_{c\psi}(\Delta y) << \Delta_\psi(\Delta y)$$

Case b: Left wheel is on the flange;

$$\Delta_{c\psi}(\Delta y) \simeq \frac{(r_L + r_R)}{a} \frac{(\delta_R - \phi)\tan(\delta_L + \phi)}{2 - \frac{1}{a}[r_L \tan(\delta_L + \phi)]}$$

$$\Delta_\psi(\Delta y) \simeq \frac{\tan(\delta_L + \phi)}{2 - \frac{1}{a}[r_L \tan(\delta_L+\phi)]}$$

The result is: $\Delta_{c\psi}(\Delta y) << \Delta_\psi(\Delta y)$

Case c: Right wheel is on the flange:

Similarly

$$\Delta_{c\psi}(\Delta y) << \Delta_\psi(\Delta y)$$

Therefore $\Delta_{c\psi}(\Delta y) << \Delta_\psi(\Delta y)$ in general, and M_{grav} reduces to: (A.6.18)

$$M_{grav} = -a\psi[F_z^*\Delta_\psi(\Delta y) + \frac{M_\phi^*}{a} \Delta_L(\Delta y)] \quad (A.6.19)$$

A.6.3 Wheelset Equations

Substitution of the equations (A.6.12) and (A.6.17) into the yaw and lateral equations and neglecting the higher order terms gives:

Lateral Equation:

$$M\ddot{y} = \psi F'_{Lx}(1 + \frac{r_L}{a} \Delta_\psi) + \psi F'_{Rx}(1 + \frac{r_R}{a} \Delta_\psi)$$

$$+ F'_{Ly}\cos(\delta_L + \phi) \cdot [1 + \frac{r_L}{a} \Delta_\psi]$$

$$+F'_{Ry}\cos(\delta_R - \phi) \cdot [1 + \frac{r_R}{a} \Delta_\psi]$$

$$-L_A \Delta_L (\Delta y) + F_{susp_y} \qquad (A.6.18)$$

Yaw Equation:

$$I_{wx}\ddot{\psi} + I_{wy}\Omega_o\dot{\phi} = a(F'_{Rx} - F'_{Lx}) + M'_{Lz}\cos(\delta_L + \phi)$$

$$+ M'_{Rz}\cos(\delta_R - \phi) + a\psi L_A \Delta_\psi(\Delta y) + M_{susp_z} \qquad (A.6.19)$$

A.7 Derivation of Creepages

Lateral, longitudinal and spin creepages are defined as relative linear and angular motions between the wheel and rail, i.e.

$$\xi_y = \frac{\text{(Lateral velocity of wheel - lateral velocity of rail) at contact point}}{\text{nominal velocity}}$$

$$\xi_x = \frac{\text{(Longitudinal velocity of wheel - longitudinal velocity of rail) at cont. pt.}}{\text{nominal velocity}}$$

$$\xi_{sp} = \frac{\text{(Angular velocity of wheel - angular velocity of rail) at contact point}}{\text{nominal velocity}}$$

Let R'_L and R'_R be the position vector of the left and right contact points from equilibrium axis, i.e.,

Left wheel:

$$R_L' = xi''' + yj''' \ \ zk''' + (a - \Delta_L)j' - r_L k'$$

$$= [x - (a - \Delta_L)\cos\phi\sin\psi - r_L\sin\phi\sin\psi]i'''$$

$$+ [y + (a - \Delta_L)\cos\phi\cos\psi + r_L\sin\phi\cos\psi]j'''$$

$$+ [z + (a - \Delta_L)\sin\phi - r_L\cos\phi]k''' \qquad (A.7.2)$$

then

$$\xi_{xL} = (\dot{R}_L' \cdot e_{1L} - V\frac{r_L}{r_o}\cos\psi)/V$$

$$\xi_{yL} = (\dot{R}_L' \cdot e_{2L})/V \qquad (A.7.3)$$

$$\xi_{spL} = (\omega \cdot e_{3L})/V$$

where

$(\cdot)$ = dot product of two vectors

$$e_{1L} = \cos\psi i''' + \sin\psi j'''$$

$$e_{2L} = -\cos(\delta_L + \phi)\sin\psi i''' + \cos(\delta_L + \phi)\cos\psi j''' + \sin(\delta_L + \phi)k'''$$

$$e_{3L} = -\sin\delta_L j' + \cos\delta_L k'$$

$$\omega = \dot{\phi}\, i' + (\Omega + \dot{\beta} + \dot{\psi}\sin\phi)j' + \dot{\psi}\cos\phi k' \qquad (A.7.4)$$

Right wheel:

$$R'_R = xi''' + yj''' + zk''' - (a + \Delta_R)j' - r_R k'$$

$$= [x + (a + \Delta_R)\cos\phi\sin\psi - r_R\sin\phi\sin\psi]i'''$$

$$+ [y - (a + \Delta_R)\cos\phi\cos\psi + r_R\sin\phi\cos\psi]j''' \qquad (A.7.5)$$

$$+ [z - (a + \Delta_R)\sin\phi - r_R\cos\phi]k'''$$

then

$$\xi_{xR} = (\dot{R}'_R \cdot e_{1R} - V \frac{r_R}{r_o}\cos\psi)/V$$

$$\xi_{yR} = (\dot{R}'_L \cdot e_{2R})/V \qquad (A.7.6)$$

$$\xi_{spR} = (\omega \cdot e_{3R})/V$$

where

$(\cdot)$ = dot product of two vectors

$$e_{1R} = \cos\psi\, i''' + \sin\psi\, j'''$$

$$e_{2R} = -\cos(\delta_R - \phi)\sin\psi i''' + \cos(\delta_R - \phi)\cos\psi j''' - \sin(\delta_R - \phi)k'''$$

$$e_{3R} = \sin\delta_R j' + \cos\delta_R k'$$

$$\omega = \dot{\phi}\, i' + (\Omega + \dot{\beta} + \dot{\psi}\sin\phi)j' + \dot{\psi}\cos\phi k' \qquad (A.7.7)$$

After some algebra and neglecting the higher order terms the creepages are obtained as:

Left wheel:

$$\xi_{xL} = \frac{1}{V}[V(1 - \frac{r_L}{r_o}) - ((a - \Delta_L)\cos\phi\cos\psi)\dot{\psi}] \cdot \cos\psi$$

$$\xi_{yL} = \frac{1}{V}[\dot{y}\cos\psi + r_L\cos\phi\ \cos^2\psi\ \dot{\phi} - V\sin\psi]\cos(\delta_L + \phi)$$

$$+ \frac{1}{V}[\dot{z} + (a - \Delta_L)\cos\phi\ \dot{\phi}]\ \sin(\delta_L + \phi) \qquad (A.7.8)$$

$$\xi_{spL} = \frac{1}{V}\ [\dot{\psi}\cos(\delta_L + \phi) - \Omega_o\sin\delta_L]$$

Right wheel:

$$\xi_{xR} = \frac{1}{V}\ [V(1 - \frac{r_R}{r_o}) + ((a + \Delta_R)\cos\phi\cos\psi)\dot{\psi}] \cdot \cos\psi$$

$$\xi_{yR} = \frac{1}{V}\ [\dot{y}\cos\psi + r_R\cos\phi\cos^2\psi\ \dot{\phi} - V\sin\psi]\cos(\delta_R - \phi)$$

$$- \frac{1}{V}\ [\dot{z} - (a + \Delta_R)\cos\phi\ \dot{\phi}]\sin(\delta_R - \phi) \qquad (A.7.9)$$

$$\xi_{spR} = \frac{1}{V}\ [\dot{\psi}\cos(\delta_R - \phi) + \Omega_o\sin\delta_R]$$

where

$\Omega_o = V/r_o$ (Nominal angular velocity)

A small roll and yaw angles assumption together with small vertical velocity of wheelset reduces the equations (A.7.8) and (A.7.9) to:

Left wheel:

$$\xi_{xL} = \frac{1}{V}[V(1 - \frac{r_L}{r_o}) - a\dot{\psi}]$$

$$\xi_{yL} = \frac{1}{V}[\dot{y} + r_L\dot{\phi} - V\psi)\cos(\delta_L + \phi) \qquad (A.7.10)$$

$$\xi_{spL} = \frac{1}{V}[\dot{\psi}\cos(\delta_L + \phi) - \Omega_o\sin\delta_L]$$

Right wheel:

$$\xi_{xR} = \frac{1}{V}[V(1 - \frac{r_R}{r_o}) + a\dot{\psi}]$$

$$\xi_{yR} = \frac{1}{V}[\dot{y} + r_R\dot{\phi} - V\psi]\cos(\delta_R - \phi) \qquad (A.7.11)$$

$$\xi_{spR} = \frac{1}{V}[\dot{\psi}\cos(\delta_R - \phi) + \Omega_o\sin\delta_R]$$

Furthermore, small contact angles assumption reduces the creepages to:

Left wheel:

$$\xi_{xL} = \frac{1}{V}[V(1 - \frac{r_L}{r_o}) - a\dot{\psi}]$$

$$\xi_{yL} = \frac{1}{V}[\dot{y} + r_L\dot{\phi} - V\psi] \qquad (A.7.12)$$

$$\xi_{spL} = \frac{1}{V}[\dot{\psi} - \Omega_o\delta_L]$$

Right wheel:

$$\xi_{xR} = \frac{1}{V}[V(1 - \frac{r_R}{r_o}) + a\dot{\psi}]$$

$$\xi_{yR} = \frac{1}{V}[\dot{y} + r_R\dot{\phi} - V\psi] \qquad (A.7.13)$$

$$\xi_{spR} = \frac{1}{V}[\dot{\psi} + \Omega_o\delta_R]$$

A.8 Simple Forms of Equations of Motion

In this section the simplification of the nonlinear wheelset equations (A.6.18 and A.6.19) under certain assumptions are presented.

A.8.1 Linear Creep Force/Creepage

The most widely accepted linear creep law is due to Kalker [53] and called "Linearized Theory". The linear creep force/creepage relations are given by:

Lateral Creep Force:

$$F_y = -f_{11}\xi_y - f_{12}\xi_{sp} \qquad (A.8.1)$$

Longitudinal Creep Force:

$$F_x = -f_{33}\xi_x \qquad (A.8.2)$$

Spin Creep Moment:

$$M_z = f_{12}\xi_y - f_{22}\xi_{sp} \qquad \text{(A.8.3)}$$

where

ξ_y = Lateral creepage

ξ_x = Longitudinal creepage

ξ_{sp} = Spin creepage

Using creepages given by equations (A.7.10) and (A.7.11) together with equations (A.8.1 to A.8.3) and also assuming that $r_L\dot{\phi}$ and $r_R\dot{\phi} \approx r_o\dot{\phi}$ in creepage equations reduces the wheelset equations (A.6.18) and (A.6.19) to:

Lateral equation:

$$M\ddot{y} + [\frac{2f_{11}}{V}(\dot{y} + r_o\dot{\phi} - V\psi) + \frac{2f_{12}}{V}\dot{\psi}] \cdot \Delta_3(\Delta y)$$

$$- \frac{2f_{12}}{r_o}\Delta_2(\Delta y) + L_A\Delta_L(\Delta y) = F_{susp_y} \qquad \text{(A.8.4)}$$

Yaw equation:

$$I_{wx}\ddot{\psi} + I_{wy}\frac{V}{r_o}\dot{\phi} + \frac{2a^2f_{33}}{V}\dot{\psi} + \frac{2af_{33}}{r_o}(\frac{r_L - r_R}{2})$$

$$+ \left[\frac{2f_{22}}{V} \dot{\psi} - \frac{2f_{12}}{V} (\dot{y} + r_o\dot{\phi} - V\psi)\right] \cdot \Delta_4(\Delta y)$$

(A.8.5)

$$- \frac{2f_{22}}{r_o} \Delta_1(\Delta y) - a\psi \quad L_A \Delta_\psi(\Delta y) = M_{susp_z}$$

where

$$\Delta_L(\Delta y) = \frac{\tan(\delta_L + \phi) - \tan(\delta_R - \phi)}{2 - \frac{1}{a}[r_L \tan(\delta_L + \phi) + r_R \tan(\delta_R - \phi)]} \qquad (A.8.6)$$

$$\Delta_\psi(\Delta y) = \frac{\tan(\delta_L + \phi) + \tan(\delta_R - \phi)}{2 - \frac{1}{a}[r_L \tan(\delta_L + \phi) + r_R \tan(\delta_R - \phi)]} \qquad (A.8.7)$$

$$\Delta_1(\Delta y) = \frac{\sin\delta_L \cdot \cos(\delta_L + \phi) - \sin\delta_R \cdot \cos(\delta_R - \phi)}{2}$$

(A.8.8)

$$\Delta_2(\Delta y) = \frac{\sin\delta_L \cdot \cos(\delta_L + \phi) - \sin\delta_R \cdot \cos(\delta_R - \phi)}{2 - \frac{1}{a}[r_L \tan(\delta_L + \phi) + r_R \tan(\delta_R - \phi)]}$$

(A.8.9)

$$\Delta_3(\Delta y) = \frac{\cos^2(\delta_L + \phi) + \cos^2(\delta_R - \phi)}{2 - \frac{1}{a}[r_L \tan(\delta_L + \phi) + r_R \tan(\delta_R - \phi)]}$$

(A.8.10)

$$\Delta_4(\Delta y) = \frac{\cos^2(\delta_L + \phi) + \cos^2(\delta_R - \phi)}{2}$$

(A.8.11)

It is clear that $\Delta_L(\Delta y)$, $\Delta_1(\Delta y)$, $\Delta_2(\Delta y)$ are odd functions and $\Delta_\psi(\Delta y)$, $\Delta_3(\Delta y)$, $\Delta_4(\Delta y)$, are even functions of wheelset excursion Δy.

In digital simulation models odd and even functions can be used. But in order not to get a bias term in equivalent gains, odd nonlinearities should be used in equivalent linearization programs. The following table shows the error introduced by replacing the even nonlinearities with their nominal values, i.e.

$$\Delta_3(\Delta y) \simeq 1$$

$$\Delta_4(\Delta y) \simeq 1$$

$$\Delta_\psi(\Delta y) \simeq \delta_o$$ (δ_o=0.0694 for New Wheel on New Rail at STD gauge)

$(\delta_{L,R} \pm \phi)$	5°	10°	20°	30°	40°	50°
$\Delta_3(\Delta y)$	1.028	1.05	1.081	1.10	1.13	1.22
$\Delta_4(\Delta y)$	0.996	0.985	0.940	0.875	0.793	0.707
$\Delta_\psi(\Delta y)$	0.045	0.094	0.207	0.358	0.584	0.994

Digital simulation of twelve degrees of freedom locomotive half carbody model at 60 mph shows that

$$|\dot{y}|_{max} < 10 \text{ in/sec}$$

$$|\dot{\psi}|_{max} < 0.5 \text{ rd/sec}$$

$$|\psi|_{max} < 0.01 \text{ rd}$$

Therefore the actual errors introduced by the nominal values of $\Delta_4(\Delta y)$ and $\Delta_\psi(\Delta y)$ in equations (A.8.4) and (A.8.5) will be negligible with respect to the error introduced by $\Delta_3(\Delta y)$ which is less than 13% when the wheelset is on a forty degrees flange.

Using these assumptions the wheelset equations further reduce to:

Lateral equation:

$$M\ddot{y} + \frac{2f_{11}}{V}(\dot{y} + r_o\dot{\phi} - V\psi) + \frac{2f_{12}}{V}\dot{\psi}$$

$$- \frac{2f_{12}}{r_o}\Delta_2(\Delta y) + L_A\Delta_L(\Delta y) = F_{susp_y} \qquad \text{(A.8.13)}$$

Yaw equation:

$$I_{wx}\ddot{\psi} + I_{wy}\frac{V}{r_o}\dot{\phi} + \frac{2a^2f_{33}}{V}\dot{\psi} + \frac{2af_{33}}{r_o}\left(\frac{r_L - r_R}{2}\right)$$

$$+ \frac{2f_{22}}{V}\dot{\psi} - \frac{2f_{12}}{V}(\dot{y} + r_o\dot{\phi} - V\psi)$$

$$- \frac{2f_{22}}{r_o}\Delta_1(\Delta y) - a\psi L_A\delta_o = M_{susp_z} \qquad \text{(A.8.14)}$$

where

$\Delta_L(\Delta y)$, $\Delta_1(\Delta y)$, $\Delta_2(\Delta y)$ are given by equations (A.8.6), (A.8.8) and (A.8.9)

A.8.2 <u>Linear Creep, Small Contact Angles</u>

Assuming small contact angles and linear creep force/creepage relations reduces equations (A.6.1) and (A.6.2) to:

Lateral equation:

$$M\ddot{y} + 2f_{33}\left[1 - \frac{(r_L + r_R)}{2r_o}\right]\psi + \frac{2f_{11}}{V}\left[\dot{y} + \frac{(r_L + r_R)}{2}\dot{\phi} - V\psi\right]$$

$$+2f_{12}\left[\frac{\dot{\psi}}{V} - \frac{\delta_L - \delta_R}{2r_o}\right] + L_A\left[\frac{\delta_L - \delta_R}{2} + \phi\right] = F_{susp_y}$$

(A.8.15)

Yaw equation:

$$I_{wx}\ddot{\psi} + I_{wy}\frac{V}{r_o}\dot{\phi} + \frac{2a^2 f_{33}}{r_o}\frac{(r_L - r_R)}{2a} - \frac{2f_{12}}{V}\left(\dot{y} + \frac{(r_L + r_R)}{2}\dot{\phi} - V\psi\right]$$

$$+ \frac{2a^2 f_{33}}{V}\dot{\psi} - 2f_{22}\left(\frac{\delta_L - \dot{\delta}_R}{2r_o}\right) - aL_A\left(\frac{\delta_L + \delta_R}{2}\right)\psi$$

$$+ \frac{2f_{22}}{V}\dot{\psi} = M_{susp_z} \qquad \text{(A.8.16)}$$

A.8.3 Linear Creep, Linear Profiled Wheel

The linear profiled wheel assumption further simplifies the equations of motion for the wheelset, i.e.,

$$\frac{(\delta_L - \delta_R)}{2} \simeq \frac{\Delta}{a}\,\Delta y$$

$$\cdot \quad \frac{(r_L - r_R)}{2a} \simeq \frac{\lambda}{a} \Delta y \tag{A.8.17}$$

$$\cdot \quad \phi \simeq \frac{a_1}{a} \Delta y$$

where

Δy = wheelset excursion = $y - y_r$

y = absolute lateral displacement of wheelset

y_r = absolute lateral displacement of the rail

Equations (A.8.15) and (A.8.16) reduce to:

$$M\ddot{y} + 2f_{33}[1 - \frac{(r_L+r_R)}{2r_o}]\psi + \frac{2f_{11}}{V}[\dot{y} + \frac{(r_L+r_R)}{2a} a_1(\dot{y}-\dot{y}_r)-V\psi]$$

$$+2f_{12}[\frac{\dot{\psi}}{V} - \frac{\Delta}{ar_o}(y - y_r)]+L_A[\frac{\Delta + a_1}{a}](y-y_r) = F_{susp_y} \tag{A.8.18}$$

Yaw equation:

$$I_{wx}\ddot{\psi}+I_{wy} \frac{V}{r_o} \frac{a_1}{a}(\dot{y}-\dot{y}_r) + \frac{2af_{33}\lambda}{r_o}(y-y_r) - \frac{2f_{12}}{V}[\dot{y}+ \frac{(r_L+r_R)}{2a}a_1(\dot{y}-\dot{y}_r)-V\psi]$$

$$+ \frac{2a^2f_{33}}{V}\dot{\psi} - 2f_{22}(\frac{\Delta}{ar_o} (y-y_r) - \frac{\dot{\psi}}{R}) - aL_A(\frac{(\delta_L+\delta_R)}{2})\psi =M_{susp_z}$$

(A.8.19)

A.8.4 Linear Creep, Conical Wheel

A conical wheel assumption together with (A.8.17) gives the most simplified equations, i.e.:

- $$\frac{(r_L - r_R)}{2a} \simeq \frac{\lambda}{a} \Delta y$$

- $$\frac{(\hat{\delta}_L - \delta_R)}{2} \simeq 0$$

- $$\phi \simeq \frac{a_1}{a} \Delta y; \quad a_1 = \lambda \qquad \text{(A.8.20)}$$

- $$\frac{(r_L + r_R)}{2} \simeq r_o$$

- $$\frac{(\delta_L + \delta_R)}{2} \simeq \delta_o$$

The wheelset equations reduce to:

$$M\ddot{y} + \frac{2f_{11}}{V} [\dot{y} + \frac{a_1 r_o}{a} \dot{y} - V\psi] + \frac{2f_{12}}{V} \dot{\psi} + \frac{L_A}{a} a_1 y - F_{susp_y} = u_L(t)$$

(A.8.21)

Yaw equation:

$$I_{wx}\ddot{\psi} + I_{wy} \frac{a_1 V}{a r_o} \dot{y} + \frac{2 a f_{33} \lambda}{r_o} y - \frac{2 f_{12}}{V} [\dot{y} + \frac{a_1 r_o}{a} \dot{y} - V\psi]$$

$$+ \frac{2a^2 f_{33}}{V} \dot{\psi} + \frac{2 f_{22}}{V} \dot{\psi} - L_A \cdot a\delta_o \psi - M_{susp_z} = u_\psi(t)$$

(A.8.22)

where

$$u_L(t) = \frac{2 f_{11} a_1 r_o}{V \cdot a} \dot{y}_r + L_A \frac{a_1}{a} y_r \qquad \text{(A.8.23)}$$

$$u_\psi(t) = \left(\frac{I_{wy} a_1 V}{a\, r_o} - \frac{2 f_{12} a_1 r_o}{a\, V}\right)\dot{y}_r + \frac{2 a f_{33} \lambda}{r_o} \dot{y}_r$$

(A.8.24)

A.9 Approximate Nonlinear Creep Force Model

The creep forces and the creep moment due to the shear stresses in the contact area between the wheel and the rail are important in the dynamic analysis of rail vehicles. For many problems in rail vehicle dynamics a linear creep force/creepage relationship has been used to determine the lateral stability and to estimate the slip boundaries for steady state curving. But recent studies [4] have shown the need for more sophisticated models of the wheel/rail interaction processes; in particular, adhesion limits on the creep force/creepage relationship should be included.

Vermuelen-Johnson [52] have formulated a nonlinear creep law which has been confirmed by laboratory experiments, this theory, however, does not include spin creepage which is known to be significant in the wheel flange region. Kalker [53] has formulated a nonlinear creep law that incorporates the effects of this spin creepage. The conversion of Kalker's Algol language computer program to Fortran is given in reference [54]. The inputs to the program are a function of the resultant normal load on the contact region. Therefore, all the creep force calculations must be on-line in a rail vehicle program. Even for Kalker's "Simplified Theory" [53] the computation time for one calculation of the creep forces is an order of magnitude greater than the simulation integration time step. Therefore, a "Heuristic Nonlinear Creep Force Model" [53] has been evaluated and found to be adequate over a broad range of creepages.

The most widely accepted linear creep law is due to Kalker [55]. The linear (unlimited) creep force/creepage relations are given by:

Lateral Creep Force:

$$F_y = -f_{11}\xi_y - f_{12}\xi_{sp} \qquad (A.9.1)$$

Longitudinal Creep Force:

$$F_x = -f_{33}\xi_x \tag{A.9.2}$$

Spin Creep Moment:

$$M_z = f_{12}\xi_y - f_{22}\xi_{sp} \tag{A.9.3}$$

where

ξ_y = lateral creepage

ξ_x = longitudinal creepage

ξ_{sp} = spin creepage

f_{11} = lateral creep coefficient

f_{12} = lateral/spin creep coefficient

f_{22} = spin creep coefficient

f_{33} = longitudinal creep coefficient

In approximate creep model, the creep forces are first computed using the linear theory and the nonlinear effect of the adhesion limit is brought in by computing:

$$\bar{F}'_R = (\bar{F}_x^2 + \bar{F}_y^2)^{1/2} \qquad (A.9.4)$$

where $\bar{F}_x = \dfrac{F_x}{\mu N}$

$\bar{F}_y = \dfrac{F_y}{\mu N}$

F_x = unlimited (linear) longitudinal creep force

F_y = unlimited (linear) lateral creep force

N = normal load at the contact region

μ = coefficient of friction

Following the Vermuelen-Johnson approach for creep without spin the limited normalized resultant force is determined by:

$$F_R = \begin{cases} (\bar{F}'_R - \frac{1}{3}\bar{F}'^2_R + \frac{1}{27}\bar{F}'^3_R) & ; \quad \bar{F}'_R \leq 3 \\ 1 & ; \quad \bar{F}_R > 3 \end{cases} \qquad (A.9.5)$$

Note that the above equation includes the spin creep contribution to the lateral creep force, F_y, in computing the resultant creep force, $\bar{F}'_R$.

Then the approximate nonlinear forces in lateral and longitudinal directions are given by:

$$F_{yN} = \frac{\bar{F}_R}{\bar{F}'_R} F_y$$

$$F_{xN} = \frac{\bar{F}_R}{\bar{F}'_R} F_x \qquad \text{(A.9.6)}$$

Figure A.4 and A.5 show the normalized creep forces vs normalized lateral creepages. The normalized creepages are a function of the normal force at the contact region and are defined as [54]:

$$UXN = \frac{\xi_x \cdot \rho}{\mu \cdot C} \qquad \text{(Normalized Longitudinal Creepage)}$$

$$UYN = \frac{\xi_y \cdot \rho}{\mu \cdot C} \qquad \text{(Normalized Lateral Creepage)}$$

$$PHN = \frac{\xi_{sp} \cdot \rho}{\mu} \qquad \text{(Normalized Spin Creepage)} \qquad \text{(A.9.7)}$$

where

$$C = \sqrt{a.b} = \text{function of normal load}$$

$$\frac{4}{\rho} = \frac{1}{R_1^+} + \frac{1}{R_1^-} + \frac{1}{R_2^+} + \frac{1}{R_2^-} \quad \text{with } R_1^+,\ R_1^-,\ R_2^+,\ R_2^-$$

being the principal radii of curvature of the two elastic bodies,

a = semi-axis of the contact ellipse in rolling direction

b = semi-axis of the contact ellipse in lateral direction

Figure A.4 and A.5 show the comparison of the Nonlinear Approximate Model with Kalker's Simplified Nonlinear Theory for thread and flange region, respectively. These figures show that Heuristic Model's results are close to Kalker's Simplified Theory results. The maximum error in lateral creep force is 11% whereas the maximum error in longitudinal creep force is less than 5%.

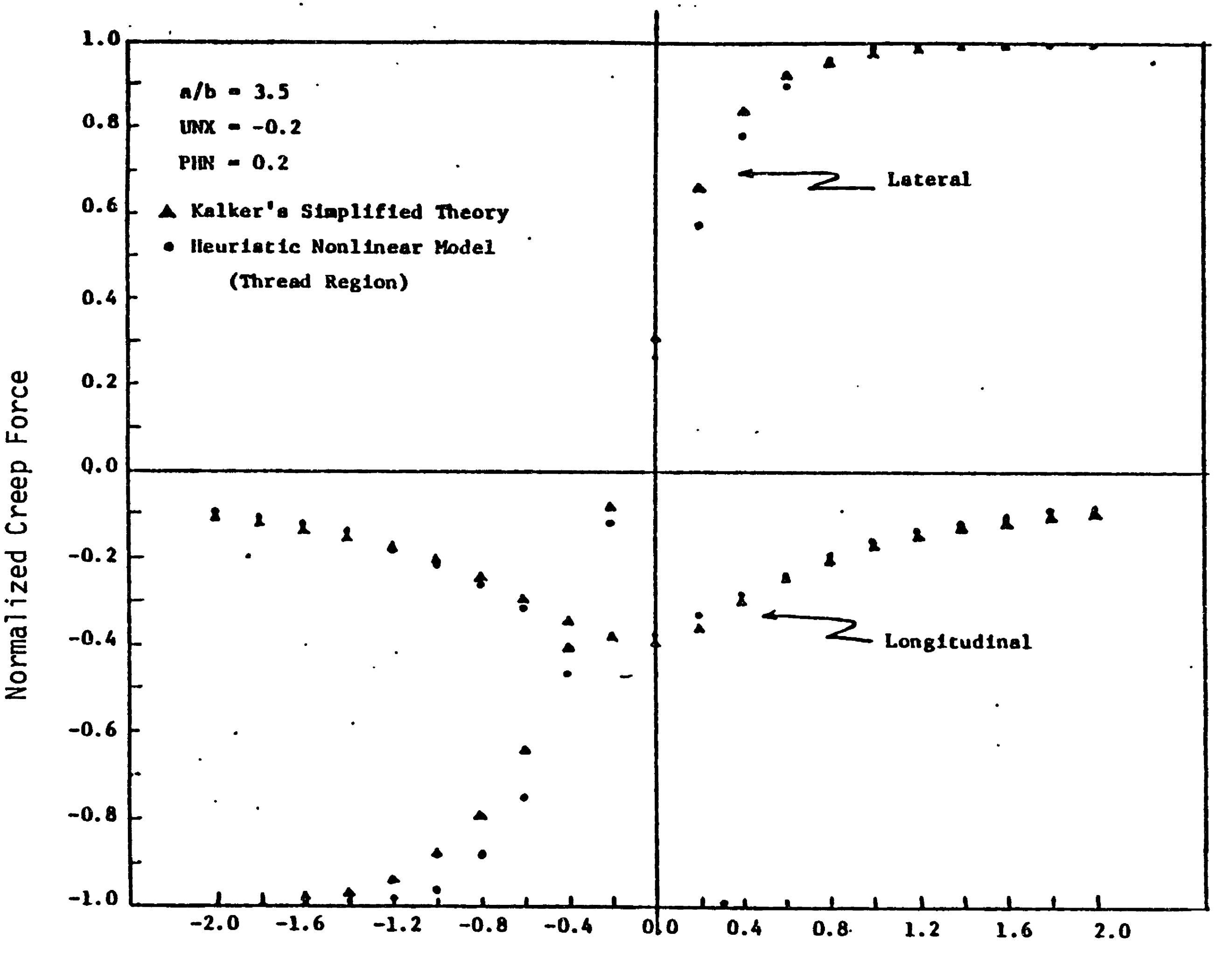

FIGURE A.4: COMPARISON OF THE "APPROXIMATE CREEP MODEL" WITH KALKER'S SIMPLIFIED NONLINEAR THEORY

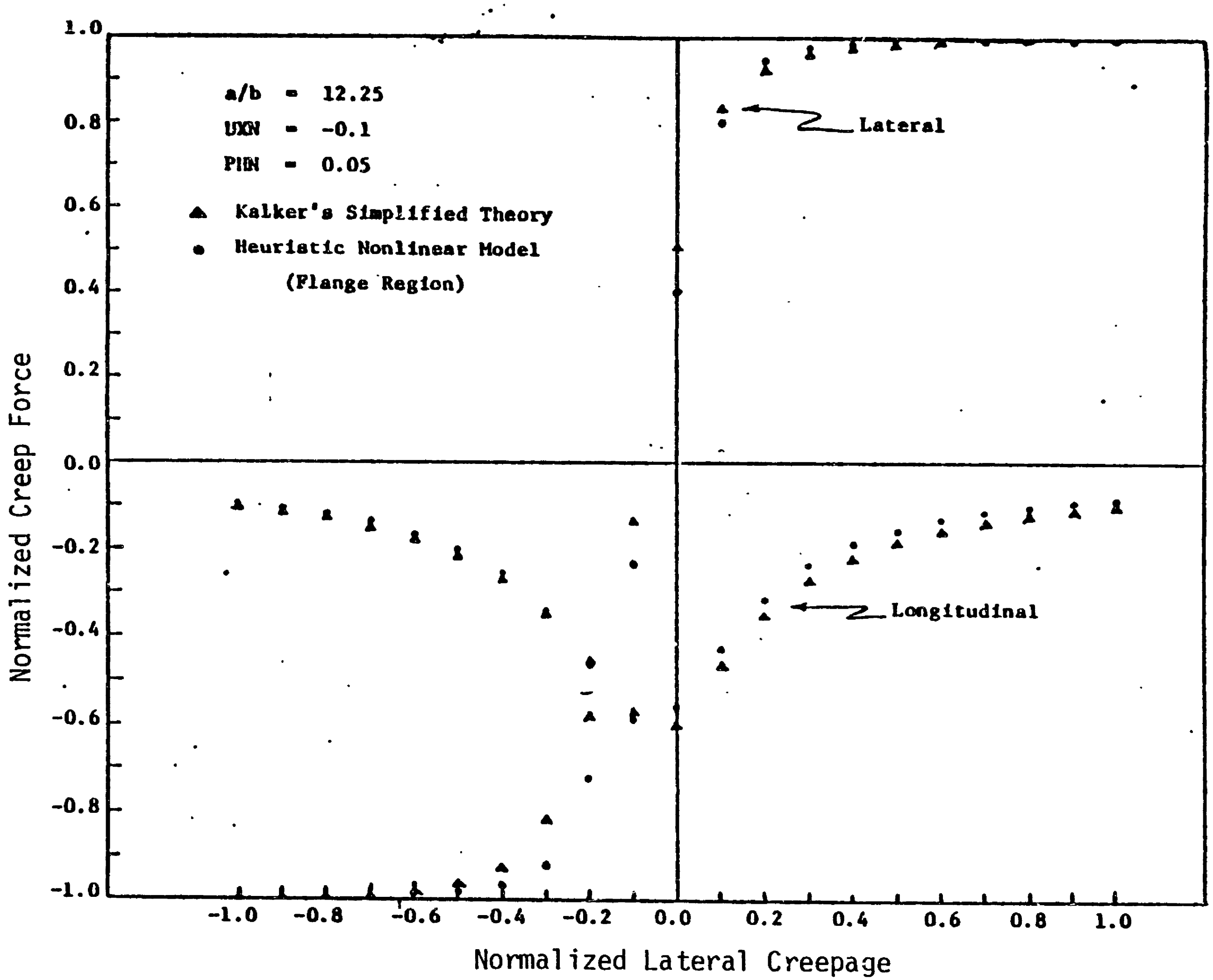

FIGURE A.5: COMPARISON OF THE "APPROXIMATE CREEP MODEL" WITH KALKER'S SIMPLIFIED NONLINEAR THEORY

APPENDIX B

LOCOMOTIVE EQUATIONS

In this appendix, the nonlinear equations of motion for the half-carbody digital locomotive model and statistically linearized equations of motion for the same model are presented. Section B.3 describes the extension of half-carbody equations to full carbody equations. Also, baseline parameters for an EMD SDP 40, six-axle locomotive are presented [21,22].

B.1 Digital Model Equations

Leading Wheelset:

Lateral Equation

$$M_w \ddot{y}_1 = [F'_{Lx}(1 + \frac{r_L}{a} \Delta_\psi) + F'_{Rx}(1 + \frac{r_R}{a} \Delta_\psi)]_1 \cdot y_2$$

$$+ \left\{ F'_{Ly}[1 + \frac{r_L}{a} \Delta_\psi] \cdot \cos(\delta_L + \phi) + F'_{Ry}[1 + \frac{r_R}{a} \Delta_\psi] \cdot \cos(\delta_R - \phi) \right\}_1$$

$$- L_A \Delta_{L_1}(y) - D_{py_1} - F_{kpy_1} \qquad \text{(B.1.1)}$$

Yaw Equation

$$I_{wx} \ddot{y}_2 + I_{wy} \frac{V}{r_o} \dot{\phi}_1 = a(F'_{Rx} - F'_{Lx})_1 + M'_{Lz_1} \cos(\delta_L + \phi)_1$$

$$+ M'_{Rz_1} \cos(\delta_R - \phi)_1 + aL_A \Delta_{\psi 1} y_2 - D_{pyaw_1} - M_{pyaw_1} \qquad \text{(B.1.2)}$$

Middle Wheelset

Lateral Equation

$$M_w\ddot{y}_3 = [F'_{Lx}(1 + \frac{r_L}{a}\Delta_\psi) + F'_{Rx}(1 + \frac{r_R}{a}\Delta_\psi)]_2\, y_4$$

$$+\left\{F'_{Ly}[1 + \frac{r_L}{a}\Delta_\psi]\cos(\delta_L+\phi) + F'_{Ry}[1 + \frac{r_R}{a}\Delta\psi]\cos(\delta_R-\phi)\right\}_2$$

$$-L_A\,\Delta_{L_2}(y) - D_{py_2} - F_{kpy_2} \qquad \text{(B.1.3)}$$

Yaw Equation

$$I_{wx}\ddot{y}_4 + I_{wy}\frac{v}{r_o}\dot{\phi}_2 = a(F'_{Rx}-F'_{Lx})_2 + M'_{Lz_2}\cos(\delta_L+\phi)_2$$

$$+ M'_{Rz_2}\cos(\delta_R-\phi)_2 + aL_A\dot{\Delta}_{\psi 2}y_4 - D_{pyaw_2} - M_{pyaw_2} \qquad \text{(B.1.4)}$$

Trailing Wheelset:

Lateral Equation

$$M_w\ddot{y}_5 = [F'_{Lx}(1 + \frac{r_L}{a}\Delta_\psi) + F'_{Rx}(1 + \frac{r_R}{a}\Delta_\psi]_3\, y_6$$

$$+\left\{F'_{Ly}[1 + \frac{r_L}{a}\Delta_\psi]\cos(\delta_L+\phi) + F'_{Ry}\,(1 + \frac{r_R}{a}\Delta_\psi]\cos(\delta_R-\phi)\right\}_3$$

$$- L_A\Delta_{L_3}(y) - D_{py_3} - F_{kpy_3} \qquad \text{(B.1.5)}$$

Yaw Equation

$$I_{wx}\ddot{y}_6 + I_{wy}\frac{v}{r_o}\dot{\phi}_3 = a(F'_{Rx} - F'_{Lx})_3 + M'_{Lz_3}\cos(\delta_L+\phi)_3$$

$$+ M'_{Rz_3}\cos(\delta_R-\phi)_3 + aL_A\Delta_{\psi_3}y_6 - D_{pyaw_3} - M_{pyaw_3} \qquad (B.1.6)$$

Truck Equations:

$$M_t\ddot{y}_7 = D_{py_1} + D_{py_2} + D_{py_3} + F_{kpy_1} + F_{kpy_2} + F_{kpy_3}$$

$$+ F_{ksy} + D_{sy} \qquad (B.1.7)$$

Yaw Equation

$$I_{tz}\ddot{y}_8 = D_{pyaw_1} + D_{pyaw_2} + D_{pyaw_3} + M_{pyaw_1} + M_{pyaw_2} + M_{pyaw_3}$$

$$- M_{syaw} + \ell_1(D_{py_1} + F_{kpy_1}) + \ell_2(D_{py_2} + F_{kpy_2})$$

$$- \ell_3(D_{py_3} + F_{kpy_3}) \qquad (B.1.8)$$

Roll Equation

$$I_{tx}\ddot{y}_9 = -D_{p\phi} - F_{kp\phi} - D_{s\phi} - F_{ks\phi} + h_{ts}(F_{ksy} + D_{sy})$$

$$+ h_{tp}(D_{py_1} + D_{py_2} + D_{py_3} + F_{kpy_1} + F_{kpy_2} + F_{kpy_3}) \qquad (B.1.9)$$

Carbody Equations:

Lateral Equation

$$M_c\ddot{y}_{10} = +F_{ksy} + D_{sy} \tag{B.1.10}$$

Roll Equation

$$I_{cx}\ddot{y}_{11} = F_{ks\phi} + D_{s\phi} + h_{cs}(F_{ksy} + D_{sy}) \tag{B.1.11}$$

where

$$\Delta_{L_i}(y) = \left[\frac{\tan(\delta_L + \phi) - \tan(\delta_R - \phi)}{2 - \frac{1}{a}[r_L\tan(\delta_L+\phi)+r_R\tan(\delta_R-\phi)]}\right]_i \qquad i = 1,2,3$$

$$\Delta_{\psi_i}(y) = \left[\frac{\tan(\delta_L + \phi) + \tan(\delta_R - \phi)}{2 - \frac{1}{a}[r_L\tan(\delta_L+\phi) + r_R\tan(\delta_R-\phi)]}\right]_i \qquad i = 1,2,3$$

$$D_{py_1} = C_{py_1}(\dot{y}_1 - \dot{y}_7 - \ell_1\dot{y}_8 - h_{tp}\dot{y}_9)$$

$$D_{py_2} = C_{py_2}(\dot{y}_3 - \dot{y}_7 - \ell_2\dot{y}_8 - h_{tp}\dot{y}_9)$$

$$D_{py_3} = C_{py_3}(\dot{y}_5 - \dot{y}_7 + \ell_3\dot{y}_8 - h_{tp}\dot{y}_9)$$

$$D_{pyaw_1} = C_{pyaw_1}(\dot{y}_2 - \dot{y}_8)$$

$$D_{pyaw_2} = C_{pyaw_2}(\dot{y}_4 - \dot{y}_8)$$

$$D_{pyaw_3} = C_{pyaw_3}(\dot{y}_6 - \dot{y}_8)$$

$$D_{p\phi} = C_{p\phi_1}(\dot{y}_9 - \dot{\phi}_1) + C_{p\phi_2}(\dot{y}_9 - \dot{\phi}_2) + C_{p\phi_3}(\dot{y}_9 - \dot{\phi}_3)$$

$$F_{kp\phi} = K_{p\phi_1}(y_9 - \phi_1) + K_{p\phi_2}(y_9 - \phi_2) + K_{p\phi_3}(y_9 - \phi_3)$$

$$F_{ksy} = K_{sy}(y_7 - y_{10} - h_{ts}y_9 - h_{cs}y_{11})$$

$$D_{sy} = C_{sy}(\dot{y}_7 - \dot{y}_{10} - h_{ts}\dot{y}_9 - h_{cs}\dot{y}_{11})$$

$$F_{ks\phi} = K_{s\phi}(y_9 - y_{11})$$

$$D_{s\phi} = C_{s\phi}(\dot{y}_9 - \dot{y}_{11})$$

F_{kpy_i}, i = 1,2,3 are given by Equation (2.1)

M_{pyaw_i}, i = 1,2,3 are given by Equation (2.2)

M_{syaw} is given by Equation (2.3)

B.2 Statistically Linearized Half Carbody Equations

Leading Wheelset:

Lateral Equation

$$M_w\ddot{y}_1 + \frac{2f_{11}}{V}(\dot{y}_1 + \frac{r_o}{a} k_{\phi_1} \dot{y}_1 - Vy_2) + \frac{2f_{12}}{V}(\dot{y}_2 - \frac{V}{r_o a} k_{\Delta_{21}} y_1)$$

$$+ L_A \frac{k_{g1}}{a} y_1 + k_{p1}(y_1 - y_7 - \ell_1 y_8 - h_{tp}y_9) \qquad (B.2.1)$$

$$+ C_{py_1}(\dot{y}_1 - \dot{y}_7 - \ell_1\dot{y}_8 - h_{tp}\dot{y}_9) = u_{1L}(t)$$

where

$$u_{1L}(t) = (\frac{L_A k_{g1}}{a} - \frac{2f_{12}}{r_o a} k_{\Delta_{21}})u_a(t) + (\frac{2f_{11} \cdot r_o}{V \cdot a} k_{\phi_1})\dot{u}_a(t)$$

(B.2.2)

Yaw Equation

$$I_{wx}\ddot{y}_2 + I_{wy} \frac{V}{r_o a} k_{\phi_1}\dot{y}_1 + \frac{2af_{33}}{r_o} \lambda_1 y_1 - \frac{2f_{12}}{V}(\dot{y}_1 + \frac{r_o}{a} k_{\phi_1}\dot{y}_1 - V \cdot y_2)$$

$$+ \frac{2a^2 f_{33}}{V} \dot{y}_2 - \frac{2f_{22}}{ar_o} k_{\Delta_{11}} y_1 + \frac{2f_{22}}{V} \dot{y}_2 - aL_A \delta_{o1} y_2$$

$$+ k_{\psi_1}(y_2 - y_8) + C_{pyaw_1}(\dot{y}_2 - \dot{y}_8) = u_{1\psi}(t) \qquad (B.2.3)$$

where

$$u_{1\psi}(t) = \left(\frac{2af_{33}}{r_o}\lambda_1 - \frac{2f_{22}}{a\,r_o}k_{\Delta_{11}}\right)u_a(t) + \left(\frac{I_{wy}\,V}{a\,r_o}k_{\phi_1}\right.$$

$$\left. - \frac{2f_{12}\cdot r_o}{a\,V}k_{\phi 1}\right)\dot{u}_a(t) \qquad \text{(B.2.4)}$$

<u>Middle Wheelset</u>:

Lateral Equation

$$M_w\ddot{y}_3 + \frac{2f_{11}}{V}\left(\dot{y}_3 + \frac{r_o}{a}k_{\phi_2}\dot{y}_3 - Vy_4\right) + \frac{2f_{12}}{V}\left(\dot{y}_4 - \frac{V}{r_o a}k_{\Delta_{22}}y_3\right)$$

$$+ L_A\frac{k_{g2}}{a}y_3 + k_{p2}(y_3 - y_7 - \ell_2 y_8 - h_{tp}y_9)$$

$$+ C_{py_2}(\dot{y}_3 - \dot{y}_7 - \ell_2\dot{y}_8 - h_{tp}y_9) = u_{2L}(t) \qquad \text{(B.2.5)}$$

where

$$u_{2L}(t) = \left(\frac{L_A k_{g2}}{a} - \frac{2f_{12}}{r_o\cdot a}k_{\Delta_{22}}\right)u_a\left(t - \frac{\ell_1 - \ell_2}{V}\right)$$

$$+ \left(\frac{2f_{11}r_o}{Va}k_{\phi_2}\right)\dot{u}_a\left(t - \frac{\ell_1 - \ell_2}{V}\right) \qquad \text{(B.2.6)}$$

Yaw Equation

$$I_{wx}\ddot{y}_4 + I_{wy}\frac{V}{r_o a}k_{\phi_2}\dot{y}_3 + \frac{2af_{33}}{r_o}\lambda_2 y_3 - \frac{2f_{12}}{V}(\dot{y}_3 + \frac{r_o}{a}k_{\phi_2}\dot{y}_3 - Vy_4)$$

$$+ \frac{2a^2 f_{33}}{V}\dot{y}_4 - \frac{2f_{22}}{a\ r_o}k_{\Delta_{12}}y_3 + \frac{2f_{22}}{V}\dot{y}_4 - aL_A\delta_{02}y_4$$

$$+ k_{\psi_2}(y_4 - y_8) + C_{pyaw_2}(\dot{y}_4 - \dot{y}_8) = u_{2\psi}(t) \qquad \text{(B.2.7)}$$

where

$$u_{2\psi}(t) = (\frac{2af_{33}}{r_o}\lambda_2 - \frac{2f_{22}}{a\ r_o}k_{\Delta_{12}})u_a(t - \frac{\ell_1 - \ell_2}{V}) + (\frac{I_{wy}V}{a\ r_o}k_{\phi_2}$$

$$- \frac{2f_{12}r_o}{a\ V}k_{\phi_2})\dot{u}_a(t - \frac{\ell_1 - \ell_2}{V}) \qquad \text{(B.2.8)}$$

<u>Trailing Wheelset:</u>

Lateral Equation

$$M_w\ddot{y}_5 + \frac{2f_{11}}{V}(\dot{y}_5 + \frac{r_o}{a}k_{\phi_3}\dot{y}_5 - Vy_6) + \frac{2f_{12}}{V}(\dot{y}_6 - \frac{V}{r_o a}k_{\Delta_{23}}y_5)$$

$$+ L_A\frac{k_{g3}}{a}y_5 + k_{p3}(y_5 - y_7 + \ell_3 y_8 - h_{tp}y_9)$$

$$+ C_{py_3}(\dot{y}_5 - \dot{y}_7 + \ell_3\dot{y}_8 - h_{tp}\dot{y}_9) = u_{3L}(t) \qquad \text{(B.2.9)}$$

where

$$u_{3L}(t) = \left(\frac{L_A\ k_{g3}}{a} - \frac{2f_{12}}{r_o a} k_{\Delta_{23}}\right) u_a\left(t - \frac{\ell_1 + \ell_3}{V}\right) + \left(\frac{2f_{11}\ r_o}{Va} k_{\phi_3}\right)$$

$$\dot{u}_a\left(t - \frac{\ell_1 + \ell_3}{V}\right) \qquad \text{(B.2.10)}$$

Yaw Equation

$$I_{wx}\ddot{y}_6 + I_{wy}\frac{V}{r_o a} k_{\phi_3}\dot{y}_5 + \frac{2af_{33}}{r_o}\lambda_3 y_5 - 2\frac{f_{12}}{V}\left(\dot{y}_5 + \frac{r_o}{a} k_{\phi_3}\dot{y}_5 - Vy_6\right)$$

$$+ \frac{2a^2 f_{33}}{V}\dot{y}_6 - \frac{2f_{22}}{a\ r_o} k_{\Delta_{13}} y_5 + \frac{2f_{22}}{V}\dot{y}_6 - aL_A\delta_{03} y_6$$

$$+ k_{\psi_3}(y_6 - y_8) + C_{pyaw_3}(\dot{y}_6 - \dot{y}_8) = u_{3\psi}(t) \qquad \text{(B.2.11)}$$

where

$$u_{3\psi}(t) = \left(\frac{2af_{33}}{r_o}\lambda_3 - \frac{2f_{22}}{a\ r_o} k_{\Delta_{13}}\right) u_a\left(t - \frac{\ell_1 + \ell_3}{V}\right) + \left(\frac{I_{wy}\ V}{a\ r_o} k_{\phi_3}\right.$$

$$\left. - \frac{2f_{12} r_o}{a\ V} k_{\phi_3}\right)\dot{u}_a\left(t - \frac{\ell_1 + \ell_3}{V}\right) \qquad \text{(B.2.12)}$$

Truck Equations

Lateral Equation

$$M_t\ddot{y}_7 + C_{py_1}(\dot{y}_7 - \dot{y}_1 + \ell_1\dot{y}_8 + h_{tp}\dot{y}_9) + C_{py_2}(\dot{y}_7 - \dot{y}_3 + \ell_2\dot{y}_8 + h_{tp}\dot{y}_9)$$

$$+ C_{py_3}(\dot{y}_7 - \dot{y}_5 - \ell_3\dot{y}_8 + h_{tp}\dot{y}_9) + k_{p1}(y_7 - y_1 + \ell_1 y_8 + h_{tp}y_9)$$

$$+ k_{p2}(y_7 - y_3 + \ell_2 y_8 + h_{tp}y_9) + k_{p3}(y_7 - y_5 - \ell_3 y_8 + h_{tp}y_9)$$

$$+ k_{sy}(y_7 - y_{10} - h_{ts}y_9 - h_{cs}y_{11}) + C_{sy}(\dot{y}_7 - \dot{y}_{10} - h_{ts}\dot{y}_9 - h_{cs}\dot{y}_{11}) = 0$$

(B.2.13)

Yaw Equation

$$I_{tz}\ddot{y}_8 + C_{pyaw_1}(\dot{y}_8-\dot{y}_2) + C_{pyaw_2}(\dot{y}_8-\dot{y}_4) + C_{pyaw_3}(\dot{y}_8-\dot{y}_6)$$

$$+ \ell_1[C_{py_1}(\dot{y}_7-\dot{y}_1 + \ell_1\dot{y}_8 + h_{tp}\dot{y}_9) + k_{p1}(y_7-y_1+\ell_1 y_8 + h_{tp}y_9)]$$

$$+ \ell_2[C_{py_2}(\dot{y}_7-\dot{y}_3 + \ell_2\dot{y}_8 + h_{tp}\dot{y}_9) + k_{p2}(y_7-y_3 + \ell_2 y_8 + h_{tp}y_9)]$$

$$- \ell_3[C_{py_3}(\dot{y}_7-\dot{y}_5 - \ell_3\dot{y}_8 + h_{tp}\dot{y}_9) + k_{p3}(y_7-y_5 - \ell_3 y_8 + h_{tp}y_9)]$$

$$+ k_{\psi_1}(y_8-y_2) + k_{\psi_2}(y_8-y_4) + k_{\psi_3}(y_8-y_6) + k_{s\psi}(y_8-y_{12}) = 0$$

(B.2.14)

Roll Equation

$$I_{tx}\ddot{y}_9 + C_{p\phi_1}(\dot{y}_9 - \frac{k_{\phi 1}}{a}\dot{y}_1) + C_{p\phi_2}(\dot{y}_9 - \frac{k_{\phi 2}}{a}\dot{y}_3) + C_{p\phi_3}(\dot{y}_9 - \frac{k_{\phi 3}}{a}\dot{y}_5)$$

$$+ k_{p\phi_1}(y_9 - \frac{k_{\phi 1}}{a}y_1) + k_{p\phi_2}(y_9 - \frac{k_{\phi 2}}{a}y_3) + k_{p\phi_3}(y_9 - \frac{k_{\phi 3}}{a}y_5)$$

$$+ C_{s\phi}(\dot{y}_9 - \dot{y}_{11}) + k_{s\phi}(y_9 - y_{11}) - h_{ts}k_{sy}(y_7 - y_{10} - h_{ts}y_9 - h_{cs}y_{11})$$

$$- h_{ts}C_{sy}(\dot{y}_7 - \dot{y}_{10} - h_{ts}\dot{y}_9 - h_{cs}\dot{y}_{11}) + h_{tp}C_{py_1}(\dot{y}_7 - \dot{y}_1 + \ell_1\dot{y}_8 + h_{tp}\dot{y}_9)$$

$$+ h_{tp}C_{py_2}(\dot{y}_7 - \dot{y}_3 + \ell_2\dot{y}_8 + h_{tp}\dot{y}_9) + h_{tp}C_{py_3}(\dot{y}_7 - \dot{y}_5 - \ell_3\dot{y}_8 + h_{yp}\dot{y}_9)$$

$$+ h_{tp}k_{p1}(y_7 - y_1 + \ell_1 y_8 + h_{tp}y_9) + h_{tp}k_{p2}(y_7 - y_3 + \ell_2 y_8 + h_{tp}y_9)$$

$$+ h_{tp}k_{p3}(y_7 - y_5 - \ell_3 y_8 + h_{tp}y_9) = u_t(t) \qquad \text{(B.2.15)}$$

where

$$u_t(t) = -C_{p\phi_1}\frac{k_{\phi 1}}{a}\dot{u}_a(t) - k_{p\phi_1}\frac{k_{\phi 1}}{a}u_a(t)$$

$$-C_{p\phi_2}\frac{k_{\phi 2}}{a}\dot{u}_a(t - \frac{\ell_1 - \ell_2}{V}) - k_{p\phi_2}\frac{k_{\phi 2}}{a}u_a(t - \frac{\ell_1 - \ell_2}{V})$$

$$-C_{p\phi_3}\frac{k_{\phi 3}}{a}\dot{u}_a(t - \frac{\ell_1 + \ell_3}{V}) - k_{p\phi_3}\frac{k_{\phi 3}}{a}u_a(t - \frac{\ell_1 + \ell_3}{V})$$

(B.2.16)

Carbody Equations

Carbody Lateral

$$M_c\ddot{y}_{10} + C_{sy}(\dot{y}_{10} - \dot{y}_7 + h_{ts}\dot{y}_9 + h_{cs}\dot{y}_{11})$$

$$+ k_{sy}(y_{10} - y_7 + h_{ts}y_9 + h_{cs}y_{11}) = 0 \quad \text{(B.2.17)}$$

Carbody Roll

$$I_{cx}\ddot{y}_{11} + k_{s\phi}(y_{11}-y_9)+C_{s\phi}(\dot{y}_{11}-\dot{y}_9)+h_{cs}k_{sy}(y_{10}-y_7+h_{ts}y_9+h_{cs}y_{11})$$

$$+ h_{cs}C_{sy}(\dot{y}_{10}-\dot{y}_7 + h_{ts}\dot{y}_9 + h_{cs}\dot{y}_{11}) = 0 \quad \text{(B.2.18)}$$

Bolster Yaw Equation

$$I_b\ddot{y}_{12} + k_{s\psi}(y_{12} - y_8) + C_{cp}\dot{y}_{12} = 0 \quad \text{(B.2.19)}$$

B.3 Statistically Linearized Full Carbody Equations

This section presents the extension of half-carbody equations to full-carbody equations. The degrees of freedom for the full-carbody are:

$y_{1,3,5}$ = Lateral displacements of wheelsets 1,2,3.

$y_{2,4,6}$ = Yaw displacements of wheelsets 1,2,3.

$y_{14,16,18}$ = Lateral displacements of wheelsets 4,5,6

$y_{15,17,19}$ = Yaw displacements of wheelsets 4,5,6

$y_{7,20}$ = Lateral displacements of trucks 1,2

$y_{8,21}$ = Yaw displacements of trucks 1,2

$y_{9,22}$ = Roll displacements of trucks 1,2

$y_{12,23}$ = Yaw displacements of bolsters

y_{10} = Lateral displacement of carbody

y_{13} = Yaw displacement of carbody

y_{11} = Roll displacement of carbody.

<u>Wheelset 1</u>

Lateral Equation

Equation (B.2.1) (B.3.1)

Equation (B.2.2) (B.3.2)

Yaw Equation

Equation (B.2.3) (B.3.3)

Equation (B.2.4) (B.3.4)

<u>Wheelset 2</u>

Lateral Equation

Equation (B.2.5) (B.3.5)

Equation (B.2.6) (B.3.6)

Yaw Equation

Equation (B.2.7) (B.3.7)

Equation (B.2.8) (B.3.8)

Wheelset 3

Lateral Equation

Equation (B.2.9) (B.3.9)

Equation (B.2.10) (B.3.10)

Yaw Equation

Equation (B.2.11) (B.3.11)

Equation (B.2.12) (B.3.12)

Leading Truck

Lateral Equation

$$[\text{Equation (B.2.13)}] - k_{sy_1} \ell \, y_{13} - C_{sy_1} \ell \, \dot{y}_{13} = 0 \qquad \text{(B.3.13)}$$

Yaw Equation

Equation (B.2.14) (B.3.14)

Roll Equation

$$[\text{Equation (B.2.15)}] + h_{ts}\ell(k_{sy_1} y_{13} + C_{sy_1} \dot{y}_{13}) = u_t(t) \qquad \text{(B.3.15)}$$

Equation (B.2.16) (B.3.16)

Wheelset 4

Lateral Equation

$$M_w \ddot{y}_{14} + \frac{2f_{11}}{V} (\dot{y}_{14} + \frac{r_o}{a} k_{\phi_4} \dot{y}_{14} - V y_{15}) + 2 \frac{f_{12}}{V} (\dot{y}_{15} - \frac{V}{r_o a} k_{\Delta_{24}} y_{14})$$

$$+ L_A \frac{k_{g4}}{a} y_{14} + k_{p4}(y_{14} - y_{20} - \ell_4 y_{21} - h_{tp} y_{22})$$

$$+ C_{py_4}(\dot{y}_{14} - \dot{y}_{20} - \ell_4 \dot{y}_{21} - h_{tp} \dot{y}_{22}) = u_{4L}(t) \qquad \text{(B.3.17)}$$

where

$$u_{4L}(t) = \left(\frac{L_A k_{g4}}{a} - \frac{2f_{12}}{r_o a} k_{\Delta_{24}}\right) u_a\left(t - \frac{\ell + \ell_1 - \ell_4}{V}\right)$$

$$+ \left(\frac{2f_{11}\, r_o}{V\, a} k_{\phi_4}\right) u_a\left(t - \frac{\ell + \ell_1 - \ell_4}{V}\right) \qquad \text{(B.3.18)}$$

Yaw Equation

$$I_{wx}\ddot{y}_{15} + I_{wy}\frac{V}{r_o a} k_{\phi_4}\dot{y}_{14} + \frac{2af_{33}}{r_o}\lambda_4 y_{14} - \frac{2f_{12}}{V}\left(\dot{y}_{14} + \frac{r_o}{a} k_{\phi_4}\dot{y}_{14} - Vy_{15}\right)$$

$$+ \frac{2a^2 f_{33}}{V}\dot{y}_{15} - \frac{2f_{22}}{ar_o} k_{\Delta_{14}} y_{14} + \frac{2f_{22}}{V}\dot{y}_{15} - aL_A\delta_{04} y_{15}$$

$$+ k_{\psi_4}(y_{15} - y_{21}) + C_{pyaw_4}(\dot{y}_{15} - \dot{y}_{21}) = u_{4\psi}(t) \qquad \text{(B.3.19)}$$

where

$$u_{4\psi}(t) = \left(-\frac{2af_{33}}{r_o}\lambda_4 - \frac{2f_{22}}{ar_o} k_{\Delta_{14}}\right) u_a\left(t - \frac{\ell + \ell_1 - \ell_4}{V}\right)$$

$$+ \left(\frac{I_{wy}V}{ar_o} k_{\phi_4} - \frac{2f_{12}r_o}{a\, V} k_{\phi_4}\right) u_a\left(t - \frac{\ell + \ell_1 - \ell_4}{V}\right)$$

$$\text{(B.3.20)}$$

Wheelset 5

Lateral Equation

$$M_w\ddot{y}_{16} + \frac{2f_{11}}{V}(\dot{y}_{16} + \frac{r_o}{a} k_{\phi_5}\dot{y}_{16} - Vy_{17}) + \frac{2f_{12}}{V}(\dot{y}_{17} - \frac{V}{r_o a} k_{\Delta_{25}}y_{16})$$

$$+ L_A \frac{k_{g5}}{a} y_{16} + k_{p5}(y_{16} - y_{20} - \ell_5 y_{21} - h_{tp}y_{22})$$

$$+ C_{py_5}(\dot{y}_{16} - \dot{y}_{20} - \ell_5\dot{y}_{21} - h_{tp}\dot{y}_{22}) = u_{5L}(t) \qquad (B.3.21)$$

where

$$u_{5L}(t) = (\frac{L_A k_{g5}}{a} - \frac{2f_{12}}{r_o a} k_{\Delta_{25}})u_a(t - \frac{\ell + \ell_1 - \ell_5}{V})$$

$$+ (\frac{2f_{11}r_o}{Va} k_{\phi_5})\ \dot{u}_a(t - \frac{\ell + \ell_1 - \ell_5}{V}) \qquad (B.3.22)$$

Yaw Equation

$$I_{wx}\ddot{y}_{17} + I_{wy}\frac{V}{r_o a} k_{\phi_5}\dot{y}_{16} + \frac{2af_{33}}{r_o}\lambda_5 y_{16} - \frac{2f_{12}}{V}(\dot{y}_{16} + \frac{r_o}{a} k_{\phi_5}\dot{y}_{16} - Vy_{17})$$

$$+ \frac{2a^2 f_{33}}{V}\dot{y}_{17} - \frac{2f_{22}}{ar_o} k_{\Delta_{15}}y_{16} + \frac{2f_{22}}{V}\dot{y}_{17} - aL_A\delta_{05}y_{17}$$

$$+ k_{\psi_5}(y_{17} - y_{21}) + C_{pyaw_5}(\dot{y}_{17} - \dot{y}_{21}) = u_{5\psi}(t) \qquad (B.3.23)$$

where

$$u_{5\psi}(t) = \left(\frac{2af_{33}}{r_o}\lambda_5 - \frac{2f_{22}}{ar_o} k_{\Delta_{15}}\right) u_a\left(t - \frac{\ell + \ell_1 - \ell_5}{V}\right)$$

$$+ \left(\frac{I_{wy}V}{a\ r_o} k_{\phi_5} - \frac{2f_{12}r_o}{a\ V} k_{\phi_5}\right) \dot{u}_a\left(t - \frac{\ell + \ell_1 - \ell_5}{V}\right) \quad \text{(B.3.24)}$$

Wheelset 6

Lateral Equation

$$M_w\ddot{y}_{18} + \frac{2f_{11}}{V}\left(\dot{y}_{18} + \frac{r_o}{a} k_{\phi_6}\dot{y}_{18} - Vy_{19}\right) + \frac{2f_{12}}{V}\left(\dot{y}_{19} - \frac{V}{r_o a} k_{\Delta_{26}} y_{18}\right)$$

$$+ L_A \frac{k_{g6}}{a} y_{18} + k_{p6}(y_{18} - y_{20} + \ell_6 y_{21} - h_{tp} y_{22})$$

$$+ C_{py_6}(\dot{y}_{18} - \dot{y}_{20} + \ell_6\dot{y}_{21} - h_{tp}\dot{y}_{22}) = u_{6L}(t) \quad \text{(B.3.25)}$$

where

$$u_{6L}(t) = \left(\frac{L_A k_{g6}}{a} - \frac{2f_{12}}{r_o a} k_{\Delta_{26}}\right) u_a\left(t - \frac{\ell + \ell_1 + \ell_6}{V}\right)$$

$$+ \left(\frac{2f_{11}r_o}{Va} k_{\phi_6}\right) \dot{u}_a\left(t - \frac{\ell + \ell_1 + \ell_6}{V}\right) \quad \text{(B.3.26)}$$

Yaw Equation

$$I_{wx}\ddot{y}_{19} + I_{wy}\frac{V}{r_o a}\ k_{\phi_6}\dot{y}_{18} + \frac{2af_{33}}{r_o}\lambda_6 y_{18} - \frac{2f_{12}}{V}(\dot{y}_{18} + \frac{r_o}{a}k_{\phi_6}\dot{y}_{18} - Vy_{19})$$

$$+ \frac{2a^2 f_{33}}{V}\dot{y}_{19} - \frac{2f_{22}}{ar_o}k_{\Delta_{16}}y_{18} + \frac{2f_{22}}{V}\dot{y}_{19} - aL_A\delta_{06}y_{19}$$

$$+ k_{\psi 6}(y_{19}-y_{21}) + C_{pyaw_6}(\dot{y}_{19}-\dot{y}_{21}) = u_{6\psi}(t) \qquad \text{(B.3.27)}$$

where

$$u_{6\psi}(t) = (\frac{2af_{33}}{r_o}\lambda_6 - \frac{2f_{22}}{ar_o}k_{\Delta_{16}})u_a(t - \frac{\ell + \ell_1 + \ell_6}{V})$$

$$+ (\frac{I_{wy}V}{ar_o}k_{\phi_6} - \frac{2f_{12}r_o}{a\ V}k_{\phi_6})\dot{u}_a(t - \frac{\ell + \ell_1 + \ell_6}{V})$$

(B.3.28)

Trailing Truck

Lateral Equation

$$M_t\ddot{y}_{20} + C_{py_4}(\dot{y}_{20}-\dot{y}_{14}+\ell_4\dot{y}_{21}+h_{tp}\dot{y}_{22}) + C_{py_5}(\dot{y}_{20}-\dot{y}_{16}+\ell_5\dot{y}_{21}+h_{tp}\dot{y}_{22})$$

$$+ C_{py_6}(\dot{y}_{20}-\dot{y}_{18}-\ell_6\dot{y}_{21}+h_{tp}\dot{y}_{22}) + k_{p4}(y_{20}-y_{14}+\ell_4 y_{21}+h_{tp}y_{22})$$

$$+ k_{p5}(y_{20}-y_{16}+\ell_5 y_{21}+h_{tp}y_{22}) + k_{p6}(y_{20}-y_{18}-\ell_6 y_{21}+h_{tp}y_{22})$$

$$+ k_{sy_2}(y_{20}-y_{10}-h_{ts}y_{22}-h_{cs}y_{11}+\ell y_{13})$$

$$+ C_{sy_2}(\dot{y}_{20}-\dot{y}_{10}-h_{ts}\dot{y}_{22}-h_{cs}\dot{y}_{11}+\ell\dot{y}_{13})=0$$

(B.3.29)

Yaw Equation

$$I_{tz}\ddot{y}_{21} + C_{pyaw_4}(\dot{y}_{21}-\dot{y}_{15}) + C_{pyaw_5}(\dot{y}_{21}-\dot{y}_{17}) + C_{pyaw_6}(\dot{y}_{21}-\dot{y}_{19})$$
$$+ \ell_4[C_{py_4}(\dot{y}_{20}-\dot{y}_{14} + \ell_4\dot{y}_{21} + h_{tp}\dot{y}_{22}) + k_{p4}(y_{20}-y_{14} + \ell_4 y_{21}+h_{tp}y_{22})]$$
$$+ \ell_5[C_{py_5}(\dot{y}_{20}-\dot{y}_{16} + \ell_5\dot{y}_{21} + h_{tp}\dot{y}_{22}) + k_{p5}(y_{20}-y_{16} + \ell_5 y_{21}+h_{tp}y_{22})]$$
$$- \ell_6[C_{py_6}(\dot{y}_{20}-\dot{y}_{18} - \ell_6\dot{y}_{21} + h_{tp}\dot{y}_{22}) + k_{p6}(y_{20}-y_{18} - \ell_6 y_{21}+h_{tp}y_{22})]$$
$$+ k_{\psi_4}(y_{21}-y_{15}) + k_{\psi_5}(y_{21}-y_{17}) + k_{\psi_6}(y_{21} - y_{19})$$
$$+ k_{s\psi_2}(y_{21}- y_{23}) = 0 \qquad \text{(B.3.30)}$$

<u>Roll Equation:</u>

$$I_{tx}\ddot{y}_{22} + C_{p\phi_4}(\dot{y}_{22} - \frac{k_{\phi 4}}{a}\dot{y}_{14}) + C_{p\phi_5}(\dot{y}_{22} - \frac{k_{\phi 5}}{a}\dot{y}_{16})$$
$$+ C_{p\phi_6}(\dot{y}_{22} - \frac{k_{\phi 6}}{a}\dot{y}_{18}) + k_{p\phi_4}(y_{22} - \frac{k_{\phi 4}}{a}y_{14})$$
$$+ k_{p\phi_5}(y_{22} - \frac{k_{\phi 5}}{a}y_{16}) + k_{p\phi_6}(y_{22} - \frac{k_{\phi 6}}{a}y_{18})$$
$$+ C_{s\phi_2}(\dot{y}_{22} - \dot{y}_{11}) + k_{s\phi_2}(y_{22} - y_{11})$$
$$- h_{ts}k_{sy_2}(y_{20} - y_{10} - h_{ts}y_{22} - h_{cs}y_{11} + \ell y_{13})$$
$$- h_{ts}C_{sy_2}(\dot{y}_{20} - \dot{y}_{10} - h_{ts}\dot{y}_{22} - h_{cs}\dot{y}_{11} + \ell\dot{y}_{13})$$
$$+ h_{tp}C_{py_4}(\dot{y}_{20} - \dot{y}_{14} + \ell_4\dot{y}_{21} + h_{tp}\dot{y}_{22})$$
$$+ h_{tp}C_{py_5}(\dot{y}_{20} - \dot{y}_{16} + \ell_5\dot{y}_{21} + h_{tp}\dot{y}_{22})$$

$$+h_{tp}C_{py_6}(\dot{y}_{20} - \dot{y}_{18} - \ell_6\dot{y}_{21} + h_{tp}\dot{y}_{22})$$

$$+h_{tp}k_{p4}(y_{20} - y_{14} + \ell_4 y_{21} + h_{tp}y_{22})$$

$$+h_{tp}k_{p5}(y_{20} - y_{16} + \ell_5 y_{21} + h_{tp}y_{22})$$

$$+h_{tp}k_{p6}(y_{20} - y_{18} - \ell_6 y_{21} + h_{tp}y_{22}) = u_{t2}(t) \qquad (B.3.31)$$

where

$$u_{t2}(t) = -C_{p\phi_4}\frac{k_{\phi 4}}{a}\dot{u}_a(t - \frac{\ell + \ell_1 - \ell_4}{V}) - k_{p\phi_4}\frac{k_{\phi 4}}{a}u_a(t - \frac{\ell + \ell_1 - \ell_4}{V})$$

$$-C_{p\phi_5}\frac{k_{\phi 5}}{a}\dot{u}_a(t - \frac{\ell + \ell_1 - \ell_5}{V}) - k_{p\phi_5}\frac{k_{\phi 5}}{a}u_a(t - \frac{\ell + \ell_1 - \ell_5}{V})$$

$$-C_{p\phi_6}\frac{k_{\phi 6}}{a}\dot{u}_a(t - \frac{\ell + \ell_1 + \ell_6}{V}) - k_{p\phi_6}\frac{k_{\phi 6}}{a}u_a(t - \frac{\ell + \ell_1 + \ell_6}{V})$$

(B.3.32)

<u>Leading Bolster</u>

$$I_b\ddot{y}_{12} + k_{s\psi_1}(y_{12} - y_8) + C_{cp_1}(\dot{y}_{12} - \dot{y}_{13}) = 0 \qquad (B.3.33)$$

<u>Trailing Bolster</u>

$$I_b\ddot{y}_{23} + k_{s\psi_2}(y_{23} - y_{21}) + C_{cp_2}(\dot{y}_{23} - \dot{y}_{13}) = 0 \qquad (B.3.34)$$

Carbody Equations

Lateral Equation

$$M_c\ddot{y}_{10} + C_{sy_1}(\dot{y}_{10} - \dot{y}_7 + h_{ts}\dot{y}_9 + h_{cs}\dot{y}_{11} + \ell\dot{y}_{13})$$

$$+ k_{sy_1}(y_{10} - y_7 + h_{ts}y_9 + h_{cs}y_{11} + \ell y_{13})$$

$$+ C_{sy_2}(\dot{y}_{10} - \dot{y}_{20} + h_{ts}\dot{y}_{22} + h_{cs}\dot{y}_{11} - \ell\dot{y}_{13})$$

$$+ k_{sy_2}(y_{10} - y_{20} + h_{ts}y_{22} + h_{cs}y_{11} - \ell y_{13}) = 0 \qquad \text{(B.3.35)}$$

Yaw Equation

$$I_{cz}\ddot{y}_{13} + C_{cp_1}(\dot{y}_{13} - \dot{y}_{12}) + C_{cp_2}(\dot{y}_{13} - \dot{y}_{23})$$

$$+ \ell k_{sy_1}(y_{10} - y_7 + h_{ts}y_9 + h_{cs}y_{11} + \ell y_{13})$$

$$+ \ell C_{sy_1}(\dot{y}_{10} - \dot{y}_7 + h_{ts}\dot{y}_9 + h_{cs}\dot{y}_{11} + \ell\dot{y}_{13})$$

$$- \ell k_{sy_2}(y_{10} - y_{20} + h_{ts}y_{22} + h_{cs}y_{11} - \ell y_{13})$$

$$- \ell C_{sy_2}(\dot{y}_{10} - \dot{y}_{20} + h_{ts}\dot{y}_{22} + h_{cs}\dot{y}_{11} - \ell\dot{y}_{13}) = 0 \qquad \text{(B.3.36)}$$

Roll Equation

$$I_{cx}\ddot{y}_{11} + k_{s\phi_1}(y_{11} - y_9) + C_{s\phi_1}(\dot{y}_{11} - \dot{y}_9) + k_{s\phi_2}(y_{11} - y_{22}) + C_{s\phi_2}(\dot{y}_{11} - \dot{y}_{22})$$

$$+ h_{cs}k_{sy_1}(y_{10} - y_7 + h_{ts}y_9 + h_{cs}y_{11} + \ell y_{13})$$

$$+ h_{cs}C_{sy_1}(\dot{y}_{10} - \dot{y}_7 + h_{ts}\dot{y}_9 + h_{cs}\dot{y}_{11} + \ell\dot{y}_{13})$$

$$+ h_{cs}k_{sy_2}(y_{10} - y_{20} + h_{ts}y_{22} + h_{cs}y_{11} - \ell y_{13})$$

$$+ h_{cs}C_{sy_2}(\dot{y}_{10} - \dot{y}_{20} + h_{ts}\dot{y}_{22} + h_{cs}\dot{y}_{11} - \ell\dot{y}_{13}) = 0 \quad \text{(B.3.37)}$$

B.4 Baseline Parameters

Input Data for EMD SDP 40, 6 Axle Locomotive [16,18]

Dimensional Data

a	-	Half distance between contact points	=	29.562	in
ℓ_1	-	Distance between truck center and leading axle	=	79.38	in
ℓ_2	-	Distance between truck center and middle axle	=	-1.25	in
ℓ_3	-	Distance between truck center and rear axle	=	85.0	in
d_p	-	Distance from truck c.g. to primary suspension	=	39.5	in
d_s	-	Distance from truck, c.g. to secondary suspension	=	35.12	in
h_{tp}	-	Height of truck c.g. above axle center	=	2.5	in

h_{cs}	-	Height of carbody c.g. above bolster spring center	= 50.2 in
h_{ts}	-	Height of bolster spring center above truck c.g.	= 5.0 in
ℓ	-	Half distance between truck centers	= 276.0 in

<u>Mass and Inertia Data</u>

M_c	-	Carbody mass	= 766.0 lb-sec^2/in
M_T	-	Truck frame mass	= 40.0 lb-sec^2/in
M_W	-	Wheelset mass	= 30.0 lb/sec^2/in
I_{wz}	-	Wheelset yaw moment of inertia	= 16,500 lb-in-sec^2
I_{wy}	-	Wheelset spin moment of inertia	= 3,600 lb-in-sec^2
I_{tz}	-	Truck yaw moment of inertia	= 178,000 lb-in-sec^2
I_{tx}	-	Truck roll moment of inertia	= 56,000 lb-in-sec^2
I_{cx}	-	Carbody roll moment of inertia	= 1,720,000 lb-in-sec^2

<u>Linear Suspension Parameters</u>

C_{py}	-	Lateral primary damping per axle	= 400 lb-sec/in
$C_{p\psi}$	-	Yaw primary damping per axle	= 19,503 lb-in-sec/rad
$C_{p\phi}$	-	Roll primary damping per axle	= 468,075 lb-in-sec/rad
C_{pz}	-	Vertical primary damping per axle	= 100 lb-sec/in
C_{sy}	-	Lateral secondary damping per truck	= 600 lb-sec/in
$C_{s\psi}$	-	Yaw secondary damping per truck	= 200,000 lb-in-sec/rad
$C_{s\phi}$	-	Roll secondary damping per truck	= 616,700 lb-in-sec/rad
k_{py}	-	Lateral primary stiffness per axle	= 5000 lb/in

$k_{p\psi}$	-	Yaw primary stiffness per axle	= 780,125,000 lb-in/rad
$k_{p\phi}$	-	Roll primary stiffness per axle	= 10,297,650 lb-in/rad
k_{pz}	-	Vertical primary stiffness per axle	= 6,600 lb/in
k_{sy}	-	Lateral secondary stiffness per truck	= 22,000 lb/in
$k_{s\psi}$	-	Yaw secondary stiffness per truck	= 10×10^6 lb-in/rad
$k_{s\phi}$	-	Roll secondary stiffness per truck	= 616,707,200 lb-in/rad

Creep Force Data (Linear Kalker Values)

f_{11}	-	Lateral creep coefficient per wheel	= 3.59×10^6 lb
f_{12}	-	Lateral/spin creep coefficient per wheel	= 462,000 in-lb
f_{22}	-	Spin creeo coefficient per wheel	= 65,952 in^2-lb
f_{33}	-	Longitudinal creep coefficient per wheel	= 3.9×10^6 lb
L_A	-	Axle load	= 66,000 lb

Nonlinear Suspension Parameters

C_{py}	-	Lateral primary damping per axle	= 150 lb-sec/in
$C_{p\psi}$	-	Yaw primary damping per axle	= 3.12×10^5 lb-in-sec/rad
$C_{p\phi}$	-	Roll primary damping per axle:	
		Leading and rear axles	= 111,818 lb-in-sec/rad
		middle axle	= 1,141,580 lb-in-sec/rad
C_{pz}	-	Vertical primary damping per axle:	
		Leading and rear axles	= 71.67 lb-sec/in
		middle axle	= 731.67 lb-sec/in
C_{sy}	-	Lateral secondary damping per truck	= 600 lb-sec/in
$C_{s\psi}$	-	Yaw secondary damping per truck	= 0.0
$C_{s\phi}$	-	Roll secondary damping per truck	= 1.665×10^6 lb-in-sec/rad

T_{cp}	-	Centerplate Coulomb breakaway torque	= 100,000 lb-in
δ_y	-	Deadband amplitude of primary lateral spring	= 0.18756 in
C_1	-	Linear spring constant for primary deadband	= 1.44×10^4 lb/in
δ_ψ	-	Linear range for primary yaw spring	= 4.74×10^{-3} rads
$k_{p\psi_1}$	-	Primary yaw stiffness in the linear range per axle	= 1.872×10^8 lb-in/rad
$k_{p\psi_2}$	-	Primary yaw stiffness after linear range per axle	= 1.248×10^9 lb-in/rad
$k_{p\phi}$	-	Primary roll stiffness per axle	= 1.144×10^7 lb-in/rad
k_{pz}	-	Vertical primary stiffness per axle	= 7333.3 lb/in
k_{sy}	-	Secondary lateral stiffness per truck	= 23,000 lb/in
$k_{s\psi}$	-	Secondary yaw stiffness per truck	= 2.7996×10^7 lb-in/rad
$k_{s\phi}$	-	Secondary roll stiffness per truck	= 5.8587×10^8 lb-in/rad

APPENDIX C

STATISTICAL LINEARIZATION STABILITY AND FORCED RESPONSE PROGRAM LISTING

The computer listing of the twelve degrees of freedom three-axle half-carbody locomotive model is presented. The computer program is coded in such a way that the user can use the program to get the frequency domain analysis of:

- -Linear model
- -Model with nonlinear wheel/rail profile geometry
- -Model with nonlinear suspension and linear profile geometry
- -Model with nonlinear wheel/rail profile geometry and nonlinear suspension

The outputs of the analysis are the rms values of states, rms values of the inputs to the nonlinearities, rms values of carbody and truck lateral accelerations, transfer functions, power spectral densities, and eigenvalues/eigenvector analysis of the equivalent linear system.

User specifies the frequency range of interest in Hertz and the number of frequency points. Also, user can use different wheel profiles at each axle. User should supply the system parameters and the equivalent gains for the wheel/rail geometry nonlinearities. For nonlinear analysis the number of iterations for convergence should be specified by the user.

```
C*********************************************************
C     STATISTICAL DESCRIBING FUNCTION PROGRAM FOR             *
C      A TWELVE D.O.F. HALF-CAR LOCOMOTIVE MODEL              *
C                                                             *
C     EQUATION 1 IS FOR LEADING WHEELSET LATERAL              *
C     EQUATION 2 IS FOR LEADING WHEELSET YAW                  *
C     EQUATION 3 IS FOR MIDDLE WHEELSET LATERAL               *
C     EQUATION 4 IS FOR MIDDLE WHEELSET YAW                   *
C     EQUATION 5 IS FOR TRAILING WHEELSET LATERAL             *
C     EQUATION 6 IS FOR TRAILING WHEELSET YAW                 *
C     EQUATION 7 IS FOR TRUCK LATERAL                         *
C     EQUATION 8 IS FOR TRUCK YAW                             *
C     EQUATION 9 IS FOR TRUCK ROLL                            *
C     EQUATION 10 IS FOR CARBODY LATERAL                      *
C     EQUATION 11 IS FOR CARBODY ROLL                         *
C     EQUATION 12 IS FOR BOLSTER YAW                          *
C                                                             *
C*********************************************************
      COMMON/COM4/A,L1,L2,L3,HTP,HTS,HCS,PZERO,MW,MT,MC,
     1     IWY,IWX,ITZ,ITX,ICX,LA,V,IBOLS
      COMMON/OPTION/IOPT
      COMMON/IPIS/IPROF,ISUSP
      CHARACTER*50 OPT1,OPT2,OPT3,OPT4,OPT5
      COMMON/RP/R,P
      INTEGER R,P
      DIMENSION  RSIG(10)
      REAL L1,L2,L3,MW,MT,MC,IWY,IWX,ITZ,ITX,ICX,LA,IBOLS
      COMMON/WA/WA
      COMMON/IGS/IGSL,IGSY
C
      R=8
      P=5
      READ(R,2) OPT1
      READ(R,2) OPT2
      READ(R,2) OPT3
      READ(R,2) OPT4
      READ(R,2) OPT5
2     FORMAT(50A)
      WRITE(P,2) OPT1
      WRITE(P,2) OPT2
      WRITE(P,2) OPT3
      WRITE(P,2) OPT4
      WRITE(P,2) OPT5
      WRITE(P,3)
3     FORMAT(//2X,'OPTIONS'/2X,'_______'//
      12X,'OPTION  1  LINEAR SYSTEM'/
      12X,'OPTION  2  NONLINEAR WHEEL/RAIL GEOMETRY'/
      12X,'OPTION  3  NONLINEAR WHEEL/RAIL GEOMETRY AND LATERAL
      1 PRIMARY'/
      12X,'OPTION  4  NONLINEAR WHEEL/RAIL AND NONLINEAR PRIMARY'/
      12X,'OPTION  5  NONLINEAR SYSTEM'/
```

```
        12X,'OPTION  6  NONLINEAR LATERAL PRIMARY'/)
        WRITE(P,4)
4       FORMAT(2X,'OPTION  7  NONLINEAR PRIMARY'/
        1       2X,'OPTION  8  NONLINEAR PRIMARY AND COULOMB DAMPER IN
        1 SECONDARY'/
        1       2X,'OPTION  9  NONLINEAR PRIMARY YAW'/
        1       2X,'OPTION 10  NONLINEAR PRIMARY YAW AND COULOMB IN
        1 SECONDARY'/
        1       2X,'OPTION 11  COULOMB IN SECONDARY'/
        1       2X,'OPTION 12  NONLINEAR WHEEL/RAIL GEOMETRY AND
        1 PRIMARY YAW'/)
        WRITE(P,5)
5       FORMAT(2X,'OPTION 13  NONLINEAR W/R,PRIMARY YAW AND COULOMB
        1 IN SECONDARY'/
        1       2X,'OPTION 14  NONLINEAR W/R,COULOMB IN SECONDARY'/
        1       2X,'OPTION 15  NONLINEAR W/R,PRIMARY YAW AND COULOMB
        1 IN SECONDARY'/
        1       2X,'OPTION 16  NONLINEAR PRIMARY LATERAL AND COULOMB
        1 IN SECONDARY'/)
        READ(P,200) VMPH,WA
200     FORMAT(F5.1,E12.5)
        VFPS=VMPH/0.68182
        V=VFPS*12.
        READ(P,201) IWP,ITC,IPROF,ISUSP,IOPT
201     FORMAT(5I2)
        READ(R,202) IGSL,IGSY
202     FORMAT(2I2)
        IF(IOPT.EQ.1) GO TO 1
        CALL RAIL(RSIG,IWP)
1       WRITE(P,20) VMPH,IWP,ITC,IPROF,IOPT
20      FORMAT(//2X,'VELOCITY      =',F6.2,' MPH'/
        1     2X,'PROFILE #     =',I1/
        1     2X,'TRACK CLASS   =',I1/
        1     2X,'PROFILE TYPE =',I1,'  LINEAR=0,NONLINEAR=1'/
        1     2X,'OPTION        =',I2)
        CALL FCFRSP(RSIG,ITC)
C*******************************************************************
C       OUTPUT THE PSDS AND RMS VALUES
C*******************************************************************
        CALL OUTPUT
C
C*******************************************************************
C       EIGENVECTOR/EIGENVALUE CALCULATIONS
C*******************************************************************
        READ(R,1001) IVEC
1001    FORMAT(I1)
        IF(IVEC.EQ.0) STOP
C
        CALL EIGVEC
        STOP
        END
.EL
```

```
      SUBROUTINE FCFRSP(RSIG,ITC)
      COMMON/NONL/ZTZR(150,10),ZTZI(150,10),ZPSD(150,10)
      COMMON/COM4/A,L1,L2,L3,HTP,HTS,HCS,PZERO,MW,MT,MC,
     1      IWY,IWX,ITZ,ITX,ICX,LA,V,IBOLS
      DIMENSION GC(10),SP(10),SIG(10)
      COMMON/OUT/DRMS(12),DPSD(150,12),FREQ(150),I22,
     1            APSDC(150),APSDFT(150),
     1            RMYC,RMFT,MAGN(150,12),PHASE(150,12)
      COMMON/RP/R,P
      COMMON/OPTION/IOPT
      INTEGER R,P,DOF
      COMMON/DOF/DOF
      REAL L1,L2,L3,M,K,MW,MT,MC,IWY,IWX,ITZ,ITX,ICX,LA,IBOLS,MAGN
      COMMON/COMC/M(12,12),K(12,12),C(12,12),
     1           B2(12,6),B1(12,6)
      COMMON/GT3/WV7(12),WV8(12)
      COMMON/GT2/WV6(10),PSD(10) ,B3R(6),B3I(6)
      DIMENSION C1(12,12),DUM1(12,12)
      DIMENSION RSIG(10)
      COMMON/GT1/RM1R(10,12),RM1I(10,12),RM2R(10),RM2I(10),
     1 TZR(10),TZI(10),WV1(10),WV2(10),WV3(10),WV4(10),WV5(10),
     1 RMS(10),TRA(12),TIA(12),BRA(12),BIA(12)
      REAL*8 DI(12,12),DR(12,12)
      R22=6.2832/(386.4*386.4)
      READ(R,2) DOF,INL
2     FORMAT(2I2)
C*****************************************************************
C     READ FREQUENCY RANGE OF INTEREST (IN HERTS)               *
C*****************************************************************
      READ(R,489) IFREQ,ITER1
489   FORMAT(2I2)
      READ(R,1)W1,W2,I22,ITER,EPS,I23,I33
1     FORMAT(2E12.5,2I3,F5.2,I3,I2)
C**********************************************
C     CONVERT FREQUENCIES TO (RAD/SEC)       *
C**********************************************
      W1=W1*6.2832
      W2=W2*6.2832
      IF(IFREQ.EQ.1) READ(R-1,447) (FREQ(I),I=1,I22)
447   FORMAT(2X,E12.5)
      W=W1
      CALL FCDE(RSIG,W,0)
C*******************************************
C    I22 EQUALLY SPACED PTS.(IN LOG SCALE) *
C*******************************************
```

```
      DO 62 I=1,INL
      RM2R(I)=0.0
      RM2I(I)=0.0
      TZR(I)=0.0
      TZI(I)=0.0
      DO 62 J=1,DOF
      RM1R(I,J)=0.0
62    RM1I(I,J)=0.0
      RM1R(1,1)=1.0
      RM1R(2,3)=1.
      RM1R(3,5)=1.0
      RM1R(4,1)=1.
      RM1R(4,7)=-1.0
      RM1R(4,8)=-L1
      RM1R(4,9)=-HTP
      RM1R(5,3)=1.0
      RM1R(5,7)=-1.0
      RM1R(5,8)=-L2
      RM1R(5,9)=-HTP
      RM1R(6,5)=1.0
      RM1R(6,7)=-1.0
      RM1R(6,8)=L3
      RM1R(6,9)=-HTP
      RM1R(7,2)=1.0
      RM1R(7,8)=-1.0
      RM1R(8,4)=1.0
      RM1R(8,8)=-1.0
      RM1R(9,6)=1.0
      RM1R(9,8)=-1.0
      IF(IOPT.EQ.1) ITER=1
      IF(IOPT.EQ.1) ITER1=1
      ILIMIT=0
      IF(IOPT.GT.5) GO TO 1363
      INL1=1
      INL2=INL
      IF(IOPT.EQ.5) GO TO 1367
      IF(IOPT-3)1364,1365,1366
1364  INL2=3
      GO TO 1367
1365  INL2=6
      GO TO 1367
1366  INL2=9
      GO TO 1367
1363  IF(IOPT.GT.8) GO TO 1368
      INL1=4
      INL2=INL
```

```
      IF(IOPT.EQ.6) INL2=6
      IF(IOPT.EQ.7) INL2=9
      GO TO 1367
 1368 IF(IOPT.GT.11) GO TO 1367
      INL1=7
      INL2=10
      IF(IOPT.EQ.9) INL2=9
      IF(IOPT.EQ.11) INL1=10
 1367 IF(IOPT.GT.11)ILIMIT=1
 591  DO 556 I6=1,ITER
      IF(I6.LT.ITER1) GO TO 487
      IF(I33.EQ.0)  GO TO 487
      I22=I23
      IFREQ=0
 487  CONTINUE
      IF(I6.NE.ITER) GO TO 488
      INL1=1
      INL2=INL
      ILIMIT=0
 488  CONTINUE
      W=W1
      IF(IFREQ.EQ.1) W=FREQ(1)*6.2832
 490  CALL FCDE(RSIG,W,1)
      DO 570 I=1,INL
 570  RMS(I)=0.
      DO 1570 I=1,DOF
 1570 DRMS(I)=0.
      DO 555 I5=1,I22
      IF(IFREQ.EQ.1) GO TO 446
      ALPHA=(W2/W1)**(1./FLOAT(I22-1))
      RK5=W
      W=W1*ALPHA**(I5-1)
      FREQ(I5)=W/6.2832
      GO TO 445
 446    RK5=W
      W=FREQ(I5)*6.2832
 445    DW=(W-RK5)/6.2832
      CALL FCDE(RSIG,W,2)
C*****************************************************
C     RAIL ALIGNMENT INPUT,REAL AND IMAGINARY PART
C*****************************************************
      B3R(1)=1.
      B3R(2)=1.
      B3R(3)=COS((L1-L2)*W/V)
      B3R(4)=B3R(3)
      B3R(5)=COS((L1+L3)*W/V)
      B3R(6)=B3R(5)
```

```
      B3I(1)=0.
      B3I(2)=0.
      B3I(3)=-SIN((L1-L2)*W/V)
      B3I(4)=B3I(3)
      B3I(5)=-SIN((L1+L3)*W/V)
      B3I(6)=B3I(5)
      RM2R(1)=-B3R(1)
      RM2R(2)=-B3R(3)
      RM2R(3)=-B3R(5)
      RM2I(2)=-B3I(3)
      RM2I(3)=-B3I(5)
C
      RM1I(10,12)=W
C***********************************************
C     INVERSION OF ((K)-(M)*W**2+J W (D))      *
C     ASSUME INVERSE=DR(REAL)+J DI(IMAGINARY)  *
C     THEN CALCULATE DR,DI                     *
C***********************************************
      DO 300 J=1,DOF
      DO 300 I=1,DOF
      C1(I,J)=-C(I,J)*W
      DI(I,J)=-M(I,J)*W*W+K(I,J)
300   DR(I,J)=DI(I,J)
      CALL INVERT(DI,DET)
      DO 20 J=1,DOF
      DO 20 I=1,DOF
      DUM1(I,J)=0.0
      DO 20 JJ=1,DOF
20    DUM1(I,J)=DUM1(I,J)+ C1(I,JJ)*DI(JJ,J)
      DO 30 J=1,DOF
      DO 30 I=1,DOF
      DO 30 JJ=1,DOF
30    DR(I,J)=DR(I,J)+DUM1(I,JJ)*C1(JJ,J)
      CALL INVERT(DR,DET)
      DO 40 J=1,DOF
      DO 40 I=1,DOF
      DI(I,J)=0.
      DO 40 JJ=1,DOF
40    DI(I,J)=DI(I,J)+DR(I,JJ)*DUM1(JJ,J)
      DO 400 I=1,DOF
      TRA(I)=0.
      TIA(I)=0.
      BRA(I)=0.
      BIA(I)=0.
400   CONTINUE
```

```
      DO 600 I=1,DOF
      DO 600 J=1,6
      BRA(I)=BRA(I)+B2(I,J)*B3R(J)-B1(I,J)*B3I(J)
      BIA(I)=BIA(I)+B2(I,J)*B3I(J)+B1(I,J)*B3R(J)
600   CONTINUE
      DO 700 I=1,DOF
      DO 700 J=1,DOF
      TRA(I)=TRA(I)+DR(I,J)*BRA(J)-DI(I,J)*BIA(J)
      TIA(I)=TIA(I)+DI(I,J)*BRA(J)+DR(I,J)*BIA(J)
700   CONTINUE
      IF(ILIMIT.EQ.1) GO TO 1217
      DO 701 I=INL1,INL2
      WV2(I)=0.
      WV3(I)=0.
      WV1(I)=0.
      WV4(I)=0.
701   CONTINUE
      DO 705 I=INL1,INL2
      DO 705 J=1,DOF
      WV1(I)=WV1(I)+RM1R(I,J)*TRA(J)
      WV2(I)=WV2(I)+RM1I(I,J)*TIA(J)
      WV3(I)=WV3(I)+RM1I(I,J)*TRA(J)
      WV4(I)=WV4(I)+RM1R(I,J)*TIA(J)
705   CONTINUE
C*****************************************************
C  COMPUTE TRANSFERFUNCTIONS FOR 10 D.F.VAR. AND PSD,S *
C*****************************************************
      CALL PSDA(W,AIPSD,I22,I5,V,ITC)
      DO 706 I=INL1,INL2
      TZR(I)=RM2R(I)+WV1(I)-WV2(I)
      TZI(I)=RM2I(I)+WV3(I)+WV4(I)
      PSD(I)=(TZR(I)**2+TZI(I)**2)*AIPSD*6.2832
706   CONTINUE
      GO TO 1218
1217  CALL GT1(W,AIPSD,I22,I5,V,ITC)
1218  IF(I6.NE.ITER) GO TO 801
      DO 802 I=1,INL
      ZTZR(I5,I)=TZR(I)
      ZTZI(I5,I)=TZI(I)
802   ZPSD(I5,I)=PSD(I)
C*******************************************************
C     DISPLACEMENT TRANSFER FUNCTIONS,MAGNITUDE AND PHASE  *
C*******************************************************
      DO 800 I=1,DOF
      MAGN(I5,I)=SQRT(TRA(I)**2+TIA(I)**2)
800   PHASE(I5,I)=ATAN(TIA(I)/TRA(I))*360./6.2832
```

```
C*********************************
C     PSD'S OF STATUS             *
C*********************************
      DO 707 I=1,DOF
707   DPSD(I5,I)=(TRA(I)**2+TIA(I)**2)*AIPSD*6.2832
801   IF(I5.EQ.1) GO TO 559
      IF(ILIMIT.EQ.1) GO TO 1219
      DO 561 I=INL1,INL2
      RMS(I)=WV6(I)+.5*DW*(PSD(I )+WV5(I))
561   CONTINUE
      GO TO 1220
1219  CALL GT2(DW)
1220  IF(I6.NE.ITER) GO TO 559
      DO 562 I=1,DOF
562   DRMS(I)=WV8(I)+.5*DW*(DPSD(I5,I)+WV7(I))
559   CONTINUE
      IF(ILIMIT.EQ.1) GO TO 1230
      DO 560 I=INL1,INL2
      WV5(I)=PSD(I)
      WV6(I)=RMS(I)
560   CONTINUE
      GO TO 1231
1230  CALL GT3
1231  IF(I6.NE.ITER) GO TO 431
      DO 563 I=1,DOF
      WV7(I)=DPSD(I5,I)
563   WV8(I)=DRMS(I)
      IF(I6.LT.ITER) GO TO 431
434   IF(I5.NE.1) GO TO 433
      RMYC=0.
      RMFT=0.
433   CONTINUE
C***************************************************
C     CAR LATERAL ACC. TRANSFER FUNCTION *
C     TRUCK ACC. TRANSFER FUNCTION                 *
C***************************************************
      ATFCR=-TRA(10)*W**2
      ATFFTR=-TRA(7)*W**2
      ATFFTI=-TIA(7)*W**2
      ATFCI=-TIA(10)*W**2
C****************************************************
C     POWER SPECTRAL DENSITIES                      *
C****************************************************
      APSDC(I5)=(ATFCR**2+ATFCI**2)*AIPSD*R22
      APSDFT(I5)=(ATFFTR**2+ATFFTI**2)*AIPSD*R22
```

```
C*************************************************************
C     RMS VALUES OF CAR BODY,AND TRUCK ACCELERATIONS          *
C*************************************************************
432     IF(I5.EQ.1) GO TO 430
        RMYC=RMYC+0.5*DW*(R24+APSDC(I5))
        RMFT=RMFT+0.5*DW*(R25+APSDFT(I5))
430     R24=APSDC(I5)
        R25=APSDFT(I5)
431     CONTINUE
555     CONTINUE
        IF(I6.LT.ITER) GO TO 467
3001    RMYC=SQRT(RMYC)
        RMFT=SQRT(RMFT)
467     CONTINUE
        DO 580 I=1,INL
        RMS(I)=SQRT(RMS(I))
580     CONTINUE
        DO 581 I=1,DOF
581     DRMS(I)=SQRT(DRMS(I))
C***************************************
C  ITERATION SCHEME FOR CONVERGENCE    *
C***************************************
        WRITE(P,92) I6
        WRITE(P,191) I22
191     FORMAT(2X,'FREQUENCY POINTS=',I3)
        TYPE 92, I6
 92     FORMAT(//1H,5X,'  ITERATION NO.  ',I3/7X,20('*')/
        1      8X,'GUESSED',7X,'COMPUTED')
        TYPE 191,I22
        DO 927 I=1,INL
        WRITE(P,93) I,RSIG(I),RMS(I)
        TYPE 93, I,RSIG(I),RMS(I)
927     CONTINUE
93      FORMAT(2X,I2,3X,E12.5,3X,E12.5)
        IF(I6.EQ.1) GO TO 1111
        GO TO 1113
1111    DO 1112 J=1,INL
        GC(J)=RMS(J)
        SIG(J)=RSIG(J)
1112    RSIG(J)=1.1*RSIG(J)
        GO TO 835
1113    IF(I6.EQ.ITER) GO TO 835
        DO 1114 J=1,INL
        IF((RSIG(J)-SIG(J)-RMS(J)+GC(J)).EQ.0.) GO TO 1819
        SP(J)=(RSIG(J)-SIG(J))/(RSIG(J)-SIG(J)-RMS(J)+GC(J))
        GO TO 1820
```

```
1819    SP(J)=SP(J)
1820    IF(ABS(SP(J)).GE.EPS) SP(J)=EPS*SIGN(1.,SP(J))
        IF(ABS(SP(J)).LE..01) SP(J)=.01*SIGN(1.,SP(J))
        GC(J)=RMS(J)
        SIG(J)=RSIG(J)
        DIFF=RMS(J)-RSIG(J)
        IF(ABS(DIFF).GT.RSIG(J)) DIFF=SIGN(1.,DIFF)*RSIG(J)
1117    RSIG(J)=RSIG(J)+SP(J)*DIFF
        IF(RSIG(J).EQ.0.) RSIG(J)=0.5*(SIG(J)+RMS(J))
1203    CONTINUE
1114    CONTINUE
835     CONTINUE
556     CONTINUE
        RETURN
        END
```

```
      SUBROUTINE FCPL(RSIG,W,II)
      COMMON/COM2/CPYAW(3),CPY(3),CPPHI(3),KPPHI(3),
     1       KSPHI,CSPHI,KSY,CSY,KSYAW,TCP,PY1(3),
     1       PYAW1(3),PYAW2(3),DLY(3),DLYAW(3),DEL0(3)
      COMMON/COM4/A,L1,L2,L3,HTP,HTS,HCS,PZERO,MW,MT,MC,
     1       IWY,IWX,ITZ,ITX,ICX,LA,V,IBOLS
      COMMON/COM5/F11,F12,F22,F33
      COMMON/GAINS/K71,K72,K73,K81,K82,K83,A11,A12,A13,
     1       KGRAV(3),KDEL(3),LAMDA(3),CCP,GPHI(3),KDELY(3)
      REAL MAGN
      COMMON/OUT/DRMS(12),DPSD(150,12),FREQ(150),I22,
     1          APSDC(150),APSDFT(150),
     1           RMYC,RMFT,MAGN(150,12),PHASE(150,12)
      COMMON/RP/R,P
      COMMON/DOF/DOF
      INTEGER R,P,DOF
      REAL KPPHI,KSPHI,KSY,KSYAW,IWY,IWX,ITZ,ITX,ICX,LA,IBOLS
     1       ,K71,K72,K73,K81,K82,K83,KGRAV,KDEL,LAMDA,M,K,KDELY
      REAL L1,L2,L3,MW,MT,MC
      DIMENSION RSIG(10)
      COMMON/AINC/AINC7,AINC8
      COMMON/COMC/M(12,12),K(12,12),C(12,12),
     1          B2(12,6),B1(12,6)
      COMMON/OPTION/IOPT
      IF(II.GE.2) GO TO 1796
      IF (II.GE.1) GO TO 1200
C*******************************************
C     VEHICLE PARAMETERS
C*******************************************
      READ(R,199) IWRITE
199   FORMAT(I1)
      READ(R,200) A,L1,L2,L3
      READ(R,200) HTP,HCS,HTS,PZERO,XNU
      READ(R,200) F11,F12,F22,F33
      READ(R,200) MW,MT,MC,LA,IBOLS
      READ(R,200) IWX,IWY,ITX,ITZ,ICX
      READ(R,200) (CPY(I),I=1,3)
      READ(R,200) (CPYAW(I),I=1,3)
      READ(R,200) (CPPHI(I),I=1,3)
      READ(R,200) (KPPHI(I),I=1,3)
      READ(R,200) KSPHI,CSPHI,KSY,CSY
      READ(R,200) (PY1(I),I=1,3)
      READ(R,200) (PYAW1(I),I=1,3)
      READ(R,200) (PYAW2(I),I=1,3)
```

```
      READ(R,200) KSYMM,TCP
      READ(R,200) (DLY(I),I=1,3)
      READ(R,200) (DLYAW(I),I=1,3)
      READ(R,200) (DEL0(I),I=1,3)
      READ(R,200) A11,A12,A13
      READ(R,200) (LAMDA(I),I=1,3)
      READ(R,200) (KDEL(I),I=1,3)
      READ(R,200) (KDELY(I),I=1,3)
      READ(R,200) (KGRAV(I),I=1,3)
      READ(R,200) K71,K72,K73
      READ(R,200) K81,K82,K83
      READ(R,200) CCP
      READ(R,200) (GPHI(I),I=1,3)
      READ(R,200) AINC7,AINC8
      IF(IWRITE.EQ.0) GO TO 203
200   FORMAT(5E12.5)
      WRITE(P,21)
21    FORMAT(1H1/2X,'LOCOMOTIVE PARAMETERS'/
     1        2X,'______________________'/
     1        2X,'______________________'/)
      WRITE(P,22)A,L1,L2,L3
22    FORMAT(5X,'DIMENSIONS'//
     1 5X,'A  (HALF LENGTH OF WHEEL BASE)
     1         =',E12.5,' IN.'/
     2 5X,'L1 (DISTANCE BETWEEN TRUCK CENTER AND LEAD AXLE)
     2     =',E12.5,' IN.'/
     3 5X,'L2 (DISTANCE BETWEEN TRUCK CENTER AND MIDDLE AXLE)
     3  =',E12.5,' IN.'/
     4 5X,'L3 (DISTANCE BETWEEN TRUCK CENTER AND TRAILING
     4 AXLE) =',E12.5,' IN.')
      WRITE(P,23)HTP,HCS,HTS,RZERO,XMU
23    FORMAT(/5X,'HTP    (HEIGHT OF TRUCK FRAME C.G. ABOVE
     1 AXLE CENTER)                 =',E12.5,' IN.'/
     2       5X,'HCS    (HEIGHT OF CARBODY C.G. ABOVE BOL
     2STER SPRING CENTER)           =',E12.5,' IN.'/
     3       5X,'HTS    (HEIGHT OF BOLSTER SPRING CENTER
     4 ABOVE TRUCK FRAME C.G.) =',E12.5,' IN.'/
     5       5X,'RZERO  (WHEEL TREAD RADIUS)
     6                                =',E12.5,' IN.'/
     7         5X,'XMU    (COEFFICIENT OF FRICTION)
     8                         =',E12.5,' IN.')
      WRITE(P,24) DLY(1),DLYAW(1)
24    FORMAT(/5X,'DLY    (DEADBAND IN PRIMARY LATERAL
     1 STIFFNESS)           =',E12.5,' IN.'/
     2       5X,'DLYAW (LIMIT OF FIRST LINEAR STIFFNESS
     3 IN PRIMARY YAW) =',E12.5,' IN.')
```

```
      WRITE(P,25)MW,MT,MC,LA
25    FORMAT(///5X,'MASS PROPERTIES'//
     1       5X,'MW (WHEELSET MASS)  =',E12.5,' LB-SEC**2
     2/IN'/
     3       5X,'MT (TRUCK MASS    )  =',E12.5,' LB-SEC**2
     4/IN'/
     5       5X,'MC (HALF-CAR MASS)  =',E12.5,' LB-SEC**2
     6/IN'/
     7       5X,'W (NOMINAL AXLE LOAD)=',E12.5,' LB')
      WRITE(P,26)IWX,IWY,ITX,ITZ,ICX,IBOLS
26    FORMAT(/5X,'IWX (ROLL & YAW MOMENT OF INERTIA OF
     1 THE WHEELSET) =',E12.5,' LB-IN-SEC**2'/
     2       5X,'IWY (SPIN MOMENT OF INERTIA OF THE
     3 WHEELSET)         =',E12.5,' LB-IN-SEC**2'/
     4       5X,'ITX (ROLL MOMENT OF INERTIA OF THE
     5 TRUCK)            =',E12.5,' LB-IN-SEC**2'/
     6       5X,'ITZ (YAW MOMENT OF INERTIA OF THE
     7TRUCK )            =',E12.5,' LB-IN-SEC**2'/
     8       5X,'ICX (HALF-ROLL MOMENT OF INERTIA OF
     9 THE CARBODY)   =',E12.5,' LB-IN-SEC**2'/
     8       5X,'IBOLS(YAW MOMENT OF INERTIA OF THE
     9 BOLSTER)          =',E12.5,' LB-IN-SEC**2')
      WRITE(P,27)F11,F12,F22,F33
27    FORMAT(//5X,'NOMINAL CREEP COEFFICIENTS'//
     1  5X,'F11 (LATERAL)   =',E12.5,' LB/WHEEL'/
     2  5X,'F12 (LAT/SPIN) =',E12.5,' LB-IN/WHEEL'/
     3  5X,'F22 (SPIN)      =',E12.5,' LB-IN**2/WHEEL'/
     4  5X,'F33 (LONGITUD.)=',E12.5,' LB/WHEEL')
      WRITE(P,28)(CPY(I),I=1,3)
28    FORMAT(1H1,///5X,'PRIMARY SUSPENSIONS (PER AXLE)'//
     1  5X,'CPY (LAT. DAMPING COEFF.)          =',
     2  E12.5,2X,E12.5,2X,E12.5,' LB-SEC/IN')
      WRITE(P,29)(CPYAW(I),I=1,3),(CPPHI(I),I=1,3)
29    FORMAT(5X,'CPYAW (YAW DAMPING COEFF.)        =',
     2  E12.5,2X,E12.5,2X,E12.5,' LB-IN-SEC'/
     3  5X,'CPPHI (ROLL DAMPING COEFF.)      =',E12.5,2X,
     4  E12.5,2X,E12.5,' LB-IN-SEC')
      WRITE(P,30)(KPPHI(I),I=1,3),(PYAW1(I),I=1,3),
     1         (PYAW2(I),I=1,3)
30    FORMAT(5X,'KPPHI (ROLL STIFFNESS)             =',E12.5,
     1  2X,E12.5,2X,E12.5,' LB-IN'/
     2  5X,'PYAW1 (FIRST STIFFNESS IN YAW)  =',E12.5,2X,
     3  E12.5,2X,E12.5,' LB-IN'/
     4  5X,'PYAW2 (SECOND STIFFNESS IN YAW) =',E12.5,2X,
     5  E12.5,2X,E12.5,' LB-IN')
```

```
      WRITE(P,32)KSPHI,CSPHI,KSY,CSY,KSYAW,TCP
32    FORMAT(//5X,'SECONDARY SUSPENSIONS (PER TRUCK)'//
     1  5X,'KSPHI (ROLL STIFFNESS)  =',E12.5,' LB-I '/
     2  5X,'CSPHI (ROLL DAMPING)    =',E12.5,' LB-IN-SEC'/
     3  5X,'KSY   (LATERAL STIFFNESS)=',E12.5,' LB/IN'/
     4  5X,'CSY   (LATERAL DAMPING)  =',E12.5,' LB-SEC/IN'/
     5  5X,'KSYAW (YAW STIFFNESS)    =',E12.5,' LB-IN'/
     6  5X,'TCP   (COULOMB BREAKAWAY)=',E12.5,' LB-IN')
      WRITE(P,33)(DEL0(I),I=1,3),A11,A12,A13,(LAMDA(I),I=1,3)
33    FORMAT(///5X,'LINEAR PARAMETERS'/
     1        5X,'_________________'//
     1       5X,'DEL0  =',3(2X,E12.5)/
     1       5X,'A1(I) =',3(2X,E12.5)/
     1       5X,'LAMDA =',3(2X,E12.5))
      WRITE(P,34)(KDEL(I),I=1,3),(KDELY(I),I=1,3),(KGRAV(I),I=1,3),
     1       K71,K72,K73,K81,K82,K83,CCP
34    FORMAT(5X,'KDEL  =',3(2X,E12.5)/
     1       5X,'KDELY =',3(2X,E12.5)/
     1       5X,'KGRAV =',3(2X,E12.5)/
     1       5X,'K7    =',3(2X,E12.5)/
     1       5X,'K8    =',3(2X,E12.5)/
     1       5X,'CCP   =',3(2X,E12.5),5(/))
203   IF(IOPT.EQ.1) GO TO 201
      CALL RSF4(RSIG,0)
C*****************************************************************
C     INITIALIZATION OF M,K,C AND INPUT COEFF. MATRICES
C******************************************************************
201     DO 650 I=1,DOF
      DO 650 J=1,DOF
      M(I,J)=0.0
      C(I,J)=0.0
      K(I,J)=0.0
 650    CONTINUE
      DO 906 I=1,DOF
      DO 906 J=1,6
      B2(I,J)=0.0
      B1(I,J)=0.0
906     CONTINUE
C***************************************************************
C THE FORM USED IN THE COEFF MATRICES IS
C     M*DDX+C*DX+K*X=0
C THE EQUATIONS ARE STILL COUPLED HERE
C**************************************************************
      M(1,1)=MW
      M(2,2)=IWX
      M(3,3)=MW
      M(4,4)=IWX
```

```
      M(5,5)=MW
      M(6,6)=IMY
      M(7,7)=MT
      M(8,8)=ITZ
      M(9,9)=ITX
      M(10,10)=MC
      M(11,11)=ICX
      M(12,12)=IBOLS
C*************************************************
C   ***SPRING CONSTANT***
C*************************************************
      K(1,2)=-2.*F11
      K(3,4)=-2.*F11
      K(5,6)=-2.*F11
      K(7,10)=-KSY
      K(7,11)=-HCS*KSY
      K(8,12)=-KSYAW
      K(9,10)=HTS*KSY
      K(9,11)=-KSPHI+HCS*HTS*KSY
      K(10,7)=-KSY
      K(10,9)=HTS*KSY
      K(10,10)=KSY
      K(10,11)=HCS*KSY
      K(11,7)=-HCS*KSY
      K(11,9)=-KSPHI+HCS*HTS*KSY
      K(11,10)=HCS*KSY
      K(11,11)=KSPHI+HCS*HCS*KSY
      K(12,8)=-KSYAW
      K(12,12)=KSYAW
      C(1,2)=2.*F12/V
      C(1,7)=-CPY(1)
      C(1,8)=-L1*CPY(1)
      C(1,9)=-HTP*CPY(1)
      C(2,2)=2.*A*A*F33/V+2.*F22/V+CPYAW(1)
      C(2,8)=-CPYAW(1)
      C(3,4)=2.*F12/V
      C(3,7)=-CPY(2)
      C(3,8)=-L2*CPY(2)
      C(3,9)=-HTP*CPY(2)
      C(4,4)=2.*A*A*F33/V+2.*F22/V+CPYAW(2)
      C(4,8)=-CPYAW(2)
      C(5,6)=2.*F12/V
      C(5,7)=-CPY(3)
      C(5,8)=L3*CPY(3)
      C(5,9)=-HTP*CPY(3)
      C(6,6)=2.*A*A*F33/V+2.*F22/V+CPYAW(3)
      C(6,8)=-CPYAW(3)
```

```
      C(7,1)=-CPY(1)
      C(7,3)=-CPY(2)
      C(7,5)=-CPY(3)
      C(7,7)=CPY(1)+CPY(2)+CPY(3)+CSY
      C(7,8)=L1*CPY(1)+L2*CPY(2)-L3*CPY(3)
      C(7,9)=HTP*(CPY(1)+CPY(2)+CPY(3))-HTS*CSY
      C(7,10)=-CSY
      C(7,11)=-HCS*CSY
      C(8,1)=-L1*CPY(1)
      C(8,2)=-CPYAW(1)
      C(8,3)=-L2*CPY(2)
      C(8,4)=-CPYAW(2)
      C(8,5)=L3*CPY(3)
      C(8,6)=-CPYAW(3)
      C(8,7)=L1*CPY(1)+L2*CPY(2)-L3*CPY(3)
      C(8,8)=CPYAW(1)+CPYAW(2)+CPYAW(3)+L1*L1*CPY(1)+L2*L2*CPY(2)
     1      +L3*L3*CPY(3)
      C(8,9)=HTP*(L1*CPY(1)+L2*CPY(2)-L3*CPY(3))
      C(9,7)=-HTS*CSY+HTP*(CPY(1)+CPY(2)+CPY(3))
      C(9,8)=HTP*(L1*CPY(1)+L2*CPY(2)-L3*CPY(3))
      C(9,9)=CPPHI(1)+CPPHI(2)+CPPHI(3)+CSPHI+HTS*HTS*CSY+
     1      HTP*HTP*(CPY(1)+CPY(2)+CPY(3))
      C(9,10)=HTS*CSY
      C(9,11)=-CSPHI+HCS*HTS*CSY
      C(10,7)=-CSY
      C(10,9)=HTS*CSY
      C(10,10)=CSY
      C(10,11)=HCS*CSY
      C(11,7)=-HCS*CSY
      C(11,9)=-CSPHI+HCS*HTS*CSY
      C(11,10)=HCS*CSY
      C(11,11)=CSPHI+HCS*HCS*CSY
      GO TO 5000
1200  CONTINUE
      IF(IOPT.EQ.1) GO TO 1201
C*********************************************************************
C     CALL DSF4 TO GET DESCRIBING FUNCTION GAINS FOR NONLINEARITIES
C*********************************************************************
      CALL DSF4(RSIG,1)
1201  K(1,1)=-2.*F12*KDEL(1)/A/RZERO+LA*KGRAV(1)/A+K71
      K(1,7)=-K71
      K(1,8)=-L1*K71
      K(1,9)=-HTP*K71
      K(2,1)=2.*A*F33*LAMDA(1)/RZERO-2.*F22*KDELY(1)/A/RZERO
      K(2,2)=2.*F12-A*LA*DEL0(1)+K81
      K(2,8)=-K81
      K(3,3)=-2.*F12*KDEL(2)/A/RZERO+LA*KGRAV(2)/A+K72
      K(3,7)=-K72
```

```
      K(3,8)=-L2*K72
      K(3,9)=-HTP*K72
      K(4,3)=2.*A*F33*LAMDA(2)/RZERO-2.*F22*KDELY(2)/A/RZERO
      K(4,4)=2.*F12-A*LA*DEL0(2)+K82
      K(4,8)=-K82
C
      K(5,5)=-2.*F12*KDLL(3)/A/RZERO+LA*MGRAV(3)/A+K73
      K(5,7)=-K73
      K(5,8)=L3*K73
      K(5,9)=-HTP*K73
C
      K(6,5)=2.*A*F33*LAMDA(3)/RZERO-2.*F22*KDELY(3)/A/RZERO
      K(6,6)=2.*F12-A*LA*DEL0(3)+K83
      K(6,8)=-K83
C
      K(7,1)=-K71
      K(7,3)=-K72
      K(7,5)=-K73
      K(7,7)=K71+K72+K73+KSY
      K(7,8)=L1*K71+L2*K72-L3*K73
      K(7,9)=-HTS*KSY+HTP*(K71+K72+K73)
      K(8,1)=-L1*K71
      K(8,2)=-K81
      K(8,3)=-L2*K72
      K(8,4)=-K82
      K(8,5)=L3*K73
      K(8,6)=-K83
      K(8,7)=L1*K71+L2*K72-L3*K73
      K(8,8)=L1*L1*K71+L2*L2*K72+L3*L3*K73+K81+K82+K83+KSYAW
      K(8,9)=HTP*(L1*K71+L2*K72-L3*K73)
C
      K(9,1)=-HTP*K71-KPPHI(1)*A11/A
      K(9,3)=-HTP*K72-KPPHI(2)*A12/A
      K(9,5)=-HTP*K73-KPPHI(3)*A13/A
      K(9,7)=HTP*(K71+K72+K73)-HTS*KSY
      K(9,8)=HTP*(L1*K71+L2*K72-L3*K73)
      K(9,9)=KPPHI(1)+KPPHI(2)+KPPHI(3)+KSPHI+HTS*HTS*KSY+
     1       HTP*HTP*(K71+K72+K73)
C
      C(1,1)=2.*F11/V*(1.+RZERO*GPHI(1)/A)+CPY(1)
      C(2,1)=IWY*V*GPHI(1)/A/RZERO-2.*F12/V*(1.+RZERO*GPHI(1)/A)
      C(3,3)=2.*F11/V*(1.+RZERO*GPHI(2)/A)+CPY(2)
      C(4,3)=IWY*V*GPHI(2)/A/RZERO-2.*F12/V*(1.+RZERO*GPHI(2)/A)
C
      C(5,5)=2.*F11/V*(1.+RZERO*GPHI(3)/A)+CPY(3)
      C(6,5)=IWY*V*GPHI(3)/A/RZERO-2.*F12/V*(1.+RZERO*GPHI(3)/A)
C
```

```
      C(9,1)=-HTP*CPY(1)-CPPHI(1)*GPHI(1)/A
      C(9,3)=-HTP*CPY(2)-CPPHI(2)*GPHI(2)/A
      C(9,5)=-HTP*CPY(3)-CPPHI(3)*GPHI(3)/A
      C(12,12)=CCP
      B2(1,1)=2.*(LA*KGRAV(1)/2.-F12*KDEL(1)/RZERO)/A
      B2(2,2)=-2.*(F22*KDELY(1)/A-A*F33*LAMDA(1))/RZERO
      B2(3,3)=2.*(LA*KGRAV(2)/2.-F12*KDEL(2)/RZERO)/A
      B2(4,4)=-2.*(F22*KDELY(2)/A-A*F33*LAMDA(2))/RZERO
      B2(5,5)=2.*(LA*KGRAV(3)/2.-F12*KDEL(3)/RZERO)/A
      B2(6,6)=-2.*(F22*KDELY(3)/A-A*F33*LAMDA(3))/RZERO
      B2(9,1)=-KPPHI(1)*A11/A
      B2(9,3)=-KPPHI(2)*A12/A
      B2(9,5)=-KPPHI(3)*A13/A
1796  CONTINUE
      B1(1,1)=2.*F11*RZERO*GPHI(1)/A/V*W
      B1(2,2)=(IWY*V/RZERO-2.*F12*RZERO/V)*GPHI(1)/A*W
      B1(3,3)=2.*F11*RZERO*GPHI(2)/A/V*W
      B1(4,4)=(IWY*V/RZERO-2.*F12*RZERO/V)*GPHI(2)/A*W
      B1(5,5)=2.*F11*RZERO*GPHI(3)/A/V*W
      B1(6,6)=(IWY*V/RZERO-2.*F12*RZERO/V)*GPHI(3)/A*W
      B1(9,1)=-CPPHI(1)*GPHI(1)/A*W
      B1(9,3)=-CPPHI(2)*GPHI(2)/A*W
      B1(9,5)=-CPPHI(3)*GPHI(3)/A*W
5000  CONTINUE
      RETURN
      END
```

```
      SUBROUTINE RAIL (RSIG,IMP)
      DIMENSION RSIG(10)
      COMMON/MINPUT/X1(51),ALM1(51),ADL1(51),APH1(51),GS1(51),
     1  ADLY1(51),X2(51),ALM2(51),ADL2(51),APH2(51),GS2(51),
     1  ADLY2(51),X3(51),ALM3(51),ADL3(51),APH3(51),GS3(51),
     1  ADLY3(51)
      COMMON/RP/R,P
      COMMON/IGS/IGSL,IGSY
      COMMON/GIGSL/Y1(120),GAIN71(120),Y2(120),GAIN72(120),
     1             Y3(120),GAIN73(120)
      COMMON/GIGSY/Y4(120),GAIN81(120),Y5(120),GAIN82(120),
     1             Y6(120),GAIN83(120)
      INTEGER R,P
      COMMON/ER/ER(201)
C*******************************************************************
C     READ STATISTICAL DESCRIBING FUNCTION TABLE FOR THREE WHEELSETS
C     X  :WHEELSET RELATIVE LATERAL DISPLACEMENT
C     ALM:EFFECTIVE CONICITY (LAMDA(*),ETC.)
C     ADL:CONTACT ANGLE COEFFS. (YDIL(*),ETC.)
C     APH:ROLL COEFFS. (A51,ETC.)
C     GS :EFFECTIVE LATERAL GRAV. STIFFNESS
C*******************************************************************
      READ(R+1,10) (X1(I),ADLY1(I),ALM1(I),APH1(I),GS1(I),ADL1(I),
     1       I=1,51)
      READ(R+2,10) (X2(I),ADLY2(I),ALM2(I),APH2(I),GS2(I),ADL2(I),
     1       I=1,51)
      READ(R+3,10) (X3(I),ADLY3(I),ALM3(I),APH3(I),GS3(I),ADL3(I),
     1       I=1,51)
10    FORMAT(6(2X,E12.5))
C*****************************************************
C     READ ERROR FUNCTION TABLE ERF(X)
C*****************************************************
      READ(R+4,2) (ER(I),I=1,201)
2     FORMAT(F7.5)
      IF(IGSL.EQ.0) GO TO 1
      READ(R+5,11) (Y1(I),GAIN71(I),I=1,120)
      READ(R+6,11) (Y2(I),GAIN72(I),I=1,120)
      READ(R+7,11) (Y3(I),GAIN73(I),I=1,120)
1     IF(IGSY.EQ.0) GO TO 22
      READ(R+8,11) (Y4(I),GAIN81(I),I=1,120)
      READ(R+9,11) (Y5(I),GAIN82(I),I=1,120)
      READ(R+10,11) (Y6(I),GAIN83(I),I=1,120)
22    CONTINUE
11    FORMAT(2(E12.5))
C********************************
C    READ GUESSED RMS VALUES
C********************************
      READ(R,30) (RSIG(I),I=1,10)
30    FORMAT(6E12.5)
      RETURN
      END
```

```
      SUBROUTINE DSF4(RSIG,I3)
      COMMON/COM2/CPYAW(3),CPY(3),CPPHI(3),KPPHI(3),
     1        KSPHI,CSPHI,KSY,CSY,KSYAW,TCP,PY1(3),
     1        PYAW1(3),PYAW2(3),DLY(3),DLYAW(3),DELB(3)
      COMMON/GAINS/K71,K72,K73,K81,K82,K83,A11,A12,A13,
     1        KGRAV(3),KDEL(3),LAMDA(3),CCP,GPHI(3),KDELY(3)
      REAL KPPHI,KSPHI,KSY,KSYAW,K71,K72,K73,K81,K82,K83,KGRAV
     1        ,KDEL,LAMDA,KDELY
      COMMON/AINPUT/X1(51),ALM1(51),ADL1(51),APH1(51),GS1(51),
     1   ADLY1(51),X2(51),ALM2(51),ADL2(51),APH2(51),GS2(51),
     1   ADLY2(51),X3(51),ALM3(51),ADL3(51),APH3(51),GS3(51),
     1   ADLY3(51)
      COMMON/GIGSL/Y1(120),GAIN71(120),Y2(120),GAIN72(120),
     1              Y3(120),GAIN73(120)
      COMMON/GIGSY/Y4(120),GAIN81(120),Y5(120),GAIN82(120),
     1              Y6(120),GAIN83(120)
      COMMON/AINC/AINC7,AINC8
      COMMON/RP/R,P
      COMMON/ER/ER(201)
      INTEGER R,P
      COMMON/IPIS/IPROF,ISUSP
      COMMON/IGS/IGSL,IGSY
      COMMON/OPTION/IOPT
      DIMENSION RSIG(10)
      IF(I3.EQ.0) READ(R,2) SIGLOW
2     FORMAT(E12.5)
      IF(IPROF.EQ.0) GO TO 20
C*****************************************************************
C     WHEEL/RAIL PROFILE EQUIVALENT GAINS
C*****************************************************************
      CALL LDP4(RSIG(1),LAMDA(1),KDEL(1),A11,KGRAV(1),KDELY(1),
     1        X1,ALM1,ADL1,APH1,GS1,ADLY1)
      CALL LDP4(RSIG(2),LAMDA(2),KDEL(2),A12,KGRAV(2),KDELY(2),
     1        X2,ALM2,ADL2,APH2,GS2,ADLY2)
      CALL LDP4(RSIG(3),LAMDA(3),KDEL(3),A13,KGRAV(3),KDELY(3),
     1        X3,ALM3,ADL3,APH3,GS3,ADLY3)
C**********************************************
C     AT THIS STAGE OF THE DEVELOPMENT GPH(I)=A1I
C**********************************************
      GPHI(1)=A11
      GPHI(2)=A12
      GPHI(3)=A13
      IF(IOPT.EQ.2) RETURN
```

```
C***************************************************************
C       SUSPENSION EQUIVALENT GAINS
C***************************************************************
20      RC=.79788
        IF(IOPT.LE.8) GO TO 50
        IF(IOPT.GE.15) GO TO 50
        GO TO 11
50      IF(IGSL.EQ.1) GO TO 10
        CALL ERF(DLY(1),RSIG(4),K71)
        CALL ERF(DLY(2),RSIG(5),K72)
        CALL ERF(DLY(3),RSIG(6),K73)
        K71=PY1(1)*(1.-K71)
        K72=PY1(2)*(1.-K72)
        K73=PY1(3)*(1.-K73)
        GO TO 11
10      CALL GK7(RSIG(4),K71,Y1,GAIN71,AINC7)
        CALL GK7(RSIG(5),K72,Y2,GAIN72,AINC7)
        CALL GK7(RSIG(6),K73,Y3,GAIN73,AINC7)
11      IF(IOPT.EQ.3) RETURN
        IF(IOPT.EQ.6) RETURN
        IF(IOPT.EQ.11) GO TO 17
        IF(IOPT.GE.14) GO TO 17
        IF(IGSY.EQ.1) GO TO 12
        CALL ERF(DLYAW(1),RSIG(7),K81)
        CALL ERF(DLYAW(2),RSIG(8),K82)
        CALL ERF(DLYAW(3),RSIG(9),K83)
        K81=PYAW1(1)+(PYAW2(1)-PYAW1(1))*(1.-K81)
        K82=PYAW1(2)+(PYAW2(2)-PYAW1(2))*(1.-K82)
        K83=PYAW1(3)+(PYAW2(3)-PYAW1(3))*(1.-K83)
        GO TO 13
12      CALL GK7(RSIG(7),K81,Y4,GAIN81,AINC8)
        CALL GK7(RSIG(8),K82,Y5,GAIN82,AINC8)
        CALL GK7(RSIG(9),K83,Y6,GAIN83,AINC8)
13      IF(IOPT.LE.4) RETURN
        IF(IOPT.EQ.12) RETURN
        IF(IOPT.EQ.9) RETURN
        IF(IOPT.EQ.7) RETURN
17      IF(RSIG(10).GE.SIGLOW) CCP=RC*TCP/RSIG(10)
        IF(RSIG(10).LT.SIGLOW) CCP=RC*TCP/SIGLOW
        RETURN
        END
```

```
      SUBROUTINE EIGVEC
      COMMON/DOF/DOF
      COMMON/DOF2/DOF2
      REAL K,M
      REAL*8 AM(12,12)
      INTEGER R,P,DOF,DOF2
      COMMON/RP/R,P
      COMMON/COMC/M(12,12),K(12,12),C(12,12),B2(12,12),B1(12,12)
      DIMENSION G(24,24),XMINV(12,12),Y(12,12),E(12,12),U(12,12),
     1          ROOTR(24),ROOTI(24),Z(24,24),DAMP(24)
      DOF2=2*DOF
      DO 2 I=1,DOF2
      DO 2 J=1,DOF2
    2   G(I,J)=0.0
      DO 3 I=1,DOF
      DO 3 J=1,DOF
      XMINV(I,J)=0.0
      Y(I,J)=0.0
      E(I,J)=0.0
    3   U(I,J)=0.0
      DO 4 I=1,DOF
    4   U(I,I)=1.0
      DUMMY=0.0
      DO 31 I=1,DOF
      DO 31 J=1,DOF
   31   AM(I,J)=M(I,J)
      CALL MATINV(AM,DOF,DUMMY,0,DETERM,DOF,MARK)
      DO 5 I=1,DOF
      DO 5 J=1,DOF
    5   XMINV(I,J)=-AM(I,J)
      DO 6 I=1,DOF
      DO 6 J=1,DOF
      Y(I,J)=0.0
      DO 6 L=1,DOF
    6   Y(I,J)=Y(I,J)+XMINV(I,L) *K(L,J)
      DO 7 I=1,DOF
      DO 7 J=1,DOF
      E(I,J)=0.0
      DO 7 L=1,DOF
    7   E(I,J)=E(I,J)+XMINV(I,L) *C(L,J)
      DO 8 I=1,DOF
      II=I+DOF
      DO 8 J=1,DOF
      JJ=J
    8   G(II,JJ)=Y(I,J)
```

```
      DO 9 I=1,DOF
      II=I+DOF
      DO 9 J=1,DOF
      JJ=J+DOF
 9      G(II,JJ)=E(I,J)
      DO 10 I=1,DOF
      II=I
      DO 10 J=1,DOF
      JJ=J+DOF
10      G(II,JJ)=U(I,J)
      CALL EISPAC(DOF2,DOF2,0,1,G,ROOTR,ROOTI,Z,IER,1011,1011,1,'SYSMATRIX'
      1 ,0)
      CALL STAB(DOF2,ROOTR,ROOTI,DAMP,1)
      CALL TRANS(ROOTR,ROOTI,Z)
      RETURN
      END
```

```
      SUBROUTINE OUTPUT
      COMMON/MODL/ZTZR(150,10),ZTZI(150,10),ZPSD(150,10)
      COMMON/CONC/M(12,12),K(12,12),C(12,12),
     1            B2(12,6),B1(12,6)
      COMMON/RP/R,P
      INTEGER R,P,DOF
      COMMON/DOF/DOF
      REAL MAGN,K71,K72,K73,K81,K82,K83,KGRAV,KDEL,LAMDA,KDELY
      COMMON/GAINS/K71,K72,K73,K81,K82,K83,A11,A12,A13,
     1      KGRAV(3),KDEL(3),LAMDA(3),CCP,GPHI(3),KDELY(3)
      COMMON/OUT/DRMS(12),DPSD(150,12),FREQ(150),I22,
     1            APSDC(150),APSDFT(150),
     1            RMYC,RMFT,MAGN(150,12),PHASE(150,12)
      REAL M,K
      DIMENSION ZMAGN(150,10),ZPHASE(150,10)
      READ(R,500) IP1,IP2,IP3,IP4,IP5
500   FORMAT(5I2)
C*********************************************
C     PRINT EFFECTIVE GAINS AT CONVERGENCE  *
C*********************************************
      WRITE(P,33)A11,A12,A13,(LAMDA(I),I=1,3)
33    FORMAT(///5X,'EFFECTIVE GAINS AT CONVERGENCE'/
     1        5X,'______________________________'//
     1       5X,'A1(I) =',3(2X,E12.5)/
     1       5X,'LAMDA =',3(2X,E12.5))
      WRITE(P,34)(KDEL(I),I=1,3),(KDELY(I),I=1,3),(KGRAV(I),I=1,3),
     1       K71,K72,K73,K81,K82,K83,CCP
34    FORMAT(5X,'KDEL  =',3(2X,E12.5)/
     1       5X,'KDELY =',3(2X,E12.5)/
     1       5X,'KGRAV =',3(2X,E12.5)/
     1       5X,'K7    =',3(2X,E12.5)/
     1       5X,'K8    =',3(2X,E12.5)/
     1       5X,'CCP   =',3(2X,E12.5))
C******************************************
C     M,K,C MATRICES AT CONVERGENCE      *
C******************************************
      WRITE(P,1201)
1201  FORMAT(1H1,4X,'M,K,C MATRICES AT CONVERGENCE'/4X,30('*'))
      WRITE(P,1205)
1205  FORMAT(9X,'M-MATRIX')
      DO 1215 I=1,DOF
      WRITE(P,1210) (M(I,J),J=1,DOF)
1210  FORMAT(12(1X,E10.3))
1215  CONTINUE
      WRITE(P,1220)
1220  FORMAT(///,9X,'C-MATRIX')
      DO 1225 I=1,DOF
      WRITE(P,1210) (C(I,J),J=1,DOF)
1225  CONTINUE
```

```
      WRITE(P,1230)
1230  FORMAT(///,9X,'K-MATRIX')
      DO 1235 I=1,DOF
      WRITE(P,1210) (K(I,J),J=1,DOF)
1235  CONTINUE
      IF(IP1.EQ.0) GO TO 501
      WRITE(P,20)
20    FORMAT(1H1)
      WRITE(P,1)
1     FORMAT(2X,'DISPLACEMENT POWER SPECTRAL DENSITIES'/42('*'))
      WRITE(P,8)
8     FORMAT(  '      FREQUENCY     W #1 LATERAL       W #1 YAW'
      1                 '     W #2 LATERAL       W #2 YAW'
      1                 '     W #3 LATERAL       W #3 YAW'/
      18X,'(HZ)',4X,'    (IN**2/HZ)
      1       (RD**2/HZ)    (IN**2/HZ)       (RD**2/HZ)     (IN**2/HZ)
      1      (RD**2/HZ)')
      WRITE(P,2) (FREQ(I),(DPSD(I,J),J=1,6),I=1,I22)
2     FORMAT(2X,E12.5,4X,E12.5,3X,E12.5,2X,E12.5,4X,E12.5,
      1       3X,E12.5,3X,E12.5)
      WRITE(P,20)
      WRITE(P,9)
9     FORMAT('      FREQUENCY  TRUCK LATERAL  TRUCK YAW   TRUCK ROLL  '
      1' CAR LATERAL    CAR ROLL   BOLSTER YAW'/
      18X,'(HZ)',4X,' (IN**2/HZ)    (RD**2/HZ)
      1   (RD**2/HZ)(IN**2/HZ)    (RD**2/HZ)     (RD**2/HZ)'/)
      WRITE(P,3) (FREQ(I),(DPSD(I,J),J=7,12),I=1,I22)
3     FORMAT(7(2X,E12.5))
501   IF(IP2.EQ.0) GO TO 502
      WRITE(P,41)
41    FORMAT(1H1,2X,'DISPLACEMENT TRANSFER FUNCTIONS'/2X,31('*')/
      1            5X,'FREQUENCY          W #1 LATERAL            W #1 YAW
      1            W #2 LATERAL          W #2 YAW   '/
      1 8X,'(HZ)          MAGNITUDE   PHASE      MAGNITUDE     PHASE       MAGNIT
      1 UDE   PHASE     MAGNITUDE   PHASE')
      WRITE(P,42) (FREQ(I),(MAGN(I,J),PHASE(I,J),J=1,4),I=1,I22)
42    FORMAT(2X,E12.5,3X,E12.5,2X,F6.2,3X,E12.5,2X,F6.2,3X,E12.5,2X,F6.2
      1,3X,E12.5,2X,F6.2)
      WRITE(P,43)
43    FORMAT(1H1,5X,'FREQUENCY       W #3 LATERAL              W #3 YAW
      1             TRUCK LATERAL                TRUCK YAW '/
      1 8X,'(HZ)          MAGNITUDE   PHASE      MAGNITUDE     PHASE       MAGNIT
      1 UDE   PHASE     MAGNITUDE   PHASE')
      WRITE(P,42) (FREQ(I),(MAGN(I,J),PHASE(I,J),J=5,8),I=1,I22)
      WRITE(P,44)
44    FORMAT(1H1,5X,'FREQUENCY        TRUCK ROLL         CAR BODY LATERAL
      1             CAR  ROLL  BOLSTER YAW'/
      1 8X,'(HZ)          MAGNITUDE   PHASE      MAGNITUDE     PHASE       MAGNIT
      1 UDE   PHASE     MAGNITUDE   PHASE')
```

```
      WRITE(P,422) (FREQ(I),(MAGN(I,J),PHASE(I,J),J=9,12),I=1,I22)
422   FORMAT(2X,E12.5,3X,E12.5,2X,F6.2,3X,E12.5,2X,F6.2,3X,E12.5,
     1      2X,F6.2,3X,E12.5,F6.2)
502   IF(IP3.EQ.0) GO TO 503
      WRITE(P,6)
6     FORMAT(1H1,2X,'ACCELERATION PSD OF CAR , AND  TRUCK C.G.'
     1 /2X,50('*'))
      WRITE(P,7)
7     FORMAT( /'      FREQUENCY     CAR BODY        TRUCK '/
     1 8X,'(HZ)',4X,' (G**2/HZ)      (G**2/HZ) '/)
      WRITE(P,11) (FREQ(I),APSDC(I),APSDFT(I),I=1,I22)
11    FORMAT(2X,E12.5,2X,E12.5,2X,E12.5)
503   IF(IP4.EQ.0) GO TO 504
      WRITE(P,505)
505   FORMAT(1H1,3X,'TRANSFER FUNCTIONS OF NONLINEARITIES'/
     1         ,3X,'*************************************')
      DO 1000 J=1,10
      DO 1000 I=1,I22
      ZMAGN(I,J)=SQRT(ZTZR(I,J)**2+ZTZI(I,J)**2)
1000  ZPHASE(I,J)=ATAN(ZTZI(I,J)/ZTZR(I,J))*360./6.2832
      WRITE(P,42)(FREQ(I),(ZMAGN(I,J),ZPHASE(I,J),J=1,4),I=1,I22)
      WRITE(P,506)
506   FORMAT(1H1)
      WRITE(P,42) (FREQ(I),(ZMAGN(I,J),ZPHASE(I,J),J=5,8),I=1,I22)
      WRITE(P,506)
      WRITE(P,510) (FREQ(I),(ZMAGN(I,J),ZPHASE(I,J),J=9,10),I=1,I22)
510   FORMAT(2X,E12.5,3X,E12.5,2X,F6.2,3X,E12.5,2X,F6.2)
504   IF(IP5.EQ.0) GO TO 565
      WRITE(P,507)
507   FORMAT(1H1,3X,'POWER SPECTRAL DENSITIES OF NONLINEARITIES'/
     1         3X,'******************************************')
      WRITE(P,2) (FREQ(I),(ZPSD(I,J),J=1,6),I=1,I22)
      WRITE(P,506)
      WRITE(P,508)(FREQ(I),(ZPSD(I,J),J=7,10),I=1,I22)
508   FORMAT(5(2X,E12.5))
565   CONTINUE
      WRITE(P,4)
4     FORMAT(1H1,3X,'DISPLACEMENT RMS VALUES (IN)'/3X,29('*'))
      WRITE(P,5) (DRMS(I),I=1,12)
5     FORMAT(3X,'LEADING WHEELSET LATERAL ',E12.5,' IN'/
     1       3X,'LEADING WHEELSET YAW     ',E12.5,' RD'/
     1       3X,'MIDDLE WHEELSET LATERAL  ',E12.5,' IN'/
     1       3X,'MIDDLE WHEELSET YAW      ',E12.5,' RD'/
     1       3X,'TRAILING WHEELSET LATERAL',E12.5,' IN'/
     1       3X,'TRAILING WHEELSET YAW    ',E12.5,' RD'/
     1       3X,'TRUCK LATERAL            ',E12.5,' IN'/
     1       3X,'TRUCK YAW                ',E12.5,' RD'/
     1       3X,'TRUCK ROLL               ',E12.5,' RD'/
     1       3X,'CARBODY LATERAL          ',E12.5,' IN'/
     1       3X,'CARBODY ROLL             ',E12.5,' RD'/
     1       3X,'BOLSTER YAW              ',E12.5,' RD')
```

```
      WRITE(P,12)
12    FORMAT(//3X,'ACCELERATION RMS VALUES OF CAR, AND TRUCK (
     1 G)'/3X,55('*'))
      WRITE(P,13) RMYC,RMFT
13    FORMAT(//3X,'CAR BODY',5X,E12.5/3X,'TRUCK          ',E12.5)
      RETURN
      END
```

```
      SUBROUTINE ERF(D,S,G)
      COMMON/ER/ER(201)
      ROOT2=1.4142
      B=D/S/ROOT2
      I1=IFIX(B/0.01)+1
      IF(I1.GE.201) GO TO 1
      YINT=(B-(I1-1)*0.01)/0.01
      I2=I1+1
      G=(ER(I2)-ER(I1))*YINT+ER(I1)
      RETURN
1       G=1.
      RETURN
      END
```

```
      SUBROUTINE PSDA(W,AIPSD,I22,I5,V,ITC)
      COMMON/RP/R,P
      DIMENSION FREQ(50)
      COMMON/WA/WAA
      INTEGER R,P
C     DIMENSION PSDI(50)
C     IF(I5.NE.1) GO TO 1
C
C     READ ALIGNMENT PSD
C     READ(R,2) (FREQ(I),PSDI(I),I=1,I22)
C   2 FORMAT(*****)
C
C     INTERPOLATION
C     W=W*6.2832
C   1 DO 50 I=1,I22
C     IF(W.LT.FREQ(I)) GO TO 70
C  50 CONTINUE
C     GO TO 90
C  70 IF(I.EQ.1) GO TO 80
C     I1=I-1
C     DW=(W-FREQ(I1))/(FREQ(I)-FREQ(I1))
C     AIPSD=(PSDI(I)-PSDI(I1))*DW+PSDI(I1)
C     GO TO 140
C  80 AIPSD=PSDI(1)
C     GO TO 140
C  90 AIPSD=PSDI(I22)
C 140 CONTINUE
C     W=W/6.2832
C
C
      IF(ITC-5) 10,11,12
C     CLASS 4
10        WC=0.2513/12.*V
      WA=WAA/12.*V
      AK=9.9E-05*12.
      GO TO 13
C    CLASS 5
11        WC=0.2513/12.*V
      WA=WAA/12.*V
      AK=2.47E-05*12.
      GO TO 13
C    CLASS   6
12        WC=0.2513/12.*V
      WA=WAA/12.*V
      AK=1.1E-05*12.
C     W :RD/SEC
C     V :IN/SEC
C     AK:RD.IN
C     UNIT OF AIPSD IS ((IN**2/(RD/SEC))
   13     AIPSD=AK*V*WC*WC/(W*W+WA*WA)/(W*W+WC*WC)
      RETURN
      END
```

```
      SUBROUTINE GT1(W,AIPSD,I22,I5,V,ITC)
      COMMON/OPTION/IOPT
      COMMON/GT3/WV7(12),WV8(12)
      COMMON/GT2/WV6(10),PSD(10) ,B3R(6),B3I(6)
      COMMON/GT1/RM1R(10,12),RM1I(10,12),RM2R(10),RM2I(10),
     1 TZR(10),TZI(10),WV1(10),WV2(10),WV3(10),WV4(10),WV5(10),
     1 RMS(10),TRA(12),TIA(12),BRA(12),BIA(12)
      IF(IOPT.GT.14) GO TO 1
      DO 701 I=1,3
      WV2(I)=0.
      WV3(I)=0.
      WV1(I)=0.
      WV4(I)=0.
701   CONTINUE
      DO 705 I=1,3
      DO 705 J=1,12
      WV1(I)=WV1(I)+RM1R(I,J)*TRA(J)
      WV2(I)=WV2(I)+RM1I(I,J)*TIA(J)
      WV3(I)=WV3(I)+RM1I(I,J)*TRA(J)
      WV4(I)=WV4(I)+RM1R(I,J)*TIA(J)
705   CONTINUE
      CALL PSLA(W,AIPSD,I22,I5,V,ITC)
      DO 706 I=1,3
      TZR(I)=RM2R(I)+WV1(I)-WV2(I)
      TZI(I)=RM2I(I)+WV3(I)+WV4(I)
      PSD(I)=(TZR(I)**2+TZI(I)**2)*AIPSD*6.2832
706   CONTINUE
      IF(IOPT.LT.14) GO TO 2
      WV2(10)=0.
      WV3(10)=0.
      WV1(10)=0.
      WV4(10)=0.
      DO 7051 J=1,12
      WV1(10)=WV1(10)+RM1R(10,J)*TRA(J)
      WV2(10)=WV2(10)+RM1I(10,J)*TIA(J)
      WV3(10)=WV3(10)+RM1I(10,J)*TRA(J)
      WV4(10)=WV4(10)+RM1R(10,J)*TIA(J)
7051  CONTINUE
      TZR(10)=RM2R(10)+WV1(10)-WV2(10)
      TZI(10)=RM2I(10)+WV3(10)+WV4(10)
      PSD(10)=(TZR(10)**2+TZI(10)**2)*AIPSD*6.2832
      RETURN
2     I2=10
      IF(IOPT.EQ.12) I2=9
      DO 1701 I=7,I2
      WV2(I)=0.
      WV3(I)=0.
      WV1(I)=0.
      WV4(I)=0.
1701  CONTINUE
```

```
      DO 1705 I=7,I2
      DO 1705 J=1,12
      WV1(I)=WV1(I)+RM1R(I,J)*TRA(J)
      WV2(I)=WV2(I)+RM1I(I,J)*TIA(J)
      WV3(I)=WV3(I)+RM1I(I,J)*TRA(J)
      WV4(I)=WV4(I)+RM1R(I,J)*TIA(J)
1705  CONTINUE
      DO 1706 I=7,I2
      TZR(I)=RM2R(I)+WV1(I)-WV2(I)
      TZI(I)=RM2I(I)+WV3(I)+WV4(I)
      PSD(I)=(TZR(I)**2+TZI(I)**2)*AIPSD*6.2832
1706  CONTINUE
      RETURN
1     I1=1
      IF(IOPT.EQ.16) I1=4
      DO 711 I=I1,6
      WV2(I)=0.
      WV3(I)=0.
      WV1(I)=0.
      WV4(I)=0.
711   CONTINUE
      DO 715 I=I1,6
      DO 715 J=1,12
      WV1(I)=WV1(I)+RM1R(I,J)*TRA(J)
      WV2(I)=WV2(I)+RM1I(I,J)*TIA(J)
      WV3(I)=WV3(I)+RM1I(I,J)*TRA(J)
      WV4(I)=WV4(I)+RM1R(I,J)*TIA(J)
715   CONTINUE
      CALL PSDA(W,AIPSD,I22,I5,V,ITC)
      DO 716 I=I1,6
      TZR(I)=RM2R(I)+WV1(I)-WV2(I)
      TZI(I)=RM2I(I)+WV3(I)+WV4(I)
      PSD(I)=(TZR(I)**2+TZI(I)**2)*AIPSD*6.2832
716   CONTINUE
      WV2(10)=0.
      WV3(10)=0.
      WV1(10)=0.
      WV4(10)=0.
      DO 1715 J=1,12
      WV1(10)=WV1(10)+RM1R(10,J)*TRA(J)
      WV2(10)=WV2(10)+RM1I(10,J)*TIA(J)
      WV3(10)=WV3(10)+RM1I(10,J)*TRA(J)
      WV4(10)=WV4(10)+RM1R(10,J)*TIA(J)
1715  CONTINUE
      TZR(10)=RM2R(10)+WV1(10)-WV2(10)
      TZI(10)=RM2I(10)+WV3(10)+WV4(10)
      PSD(10)=(TZR(10)**2+TZI(10)**2)*AIPSD*6.2832
      RETURN
      END
```

```
          SUBROUTINE GT2(DW)
          COMMON/OPTION/IOPT
          COMMON/GT3/WV7(12),WV8(12)
          COMMON/GT2/WV6(10),PSD(10) ,P3R(6),P3I(6)
          COMMON/GT1/BM1R(10,12),BM1I(10,12),BM2R(10),BM2I(10),
          1 T2R(10),T2I(10),WV1(10),WV2(10),WV3(10),WV4(10),WV5(10),
          1 RMS(10),TRA(12),TIA(12),BRA(12),BIA(12)
          IF(IOPT.GT.14) GO TO 1
          DO 701 I=1,3
          RMS(I)=WV6(I)+.5*DW*(PSD(I )+WV5(I))
701       CONTINUE
          IF(IOPT.LT.14) GO TO 2
          RMS(10)=WV6(10)+.5*DW*(PSD(10 )+WV5(10))
          RETURN
2         I2=10
          IF(IOPT.EQ.12) I2=9
          DO 1701 I=7,I2
          RMS(I)=WV6(I)+.5*DW*(PSD(I )+WV5(I))
1701      CONTINUE
          RETURN
1         I1=1
          IF(IOPT.EQ.16) I1=4
          DO 711 I=I1,6
          RMS(I)=WV6(I)+.5*DW*(PSD(I )+WV5(I))
711       CONTINUE
          RMS(10)=WV6(10)+.5*DW*(PSD(10 )+WV5(10))
          RETURN
          END


          SUBROUTINE GF7(A,GAIN,X,GAIN78,AINC)
C*****************************************************************
C     INTERPOLATES VALUES FOR THE DESCRIBING FUNCTIONS FROM
C       THE TABLE
C*****************************************************************
          DIMENSION X(120),GAIN78(120)
          NDF=120
          IF(A.GE.X(NDF)) GO TO 1
          I1=IFIX(A/AINC)+1
          I2=I1+1
          DX=A-X(I1)
          GAIN=GAIN78(I1)+(GAIN78(I2)-GAIN78(I1))*DX/AINC
          RETURN
1         GAIN=GAIN78(NDF)
          RETURN
          END
```

```
      SUBROUTINE GT3
      COMMON/OPTION/IOPT
      COMMON/GT3/WV7(12),WV8(12)
      COMMON/GT2/WV6(10),PSD(10) ,B3R(6),B3I(6)
      COMMON/GT1/PM1R(10,12),PM1I(10,12),PM2R(10),PM2I(10),
     1 TZR(10),TZI(10),WV1(10),WV2(10),WV3(10),WV4(10),WV5(10),
     1 RMS(10),TRA(12),TIA(12),RPA(12),PIA(12)
      IF(IOPT.GT.14) GO TO 1
      DO 701 I=1,3
      WV5(I)=PSD(I)
      WV6(I)=RMS(I)
701   CONTINUE
      IF(IOPT.LT.14) GO TO 2
      WV5(10)=PSD(10)
      WV6(10)=RMS(10)
      RETURN
2     I2=10
      IF(IOPT.EQ.12) I2=9
      DO 1701 I=7,I2
      WV5(I)=PSD(I)
      WV6(I)=RMS(I)
1701  CONTINUE
      RETURN
1     I1=1
      IF(IOPT.EQ.16) I1=4
      DO 711 I=I1,6
      WV5(I)=PSD(I)
      WV6(I)=RMS(I)
711   CONTINUE
      WV5(10)=PSD(10)
      WV6(10)=RMS(10)
      RETURN
      END
```

```
      SUBROUTINE LDF4(A,LAM,DEL,PHI,GRAV,DELY,X,ALM,ADL,APH,GS,ADLY)
C*****************************************************************
C LDF INTERPOLATES VALUES FOR THE DESCRIBING FUNCTIONS FROM
C  THE DESCRIBING FUNCTION TABLE
C*****************************************************************
      REAL LAM
      DIMENSION X(51),ALM(51),ADL(51),APH(51),GS(51),ADLY(51)
      NDF=51
      IF(A.GE.X(NDF)) GO TO 1
      I1=IFIX(A/0.01)+1
      I2=I1+1
      DX=A-X(I1)
      LAM=ALM(I1)+(ALM(I2)-ALM(I1))*DX/0.01
      DEL=ADL(I1)+(ADL(I2)-ADL(I1))*DX/0.01
      PHI=APH(I1)+(APH(I2)-APH(I1))*DX/0.01
      GRAV=GS(I1)+(GS(I2)-GS(I1))*DX/0.01
      DELY=ADLY(I1)+(ADLY(I2)-ADLY(I1))*DX/0.01
      RETURN
1       LAM=ALM(NDF)
      DEL=ADL(NDF)
      PHI=APH(NDF)
      GRAV=GS(NDF)
      RETURN
      END


      SUBROUTINE LDF5(B,GRAV)
      DIMENSION X(51)
      COMMON/COM21/CAD(51)
       NDF=51
      DO 1 I=1,NDF
1       X(I)=(I-1)*0.01
      A=B
      DO 50 I=1,NDF
      IF(A.LT.X(I)) GO TO 70
50      CONTINUE
      IF(A.EQ.X(I)) GO TO 100
      GO TO 90
  70    IF(I.EQ.1) GO TO 80
      I1=I-1
      XX=(A-X(I1))/(X(I)-X(I1))
      GRAV=((CAD(I)-CAD(I1))*XX+CAD(I1))*29.562
      GO TO 140
 80     CONTINUE
      GRAV=CAD(1)*29.562
      GO TO 140
 90     CONTINUE
 100    GRAV=CAD(NDF)*29.562
 140    CONTINUE
      RETURN
      END
```

```
      SUBROUTINE INVERT(A,D)
      REAL*8 B(12,12)
      REAL*8 A(12,12)
      REAL*8 DET
      INTEGER L(12),M(12),DOF
      COMMON/DOF/DOF
       DO 10 I=1,DOF
      DO 10 J=1,DOF
10      B(I,J)=A(I,J)*1.E-05
      CALL MATINV(B,DOF,DUMMY,0,DET,DOF,MARK)
      DO 15 I=1,DOF
      DO 15 J=1,DOF
15      A(I,J)=B(I,J)*1.E-05
      D=DET
      RETURN
      END


      SUBROUTINE MATINV(A,N,B,M,DETERM,NY,MARK)
      IMPLICIT REAL*8(A-H,O-Z)
      INTEGER R,P
      COMMON/RP/R,P
C
C MATRIX INVERSION WITH ACCOMPANYING SOLUTION OF LINEAR EQUATION
C
      DIMENSION IPIVOT(100),INDEX(100,2),A(NY,NY),B(100,1),PIVOT(100)
      EQUIVALENCE(IROW,JROW),(ICOLUM,JCOLUM),(AMAX,T,SWAP)
C     INITIALIZATION
C
  5     MARK=0
 10     DETERM=1.0
 15     DO 20 J=1,N
 20     IPIVOT(J)=0
 30     DO 550 I=1,N
C C
C SEARCH FOR PIVOT ELEMENT
C
 40     AMAX=0.0
 45     DO 105 J=1,N
 50     IF (IPIVOT(J)-1) 60,105,60
 60     DO 100 K=1,N
 70     IF (IPIVOT(K)-1) 80,100,723
 80     IF (DABS(AMAX)-DABS(A(J,K))) 85,100,100
 85     IROW=J
 90     ICOLUM=K
 95     AMAX=A(J,K)
100     CONTINUE
105     CONTINUE
```

```
  110      IPIVOT(ICOLUM)=IPIVOT(ICOLUM)+1
C C
C     INTERCHANGE ROWS TO PUT PIVOT ELEMENT ON DIAGONAL
C
  103      IF (IROW-ICOLUM) 140,260,140
  140      DETERM=-DETERM
  150      DO 200 L=1,N
  160      SWAP=A(IROW,L)
  170      A(IROW,L)=A(ICOLUM,L)
  200      A(ICOLUM,L)=SWAP
  205      IF(M) 260,260,210
  210      DO 250 L=1,M
  220      SWAP=B(IROW,L)
  230      B(IROW,L)=B(ICOLUM,L)
  250      B(ICOLUM,L)=SWAP
  260      INDEX(I,1)=IROW
  270      INDEX(I,2)=ICOLUM
  310      PIVOT(I)=A(ICOLUM,ICOLUM)
  315      IF(DABS(DETERM).LT.1.0D+36) GO TO 320
  316      DETERM = DETERM/1.0D+20
C**************************
C       CORRECT  ONE IS THE FOLLOWING
C 320   DETERM=DETERM*PIVOT(I)
C**************************
  320      DETERM=1.
C C
C     DIVIDE PIVOT ROW BY PIVOT ELEMENT
C
  321      IF(DABS(PIVOT(I)).LE.1.0D-25) GO TO 720
  330      A(ICOLUM,ICOLUM)=1.0
  340      DO 350 L=1,N
  350      A(ICOLUM,L)=A(ICOLUM,L)/PIVOT(I)
  355      IF(M) 380,380,360
  360      DO 370 L=1,M
  370      B(ICOLUM,L)=B(ICOLUM,L)/PIVOT(I)
C C
C     REDUCE NON-PIVOT ROWS
C
  380      DO 550 L1=1,N
  390      IF(L1-ICOLUM) 400,550,400
  400      T=A(L1,ICOLUM)
  420      A(L1,ICOLUM)=0.0
  430      DO 450 L=1,N
  450      A(L1,L)=A(L1,L)-A(ICOLUM,L)*T
  455      IF(M) 550,550,460
  460      DO 500 L=1,M
  500      B(L1,L)=B(L1,L)-B(ICOLUM,L)*T
  550      CONTINUE
```

```
C C
C       INTERCHANGE COLUMNS
C
  600      DO 710 I=1,N
  610      L=N+1-I
  620      IF (INDEX(L,1)-INDEX(L,2)) 630,710,630
  630      JROW=INDEX(L,1)
  640      JCOLUM =INDEX(L,2)
  650      DO 705 K=1,N
  660      SWAP=A(K,JROW)
  670      A(K,JROW)=A(K,JCOLUM)
  700      A(K,JCOLUM)=SWAP
  705      CONTINUE
  710      CONTINUE
  715      RETURN
  720      WRITE(P,721)
  721      FORMAT(1H,15HMATRIX SINGULAR)
  722      MASK=1
  723      RETURN
         END
```

```
      SUBROUTINE STAB(M,ROOTR,ROOTI,DAMP,ISTATE)
      DIMENSION ROOTR(M),ROOTI(M),DAMP(M)
      INTEGER R,P
      COMMON/RP/R,P
      IF(ISTATE.EQ.0)  GO TO 3
      K1=0
      K2=0
      K3=0
      DO 15 I=1,M
      IF(ROOTR(I))20,30,40
   20   K1=K1+1
      GO TO 15
   30   K2=K2+1
      GO TO 15
   40   K3=K3+1
   15   CONTINUE
      IF(K1.EQ.M) GO TO 21
      IF(K2.NE.0) GO TO 31
   32   IF(K3.NE.0) GO TO 41
      GO TO 3
   31   WRITE(P,11)K2
      GO TO 32
   41   WRITE(P,12)K3
      GO TO 3
   21   WRITE(P,8)
    3   DO 1 I=1,M
    1   DAMP(I)= COS(ATAN2(ABS(ROOTI(I)),-ROOTR(I)))
      IF(ISTATE.EQ.0) RETURN
      WRITE(P,9)
      DO 2 I=1,M
      IF(DAMP(I).EQ.1.) GO TO 4
      WRITE(P,10)ROOTR(I),ROOTI(I),DAMP(I),ROOTR(I),ROOTI(I)
      GO TO 2
    4   WRITE(P,13)ROOTR(I),ROOTI(I),ROOTR(I),ROOTI(I)
    2   CONTINUE
11      FORMAT(1H0,'SYSTEM IS NEUTRALLY STABLE, K2 =',I5,' ROOTS WITH
      1       ZERO REAL PARTS'//)
   12   FORMAT(1H0,'   SYSTEM UNSTABLE, K3 =',I5,'  ROOTS WITH POSITIVE
      1       REAL PARTS'//)
8       FORMAT(1H0,'SYSTEM STABLE, ALL ROOTS HAVE NEGATIVE REAL PARTS'//)
9       FORMAT(1H0,40X,'THE EIGENVALUES AND DAMPING FACTORS ARE'///6X,
      1 'REAL PART',4X,' IMAGINARY PART',4X,' DAMPING FACTOR',4X,
      1 ' REAL PART',4X,' IMAGINARY PART'///)
   10   FORMAT(1H ,E15.8,4X,E15.8,6X,E15.8,6X,E15.8,4X,E15.8/)
   13   FORMAT(1H ,E15.8,4X,E15.8,6X,'     APERIODIC ',6X,E15.8,4X,E15.8/
      1 )3
      RETURN
      END
```

```
      SUBROUTINE TRANS (UR,UI,Z)
      DIMENSION UR(24),UI(24),Z(24,24),B(24,24),C(24,24),BR(12,24),CR(12,1
     1 3),XMOD(12,24),EIGMOD(12,24),EIGARG(12,24),XNORM(24)
      INTEGER R,P,DOF,DOF2
      COMMON/RP/R,P
      COMMON/DOF/DOF
      COMMON/DOF2/DOF2
      K=1
      N=DOF2
      NHALF=N/2
1000  IF (K.GT.24) GO TO 5000
      IF(UI(K).EQ.0.0) GO TO 3000
      DO 2000 I=1,N,1
      B(I,K)=Z(I,K)
      C(I,K)=Z(I,K+1)
      B(I,K+1)=B(I,K)
      C(I,K+1)=-C(I,K)
2000  CONTINUE
      K=K+2
      GO TO 1000
3000  DO 4000 I=1,N,1
      B(I,K)=Z(I,K)
      C(I,K)=0.00
4000  CONTINUE
      K=K+1
      GO TO 1000
5000  DO 6000 I=1,NHALF
      DO 6000 K=1,N
6000  XMOD(I,K)=B(I,K)*B(I,K)+C(I,K)*C(I,K)
      DO 7500 K=1,N
      XMAX=XMOD(1,K)
      DO 6500 JJ=2,NHALF
      IF (XMOD(JJ,K).LE.XMAX) GO TO 6500
      XMAX=XMOD(JJ,K)
6500  CONTINUE
      XNORM(K)=XMAX
      DO 7000 I=1,NHALF
7000  IF (XNORM(K).EQ.XMOD(I,K)) LL=I
      DO 7500 L=1,NHALF
      BR(L,K)=(B(L,K)*B(LL,K)+C(L,K)*C(LL,K))/XNORM(K)
      CR(L,K)=(C(L,K)*B(LL,K)-B(L,K)*C(LL,K))/XNORM(K)
      EIGMOD(L,K)=SQRT(BR(L,K)*BR(L,K)+CR(L,K)*CR(L,K))
      IF(EIGMOD(L,K).NE.0.00) GO TO 7501
      EIGARG(L,K)=0.
      GO TO 7500
```

```
7501      EIGARG(L,K)=57.3*ATAN2(CR(I,K),CA(L,K))
7500      CONTINUE
8000      CONTINUE
      WRITE(P,9200) NHALF
      KLJ=1
      KLJJ=4
8100      WRITE (P,9300) (K,K,K=KLJ,KLJJ)
      WRITE (P,9400)   (WR(K),WI(K),K=KLJ,KLJJ)
      WRITE (P,9500)
      DO 8200 L=1,NHALF
8200      WRITE (P,9600) L, (EIGMOD(L,K),EIGARG(L,K),K=KLJ,KLJJ)
      IF (KLJJ-N) 8500,9700,9700
8500      CONTINUE
      KLJ=KLJ+4
      KLJJ=KLJJ+4
      IF(KLJJ.LT.N) GO TO 8100
      KLJ=N-3
      KLJJ=N
      GO TO 8100
9200      FORMAT(1H0,20X,'EIGENVALUES AND EIGENVECTORS, FIRST ELEMENT IS'/
      1    20X,' THE EIGENVALUE, NEXT ',I2,' ELEMENTS ARE COMPONENTS OF'/
      1    20X,' THE DISPLACEMENT EIGENVECTOR IN MAG-PHASE FORM'/)
9300      FORMAT (1H0,'*****************************************************'/
      1         1H ,6X,4('RR(',I2,')',8X,'RI(',I2,')',8X))
9400      FORMAT (1H ,3X, 8E14.5)
9500      FORMAT (1H0,20X,'EIGENVECTOR COMPONENTS'/
      1    1H ,6X,4('MODULUS    ','  PHASE DEG      '))
9600      FORMAT (1H ,I3,(8E14.5))
9700      RETURN
      END
```

```
 STATISTICAL DESCRIBING FUNCTION PROGRAM FOR
  A TWELVE D.O.F. HALF-CAR LOCOMOTIVE MODEL
 NEW AAR ON NEW RAIL
 PARAMETRIC STUDIES (** FOR CRITICAL SPEED **)
 DEADBAND IS REDUCED BY 50% IN ALL AXLES
115.0 0.0314E 00                                  VELOCITY,
 1 6 1 5 5,                                            IWP,ITC,IPROF,ISUSP,IOPT
 1 0,                                  IGEL,IGSY
 0.19429E 00 0.18698E 00 0.18484E 00 0.20000E 00 0.22000E 00 0.36000E 00
 0.10496E-02 0.44526E-03 0.67660E-03 0.11504E-02
1210,                               DOF,INL
 0 4,                                     IFREQ,ITERM
 0.40000E 00 0.10000E 02 50  7 1.00 50 1, W1,W2,I22,ITER,EPS,I23,I33
0,                                 INRITE
 0.29562E 02 0.79380E 02-0.12500E 01 0.85000E 02,          A,L1,L2,L3
 0.25000E 01 0.50200E 02 0.50000E 01 0.20000E 02 0.20000E 00,HTP,HCG,HTC,HZERO,YTL
 0.35900E 07 0.45240E 06 0.58860E 05 0.40550E 07,     F11,F12,F22,F33
 0.30000E 02 0.40000E 02 0.38300E 03 0.66000E 05 0.17800E 04,MW,MT,MC,LA,IROLL
 0.16500E 05 0.36000E 04 0.56000E 05 0.17800E 06 0.36000E 06,IWX,IWY,ETC
 0.75000E 02 0.75000E 02 0.75000E 02,    CPY(I)
 0.21666E 04 0.21666E 04 0.21666E 04,    CPYAW(I)
 0.11180E 06 0.11420E 07 0.11180E 06,     CPPHI(I)
 0.11440E 08 0.11440E 08 0.11440E 08,     KPPHI(I)
 0.58587E 09 0.16651E 07 0.23000E 05 0.60000E 03,  KSPHI,CSPHI,KSY,CSY
 0.14400E 05 0.14400E 05 0.14400E 05,     PY1(I)
 0.18720E 09 0.18720E 09 0.18720E 09,     PYAW1(I)
 0.12480E 10 0.12480E 10 0.12480E 10,     PYAW2(I)
 0.27996E 08 0.10000E 06,                 KSYAW,TCP
 0.18756E 00 0.18756E 00 0.18756E 00,     DLY(I)
 0.47400E-02 0.47400E-02 0.47400E-02,     DLYAW(I)
 0.36600E-01 0.36600E-01 0.36600E-01,        DELJ(1-3)
 0.67993E-01 0.67993E-01 0.67993E-01,        A11,A12,A13
 0.66948E-01 0.66948E-01 0.66948E-01,       LAMDA(1-3)
 0.38708E-02 0.38708E-02 0.38708E-02,          KDEL
 0.99446E 00 0.99446E 00 0.99446E 00,         KDELY
 0.10329E 01 0.10329E 01 0.10329E 01,       KGRAV
 0.14400E 05 0.14400E 05 0.14400E 05,                K71,K72,K73
 0.18720E 09 0.18720E 09 0.18720E 09,          K81,K82,K83
 0.06000E 07,                              CCP
 0.10865E 00 0.10358E 00 0.92433E-01,      GPHI
 0.01000E 00 0.00010E 00,                                AINC7,AINC8
 0.00100E 00,                            SIGLOW
 0 0 1 0 1, DISP PSD,DISP TF,ACC PSD CAR &TRUCK, NL TF,NL PSD,
 1,                    EVEC/EVAL OPTION
```

APPENDIX D

DESCRIBING FUNCTION TABLES FOR HEUMANN AND NEW WHEEL ON NEW RAIL AT STANDARD GAUGE

TABLE D.1: HEUMANN WHEEL ON NEW RAIL AT 56.5" GAUGES
GAUSSIAN PROBABILITY DENSITY FUNCTION

σ	K_{Δ_1}	λ	K_{ϕ}
0.00	0.24514E+01	0.88869E-01	0.38675E-01
0.01	0.24514E+01	0.88869E-01	0.38675E-01
0.02	0.30842E+01	0.10188E+00	0.38799E-01
0.03	0.37186E+01	0.11497E+00	0.39449E-01
0.04	0.43514E+01	0.12806E+00	0.41717E-01
0.05	0.49812E+01	0.14116E+00	0.46253E-01
0.06	0.56067E+01	0.15425E+00	0.52270E-01
0.07	0.62258E+01	0.16734E+00	0.58889E-01
0.08	0.68365E+01	0.18047E+00	0.65626E-01
0.09	0.74378E+01	0.19382E+00	0.72301E-01
0.10	0.80284E+01	0.20793E+00	0.78968E-01
0.11	0.86041E+01	0.22365E+00	0.85933E-01
0.12	0.91560E+01	0.24186E+00	0.93720E-01
0.13	0.96719E+01	0.26314E+00	0.10293E+00
0.14	0.10141E+02	0.28755E+00	0.11404E+00
0.15	0.10556E+02	0.31471E+00	0.12733E+00
0.16	0.10912E+02	0.34394E+00	0.14281E+00
0.17	0.11210E+02	0.37439E+00	0.16027E+00
0.18	0.11450E+02	0.40523E+00	0.17934E+00
0.19	0.11638E+02	0.43570E+00	0.19959E+00
0.20	0.11775E+02	0.46518E+00	0.22056E+00
0.21	0.11866E+02	0.49320E+00	0.24182E+00
0.22	0.11917E+02	0.51945E+00	0.26300E+00
0.23	0.11930E+02	0.54369E+00	0.28376E+00
0.24	0.11911E+02	0.56584E+00	0.30386E+00
0.25	0.11864E+02	0.58588E+00	0.32309E+00
0.26	0.11794E+02	0.60383E+00	0.34131E+00
0.27	0.11704E+02	0.61980E+00	0.35843E+00
0.28	0.11599E+02	0.63389E+00	0.37440E+00
0.29	0.11482E+02	0.64627E+00	0.38920E+00
0.30	0.11357E+02	0.65706E+00	0.40286E+00
0.31	0.11226E+02	0.66644E+00	0.41540E+00
0.32	0.11092E+02	0.67456E+00	0.42688E+00
0.33	0.10957E+02	0.68155E+00	0.43736E+00
0.34	0.10823E+02	0.68756E+00	0.44691E+00
0.35	0.10691E+02	0.69271E+00	0.45560E+00
0.36	0.10562E+02	0.69712E+00	0.46349E+00
0.37	0.10437E+02	0.70088E+00	0.47067E+00
0.38	0.10316E+02	0.70408E+00	0.47719E+00
0.39	0.10199E+02	0.70680E+00	0.48312E+00
0.40	0.10088E+02	0.70911E+00	0.48851E+00

σ (in)	K_g	K_{Δ_2}
0.00	0.25533E+01	0.25033E+01
0.01	0.25533E+01	0.25033E+01
0.02	0.32064E+01	0.31522E+01
0.03	0.38669E+01	0.38063E+01
0.04	0.45351E+01	0.44634E+01
0.05	0.52134E+01	0.51234E+01
0.06	0.59031E+01	0.57862E+01
0.07	0.66066E+01	0.64512E+01
0.08	0.73333E+01	0.71188E+01
0.09	0.81286E+01	0.77956E+01
0.10	0.91102E+01	0.84997E+01
0.11	0.10451E+02	0.92551E+01
0.12	0.12297E+02	0.10077E+02
0.13	0.14697E+02	0.10961E+02
0.14	0.17580E+02	0.11884E+02
0.15	0.20792E+02	0.12811E+02
0.16	0.24141E+02	0.13707E+02
0.17	0.27442E+02	0.14541E+02
0.18	0.30543E+02	0.15287E+02
0.19	0.33333E+02	0.15932E+02
0.20	0.35745E+02	0.16468E+02
0.21	0.37748E+02	0.16894E+02
0.22	0.39341E+02	0.17213E+02
0.23	0.40540E+02	0.17433E+02
0.24	0.41379E+02	0.17564E+02
0.25	0.41896E+02	0.17616E+02
0.26	0.42135E+02	0.17600E+02
0.27	0.42141E+02	0.17528E+02
0.28	0.41955E+02	0.17409E+02
0.29	0.41616E+02	0.17254E+02
0.30	0.41159E+02	0.17072E+02
0.31	0.40614E+02	0.16869E+02
0.32	0.40007E+02	0.16653E+02
0.33	0.39358E+02	0.16429E+02
0.34	0.38685E+02	0.16200E+02
0.35	0.38002E+02	0.15972E+02
0.36	0.37319E+02	0.15746E+02
0.37	0.36646E+02	0.15524E+02
0.38	0.35987E+02	0.15309E+02
0.39	0.35347E+02	0.15100E+02
0.40	0.34730E+02	0.14900E+02

TABLE D.2: HEUMANN WHEEL ON NEW RAIL AT 56.5" GAUGES
TRAPEZOIDAL PROBABILITY DENSITY FUNCTION

σ (in)	K_{Δ_1}	λ	K_ϕ
0.00	0.21963E+01	0.84019E-01	0.38431E-01
0.01	0.21963E+01	0.84019E-01	0.38431E-01
0.02	0.27033E+01	0.94386E-01	0.38431E-01
0.03	0.33201E+01	0.10717E+00	0.38667E-01
0.04	0.38873E+01	0.11895E+00	0.39155E-01
0.05	0.44716E+01	0.13112E+00	0.40718E-01
0.06	0.50486E+01	0.14317E+00	0.45390E-01
0.07	0.56188E+01	0.15514E+00	0.51734E-01
0.08	0.60117E+01	0.16343E+00	0.56320E-01
0.09	0.62403E+01	0.16822E+00	0.58590E-01
0.10	0.66361E+01	0.17658E+00	0.63737E-01
0.11	0.71312E+01	0.18714E+00	0.69607E-01
0.12	0.76393E+01	0.19812E+00	0.75041E-01
0.13	0.81749E+01	0.20989E+00	0.80850E-01
0.14	0.87164E+01	0.22206E+00	0.86759E-01
0.15	0.92518E+01	0.23444E+00	0.92542E-01
0.16	0.97719E+01	0.24690E+00	0.98086E-01
0.17	0.10276E+02	0.25952E+00	0.10332E+00
0.18	0.10902E+02	0.27821E+00	0.10862E+00
0.19	0.11478E+02	0.30806E+00	0.11602E+00
0.20	0.11870E+02	0.34539E+00	0.12759E+00
0.21	0.12094E+02	0.38664E+00	0.14549E+00
0.22	0.12230E+02	0.42954E+00	0.16930E+00
0.23	0.12322E+02	0.47115E+00	0.19619E+00
0.24	0.12389E+02	0.51040E+00	0.22476E+00
0.25	0.12441E+02	0.54601E+00	0.25330E+00
0.26	0.12471E+02	0.57728E+00	0.28096E+00
0.27	0.12470E+02	0.60468E+00	0.30744E+00
0.28	0.12435E+02	0.62832E+00	0.33212E+00
0.29	0.12362E+02	0.64870E+00	0.35520E+00
0.30	0.12255E+02	0.66592E+00	0.37626E+00
0.31	0.12113E+02	0.68042E+00	0.39559E+00
0.32	0.11944E+02	0.69242E+00	0.41305E+00
0.33	0.11757E+02	0.70233E+00	0.42886E+00
0.34	0.11561E+02	0.71037E+00	0.44302E+00
0.35	0.11356E+02	0.71671E+00	0.45568E+00
0.36	0.11144E+02	0.72157E+00	0.46692E+00
0.37	0.10925E+02	0.72511E+00	0.47688E+00
0.38	0.10702E+02	0.72747E+00	0.48565E+00
0.39	0.10476E+02	0.72874E+00	0.49335E+00
0.40	0.10251E+02	0.72905E+00	0.50006E+00

σ (in)	K_g	K_{Δ_2}
0.00	0.22911E+01	0.22426E+01
0.01	0.22911E+01	0.22426E+01
0.02	0.28127E+01	0.27615E+01
0.03	0.34508E+01	0.33951E+01
0.04	0.40419E+01	0.39804E+01
0.05	0.46581E+01	0.45872E+01
0.06	0.52776E+01	0.51909E+01
0.07	0.59015E+01	0.57928E+01
0.08	0.63381E+01	0.62110E+01
0.09	0.65872E+01	0.64518E+01
0.10	0.70295E+01	0.68741E+01
0.11	0.75982E+01	0.74098E+01
0.12	0.82010E+01	0.79683E+01
0.13	0.88632E+01	0.85674E+01
0.14	0.95674E+01	0.91855E+01
0.15	0.10308E+02	0.98110E+01
0.16	0.11082E+02	0.10435E+02
0.17	0.11912E+02	0.11061E+02
0.18	0.13964E+02	0.12007E+02
0.19	0.19133E+02	0.13368E+02
0.20	0.25514E+02	0.14849E+02
0.21	0.31933E+02	0.16235E+02
0.22	0.37799E+02	0.17354E+02
0.23	0.42422E+02	0.18186E+02
0.24	0.45730E+02	0.18776E+02
0.25	0.47905E+02	0.19175E+02
0.26	0.49267E+02	0.19426E+02
0.27	0.49902E+02	0.19535E+02
0.28	0.49953E+02	0.19521E+02
0.29	0.49529E+02	0.19397E+02
0.30	0.48773E+02	0.19187E+02
0.31	0.47745E+02	0.18901E+02
0.32	0.46547E+02	0.18561E+02
0.33	0.45221E+02	0.18181E+02
0.34	0.43836E+02	0.17782E+02
0.35	0.42411E+02	0.17367E+02
0.36	0.40981E+02	0.16943E+02
0.37	0.39551E+02	0.16512E+02
0.38	0.38146E+02	0.16079E+02
0.39	0.36770E+02	0.15648E+02
0.40	0.35439E+02	0.15225E+02

TABLE D.3: NEW WHEEL ON NEW RAIL AT 56.5" GAUGES
GAUSSIAN PROBABILITY DENSITY FUNCTION

σ (in)	K_{Δ_1}	λ	K_{ϕ}
0.00	0.15060E+01	0.75129E-01	0.69232E-01
0.01	0.15060E+01	0.75129E-01	0.69232E-01
0.02	0.15091E+01	0.77102E-01	0.69956E-01
0.03	0.14374E+01	0.74722E-01	0.69974E-01
0.04	0.13539E+01	0.73053E-01	0.69867E-01
0.05	0.12280E+01	0.72425E-01	0.69719E-01
0.06	0.10655E+01	0.72331E-01	0.69598E-01
0.07	0.88967E+00	0.72262E-01	0.69505E-01
0.08	0.72025E+00	0.72099E-01	0.69399E-01
0.09	0.57759E+00	0.72350E-01	0.69351E-01
0.10	0.49279E+00	0.74380E-01	0.69729E-01
0.11	0.50340E+00	0.80121E-01	0.71258E-01
0.12	0.63810E+00	0.91307E-01	0.74836E-01
0.13	0.90600E+00	0.10883E+00	0.81229E-01
0.14	0.12962E+01	0.13258E+00	0.90859E-01
0.15	0.17843E+01	0.16164E+00	0.10374E+00
0.16	0.23395E+01	0.19466E+00	0.11957E+00
0.17	0.29311E+01	0.23017E+00	0.13780E+00
0.18	0.35321E+01	0.26679E+00	0.15781E+00
0.19	0.41205E+01	0.30334E+00	0.17898E+00
0.20	0.46801E+01	0.33891E+00	0.20072E+00
0.21	0.51995E+01	0.37282E+00	0.22252E+00
0.22	0.56717E+01	0.40463E+00	0.24400E+00
0.23	0.60934E+01	0.43406E+00	0.26481E+00
0.24	0.64636E+01	0.46097E+00	0.28474E+00
0.25	0.67836E+01	0.48534E+00	0.30362E+00
0.26	0.70560E+01	0.50722E+00	0.32133E+00
0.27	0.72844E+01	0.52673E+00	0.33783E+00
0.28	0.74727E+01	0.54400E+00	0.35310E+00
0.29	0.76255E+01	0.55923E+00	0.36715E+00
0.30	0.77469E+01	0.57258E+00	0.38001E+00
0.31	0.78414E+01	0.58424E+00	0.39176E+00
0.32	0.79127E+01	0.59440E+00	0.40245E+00
0.33	0.79646E+01	0.60322E+00	0.41215E+00
0.34	0.80001E+01	0.61087E+00	0.42095E+00
0.35	0.80221E+01	0.61749E+00	0.42892E+00
0.36	0.80330E+01	0.62321E+00	0.43614E+00
0.37	0.80350E+01	0.62816E+00	0.44267E+00
0.38	0.80298E+01	0.63243E+00	0.44858E+00
0.39	0.80189E+01	0.63612E+00	0.45393E+00
0.40	0.80035E+01	0.63930E+00	0.45879E+00

σ (in)	K_g	K_{Δ_2}
0.00	0.16577E+01	0.15640E+01
0.01	0.16577E+01	0.15640E+01
0.02	0.16616E+01	0.15672E+01
0.03	0.15858E+01	0.14925E+01
0.04	0.14974E+01	0.14056E+01
0.05	0.13645E+01	0.12748E+01
0.06	0.11933E+01	0.11060E+01
0.07	0.10094E+01	0.92370E+00
0.08	0.85018E+00	0.75104E+00
0.09	0.82129E+00	0.62312E+00
0.10	0.11460E+01	0.60451E+00
0.11	0.20950E+01	0.77399E+00
0.12	0.38438E+01	0.11868E+01
0.13	0.63910E+01	0.18509E+01
0.14	0.95759E+01	0.27302E+01
0.15	0.13151E+02	0.37615E+01
0.16	0.16855E+02	0.48744E+01
0.17	0.20462E+02	0.60044E+01
0.18	0.23805E+02	0.70998E+01
0.19	0.26776E+02	0.81232E+01
0.20	0.29316E+02	0.90506E+01
0.21	0.31411E+02	0.98691E+01
0.22	0.33071E+02	0.10574E+02
0.23	0.34327E+02	0.11168E+02
0.24	0.35220E+02	0.11655E+02
0.25	0.35794E+02	0.12046E+02
0.26	0.36098E+02	0.12348E+02
0.27	0.36176E+02	0.12573E+02
0.28	0.36072E+02	0.12732E+02
0.29	0.35822E+02	0.12835E+02
0.30	0.35461E+02	0.12890E+02
0.31	0.35017E+02	0.12907E+02
0.32	0.34514E+02	0.12893E+02
0.33	0.33971E+02	0.12854E+02
0.34	0.33405E+02	0.12796E+02
0.35	0.32828E+02	0.12723E+02
0.36	0.32250E+02	0.12641E+02
0.37	0.31679E+02	0.12550E+02
0.38	0.31119E+02	0.12455E+02
0.39	0.30575E+02	0.12357E+02
0.40	0.30049E+02	0.12258E+02

TABLE D.4: NEW WHEEL ON NEW RAIL AT 56.5" GAUGES
TRAPEZOIDAL PROBABILITY DENSITY FUNCTION

σ (in)	k_{Δ_1}	λ	k_ϕ
0.00	0.99446E+00	0.66948E-01	0.67993E-01
0.01	0.99446E+00	0.66948E-01	0.67993E-01
0.02	0.10210E+01	0.78693E-01	0.69455E-01
0.03	0.10505E+01	0.76014E-01	0.69594E-01
0.04	0.10744E+01	0.73903E-01	0.69518E-01
0.05	0.10957E+01	0.72095E-01	0.69429E-01
0.06	0.11136E+01	0.71859E-01	0.69248E-01
0.07	0.11282E+01	0.72282E-01	0.69014E-01
0.08	0.11367E+01	0.72605E-01	0.68981E-01
0.09	0.11428E+01	0.72653E-01	0.68915E-01
0.10	0.11506E+01	0.72989E-01	0.68849E-01
0.11	0.11570E+01	0.73491E-01	0.69066E-01
0.12	0.11605E+01	0.72673E-01	0.69179E-01
0.13	0.11607E+01	0.71540E-01	0.69025E-01
0.14	0.11582E+01	0.70451E-01	0.68639E-01
0.15	0.11529E+01	0.69458E-01	0.68081E-01
0.16	0.11433E+01	0.68510E-01	0.67406E-01
0.17	0.11525E+01	0.68498E-01	0.66757E-01
0.18	0.17034E+01	0.90372E-01	0.68679E-01
0.19	0.25348E+01	0.13256E+00	0.78695E-01
0.20	0.34212E+01	0.18537E+00	0.97744E-01
0.21	0.43081E+01	0.24196E+00	0.12344E+00
0.22	0.51613E+01	0.29811E+00	0.15298E+00
0.23	0.59327E+01	0.35035E+00	0.18335E+00
0.24	0.66130E+01	0.39780E+00	0.21361E+00
0.25	0.71933E+01	0.43989E+00	0.24265E+00
0.26	0.76798E+01	0.47674E+00	0.27000E+00
0.27	0.80791E+01	0.50887E+00	0.29554E+00
0.28	0.83936E+01	0.53662E+00	0.31889E+00
0.29	0.86400E+01	0.56058E+00	0.34038E+00
0.30	0.88241E+01	0.58094E+00	0.35973E+00
0.31	0.89540E+01	0.59825E+00	0.37729E+00
0.32	0.90366E+01	0.61273E+00	0.39301E+00
0.33	0.90761E+01	0.62477E+00	0.40712E+00
0.34	0.90786E+01	0.63463E+00	0.41967E+00
0.35	0.90485E+01	0.64258E+00	0.43084E+00
0.36	0.89919E+01	0.64884E+00	0.44070E+00
0.37	0.89121E+01	0.65360E+00	0.44942E+00
0.38	0.88144E+01	0.65704E+00	0.45706E+00
0.39	0.87026E+01	0.65930E+00	0.46375E+00
0.40	0.85787E+01	0.66056E+00	0.46957E+00

σ (in)	K_g	K_{Δ_2}
0.00	0.11180E+01	0.10329E+01
0.01	0.11180E+01	0.10329E+01
0.02	0.11473E+01	0.10604E+01
0.03	0.11781E+01	0.10908E+01
0.04	0.12028E+01	0.11154E+01
0.05	0.12248E+01	0.11373E+01
0.06	0.12431E+01	0.11557E+01
0.07	0.12578E+01	0.11707E+01
0.08	0.12664E+01	0.11793E+01
0.09	0.12726E+01	0.11856E+01
0.10	0.12805E+01	0.11935E+01
0.11	0.12871E+01	0.12000E+01
0.12	0.12905E+01	0.12034E+01
0.13	0.12903E+01	0.12034E+01
0.14	0.12870E+01	0.12007E+01
0.15	0.12805E+01	0.11950E+01
0.16	0.12695E+01	0.11849E+01
0.17	0.14593E+01	0.12200E+01
0.18	0.62259E+01	0.24455E+01
0.19	0.13806E+02	0.45349E+01
0.20	0.21790E+02	0.67288E+01
0.21	0.28978E+02	0.87005E+01
0.22	0.34487E+02	0.10355E+02
0.23	0.38363E+02	0.11680E+02
0.24	0.41038E+02	0.12732E+02
0.25	0.42719E+02	0.13539E+02
0.26	0.43608E+02	0.14136E+02
0.27	0.43885E+02	0.14558E+02
0.28	0.43711E+02	0.14830E+02
0.29	0.43183E+02	0.14982E+02
0.30	0.42419E+02	0.15037E+02
0.31	0.41467E+02	0.15011E+02
0.32	0.40406E+02	0.14922E+02
0.33	0.39254E+02	0.14777E+02
0.34	0.38056E+02	0.14590E+02
0.35	0.36827E+02	0.14365E+02
0.36	0.35595E+02	0.14114E+02
0.37	0.34367E+02	0.13842E+02
0.38	0.33161E+02	0.13556E+02
0.39	0.31982E+02	0.13260E+02
0.40	0.30836E+02	0.12958E+02